HYDROCYCLONE FRACTIONATION OF CHICKPEA FLOUR AND MEASUREMENT OF PHYSICAL AND FUNCTIONAL PROPERTIES OF FLOUR AND STARCH AND PROTEIN FRACTIONS

A Thesis Submitted to the College of Graduate Studies and Research

in Partial Fulfillment of the Requirements

for the Degree of Doctor of Philosophy

in the Department of Agricultural and Bioresource Engineering

University of Saskatchewan, Saskatoon

Canada

By

Seyed Shahram Tabaeh Emami

COPYRIGHT

ABSTRACT

Chickpea grain contains a high amount of starch and valuable protein. Many grain legumes (pulses) can be processed by pin milling and air classification with high separation efficiency. However, chickpea exhibits low separation efficiency because it has a relatively high fat content compared to other pulses. Therefore, the main goal of this research was to improve the starch-protein separation from chickpea flour in order to increase the economic value of chickpea grain.

The chemical composition of pin-milled chickpea flour was determined. The functional and physical properties of chickpea flour affecting starch-protein separation were determined. No chemical interactive force was detected between starch granules and protein particles. Therefore, a physical separation technique, i.e. applying centrifugal force in a hydrocyclone, was employed to separate starch granules from protein particles.

Using a hydrocyclone, centrifugal force was applied to chickpea flour particles. Chickpea flour was suspended in two different media, isopropyl alcohol or deionized water. In both media, high inlet pressure resulted in smaller geometric mean diameter of particles collected in the overflow and underflow. Isopropyl alcohol as a medium resulted in particles with smaller geometric mean diameter than did deionized water. Starch and protein separation efficiencies were higher at greater inlet pressures. The application of a double-pass hydrocyclone process increased the purity of starch in the underflow and of protein in the overflow, although this process reduced separation efficiencies. Starch granules and protein particles were separated at higher purities in deionized water than in isopropyl alcohol. Separation in deionized water resulted in higher starch separation efficiency and lower protein separation efficiency than did separation in isopropyl alcohol. This difference was due to the difference in density and viscosity of the two media. The higher viscosity of isopropyl alcohol reduced the likelihood of starch granules reaching the inner hydrocyclone

wall. Thus, some starch granules were retained in the overflow instead of in the underflow. Additionally, the centrifugal force and drag force applied to the chickpea flour particles differed between the two different media. Hydrocyclone operation resulted in higher centrifugal force and lower drag force in deionized water than in isopropyl alcohol. Since the drag force in isopropyl alcohol was higher than that in deionized water, some small starch granules were diverted to the overflow which caused reduction of protein purity.

The use of pH 9.0 and defatting of chickpea flour improved both starch and protein separation efficiencies. Chickpea flour in deionized water at a feed concentration of 5% yielded a pumpable slurry which was delivered efficiently to the hydrocyclone at an inlet pressure of 827 kPa Fractionation of starch and protein from chickpea flour in deionized water using an integrated separation process resulted in starch and protein fractions containing 75.0 and 81.9% (d.b.) starch and protein, respectively. This process resulted in starch and protein separation efficiencies of 99.7 and 89.3%, respectively.

Experiments were also conducted to determine the physical and functional properties of chickpea flour and starch and protein fractions. Thermal conductivity, specific heat, and thermal diffusivity were determined and the polynomial linear models were fitted very well to experimental data. Internal and external friction properties of chickpea flour and starch and protein fractions were determined. Samples were subjected to uniaxial compression testing to determine force-time relationships. The samples' particles underwent rearrangement rather than deformation during compression. The asymptotic modulus of samples was also computed, and it was linearly related to maximum compressive pressure. The functional properties of fractionated products were highly affected by the separation process. The water hydration capacity of starch fraction increased, whereas the emulsion capacity and foaming capacity of starch and protein fractions were reduced, compared to that of chickpea flour.

DEDICATION

This thesis is dedicated to

my beloved Lily.

ACKNOWLEDGEMENTS

Firstly, I would like to thank God, the most gracious and the most merciful, for giving me the opportunities to learn and study through my life and also to complete this research.

I would like to extend my heartfelt gratitude to my supervisor, Dr. L.G. Tabil, for his generous support and scientific advices, as well as his friendship, patience, and understanding in every stage of this work. The guidance and opportunities that he provided me were invaluable in my training.

Sincere thanks to Dr. R.T. Tyler for providing me some facilities in the Department of Applied Microbiology and Food Science, as well as for his priceless advice and constructive guidance during my graduate work. Many thanks and acknowledgement to other member of my Graduate Advisory Committee, Drs. R.L. Kushwaha, O.D. Baik, and V. Meda, for their time and valuable comments and suggestions. Their comments always helped me to improve this manuscript and throughout my graduate program. I thank Dr. K. Muthukumarappan, of the Agricultural and Biosystems Engineering, South Dakota State University, for serving as external examiner and also for suggesting some informative revisions.

I would like to thank the POS Pilot Plant Corp., for lending hydrocyclone and relevant equipment. My acknowledgements to Mr. W.G. Crerar in the Department of Agricultural and Bioresource Engineering, Ms. C.E. Perron and Mr. D. Hassard in the Crop Development Centre, Dr. Todd Pugsley and Mr. M. Wormsbecker in the Department of Chemical Engineering, and Ms. H. Qi in the Alberta Agriculture, Food and Rural Development and the Saskatchewan Structural Sciences Centre for their technical support. I thank the Natural Sciences and Engineering Research Council, Agriculture Development Fund, and University of Ssakatchewan Devolved Graduate Scholarship.

I sincerely extend my deepest thanks to my beloved wife, Lily, for her understanding, support, and patience. She provided me the best support in my study and focus on my research. Many thanks to my relatives, my mother and mother in-law, my father and father in-law, for their moral support.

TABLE OF CONTENTS

LIST OF TABLES

LIST OF FIGURES

NOMENCLATURE

ϕ_i = angle of internal friction (degree)

ε = porosity (%)

ϕ_e = angle of external friction (degree)

$\overline{F}$ = average form factor

$\overline{v}$ = average linear velocity of fluid (m/s)

ρ_b = bulk density (kg/m^3)

$\Delta\rho_b$ = error of bulk density (kg/m^3)

$\Delta\rho_t$ = error of particle density (kg/m^3)

$\Delta\varepsilon$ = error of porosity (%)

Δc_p = error of specific heat (J kg^{-1} °C^{-1})

Δk = error of thermal conductivity (W m^{-1} °C^{-1})

ρ_f = fluid density (kg/m^3)

μ = fluid viscosity (Pa s)

ρ_0 = initial bulk density (kg/m^3)

σ = normal stress (Pa)

ρ_p = particle density (kg/m^3)

ρ_t = particle density (kg/m^3)

ΔT = temperature change (°C)

$\overline{D}$ = average size of starch granules (μm)

ΔH = enthalpy (J/g)

ΔH_d = enthalpy of protein denaturation/aggregation (J/g)

ΔH_p = enthalpy of starch gelatinization (J/g)

ΔS = entropy ($J°C^{-1}\ mol^{-1}$)

ΔT = width of the peak (°C)

μ = coefficient of friction which is $tan\,\phi$

μ_e = coefficient of external friction

μ_i = coefficient of internal friction

a = constant

a = redness (positive) or greenness (negative) in the Hunter **L**, **a**, and **b** colour coordinate

A = biopolymer-ligand interaction

A = cell cross sectional area (m^2)

a_1 = constant

a_2 = constant

a_c = centrifugal acceleration (m^2/s)

A_i = cross-sectional area of inlet (m^2)

A_p = projected area of the particle (m^2)

b = constant

b = yellowness (positive) or blueness (negative) in the Hunter **L**, **a**, and **b** colour coordinate

B = dilution of ligand on injection to the sample

c = constant

C = degree of volume reduction

C = dilution of biopolymer by adding ligand

C_c = cohesion (Pa)

C_D = dimensionless drag coefficient

C_F = component content in the feed material (% d.b.)

c_p = specific heat (J kg^{-1} $°C^{-1}$)

C_P = component content in the product (% d.b.)

d = constant

D = mechanical mixing

d.b. = dry basis (%)

df = degree of freedom

d_i = diameter of pipe (m)

D_n = diameter of a circle with the same area as the area of granule number n (μm)

d_p = particle diameter (m)

D_p = probe diameter (m)

D_{sa} = sample diameter (m)

E_A = asymptotic modulus (Pa)

F = form factor

$F_{(t)}$ = decaying force after time t (N)

F_0 = initial force (N)

F_c = centrifugal force (N)

F_D = drag force (N)

F_f = friction force (N)

F_g = force of gravity (N)

F_n = normal force (N)

GMD = geometric mean diameter (μm)

I = current (A)

ITC = isothermal titration calorimeter

k = thermal conductivity (W m^{-1} °C^{-1})

k_1 = constant

k_2 = constant

K_B = binding constants

k_c = corrected thermal conductivity (W m^{-1} °C^{-1})

k_m = measured thermal conductivity (W m^{-1} °C^{-1})

l = length traveled by fluid (m)

L = lightness (**L** = 100 for white) or darkness (**L** = 0 for black) in the Hunter **L**, **a**, and **b** colour coordinate

m = mass (kg)

n = stoichiometry of the reaction

NSI = nitrogen solubility index

O1 = overflow of the first-pass

OO1 = overflow of the second-pass of O1

OU1 = overflow of the second-pass of U1

P = compressive pressure (Pa)

P = probability

$P1$ = pressure reading after pressurizing the reference volume (psi)

$P2$ = pressure reading after including volume of the cell (psi)

P_i = perimeter of the granule image (μm^2)

q = heat (J)

Q = volume flow rate (m^3/s)

r = radius of path of particle which is hydrocyclone inner radius (m)

R = specific resistance of the heating wire (Ω/m)

R^2 = coefficient of determination

Re = Reynolds number

Re_p = Reynolds number of particle

S = maximum slope

S.E. = standard error

SE = separation efficiency (%)

SE = sediment

SEE = standard error of estimate

S_{gw} = geometric standard deviation of particle diameter (μm)

S_i = area of granule image (μm^2)

SU = supernatant

t = time (s)

T = temperature (°C)

T_d = peak denaturation/aggregation temperature (°C)

TDF = total dietary fibre

T_p = peak gelatinization temperature (°C)

TS_F = total solid of feed material (kg)

TS_P = total solid of product (kg)

u = relative velocity between the fluid and particle (m/s)

U1 = underflow of the first-pass

UO1 = underflow of the second-pass of O1

UU1 = underflow of the second-pass of U1

v = tangential velocity of the particle (m/s)

V = volume of compacted sample at pressure P (m^3)

V = volume of fluid (m^3)

V_0 = volume of sample at zero pressure (m^3)

V_c = volume of cylinder (m^3)

V_{cell} = volume of the cell (cm^3)

v_f = whole volume after whipping (mL)

V_f = foam volume (mL)

V_i = whole volume before whipping (mL)

V_r = volume of released water from emulsion (mL)

VR = reference volume for the large cell (cm^3)

V_s = volume of solid (cm^3)

V_w = total volume of water in the emulsion (mL)

W = weight of sample (g)

w.b. = wet basis (%)

W_d = moisture content (% d.b.)

WHC = water hydration capacity

W_w = moisture content (% w.b.)

x = particle size (μm)

y = cumulative undersize fraction (% volume)

ZP = zeta potential (mV)

α = thermal diffusivity (m^2/s)

ε = strain

σ_0 = initial stress (MPa)

τ = shear stress (Pa)

1. INTRODUCTION

1.1 Background

Canadian pulse crops include dry pea, lentil, dry bean, and chickpea. Chickpea (*Cicer arietinum* L.) is a valuable source of protein and starch. According to Agriculture and Agri-Food Canada (2005) and Saskatchewan Agriculture and Food (2005), the total amount of pulse production in Canada and Saskatchewan in 2004-05 was 5.23 and 4.35 million tonnes from seeded areas of 3.14 and 2.21 million hectares, respectively. This shows that Saskatchewan accounted for 83% of the production and 70% of the seeded area of Canadian pulse crops in 2004-05. Among pulses, chickpea production was 51,000 tonnes, which was 0.1% of Canadian pulse crop production. Export and domestic use of Canadian chickpea seed was 35,000 and 36,000 tonnes, respectively (AAFC 2005). These values show that chickpea grain is becoming an important crop in Canada and one that needs value-added processing to increase its uses and economic value. Most Canadian pulses, like chickpea, are exported as raw product without any processing, except cleaning and grading operations. Increased processing of pulses would contribute to the diversification of agriculture in Western Canada. It is believed that more processing of chickpea would lead to an improvement in the final export value of chickpea and chickpea products. For example, grain products, such as dehulled chickpea (desi), canned chickpea, isolated protein and starch, and concentrated protein and starch would have more economic value than would chickpea grain.

Chickpea grain, from a nutritional point of view, is used in a variety of human foods and serves as an economical protein source. Chickpea is consumed as a staple food in many countries, such as India, and served as a cooked dehulled or whole grain. It is also a main culinary ingredient used in chickpea-based products such as dhokla and dosa (fermented products) as well as laddu and puran poli (sweetened products). Chickpea grain contains a high level of valuable protein (12.4% to 30.6%) and carbohydrates (52.4% to 70.9%) (Chavan et al. 1986). Starch constitutes the majority of the carbohydrate in chickpea. Therefore, chickpea grains can be used as raw material in the production of starch and protein fractions. Fractionation of protein and starch in non-oilseed legumes can be efficiently done by dry processing, i.e. dry milling and air classification (Owusu-Ansah and Mc Curdy 1991). Although chickpea is categorized as a non-oilseed pulse crop, it has a relatively high fat content compared to other pulses. A study by Sosulski co-workers (1987) showed that air classification of pin-milled chickpea flour did not yield as high of a separation efficiency as did other legumes, and protein fraction recovery was very low. The high fat content of chickpea flour causes problem in other processing methods, including isolation. Protein concentrates and isolates can be prepared from pulse grains by wet processing. Wet processing is based on dispersing the protein at alkaline pH followed by precipitation at isoelectric pH to recover protein (Tabil et al. 1995; Owusu-Ansah and Mc Curdy 1991; Swanson 1990). Other wet processing methods include salting out, hydrophobic out, and ultra-filtration (Owusu-Ansah and Mc Curdy 1991). There exists a lack of information on the fractionation of starch and protein from chickpea flour, and value-added processing is required to enhance the economic value of chickpea grain.

1.2 Objectives

The main objective of this research was to develop an efficient separation process for starch and protein fractions from chickpea flour by taking advantage of the physical, chemical, and functional properties of chickpea flour and its components. There exists a lack of information on starch-protein separation from higher-fat content legumes using a hydrocyclone. The hydrocyclone separates particles from a liquid based on their size and density. The feed liquid entering the hydrocyclone tangentially is fractionated to a coarse fraction in to the underflow and a fine fraction in the overflow. In terms of particle size, starch granules and protein particles are quite different. Therefore, since the hydrocyclone separation is particle-size dependent (Svarovsky 1984), the hydrocyclone was employed in this study to separate starch and protein from chickpea flour. Overall, this research was conducted to optimize the operating conditions of a hydrocyclone in the separation of starch and protein from chickpea flour and to determine the chemical, physical, and functional properties of chickpea flour and products. The specific objectives of this research were:

1. to determine the physical and functional properties of chickpea flour and use these properties in a starch-protein fractionation;
2. to optimize the separation process in the hydrocyclone in terms of the following:
    a) selection of the appropriate liquid medium, pressure drop, and feed concentration;
    b) investigation of the effect of defatting of chickpea flour and pH adjustment on the fractionation;
    c) improvement and optimization of starch and protein separation efficiencies from chickpea flour using the hydrocyclone;

d) determination of the highest feed concentration in the hydrocyclone process which would result in an acceptable separation efficiency;

3. to determine physical and functional properties of chickpea fractions and relate these properties to chemical composition changes during separation and overall processing of the product; and
4. to investigate possible utilization models for the starch and protein fractions from information on physicochemical properties generated in this research.

Knowledge of the physical, chemical, and functional properties of final products is necessary for the design, calculation, modeling, and optimization of food processing operations, including mixing, rewetting, drying, transportation, heat treatment, solid flow, storage, etc., that are involved in starch and protein separated from chickpea flour.

1.3 Organization of the thesis

This research is presented in six main chapters including Literature Review, Materials and Methods, Results, Discussion, Summary and Conclusions, and Recommendations for Future Research. The Literature Review is presented in the following order: specifications of chickpea grain; chemical and physical properties employed in starch-protein separation; starch-protein separation from pulse grains; and some useful physical and functional properties. In the Materials and Methods section, techniques used for measuring chemical composition and physical properties are described. This part is followed by a description of the separation techniques employed, focusing on the method using elevated pH, isoelectric precipitation, and hydrocyclone operation. This chapter ends with an explanation of the techniques and methods used for measurement of useful physical and functional properties

of the raw material and products. The Results section presents the numerical values obtained from measurement of chemical composition, physical properties, and functional properties which were applicable to the separation. This chapter also presents the efficiencies resulting from the separation techniques, as well as the physical and functional properties of chickpea flour and starch and protein fractions. In the Discussion section, the variability of data, statistical analysis, comparison of different treatments, and mathematical modeling are discussed in the same order as in the Results section. The Summary and Conclusions and Recommendations for Future Research follow in order.

2. LITERATURE REVIEW

This literature review is presented in four main parts. The first part is a description of chickpea grain. The second part explains the chemical, physical, and functional properties useful in starch-protein separations. The third part focuses on the starch-protein separation techniques applicable for pulse including the hydrocyclone process. The last part describes some useful physical and functional properties of starch and protein fractions.

2.1 Chickpea grain

Pulse grains, such as chickpea, and their products have become an important part of human food in many parts of word (Jood et al. 1998). Chickpea is called by different names including viz., Bengal gram, boot, chana, chola, chhole, garbanzo bean, gram, hommes, and pois chiche. Chickpea is available in different types and used as staple food in some tropical and subtropical countries (Chavan et al. 1986).

2.1.1 History and origin

The word of "pulse" is derived from the Latin word of "puls, pultis", which is a thick soup. This word is applied for dried, edible legume seeds. Pulse crops refer to the seeds of legumes which are used as food. They include peas, beans, lentils, chickpeas, and fababeans. Chickpea (*Cicer arietinum* L.) belong to the family Leguminoseae and originate in the Asia

(Saskpulse 2005). India, Central Asia, Near Eastern, and Mediterranean countries are the primary sources and Ethiopia is a secondary source of origin of chickpea seeds. Old Sanskrit and carbonized names state the existence chickpea seeds in India since 2,000 B.C. (Chavan et al. 1986).

2.1.2 Distribution and production

Chickpea is produced in developing countries, accounting for more than 90% of world chickpea production. The most important consumer of chickpea is India, which produces and consumes 90% of the world's chickpea crop. The major countries that import chickpea are Spain, Algeria, India, Pakistan, Iran, Libya, Lebanon, and the USA. The major exporting countries include Turkey, Australia, Syria and Mexico. Food and Agriculture Organization (FAO 2006) reported that chickpea production in 2005 was 9.16×10^{12} tonnes in total seeded area of 1.12×10^{7} hectares. Table 2.1 shows the worldwide seeded area and production of chickpea. In 2004, Asia produced 90% of world's chickpea followed by North and Central America and Africa.

Pulse grains, being specialty crop in Canada, are one of the most important foods in many countries of Asia, Africa, and Latin American, forming part of the staple diet of the population in these countries. Since pulses have high protein and dietary fibre content, a number of researchers have been working on them. Pulses are used in a variety of human foods and supply as an economical protein source. In many underdeveloped and developing countries, people who cannot afford to buy animal protein sources, use pulses as protein source (Tabil et al. 1995; Bishnoi and Khetarpaul 1993). In addition, vegetarians consume pulses for the necessary protein requirement (Bishnoi and Khetarpaul 1993). Some pulses

Table 2.1 Seeded area and production of chickpea in the world (FAO 2006).

Continent	Seeded area ($\times 10^5$ hectare)					Production ($\times 10^{11}$ tonnes)				
	2001	2002	2003	2004	2005	2001	2002	2003	2004	2005
Africa	5.01	4.82	4.42	4.83	4.92	3.45	3.72	3.05	3.24	3.28
Asia	79.63	93.13	85.76	102.38	102.16	54.12	72.73	62.22	77.71	82.58
Europe	0.97	1.04	1.00	0.97	0.79	0.75	0.89	0.69	0.76	0.36
North & Central America	6.62	3.01	2.13	1.89	2.15	7.81	3.92	3.08	2.91	3.38
South America	0.11	0.07	0.07	0.07	0.07	0.12	0.08	0.07	0.07	0.07
Oceania	1.95	2.01	1.52	1.06	1.95	2.58	1.36	1.78	1.40	1.89
World	94.29	104.08	94.91	111.20	112.05	68.82	82.70	70.89	86.08	91.56

like peas, lentils, beans, and chickpeas are good protein sources in the form of flours, concentrates, and isolates (Swanson 1990). Pulses are fibre-rich foods that can reduce the risk of certain kind of cancer and can also lower blood cholesterol.

2.1.3 Commercial chickpea types

The two main commercial types of chickpea are desi and kabuli. The desi type (Indian origin) has a thick, coloured seed coat, and coloured flowers (Salunkhe et al. 1985). Its seed is wrinkled at beak with brown, light brown, fawn, yellow, orange, black or green colour (Chavan et al. 1986). The desi type has smaller seed than the kabuli type. Desi chickpea has been produced in the Indian subcontinent and milled for making some food products. However, the desi type is not preferred by consumers. The kabuli type, which is called garbanzo bean, has a thin, white seed coat with white flowers which is also used mainly in salad bars and vegetable mixes (Salunkhe et al. 1985). The kabuli type seed is white to cream in colour and has larger seed than the desi type. The kabuli type chickpea originate in the Mediterranean and Middle Eastern countries (Chavan et al. 1986; Salunkhe et al. 1985).

2.2 Chemical, physical, and functional properties useful in starch-protein separation

The utilization of legume flour, such as chickpea flour, and their fractions is growing. Legume flours and their fractions can be utilized in processing of different food and non-food products. The quality and functionality of products depends on composition, physical, and functional properties of raw materials. In addition, study on the structure and functional properties of legumes flour and their fractions extend their utilization in different industries and food processing (Hoover and Sosulski 1991).

2.2.1 Chemical composition

The cotyledons are the major source of nutrients in pulse grains. For chickpea, cotyledons constitute 84% of the whole seed weight (Sokhansanj and Patil 2003; Chavan et al. 1986). The embryo has also considerable amount of protein, fat, and minerals, but its contribution in total seed weight is small (Table 2.2). The seed coat contains most of the non-digestible carbohydrates and relatively higher proportion of calcium (Chavan et al. 1986). Dehulling removes seed coat by abrasion; crude fibre and ash levels decrease while protein, total carbohydrates and lipids content increase (Table 2.3).

2.2.1.1 Protein

The protein content of chickpea seeds is influenced by genetic and environmental factors (Owusu-Ansah and Mc Curdy 1991; Swanson 1990; Chavan et al. 1986). Chickpeas are highly valuable and economical source of vegetable protein that includes essential amino acids (Clemente et al. 2000; Menkov 2000). The storage proteins of chickpea seeds include albumins (water soluble), globulins (salt soluble), prolamines (alcohol soluble), glutelins (acid/alkali soluble) and residual proteins. The globulins, consisting mainly of legumin and vicilin, constitute the major storage protein (56%) followed by glutelins (18.1%), albumins (12.0%), and the least are prolamines (2.8%). The cotyledon is the largest component of a chickpea seed; hence, it contains the majority of the globulins, glutelins, and albumins (Chavan et al. 1986). Studies have shown that the globulins do not contain methionine and cystine (sulfur amino acids). However, albumins and glutelins have higher level of these two amino acids (Clemente et al. 2000; Swanson 1990; Kurien 1987). Hence, the poor nutritive value of chickpea is due to globulins fractions (Chavan et al. 1986). Generally, legume

Table 2.2 Relative distribution of nutrients in different anatomical parts of chickpea (%) (Chavan et al. 1986).

Nutrient	Seed coat (14.5%)		Cotyledon (84.0%)		Embryo (1.5%)		Whole seed (100%)
	a	b	a	b	a	b	
Protein*	3.0	2.0	25.0	95.5	37.0	2.5	22.0
Fat	0.2	0.6	5.0	94.0	13.0	5.0	4.5
Ash	2.8	15.0	2.6	81.0	5.0	3.0	2.7
Crude fibre	48.0	87.0	1.2	13.0	------	------	8.0
Carbohydrates	46.0	11.0	66.0	88.0	42.0	1.0	63.0
Phosphorus	24.0 mg†	1.5	290.0 mg	94.0	740.0 mg	4.5	260.0 mg
Iron	8.0 mg	20.0	5.5 mg	77.0	11.0 mg	3.0	6.0 mg
Calcium	1000.0 mg	72.0	70.0 mg	29.0	110.0 mg	0.8	200.0 mg

a: Nutrient content in each anatomical part

b: Relative distribution of nutrients in whole seed

* % N × 6.25

† mg/100 g

Table 2.3 Chemical composition of chickpea (Chavan et al. 1986).

Composition (g/100g)	Whole seed		Dehulled seed	
	Range	Mean	Range	Mean
Protein*	12.4 - 30.6	21.5	20.5 - 30.5	25.5
Total carbohydrates	52.4 - 70.9	61.7	63.0 - 65.0	64.0
Ash	2.5 - 4.67	3.6	2.1 - 3.7	2.9
Lipids	3.1 - 6.9	5.0	4.5 - 7.5	6.0
Crude fibre	1.2 - 13.5	8.0	0.9 - 1.5	1.2

* % N × 6.25

protein fractions are poor in sulfur-containing amino acids and tryptophan; however, they are richer in lysine compared to cereals. Additionally, in terms of protein quantity, pulse grains have 2 to 3 times more protein than cereals. Therefore, care must be applied to provide a good balance of amino acids in human nutrition by combination of legumes and cereals (Swanson 1990; Chavan et al. 1986; Salunkhe et al. 1985; Makhmudov 1980; Jaya and Venkataraman 1979).

2.2.1.2 Carbohydrates

Carbohydrates constitute the major component of legumes. Legumes are good dietary carbohydrates source. The total carbohydrates of dry legumes vary from 24 to 68%. These include mono-, oligo-, and polysaccharides including starch. Starch is a polysaccharide, which is digestible by humans. Chickpea contains 52.4 to 70.9% total carbohydrates that constitute a major portion of the seed (Chavan et al. 1986; Salunkhe et al. 1985).

Starch is the major component of chickpea and constitutes 37.2 to 50.8% of the whole seed and 55.3 to 58.1% of the dehulled seed. The desi type contains less starch than

the kabuli type. Chickpea starch contains 31.8 to 45.8% amylose and the rest is amylopectin. The amount of amylopectin is higher than amylose, making this starch useful for special applications. The gelatinization temperature of isolated starch is 63.5 to 68°C. With starch containing a long-chain molecule, it has lower digestibility and may cause flatulence in humans (Chavan et al. 1986; Biliaderis et al. 1981).

Most of the remaining carbohydrates in chickpea include reducing and non-reducing sugars and crude fibre. The kabuli type chickpea has higher level of soluble sugar than the desi type. Among legumes, chickpea contains high amounts of raffinose, stachyose, verbascose and manninotriose. These oligosaccharides cause flatulence in humans, because they cannot produce α-galactosidase required for digesting them. Therefore, the presence of these oligosaccharides is one of the most important reasons, which inhibits its use as convenience food (Chavan et al. 1986).

Fibre constitutes a considerable proportion in human nutrition. Crude fibre in chickpea ranges between 7.1 and 13.5% and includes cellulose and hemicellulose. Crude fibre is mainly concentrated in the seed coat. The kabuli type has higher calorific value and nutrients because it contains less hemicellulose and cellulose in the whole seed and dehulled seed than the desi type. Studies have shown that dietary fibre is useful in reducing blood cholesterol levels (Chavan et al. 1986).

2.2.1.3 Lipids

Legumes generally contain higher level of lipids than cereals (Salunkhe et al. 1985). The total lipid content in whole and dehulled chickpea ranges between 3.1 and 6.9% and between 4.5 and 7.5%, respectively (Table 2.3). Lipids are a heterogeneous group.

Triglycerides are the major components of neutral lipids and lecithin is the major component of polar lipids (Kurien 1987; Chavan et al. 1986). Unsaturated fatty acids constitute 67.13% of the total lipids that include oleic acid (21.84%), linoleic acid (43.29%) and linolenic acid (2.0%). Saturated fatty acids constitute 10.42% of the total lipids, which include palmitic acid (9.22%) and stearic acid (1.20%) (Chavan et al. 1986; Salunkhe et al. 1985). In mature legumes, most of the lipids are stored in oil bodies or spherosomes or lipid-containing vesicles, which are located in the cotyledons. Most legume lipids are a good source of essential fatty acids such as linoleic and linolenic acids (Salunkhe et al. 1985; Mahadevappa and Raina 1978). Essential fatty acids are required for growth, physiological functions, and functions of brain and retina. Oleic and linoleic acids are the major fatty acids in chickpeas, peanuts, soybeans, lentils, garden peas, and broad beans. The unsaturated fatty acids of legume lipids have been involved in lowering blood serum and liver cholestrol levels (Chavan et al. 1986; Salunkhe et al. 1985).

2.2.1.4 Minerals

Food legumes are good sources of minerals. The most important minerals contained in chickpea are calcium, phosphorus, magnesium, iron, copper, zinc, sodium, and potassium. Most of the seed calcium is located in the seed coat. Therefore, the consumption of whole seed would be useful in calcium-deficient diets. Chickpea is also a good source of iron. It contains higher level of iron in comparison to other legumes (Kurien 1987; Chavan et al. 1986; Salunkhe et al. 1985).

2.2.1.5 Vitamins

Food legumes are good sources of vitamins such as thiamine, riboflavin, and niacin (Salunkhe et al. 1985). Chickpea contains considerable concentration of ascorbic acid. There is no significant difference between the amount of vitamins in dehulled seeds and whole seeds. However, there appears to be a large variation in ascorbic acid content among the cultivars (Chavan et al. 1986).

2.2.1.6 Anti-nutritional factors

Although pulse grains are a good source of protein, they do not have enough sulfur-containing amino acid such as methionine and cystine (Tabil et al. 1995; Kurien 1987). The main limiting nutritional factors attributed to the low utilization of pulse grains in developed countries are poor digestibility and availability of nutrients, flatulence factors, inherent beany flavor, and presence of anti-nutritional factors. The level of several anti-nutritional factors is reduced by heat treatment such as sterilization, micronizing, and microwave heat treatment. Among the heat treatment procedures, micronizing and microwave heating can reduce the level of anti-nutritional factors effectively without reduction of lysine, in comparison with original levels in seeds (Tabil et al. 1995). The most important anti-nutritional factors contain protease inhibitor, some oligosaccharides (such as raffinose, stachyose, and verbascose), tannins, lipoxygenase, lectins, and phytic acid (Tabil et al. 1995; Owusu-Ansah and Mc Curdy 1991; Chavan et al. 1986; Salunkhe et al. 1985; Valdebouze et al. 1980; Rackis et al. 1979).

2.2.2 Physical and functional properties

Physical and functional properties of chickpea flour and its components are important in the starch-protein fractionation. These properties are also applicable in food and feed industries for storage, handling, and processing.

2.2.2.1 Zeta potential

Zeta potential is a physical property exhibited by a particle in a suspension (Malvern Instruments 2005a). Zeta potential is an index showing the magnitude of the repulsion or attraction between particles. It is very important in many industries including brewing, ceramics, pharmaceutical, medicine, etc. (Malvern Instruments 2005b). For example, one of the methods of obtaining information about the chemical classification of food materials used by microorganism is to obtain their surface charge; the surface charge provides some ideas about multivalent ion containing positive or negative charge. The ions are affected by pH of medium (Hammer et al. 1999). It also has an important role in protein separation as protein interaction is influenced by electrostatic forces. The protein surface charge density is measured as zeta potential (Malvern Instruments 2005b). In order to explain zeta potential concept, a colloidal model with a net electronegative particle is assumed (Figure 2.1). The distribution of charge at the particle surface affects positive ions surrounding the particle; ions make double layer and are close to the surface (Malvern Instruments 2005a; Svarovsky 1990). The innermost layer of ions is called Stern layer where the ions are stationary and are strongly bonded. Beyond the Stern layer, the charges extend to a region that can move more easily and that region is called diffuse layer containing a net charge or opposite charge of Stern layer (Watson and Tuzinski 1989). In the diffuse layer, there is a notional boundary in

which ions and particles make a stable entity. When the particle moves (such as movement due to gravity), the ions in the boundary move it and those ions beyond the boundary stay with the bulk dispersant. The potential at this boundary is the zeta potential (Malvern Instruments 2005a). In other words, the potential between the shear plane, the plane between double layer and bulk dispersant is termed as zeta potential (Svarovsky 1990).

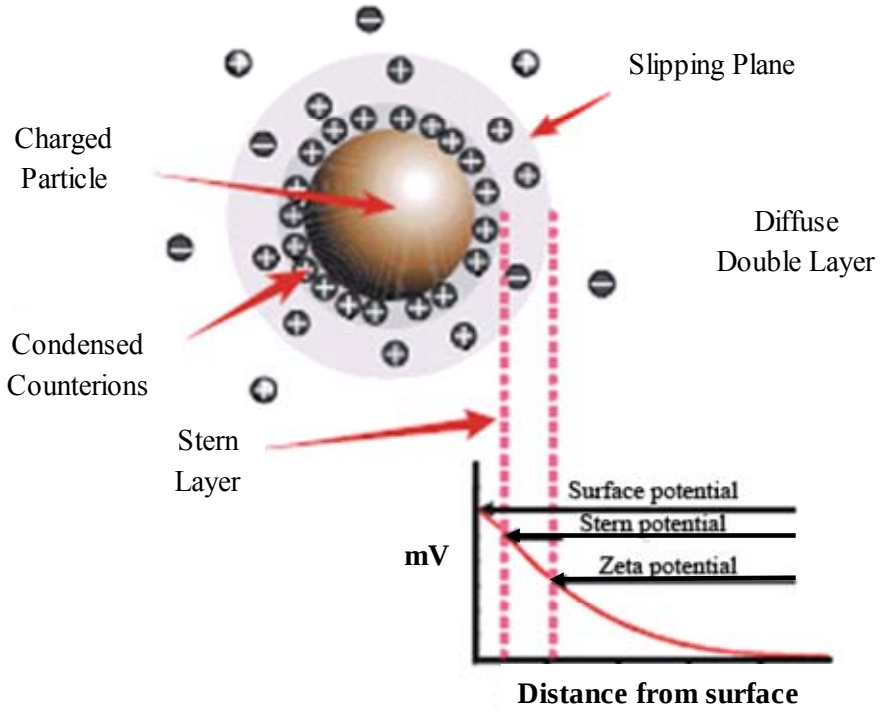

Figure 2.1 Schematic of Stern layer in the colloidal model (Malvern Instruments 2005b). *This figure was reproduced with permission of Malvern Instruments Ltd.*

Factors affecting zeta potential include pH, electrical conductivity, and concentration of components. The zeta potential varies by pH of the medium; it will be positive at acidic pH and negative in alkaline pH. At zero zeta potential, called isoelectric point, the colloid system has the lowest stability. The effect of conductivity is associated with thickness of double layer which depends on the concentration of ions in solution. This concentration is affected by ion strength and valency. As the strength or valency of the ion increases, the double layer is compressed more. The concentration of component can affect the zeta potential, thus affecting the stability of a product (Malvern Instruments 2005a; Malvern Instruments 2005c).

2.2.2.2 Shape and size of starch granules

According to Banks and Greenwood (1975), starch is a solid material with an approximate density 1.5 g/cm^3. Starch granules have been found to be different in shape (sphere to rods) and size (2 to 175 μm). The differences are due to their sources and variety and strictly speaking, due to genetic reasons. Researchers have used scanning electron microscopy (SEM) to study the size and shape of legume starch granules (Ratnayake et al. 2001; Davydova et al. 1995; Gujska et al. 1994; Hoover and Sosulski 1991; Tyler 1984; Reichert and Youngs 1978; Vose 1977). Pinto bean, navy bean, field pea, and chickpea have average starch granule size of 19.0, 19.7, 20.6 μm (Gujska et al. 1994), and 14.9 μm (Han and Khan 1990a), respectively. Davydova and co-researchers' (1995) study indicated that the average starch granule size of five different varieties of smooth pea ranged between 23 to 30 μm. They used form factor as an index of how circular is a starch granule. A form factor of 1.0 shows that particle is an ideal circle; a form factor lower than 1.0 confirms that

starch granules have deviation from the ideal circle, e.g. oval, ellipse, rod. The form factor reported ranged from 0.75 to 0.77. Hoover and Sosulski (1991) found that the surface of chickpea starch granules was smooth without any evidence of fissuring. They reported that chickpea starch granules had oval and spherical shapes and their size ranged from 8 to 54 μm. Another study also indicated that, starch granules of pea were round to elliptical with smooth surface (Ratnayake et al. 2001). Reichert and Youngs (1978) reported an uneven pea starch granule surface which included protein bodies and agglomerates. There is lack of information on the size of chickpea protein and density of chickpea protein and lipid.

2.2.2.3 Starch-protein interactive force

There is lack of information on interactive force between starch granules and protein particles of plant materials. Scanning electron micrograph of chickpea flour has revealed that protein particles are on the surface of starch granule surrounding it. It is important to investigate if there is any significant chemical interactive force between starch granules and protein particles in the chickpea flour. If there is any, application of chemical treatment will be required. If there is no chemical interactive force, starch and protein particles can be separated by applying physical forces such as gravitational and centrifugal separation.

Isothermal titration calorimeter (ITC) is an apparatus that monitors the thermodynamic reactions which occur by adding a binding component to another component. ITC techniques have been used in medicine and biology to evaluate interaction between, protein-DNA, antibody-antigen, hormone-receptor, and many others. It has been designed to study biopolymer-ligand (an ion, a molecule, receptor, antibody or a molecular group that binds to another chemical component to form a larger complex) interactions.

Binding substrate results in either generation, called exothermic reaction, or absorption, called endothermic reaction, of heat energy. ITC is able to measure this energy leading to calculation of the following values:

- binding constants (K_B);
- enthalpy (ΔH);
- entropy (ΔS); and
- stoichiometry of the reaction (n).

Therefore, the thermodynamic profile of a molecular interaction can be derived. Widespread application of ITC has been intended to analyze protein interactions with other components such as another protein, peptide, metal, or nucleic acid. There are different studies on the protein-protein interactions using ITC in the medical field; however, there is lack of study on the protein-starch interactions in biomaterials.

An ITC comprises of two identical cells of high thermal conductivity and surrounded by an adiabatic jacket (Figure 2.2). One cell, called the reference cell, contains buffer, solvent or any material, which is used as solvent in the other cell, except biopolymers. The other cell, called sample cell, contains biopolymer solution. Using a syringe as a burette at constant temperature, a ligand solution is titrated into the sample cell. In the sample cell, the ligand and biopolymer interact with each other and heat energy is released or absorbed depending on whether the molecular reaction is exothermic or endothermic. This energy is directly proportional to the amount of binding and represented as a heat pulse and shown as a peak. As the biopolymer in the reaction cell gets saturated, the recorded heat reduces until

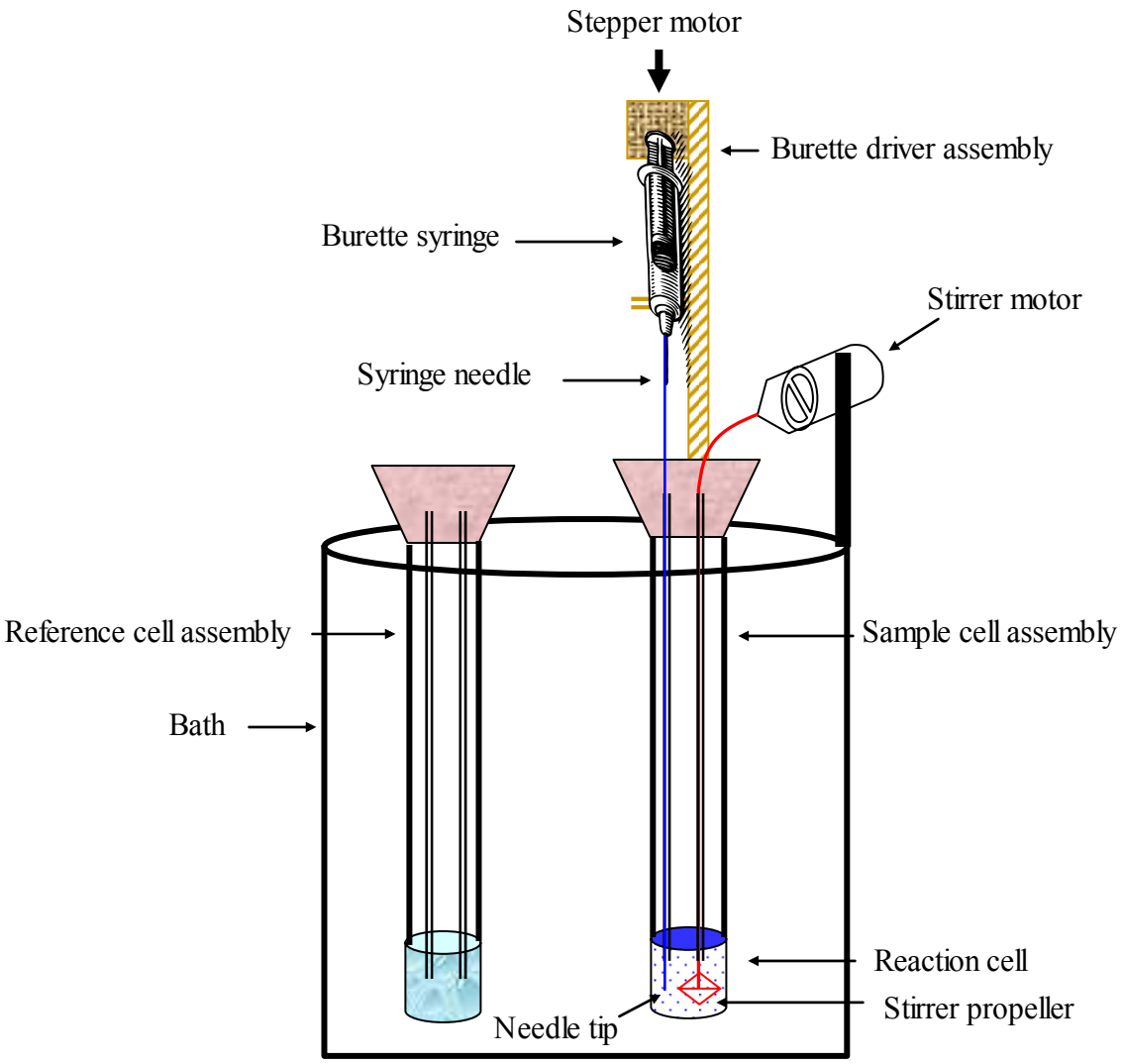

Figure 2.2 Schematic diagram of an isothermal titration calorimeter.

only the background heat of dilution called baseline is evidenced (MicroCal 2005; Pierce et al. 1999). There are four sources of heat during an interaction:

A. biopolymer-ligand interaction (that is of interest);

B. dilution of ligand on injection to the sample;

C. dilution of biopolymer by adding ligand; and

D. mechanical mixing.

The heat of interaction between biopolymer and ligand, which is of interest, can be determined by the following equation:

$$A = (1) + (4) – (2) – (3) \quad (2.1)$$

where numbers 1, 2, 3, and 4 refer to heat effect of each titration number in Table 2.4 (Cooper and Johnson 1994).

Table 2.4 Requirement measurements of heat effect (Cooper and Johnson 1994).

Titration number	Titration	Heat effect
1	Biopolymer-ligand	A + B + C + D
2	Biopolymer-buffer	C + D
3	Buffer-ligand	B + D
4	Buffer-buffer	D

2.2.2.4 Nitrogen solubility index

Nitrogen solubility index (NSI) is used as an index to show the pH in which chickpea flour protein has the highest and lowest solubility. The NSI plot presents nitrogen solubility profile of chickpea flour. Han and Khan (1990b) measured the NSI of air-classified legumes in the pH range between 2 to 10. They reported that the lowest and highest NSI for all fractions were at pH 4.0 and 10.0, respectively. Their study showed that starch-rich fraction had higher NSI than protein-rich fractions. They claimed that this phenomenon was due to the lower protein content of starch-rich fraction compared to protein-rich fractions.

2.3 Starch-protein separation from pulse grains

Legumes, such as chickpea are consumed as a whole seed. They can be used as raw material for producing such products as starch and protein fractions by dry or wet processing. Separation of starch and protein increases their use and economic value. There are two kinds of separation techniques: dry and wet processing. Under wet processing technique, the different methods will be discussed. The protein and starch fractions of legumes can be used as ingredients in food processing (Tian et al. 1999) including human food, pet food, animal feed, as well as in non-food products (Sánchez-Vioque et al. 1999). Starch is especially utilized in some industries for binding, sizing, dyeing, filling, etc. Some important industries using starch are: food industry, animal feed industry, hygiene industry, pharmaceutical industry, paper industry, cosmetic industry, and textile industry (International Starch Institute 2003).

2.3.1 Dry processing technique

Dry processing includes fine grinding of dehulled seed in a pin-mill followed by air classification to separate the protein-rich (light fraction) and starch-rich (heavy fraction) fractions. In air classification, opposing centrifugal force and density are employed to separate protein and starch granules as protein and starch concentrates from cereal and pulse grain flours. The air classification process separates more than 90% of the starch into the coarse fraction, but the separation of protein in the fine fraction depends on the kind of air classifier and the legume. The protein separated in the fine fraction ranges between 19.2% and 50.2%. Reichert and Youngs (1978) reported that the protein and starch of legumes cannot be separated completely by pin-mill and air classifier. The remaining protein in the

starch-rich fraction is mainly protein bodies, agglomerates, chloroplast membrane which surround the starch granules, remaining and water-soluble fractions.

Air classification of pea starch fraction can result in the removal of most of the protein bodies and agglomerates from pea flour (Ratnayake et al. 2002). Tyler and co-workers (1981) reported that the starch fraction from regrinding and reclassifying of eight legumes had 4.0 to 10.4% protein content. Whereas, the first and second protein fractions from the air classifier contained 0.0% to 4.6% and 0.4% to 16.6% starch, respectively. Similar results have been shown in cereals (e.g. wheat). In the case of cereals, the protein attached to the air-classified starch is called adherent protein. This kind of protein was reported by Reichert (1982), Tyler (1984), Sosulski and co-workers (1987), Han and Khan (1990a), and Swanson (1990). According to Swanson (1990), air classification of lipid-rich legumes does not result in high separation efficiency. Sosulski and co-workers (1987) reported that the high oil content of chickpea decreases the separation efficiency of air classification. The oil content of dehulled chickpea ranges between 4.5% and 7.5% (Chavan et al. 1986). This amount is unique among legumes. An average protein recovery of 35% was reported in the air classification of pin-milled chickpea flours, which is very low compared to other pulse grains. Sosulski and co-workers (1987) demonstrated that the C-E Bauer Centri-Sonic classifier (C-E Bauer, a subsidiary of Combustion Engineering, Inc., Springfield, OH) separated 50.2% of proteins into fine fraction and 92.0% of starch into the coarse fraction. They showed that this classifier was effective for air classification of pin-milled flour of chickpea. The relatively high fat content of chickpea flour will not result in high separation efficiency during air classification. Starch granules of legumes are associated with lipids, which are located on the surface and the inside. The surface lipids are

mainly triglycerides with some free fatty acids, glycolipids, and phospholipids. (Vasanthan and Hoover 1992).

The fine fraction of pin-milled flours contains much of the lipid, the ash and, to a lesser amount, the crude fibre along with the proteins (Sosulski et al. 1987). Reichert (1982) found a negative correlation between protein content of dehulled pea on one hand and their starch, lipid, and cell wall material contents on the other hand. This study confirmed that there is a positive correlation between protein content of air-classified fractions and protein content of dehulled pea. Sosulski and Zadernowski (1980) reported that defatting (oil extraction) of rapeseed followed by desolventization, pin-milling, and air classification increased the protein level by 6% and decreased the fibre content in the range of 7 to 10% in protein-rich fraction.

2.3.2 Wet processing technique

Wet processing is used to prepare more highly purified protein and starch. Protein concentrate and protein isolate (high protein concentration) from pulse grains are prepared by wet processing (Owusu-Ansah and Mc Curdy 1991). Protein concentrate obtaining from soybean has at least 65% protein (Pokatong 1994). Protein isolate obtaining from soybean contains 90% d.b. protein. Starch isolate resulting from processing of corn has 98-100% d.b. Wet processing involves dispersing the protein followed by precipitation at isoelectric pH to recover proteins (Tabil et al. 1995; Owusu-Ansah and Mc Curdy 1991; Swanson 1990; Sumner et al. 1981). Other methods under this process include salting out, hydrophobic out, and ultrafiltration (Owusu-Ansah and Mc Curdy 1991).

2.3.2.1 Isoelectric precipitation method

The isoelectric precipitation method of protein isolate production includes dehulling and milling of pulse grains, followed by suspending the flour in an alkaline solution (pH 9-10, using 1.0 *N* NaOH) and centrifugation to remove insoluble components. The dispersed proteins are precipitated by acidification of the supernatant near the isoelectric point. The mean isoelectric points of pea globulins and albumins are pH 4.4 - 4.6 and 6.0, respectively (Swanson 1990). The isoelectric point, which is used for precipitating the major protein constituent, globulins, is pH 4.5. The flocculated and precipitated proteins are collected by centrifugation or filtration (Owusu-Ansah and Mc Curdy 1991; Swanson 1990). The precipitated protein can also be recovered using a hydrocyclone. The protein is dried resulting in isoelectric protein isolate. If neutralized and dried, it yields a cationic-protein isolate (Owusu-Ansah and Mc Curdy 1991).

A number of parameters, such as particle size of the flour, type of suspension agent, pH of solution, and precipitation, affect the yield of isoelectric protein isolate. The optimum particle size of the flour is between 100 to 150 μm in dispersed protein. Larger flour particle sizes result in higher percentage of protein remaining in the residue fraction, thus, causing lower protein yield (Owusu-Ansah and Mc Curdy 1991).

From the protein yield point of view, there is no difference between sodium hydroxide and potassium hydroxide as protein suspension agents. Owusu-Ansah and Mc Curdy (1991) reported that calcium hydroxide disperses less than 90% of pea protein, because of the salting-out effect caused by calcium ions. The salting-out effect by calcium ions is most probably due to its two positive charges. The phenomenon of salting-in or salting-out is done on the media containing protein. The solubility of proteins depends on

different parameters including salt concentration. At low salt concentration, ions resulting from salt stabilize charged group on the protein and improve solubility. This phenomenon is called salting-in. The ions react with protein charges and diminish the electrostatic attraction between opposite charge groups of neighboring molecules. Therefore, the solubility of proteins in water increases. However, increasing the salt concentration affects the polar charge of water; there will be a competition between proteins and salt ions for water molecules, necessary for their solubility. Therefore, at high salt concentration there are not enough water molecules to dissolve proteins. Therefore, protein starts precipitating. This phenomenon is named salting-out (Cheftel et al. 1985).

The majority of common acids, except sulfuric acid, can be used as dispersing agent. Sulfuric acid only disperses about 40% of the proteins compared to that of other acids, which may be caused by the precipitating effect of the sulfur ion (Owusu-Ansah and Mc Curdy 1991).

The nutritive value of protein is diminished if too strong an alkaline solution is used. This is due to racemization of amino acids and formation of lysinoalanine. Dispersing food protein for long time in strong alkaline solution, heat, or their combination, may cause reduction of protein solubility, amino acid cross-linking, degradation and formation of a complex with sugars (Tabil et al. 1995).

2.3.2.2 Ultrafiltration method

Ultrafiltration can be used in the recovery of extracted protein. The proteins are dispersed and fed under pump pressure to the membrane module. The membrane module numbers must be adequate to provide enough surface area for separation at the required rate. The

permeate is passed through the membranes and taken off. The protein-enriched retentate can then be spray-dried to produce an ultrafiltered protein isolate (Owusu-Ansah and Mc Curdy 1991). The recovery yield of ultrafiltration is similar to the isoelectric precipitation process. The main problem in the use of ultrafiltration is its low flow rate and the plugging of membranes (Owusu-Ansah and Mc Curdy 1991; Swanson 1990). Pea protein isolate produced by ultrafiltration was reported to have high level of lipids (6.1%) (Owusu-Ansah and Mc Curdy 1991).

2.3.2.3 Salting-out method

Salt solution with high ionic strength can be used for protein extraction. As such, the concentration of ammonium sulfate is increased to 35% of saturation level. This will cause the precipitation of some proteins along with nucleic acids, which is then separated by centrifugation. To obtain the remaining proteins in the solution, salt concentration is increased in the range of 65 to 100% of the saturation level of ammonium sulfate. The sequential fractional salting-out is a good way of separating the main and secondary proteins from each other (Owusu-Ansah and Mc Curdy 1991).

2.3.2.4 Application of wet processing

Wet processing techniques have been used in separation of protein, starch, and fibre fraction from pulse grains. Murray and co-workers (1979) used salting-out method to produce purified protein and starch fractions. Tian and co-researchers (1999) employed a combination of isoelectric precipitation and salting-out methods to produce protein isolate from field pea. Thompson (1977) applied isoelectric precipitation method on mungbean

flour with repeated increase and decrease of pH to produce isolated protein. Sumner and co-workers (1981) used the same technique with pH increased to pH 9.0 and decreased to pH 4.5 to obtain two purified fractions from field pea. Besides these methods, sieving during wet processing can be employed to purify starch granules. Like isoelectric precipitation, the protein is dispersed to appropriate pH. Then the slurry is either centrifuged or passed through a sieve. If sieving is used, starch granules and fibre are retained on the sieve; however, protein particles pass through as permeate. Starch granules, either collected from the sieve or centrifuge, still are contaminated with other fractions including fibre and cell wall material. To remove contaminations, starch is washed on the sieve several times. Since fibre fractions are larger than starch granules, they stay on the sieve and starch fraction passes through the sieve. Sieving was used by Lineback and Ke (1975), Anderson and Romo (1976), and Colonna and co-workers (1981) in the wet processing of pulse grains. Sosulski and Sosulski (1986) also used sieving in combination with isoelectric precipitation method to produce purified starch, protein, and fibre fractions.

2.3.3 Starch-protein separation using hydrocyclone

Hydrocyclone is used in different industries to separate two phases in a liquid medium. Examples of hydrocyclone applications include: liquid clarification, slurry thickening, solids washing, degassing of liquids, solids classification, or sorting based on density or particle shape. The advantages of hydrocyclone are as follows:

1. They are flexible in application. They can be employed in clarification, thickening, washing, degassing, sorting, or separation of two immiscible liquids (Svarovsky 1984).

2. They can be used by different degree of separation by changing loading conditions or geometric proportions (Cheremisinoff 1995).
3. They are simple in design and cheap in the installation, running, and maintenance (Cheremisinoff 1995; Svarovsky 1984).
4. They are small and occupy small space.
5. They provide high shear force which can break agglomerates (Svarovsky 1984).

2.3.3.1 Description of hydrocyclone

Hydrocyclone employs fluid pressure energy to generate rotational fluid motion (Bradley 1965). The cyclone and the centrifuge use very similar principle of separation. Compared to the centrifuge, the cyclone has no moving parts. The required vortex motion is caused by rotational fluid motion (Svarovsky 1990). The cyclone is applied in various fields of industry including gas cleaning, burning, spraying, atomizing, powder classification, etc. Those types of cyclone, which are used to separate solid and liquid are called liquid cyclone. When water is used as the fluid media, the liquid cyclone is referred to as hydraulic cyclone, hydrocyclone, or hydroclone. In a hydrocyclone, the suspension of particles in a liquid is injected tangentially into the inlet opening located in the upper part of the cyclone to produce rotational motion (Figures 2.3 and 2.4). The hydrocyclone inlet is either circular or rectangular is cross-section. The vessel at the part of entry usually has a cylindrical shape, which results in a strong swirling motion as the suspension liquid is injected. The tangential entry of suspension liquid results in a strong spinning motion within the cyclone (Svarovsky 1990; Bradley 1965). Consequently, particles of the suspended material undergo two opposing forces. The first force has an outward radial direction which is due to centrifugal

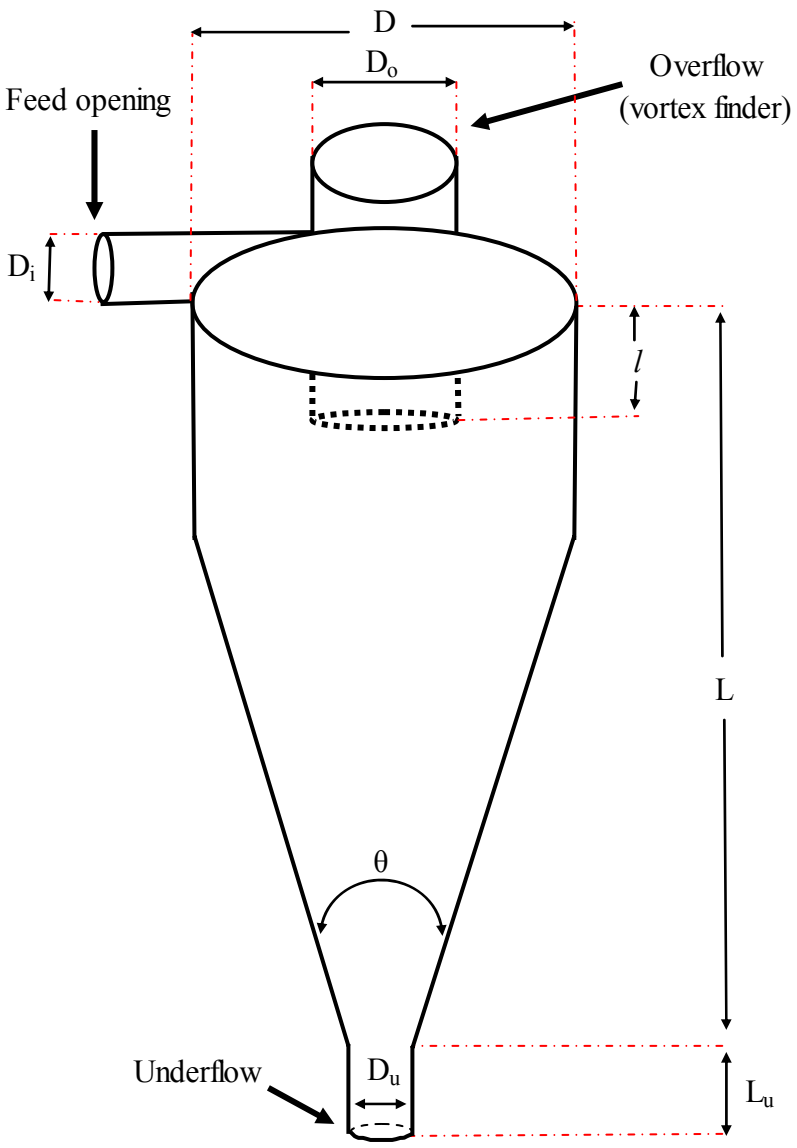

Figure 2.3 Schematic diagram of a hydrocyclone presetting important dimensions (Svarovsky 1984). D = inside diameter of hydrocyclone, D_i = inlet diameter, D_o = overflow diameter, D_u = underflow diameter, H_c = l = length of vortex finder, L = length of hydrocyclone, L_u = length of underflow, θ = angle of the apex cone.

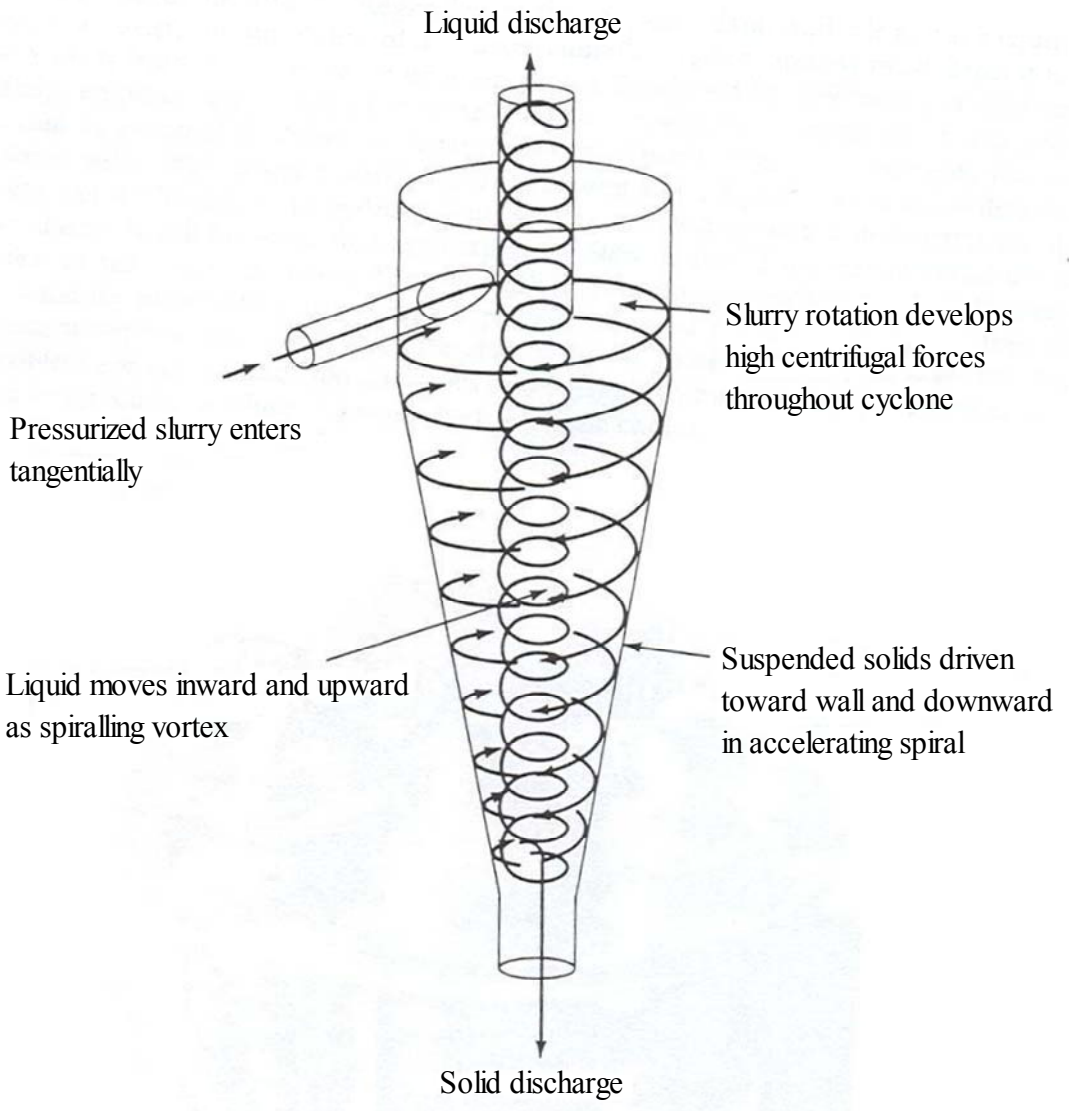

Figure 2.4 Schematic representation of the spiral flow in a hydrocyclone (Day et al. 1997). *This figure was reproduced with permission of The McGraw-Hill Companies.*

acceleration. The second one has an inward radial direction resulting from the drag force of the inward moving fluid (Svarovsky 1990; Bradley 1965). The centrifugal force is opposite of drag force. Both centrifugal and drag forces are depend on particle size; large particles are separated under influence of centrifugal force more readily (Svarovsky 1984). The magnitude of these forces depends on the physical properties of the fluid and the suspended

material such as the size, the shape, the density, and the porosity of the particle, as well as the viscosity and density of the fluid (Jones and McGinnis 1991; Svarovsky 1990; Bradley 1965). These properties are used to separate one material from the other or from the fluid (Svarovsky 1990; Svarovsky 1984; Bradley 1965). While the suspension undergoes swirling motion and moves downward, the solid particles in the suspension are derived outward radial direction by centrifugal force to inner wall of hydrocyclone (Day et al. 1997). The particles along a small portion of liquid are discharged on the periphery of the cylinder at the apex of the cone, called the underflow orifice. In the mean time, by approaching to the apex, the fluid reverses axial direction and spirals upward. Since the majority of particles, particularly large ones, have been discharged through the apex, the liquid along with the fine particles of the suspension liquid are released through the cylindrical tube located in the centre of the top (Day et al. 1997; Svarovsky 1990; Svarovsky 1984; Bradley 1965).

Separation in a hydrocyclone has been explained using different theories. The two most important theories are “equilibrium orbit theory” and “residence time theory”. Equilibrium orbit theory is based on the equilibrium radius. Particles at a given size reach a radial orbit position in the hydrocyclone, where their terminal settling velocity is identical to the radial velocity of the liquid. According to the balance of centrifugal and drag forces, the particles are elutriated by the inward flow and move to the overflow. Based on this theory, small particles reach equilibrium on small radius and move to the overflow; however, large particles are released to the hydrocyclone wall and move to the underflow. The residence time theory asserts that if a particle reaches the hydrocyclone wall within the residence time, it will move to the underflow. Therefore, the particle radial setting, time, and fluid velocity affect particle separation (Svarovsky 1990; Svarovsky 1984).

2.3.3.2 Hydrocyclone operation

Two important operating parameters in a hydrocyclone are the fluid pressure, which causes rotational motion (Bradley 1965) and flow resistance. As the flow resistance of hydrocyclone increases, the solid recovery improves and vice versa. This is valid for any parameter of the cyclone body within a certain reasonable limit, except cyclone length. For instance, decreasing the inlet and outlet opening increases the mass recovery (Svarovsky 1984). Cyclone performance is expressed in terms of efficiency, which is defined as the degree of separation of each particle from feed material to the underflow (Jones and McGinnis 1991). The efficiency of separation is affected by operating conditions; for instance, with increased pressure drop (pressure difference between inlet and overflow), the separation efficiency increases. The pressure drop ranges between 34 and 600 kPa. Smaller cyclones usually run at higher pressure drops than the larger ones (Svarovsky 1984). Moreover, the particle size distribution of the solids is an important parameter affecting separation efficiency (Jones and McGinnis 1991). As the concentration of the feed increases, the separation efficiency drops. Therefore, when high mass recovery is an objective, cyclone operation is performed with the dilute feeds. The concentration of solids in the underflow is less than 45% or 50% by volume, depending on the size and design of the cyclone, the operating conditions, and the solid being separated. The dimension of the underflow orifice is also very important. The orifice diameter is adjusted after the start-up of the hydrocyclone plant and during its operation when some other operating conditions are adjusted (Svarovsky 1984). The flow rate in hydrocyclone should be selected so that the maximum efficiency of the finest particles is achieved (Jones and McGinnis 1991). The diameter of the cyclone varies from 10 mm to 2.5 m and the flow rates between 0.1 and 7200 m^3/h (Svarovsky

1990). Another factor affecting the operation is the cut-size. Cut-size is the size in which the majority of finer particles go to the overflow and the larger particles fall in the underflow (Singh and Eckhoff 1995). The cut-size for most solids ranges between 2 and 250 μm (Svarovsky 1990). As mentioned earlier, fluid viscosity affects hydrocyclone performance. Increasing the viscosity, raises the flow rate at given pressure drop and increases the volume split. By increasing viscosity, the ratio of overflow to underflow reduces exponentially somehow and it reaches a constant value (Bradley 1965).

2.3.3.3 Design variation of hydrocyclones

Each cyclone is characterized by several dimensions shown in Figure 2.3; the size of a cyclone is normally given by its cylindrical section diameter (D) which is discussed later. The angle of the apex cone (θ) is an important factor in cyclone design. Increasing the angle of cone results in circulation fluid in the main body, which is suitable for classification and sorting. According to use and angle of cone, cyclones have been designed and grouped in the following:

1. conventional, narrow-angle cyclone;
2. wide-angle cyclone;
3. flat-bottom cyclone with central solids discharge;
4. cylindrical cyclone with peripheral solids discharge;
5. cyclone for liquid-liquid separation; and
6. cyclone for gas separation.

Based on the application of the cyclone, its shape differs with another one. The narrow-angle cyclone is the most conventional cyclone used in industries. This cyclone

comprises of a long body with four to seven times of the body diameter. The angle of cone is less than 25°. This kind of cyclone is used for recovering very small particles and employed in liquid classification and solid classification duties (Svarovsky 1984). This is more suitable for separation than wide-angle cyclone (Jones and McGinnis 1991). The wide-angle cyclone has an angle of cone greater than 25°. As the angle of cone increases, the recovery of particles decreases and selectivity with respect to particle shape improves. This kind of cyclone is employed in solid classification and sorting based on particle shape and density (Jones and McGinnis 1991; Svarovsky 1984). The flat-bottom cyclone has a 180° cone angle; in other words, it does not have a cone. All features of the flat-bottom cyclone make it suitable as preliminary stage in a two-stage process, also for classification based on particle size, for sorting based on particle shape, and for separation of heavy media. The fourth group of cyclones is the cylindrical cyclone. It is used in mineral processing for recovery of metal; it is used, as well as in coal cleaning and oil floatation from water. The liquid-liquid separation cyclone is another type of cyclone that has a different shape compared with conventional cyclones, e.g., presence of twin tangential inlets at the top with an angle of 180° from each other. It has been designed for two kinds of separation. It is used for separating light liquids at fairly low concentration from another, such as oil in water or brine. It is also used for separating of heavy liquids in concentrations up to 30% in another liquid, such as water in kerosene. The sixth group of cyclones is cyclone for gas separation. The low pressure in the cyclone core supplies a condition for degassing of liquids by hydrocyclones. It contains a wider overflow pipe and smaller cone angle and larger underflow orifice than most hydrocyclones. The most widespread application of this kind of cyclone is in degassing of crude oil on offshore oil platforms **(**Svarovsky 1984).

2.3.3.4 Centrifugal force

In a centrifugal separator, such as hydrocyclone, the centrifugal action supplies settling rates; twisting path provides enough time for particles to be separated. The centrifugal acceleration and centrifugal force applied to a particle in the centrifugal field are given by the Equations 2.2 and 2.3, respectively (Anon. 2005; McCabe et al. 2005; McCabe et al. 1993; Earle 1983; Alonso and Finn 1980; McCabe and Smith 1976):

$$a_c = \frac{v^2}{r} \tag{2.2}$$

$$F_c = \frac{mv^2}{r} \tag{2.3}$$

where: a_c = centrifugal acceleration (m^2/s);

v = tangential velocity of the particle (m/s);

r = radius of path of particle which is hydrocyclone inner radius (m);

F_c = centrifugal force (N); and

m = mass of the particle (kg).

Equation 2.3 confirms that centrifugal force increases with increase of mass and tangential velocity of particle and decrease of hydrocyclone radius. Therefore; a hydrocyclone having small diameter can collect smaller particles in the underflow and have higher efficiency than large-diameter hydrocyclone. The problem associated with small-diameter hydrocyclone is the capital cost for providing sufficient output and the pressure drop (Earle 1983).

The ratio of centrifugal force to gravitational force is conventionally called separation factor or *g*-force (× *g*) and is shown below as (Rushton et al. 1996; McCabe et al. 1993):

$$g\text{-force} = \frac{F_c}{F_g} \tag{2.4}$$

where: F_c = centrifugal force (N); and

F_g = force of gravity (N) which equals mg.

Value of F_c from Equation 2.3 and value of F_g are substitute in Equation 2.4:

$$g\text{-force} = \frac{mv^2 / r}{mg} = \frac{v^2}{rg} \tag{2.5}$$

Therefore, the centrifugal force of a particle in a hydrocyclone equals its *g*-force multiplied by particle's mass and acceleration due to gravity. The *g*-force value depends on tangential velocity of particle and hydrocyclone diameter; it ranges between 300 × *g* (in large-diameter hydrocyclone) and 50,000 × *g* (in small-diameter hydrocyclone) (Rushton et al. 1996).

2.3.3.5 Reynolds number

Fluid can flow through a pipe or channel at varying flow rates (low to high). The pressure drop in the fluid increases directly with fluid velocity when flow rate is low. However, it increases with almost square of fluid velocity at high flow rates. Osborn Reynolds, in 1874, distinguished between flow rates using a series of experiment. It was found that the change of flow from one type to other depends on the diameter of the pipe and the average linear velocity, viscosity, and density of the fluid. These variables were combined to reach a dimensionless value called Reynolds number (Equation 2.6).

$$\text{Re} = \frac{\rho_f \, \bar{v} \, d_i}{\mu} \tag{2.6}$$

where: Re = Reynolds number;

ρ_f = fluid density (kg/m^3);

$\bar{v}$ = average linear velocity of fluid (m/s);

d_i = diameter of pipe (m); and

μ = fluid viscosity (Pa s).

The magnitude of Reynolds number shows how a fluid would behave either in a pipe or on the surface of solid object. Fluid flow is laminar in the pipe at Reynolds number less than 2100 and turbulent at Reynolds number higher than 4000. Fluid flow at Reynolds number between 2100 and 4000 is called transition region, where the fluid shows either laminar or turbulent behaviour, depending on entrance conditions of the pipe (Singh and Heldman 2001; McCabe et al. 1993; McCabe and Smith 1976). When the dynamic behaviour of a particle in a fluid is studied, Reynolds number of particle is required. Reynolds number of particle affects drag coefficient and is calculated using the following equation (Rushton et al. 1996; Svarovsky 1984):

$$\mathrm{Re}_p = \frac{\rho_f \, u \, d_p}{\mu} \tag{2.7}$$

where: Re_p = Reynolds number of particle;

ρ_f = fluid density (kg/m^3);

u = relative velocity between the fluid and particle (m/s);

d_p = particle diameter (m); and

μ = fluid viscosity (Pa s).

The particle is in the Stokes' law range at Reynolds number of less than 2. The intermediate range happens when Reynolds number of particle is between 2 and 500. The particle is in the Newton's law range if Reynolds number of particle lies between 500 and 200,000 (McCabe and Smith 1976). Since the relative velocity between the fluid and particle

diameter are low in hydrocyclones, Reynolds number of particle is low and most of the times the Stokes' law range is applicable (Svarovsky 1984).

2.3.3.6 Drag force

Drag force is the summation of aerodynamic or hydrodynamic forces applied by the fluid on the solid whenever a solid object moves through a fluid and a relative motion between the solid and the fluid exists. Drag force is in the direction of the external fluid flow and opposes the motion of the solid (McCabe et al. 2005; McCabe et al. 1993). The drag force is conventionally calculated by (Statie et al. 2002; Rushton et al. 1996; McCabe et al. 1993; Mohsenin 1986; Svarovsky 1984; McCabe and Smith 1976):

$$F_D = \frac{1}{2} C_D \rho_f A_p u^2 \tag{2.8}$$

where: F_D = drag force (N);

C_D = dimensionless drag coefficient;

ρ_f = fluid density (kg/m^3);

A_p = projected area of the particle (m^2); and

u = relative velocity between the fluid and particle (m/s).

When a particle moves outward radially in a centrifugal field, it accelerates to reach its terminal velocity immediately. Hence, the relative velocity of particles will be equal to its terminal velocity which is used for calculation of drag force (Rushton et al. 1996; Svarovsky 1984; McCabe and Smith 1976). In the hydrocyclone, coarse particles move fast and the drag force is mostly caused by inertia of the fluid; therefore, the drag coefficient is constant. However, fine particles move more slowly; the drag coefficient depends on the Reynolds number of particle. The drag coefficient is inversely proportional to Reynolds number of

particle (Svarovsky 1984). Studies have conducted to express the relationship between drag coefficient and Reynolds number of particle (McCabe et al. 2005). For example, using Reynolds number of particle, the drag coefficient and relative velocity of spherical particle can be calculated using the following set of equations (McCabe et al. 1993; McCabe and Smith 1976):

when $\mathrm{Re}_p < 2$, which is Stokes' law range:

$$C_D = \frac{24}{\mathrm{Re}_p} \tag{2.9}$$

$$u = \frac{a_c d_p^2 (\rho_p - \rho_f)}{18\mu} \tag{2.10}$$

when $2 < \mathrm{Re}_p < 500$:

$$C_D = \frac{18.5}{\mathrm{Re}_p^{0.6}} \tag{2.11}$$

$$u = \frac{0.153\ a_c^{0.71} d_p^{1.14} (\rho_p - \rho_f)^{0.71}}{\rho_f^{0.29} \mu^{0.43}} \tag{2.12}$$

when $500 < \mathrm{Re}_p < 200{,}000$:

$$C_D = 0.44 \tag{2.13}$$

$$u = 1.75 \sqrt{\frac{a_c d_p (\rho_p - \rho_f)}{\rho_f}} \tag{2.14}$$

where: a_c = centrifugal acceleration (m/s^2);

d_p = particle diameter (m);

ρ_p = particle density (kg/m^3);

ρ_f = fluid density (kg/m^3); and

μ = fluid viscosity (Pa s).

2.3.3.7 Application of hydrocyclone in processing biomaterials

Ridlehuber and Gardner (1974) and Gardner and co-workers (1976) investigated the differential settling of slurry containing ruptured cottonseed meats and hexane in a glassy cylinder. The hulls and coarse meal particles settled rapidly on the bottom of the cylinder followed by whole pigment glands. Although the very fine meal particles had a higher specific gravity than the pigment glands, they settled slowly on the top of the pigment glands. This phenomenon is due to the large surface area per unit weight of the particles. Thus, fine particles resist settling and have slow settling rate. Wan and co-workers (1979) used the hydrocyclone process to separate gland pigment from cottonseed. Ridlehuber and Gardner (1974) and Gardner and co-workers (1976) explained the utilization of settling rate information in the hydrocyclone process. Dry milling (in pin-mill) or solvent milling (in stone mill) of hull-free seeds was suggested as a first step. In the case of pin-milling, the fine flour was slurried in hexane (as solvent and fluid) with a concentration of 20-22% solids. The slurry was pumped into the cyclone under a gage pressure of 270 kPa. The cyclone resulted in two fractions, namely, the overflow fraction containing protein and miscella, and the underflow fraction containing the pigment glands and the coarse meal. Therefore, the difference in the relative size of the pigment glands on the one hand, and protein and miscella on the other, makes it possible to separate them. It is notable that turbulence in the underflow should be avoided. It leads to the disruption of the classification order and to the appearance of pigment glands in the overflow. Turbulence in the underflow is avoided by controlling the solids content of the feed slurry.

Singh and Eckhoff (1995) used a 10-mm hydrocyclone to separate starch and protein from wet milled corn. The dehulled corn was milled then slurried in water to attain a specific gravity range between 1.0069 and 1.0140. An inlet gage pressure ranging between 896 and 965 kPa was used. Controlling inlet pressure is critical in the separation of starch and protein using the hydrocyclone. Increasing the pressure to greater than 965 kPa, leads to the appearance of large protein particles in the starch fraction (underflow). Furthermore, smaller feed diameter increases the separation efficiency and lowers the cut-size significantly. Thus, in order to increase the cut-size, the differential pressure should be lowered. Reducing the pressure to less than 896 kPa, causes smaller sized starch to be thrown into the protein fraction (overflow). Singh and Eckhoff (1995) demonstrated that the hydrocyclone reduced the starch and protein separation time by 75%, needed smaller area for operation, and reduced the risk of operation error. Sosulski and Zadernowski (1980, 1981) used hydrocyclone to fractionate rapeseed meal into flour and hull components. This technique could be applied to expeller (prepress) meal or to the marc after solvent extraction. Non-aqueous solvents can be used including: a) hydrocarbon liquids such as pentene, hexane, octane, decane or highly refined petroleum fractions; b) alcohols such as methanol, ethanol, isopropyl alcohol, butanol; c) benzene; d) liquid ethers as diethyl ether; e) chlorinated hydrocarbon liquids such as chloroform, methylene chloride trichlorotrifluoroethane, carbon tetrachloride, and mixtures of these.

The solvent should not dissolve the protein. The decanter centrifuge works particularly well with isopropyl alcohol and hexane solvents. Hexane can effectively reduce residual oil in the products (Sosulski and Zadernowski 1981; Sosulski and Zadernowski 1980). Solvent types distilled in narrower temperature range, such as hexane-type naphthas

(boiling range between 63 and 69ºC), are preferred in oil extraction. This class of solvent makes the management of evaporation and the solvent recovery easier. Therefore, the residual solvent in the oil and meal is reduced (Johnson 1997). The presence of 1% wt. or more of water in the solvent leads to the absorption of water by meal fractions and to the swelling of particles. Thus, the sedimentation pattern of particles is distorted. Therefore, a solvent with less than 0.5% wt. water is desired (Jones and McGinnis 1991; Sosulski and Zadernowski 1980).

According to Sosulski and Zadernowski (1980, 1981) the separation of hull and protein from rapeseed could be done by milling (dry milling) meal to obtain finely ground particles (less than 103 μm) followed by suspending the resulting meal in non-aqueous solvent which do not dissolve the protein. The solid content should be between 5% and 33% w/w preferably from 16% to 22%. The meal suspension with a moisture content below 10% is subjected to centrifugal or gravity liquid separation to separate oil fraction as miscella. The remaining materials from the centrifuge are passed through the hydrocyclone resulting in the flour slurry as overflow and the hull slurry as underflow. Then, the solvent is separated from flour and hull and recycled.

Jones and McGinnis (1991) developed a method to separate oilseed components using hydrocyclone. The seed with a moisture content of less than 8% (d.b.) was slurried in a non-aqueous solvent, which dissolved the oil but not the protein. The solid content ranged between 5% to 15% w/v. The seed was crushed in the slurry by feeding it to an enclosed flow-through macerator which crushed the seed to small particles and reduced the particle size to less than 420 μm. Then, the slurry was passed through at least two stages of hydrocyclone separators. The first cyclone stage resulted in overflow and underflow

fractions. The overflow had high concentration of oil miscella and protein-rich fraction, while the underflow contained protein-rich and fibre-rich seed coat meal. The components of each flow were fractionated using the second cyclone stage. The underflow of the first cyclone stage was passed through the second cyclone stage, which resulted in protein-rich fraction as overflow and fibre-rich fraction as underflow. Similarly, the overflow of the first cyclone stage was passed through the second cyclone stage, which resulted in protein-rich fraction as underflow and oil-rich fraction as overflow. Finally the oil and the protein and fibre-rich fractions were recovered using distillation and centrifuge separation, respectively. Jones and McGinnis (1991) suggested a cyclone with a diameter range between 3 and 10 cm, and a flow rate of 150 to 750 mL/s to be used. Hexane was the solvent used in this process.

2.4 Physical and functional properties of pulse grains and fractions

All biomaterials and their fractions are subjected to different physical treatments such as mechanical and thermal treatments. These treatments happen from production to the consumer. Physical properties have very important role in solving problems associated with design of specific machine, analysis of the product behaviour, as well as prediction of materials' behaviour during different unit operations in handling and processing of the product (Mohsenin 1986).

Functionality is a group of properties of raw materials and food products in food processing. In many application fields, functional properties are placed in very important characteristics and they have been classified as those physical and chemical properties that

influence the behaviour of raw materials and final product during storage, processing, and consumption (deMan 1990).

2.4.1 Thermal properties

Thermal properties including thermal conductivity, specific heat, and thermal diffusivity of foodstuffs are necessary in the design, calculations, modeling, and optimization of food processing operations involving heat transfer such as freezing, thawing, cooking, drying, pasteurization, and sterilization (Drouzas et al. 1991; Drouzas and Saravacos 1988; Nesvadba 1982). This information can also be used in study of packaging and shelf-life of the product. Thermal properties of some food materials are available in the literature; however, those of processed materials with different compositions and porosities in a non-homogenous structure are more difficult to predict or find in the literature and need to be measured using experimental methods (Drouzas et al. 1991). Thermal properties of biomaterials are influenced by different parameters. For example, thermal properties of starch can be affected by its crystalline structure (Kerr et al. 2000).

2.4.1.1 Thermal conductivity

During storage of food granules, such as starch, microbial growth or exothermic reactions, such as oxidation and crystallization, cause some localized heat generation. To cool down the food powder, knowledge of thermal conductivity is required (Krokida et al. 2001). Food materials contain different substances in various states, e.g. particles of food powders along with air spaces among particles. Therefore, the heat is transferred through the foodstuffs not only by conduction but also by convection. Inside solid foods, it is often

assumed that heat transfer is through conduction only and the measured thermal conductivity is referred as effective thermal conductivity. Thermal conductivity is affected by the moisture content and temperature, like specific heat, as well as by the bulk density. Studies on starch granules and cumin seeds have shown that as moisture content and temperature increase, thermal conductivity increases (Singh and Goswami 2000; Drouzas et al. 1991). Drouzas and Saravacos (1988) showed that thermal conductivity increased linearly with bulk density. Increasing the temperature resulted in an increase of thermal conductivity; this effect was greater in moisture content of 6.5% and higher. Similar results were obtained by Fang and co-workers (2000) on granular rice starch and Lan and co-researchers (2000) on tapioca starch. In biomaterials, the effect of bulk density and moisture content on thermal conductivity is greater than temperature (Mohsenin 1980).

Empirical relationships have been obtained to estimate the thermal conductivity of food products by Rahman (1995). Additionally, theoretical models, such as series, parallel, random, Maxwell, Maxwell-Eucken, and Kopelman models, have been mentioned in literature. In food materials that are complex systems, application of theoretical models is difficult since they assume that the system contains a structural arrangement. However, a food system, in most cases, is devoid of a structural arrangement (Krokida et al. 2001; Saravacos and Maroulis 2001). Thus, thermal conductivity measurement of food products having different components and structural arrangements is important and required.

Thermal conductivity measurements techniques are grouped in three categories: 1) steady state techniques; 2) quasi-steady state techniques; and 3) transient techniques (Rahman 1995; Nesvadba 1982; Mohsenin 1980). There are several experimental techniques under each category. The steady state techniques include guarded hot plate, concentric

cylinder, and heat-flux methods. The quasi-steady state techniques comprise the Fitch, Cenco-Fitch, Zuritz et al.-Fitch, and Rahman-Fitch techniques, as well as temperature profile of a heated slab method. The line heat source method, a transient technique, is the most widely used for food materials (Rahman 1995) because it is simple, quick, accurate, low cost, and usable for any geometry of a sample (Rahman 1995; Wang and Hayakawa 1993). This method has been used for measuring thermal conductivity of corn starch granules (Drouzas et al. 1991), barley, lentil, and pea (Alagusundaram et al. 1991), cumin seed (Singh and Goswami 2000), apple, banana, carrot, cheese, chicken breast, and beef muscle (Fontana et. al. 2001), and borage seed (Yang et al. 2002). The use of line heat source method started when Van der Held and Van Drunen (1949) developed a probe using a high thermal conductivity cylinder. Inside the cylinder is a heater wire throughout its length and a thermocouple in the middle of its length (Mohsenin 1980). The remaining space in the probe tube is filled with high thermal conductivity paste. The probe is inserted into a sample having a uniform temperature and heated at a constant rate. The temperature adjoining the line heat source is measured using the thermocouple. After a brief period, the slope resulting from the plot of the natural logarithm of time versus temperature is determined. The slope equals $q'/(4\pi k)$ (Sweat 1995), where q' is heat generated in the heating wire I^2R. This method is based on the following assumptions:

1. the line heat source has no mass and volume;
2. the line heat source is placed in an infinite conduction heating and homogenous medium which has uniform initial distribution;
3. the line heat source is placed in a medium with constant thermoplastic properties during measurement;

4. the thermal conductivity of the probe extremely is high;
5. the rate of heat generation throughout the probe body is constant; and
6. only radial temperature gradient exits (Fontana et al. 2001; Rahman 1995; Wang and Hayakawa 1993; Mohsenin 1980).

The heat flow from the probe in an infinite sample is given by the Fourier equation (Fontana et al. 2001; Singh and Goswami 2000):

$$\frac{\partial \theta}{\partial t} = \alpha \left[\frac{\partial^2 \theta}{\partial r^2} + \frac{1}{r} \frac{\partial \theta}{\partial r} \right] \tag{2.15}$$

This equation has been solved by several researchers including Hooper and Lepper (1950) and Nix and co-workers (1967); they discussed the basic theory behind the use of line heat source. The solution of Equation 2.15 is as follows (Iwabuchi et al. 1999; Mohsenin 1980):

$$k = \frac{I^2 R}{4\pi (T_2 - T_1)} \ln \frac{t_2}{t_1} \tag{2.16}$$

where: k = thermal conductivity of the sample infinite in size surrounding the heat source ($W\ m^{-1}\ °C^{-1}$)

I = current (A);

R = specific resistance of the heating wire (Ω/m);

T = temperature (°C);

t = time (s); and

subscripts *1* and *2* are the first and last related values in each sequence of data.

Heating of the sample starts at constant rate along the line heat source; the temperature and time are recorded. Thermal conductivity value is calculated using the maximum slope method. The slope of the straight line graph of temperature differences versus ln t is calculated (Wang and Hayakawa 1993):

$$S = \frac{T_2 - T_1}{\ln \frac{t_2}{t_1}} \tag{2.17}$$

where S is the slope. Substitution of S value from Equation 2.17 in Equation 2.16 gives the thermal conductivity as shown in Equation 2.18:

$$k = \frac{I^2 R}{4\pi S} \tag{2.18}$$

The same calculation method was used to determine thermal conductivity of barley, lentil, pea (Alagusundaram et al. 1991), tapioca starch (Lan et al. 2000), and timothy hay (Opoku et al. 2006). In the line heat source method, the probe diameter should meet the following equation (Rahman 1995):

$$D_p < \frac{4}{5}\left(\frac{\alpha t}{2}\right)^{0.5} \tag{2.19}$$

where: D_p = probe diameter (m);

α = thermal diffusivity (m^2/s); and

t = time (s).

Additionally, the ratio of the probe length to diameter should be higher than 25 (Sweat 1995). Since it has been assumed that the sample size is finite, any fluctuations in sample boundaries can make an error during thermal conductivity measurement. To avoid the effect of edge, the following condition should be met (Rahman 1995):

$$D_{sa} < 5.2(\alpha t)^{0.5} \tag{2.20}$$

where: D_{sa} = sample diameter (m);

α = thermal diffusivity (m^2/s); and

t = time (s).

2.4.1.2 Specific heat

Specific heat of agricultural material can be measured or predicted using: 1) method of indirect mixtures; 2) determination of foodstuffs composition followed by applying prediction equation calculating the specific heat; or 3) differential scanning calorimetry (DSC) (Singh and Goswami 2000; Nesvadba 1982). Being a direct technique, the method of mixtures is not as accurate as the DSC (Singh and Goswami 2000) and using of prediction equation gives an approximate value. The DSC has been utilized to investigate thermodynamic properties of legume flours or their fractions (Ratnayake et al. 2001; Kerr et al. 2000; Davydova et al. 1995; Zeleznak and Hoseney 1987; Sosulski et al. 1985; Colonna et al. 1982). Drouzas and co-workers (1991) measured thermal properties including specific heat of corn starch granules using the DSC. They reported that the value ranged from 1.230 to 1.850 kJ kg^{-1} $°C^{-1}$ in the moisture content range from 0% to 30%. Moreover, they mentioned that there was no difference between high-amylose and high-amylopectin starches. However, specific heat is affected by moisture content and temperature and increases almost linearly with increasing moisture content (Lan et al. 2000; Singh and Goswami 2000; Drouzas et al. 1991). Studies on cereal grains have shown that their specific heat has a linear relationship with moisture content and a quadratic relationship with temperature in moisture content and temperature range from 0 to 54% (d.b.) and 10 to 70°C, respectively (Murata et al. 1987). However, Singh and Goswami (2000) reported that the specific heat of cumin seed increased as moisture content increased but not linearly.

Generally, DSC is a technique employed to evaluate behaviour of polymer when it is heated under programmed condition. This technique is a thermal analysis which monitors conformation transitions and phase transitions as a function of temperature (Kaletunc and

Breslauer 2003). In DSC, the reference pan and sample pan are heated at an equal and programmed rate stated as °C/min. Since sample pan contains extra material, it requires more heat to keep its temperature equal to the reference pan which is empty. Such extra heat flow is measured by the DSC and shown as thermogram. The heat flow and heating rate are shown as the following equations:

$$\text{Heat flow} = \frac{\Delta q}{t} \tag{2.21}$$

$$\text{Heating rate} = \frac{\Delta T}{t} \tag{2.22}$$

where: q = heat (J);

t = time (s); and

ΔT = temperature change (°C).

As Equation 2.23 shows dividing heat flow by the heating rate results in heat capacity:

$$\frac{\Delta q / t}{\Delta T / t} = \frac{\Delta q}{\Delta T} = H_c \tag{2.23}$$

where H_c is heat capacity and its unit is J/°C. (Differential Scanning Calorimetry 1997; Widmann and Reissen 1987; Mohsenin 1980). Therefore, the specific heat is obtained using Equation 2.24:

$$c_p = \frac{H_c}{m} \tag{2.24}$$

where: c_p = specific heat (J kg^{-1} °C^{-1}); and

m = mass of sample (kg).

2.4.1.3 Phase transition and glass transition temperature

During heating of a sample, for example from room temperature to its decomposition, some positive and negative heat flow peaks are monitored in the thermogram. The peaks associated with heat absorption and heat release are called the endotherm and exotherm, respectively. For instance, Colonna and co-researchers (1982) reported that wrinkled pea starch has a single endotherm between 117 and 133°C with energy associated with transition, ΔH of 0.7 cal/g dry starch. Endothermic peak includes melting, denaturation, or gelatinization of polymers such as starch. However, exothermic peak is associated with crystallization of starch and aggregation of denatured proteins. Sosulski and co-workers (1985) employed DSC to determine gelatinization temperature of starch, peak denaturation/aggregation temperature of protein, enthalpy associated with the gelatinization of starch, and enthalpy of denaturation/aggregation of protein.

In the presence of crystalline and amorphous structure, a transition phase is recorded before exothermic and endothermic called glass transition. The glass transition is associated with amorphous materials or crystalline materials with amorphous regions (Kaletunc and Breslauer 2003). The glass transition temperature (T_g) can be extracted from DSC. T_g is the temperature in which amorphous materials are modified from a glassy form to a flexible form. The glass transition is not a true phase transition; however, in the DSC thermogram, the T_g is monitored as a sharp decrease in the heat capacity on cooling and abrupt increase in heat capacity on heating. In other words, polymers show a higher heat capacity above the T_g than below it. Since this change does not occur suddenly, the middle of tilted line is recognized as T_g. Below T_g, the motions of the molecular structure are delayed. Because the mechanical behaviour of polymers changes at T_g, it is an important character for all

polymers. For instance, crystallization takes place above the T_g, which is in the flexible stage of DSC thermogram (Kaletunc and Breslauer 2003). Studies show that as the degree of crystallinity rises, T_g increases, or as the amorphous region increases T_g decreases. The T_g of starch depends highly on moisture content. The T_g of wheat starch is detectable only in narrow moisture content range. As moisture content increases, T_g decreases (Zeleznak and Hoseney 1987). Ratnayake and co-workers (2001) also used DSC to investigate T_g and corresponding enthalpy of different cultivars of field pea. The T_g of starch ranges between –6 and 2°C (Rahman 1995).

2.4.1.4 Thermal diffusivity

Thermal diffusivity is another thermal property which is used to determine rate of heat transfer in solid foods. It is an index showing the tendency of material to conduct heat rather than store heat. Thermal diffusivity can be measured by different techniques including transient heating technique, a line heat source thermal conductivity probe with an auxiliary thermocouple, transient heating computer technique, and experimental measurement of thermal conductivity, specific heat, and bulk density (Sweat 1995). The transient heating technique needs large sample; the technique using the line heat source thermal conductivity probe, called direct method (Drouzas et al. 1991), is limited in usage because of the high sensitivity of results to the distance between probes. The transient heating computer technique requires powerful computer analytical techniques and boundary temperatures and distances should be precisely measured and controlled; however, it is a very good technique (Sweat 1995). The most often recommended technique which is called the indirect method (Drouzas et al. 1991) includes experimental measurement of thermal conductivity, specific

heat, and bulk density and then calculation of thermal diffusivity using the following equation (Sweat 1995):

$$\alpha = \frac{k}{\rho_b c_p} \tag{2.25}$$

where: α = thermal diffusivity (m^2/s);

k = thermal conductivity (W m^{-1} °C^{-1});

ρ_b = bulk density (kg/m^3); and

c_p = specific heat (J kg^{-1} °C^{-1}).

Drouzas and co-workers (1991) have shown that indirect method was more accurate than direct method in determination of thermal diffusivity of starch granules. Singh and Goswami (2000) showed that thermal diffusivity of cumin seed increased when temperature increased at a moisture content of 7.8% d.b.; however, it decreased at a moisture content of 11.1% and increased at 20.5% d.b.

2.4.2 Flowability and friction

Knowledge of frictional properties of biomaterials against one another and against equipment parts is very important in design of equipment for handling, production, and solid flow and in storage structure, as well as in processing operations such as storage in hoppers, formulation, mixing, compression, and packaging (Teunou et al. 1999; Puchalski and Brusewitz 1996; Mohsenin 1986). According to classical law of friction, the frictional force is directly proportional to the normal force; however, it does not depend on the sliding area. Studies have shown that, such a concept cannot be taken in practice as Mohsenin (1986) reported that friction force is a consequence of shearing and deformation severity, adhesion,

and cohesion (Puchalski and Brusewitz 1996). The following equation shows the classic relationship between the friction force and normal force:

$$F_f = \mu F_n \tag{2.26}$$

where: F_f = friction force (N);

μ = coefficient of friction which equals $tan\phi$; and

F_n = normal force (N).

Studies by Peleg and co-workers (1973), Chancellor (1994), Duffy and Puri (1996), and Puchalski and Brusewitz (1996) proved that Mohr-Coulomb equation was valid for agricultural materials:

$$\tau = C_c + tan\phi_i \ \sigma \tag{2.27}$$

where: τ = shear stress (Pa);

C_c = cohesion (Pa);

ϕ_i = angle of internal friction (degree); and

σ = normal stress (Pa).

The flow factor tester designed by Jenike (1967) can measure shear force versus displacement at a constant normal force. Such data are used to plot normal stress versus shear stress; the angle of plotted line with normal stress is defined as the angle of friction, and the tangent of corresponding angle is the coefficient of friction. If the shear force of sample upon itself is measured, the corresponding angle and its tangent will be the angle of internal friction and the coefficient of internal friction, respectively (Tabil and Sokhansanj 1997; Peleg 1977; Peleg et al. 1973). However, if the shear force of sample is measured upon an external surface, such as concrete and plastic, the corresponding angle and its tangent will be the angle of external friction and the coefficient of external friction,

respectively. The relationship between coefficient of friction and normal stress has been studied. The resultant studies showed that the coefficient of friction of biomaterials is independent of the applied normal pressure (Mohsenin 1986). The angle of external friction is affected by the material moisture content (Puchalski and Brusewitz 1996; Peleg 1977). As the moisture content increases, the angle of friction decreases. For instance, the angle of friction of corn starch decreased from 33° to 31°, when its moisture content increased from 0% to 18.5% (Peleg 1977). Duffy and Puri (1996) showed that as moisture content increased, the angle of internal friction of sugar and detergent powder decreased.

Another important extractable parameter from normal stress versus shear stress plot is cohesion/adhesion defined as the value of shear stress at zero normal stress. This value can be extrapolated from the plot. Cohesion is obtained from internal friction plot (Duffy and Puri 1996; Peleg et al. 1973) while adhesion is acquired from external friction plot (Puchalski and Brusewitz 1996; Chancellor 1994; Zhang and Kushwaha 1993). The intersection of the plot of shear stress versus normal stress (yield loci curve) with shear axis results in the cohesion/adhesion value (Peleg et al. 1973). Sample cohesion has an important role in mechanical properties of powder bed; it can diminish the flowability and stop flow by forming bridges between particles commonly known as agglomeration or caking (Peleg 1977). Cohesion is affected by the property of the powders and the pre-consolidation pressure (Peleg et al. 1973). In addition, the moisture content of a sample affects cohesion; for instance, Duffy and Puri (1996) demonstrated that as moisture content increased, cohesion of sugar and detergent increased. In food powder, such as flour, skim-milk, tea, and whey-permeate, an increase in moisture content resulted in decreased flowability and increased cohesion, which led to powder caking (Teunou et al. 1999). High normal stress

also affects adhesion; as the normal stress increases, the surface contact increases. This closing contact causes an increase in cohesion (Chancellor 1994).

2.4.3 Compressibility of powdered materials

An inherent problem with food powders is agglomeration and compaction during storage, which is undesirable from the standpoint of handling. Bulk density of powder materials considerably increases during transportation, handling, and storage. This increase is caused by vibration and tapping during transportation and handling or by normal load during storage (Kaletunc and Breslauer 2003). The behaviour of food powders under compressive stress is important during formulation and processing. The compression of fine powder involves two stages. In the first stage, particles move and voids are filled with particles of the same size or smaller. In the second stage, the smaller voids are filled by some particles that have undergone elastic deformation, plastic deformation, and/or fragmentation (Kaletunc and Breslauer 2003). Different compression models have been proposed for food and non-food materials. Walker (1923) proposed a linear model for prediction of volume change of calcium carbonate and tetranitro-methylaniline as a function of applied pressure (Equation 2.28). This model was employed by Adapa and co-workers (2002) and Shaw and co-researchers (2005) to determine the compressibility of biomaterials.

$$\frac{V}{V_0} = a \ \ln P + b \tag{2.28}$$

where: V = volume of compacted sample at pressure P;

V_0 = volume of sample at zero pressure;

P = compressive pressure; and

a, b = constants of the model.

The constant *a* is compressibility.

Jones (1960) suggested a linear model expressing the relationship between bulk density change and the pressure applied to the sample. This model was used by Peleg and co-workers (1973), Moreyra and Peleg (1981), Scoville and Peleg (1981), Tabil and Sokhansanj (1997), Adapa and co-researchers (2002), and Shaw and co-workers (2005) in determining compressibility of powdered material:

$$\ln \rho_b = a \ \ln P + b \tag{2.29}$$

where: ρ_b = bulk density;

P = compressive pressure; and

a, b = constants of the model.

The constant *a* is compressibility.

A similar model was reported by Barbosa-Cánovas and co-workers (1987) and Kaletunc and Breslauer (2003) to show the relationship between normal stress and density:

$$\frac{\rho - \rho_0}{\rho_0} = a \log \sigma + b \tag{2.30}$$

where: ρ = bulk density in applied normal stress σ;

ρ_0 = initial bulk density;

σ = normal stress; and

a, b = constants of the model.

Constant *a* represents the compressibility of the powder.

Cooper and Eaton (1962) proposed the following model to describe the volume changes during compression of several ceramic powders. This model was used by Adapa

and co-workers (2002), Mani and co-workers (2004b), and Shaw and co-workers (2005) to determine the compressibility of biomaterials:

$$\frac{V_0 - V}{V_0 - V_s} = a_1 \exp\left(\frac{-k_1}{P}\right) + a_2 \exp\left(\frac{-k_2}{P}\right) \tag{2.31}$$

where: V_0 = volume of compacted sample at zero pressure;

V = volume of compacted sample at pressure P;

V_s = volume of void free solid material; and

a_1, a_2, k_1, k_2 = constants of the model.

The magnitude of constants of a_1 and a_2 shows the compression mechanism. If a_1 is greater than a_2, rearrangement of particles during compression is the major mechanism of compaction. On the other hand, if a_2 is greater than a_1, deformation of particles is the major mechanism of compaction (Shaw et al. 2005).

Kawakita and Lüdde (1971) proposed the following model (Equation 2.32) to express the volume change of metallic and medical powder under the compression. This model was also used by Mani and co-workers to (2004b) to predict yield strength of some biomass materials using 1/b.

$$\frac{P}{C} = \frac{1}{ab} + \frac{P}{a} \tag{2.32}$$

where: P = compressive pressure;

C = degree of volume reduction which equals $\frac{V_0 - V}{V_0}$; and

a, b = constants of the model.

2.4.4 Stress relaxation behaviour

Stress relaxation is the decay of stress with time when the material is deformed at a constant strain (Mohsenin 1986). The stress relaxation behaviour of powder materials is an important characteristic showing the solidity of powder during loading such as when the load is applied to powder materials during storage. It also shows what portion of the applied initial stress is relaxed after a specific period of time. Peleg and Moreyra (1979) and Peleg (1979) presented a method for normalizing the force-relaxation curves of compacted powder:

$$\frac{F_0\ t}{F_0 - F_{(t)}} = k_1 + k_2\ t \tag{2.33}$$

where: F_0 = initial force (N);

$F_{(t)}$ = decaying force after time t (N);

t = time (s); and

k_1, k_2 = empirical constants.

Using k_2 value, Moreyra and Peleg (1981) and Scoville and Peleg (1981), calculated the asymptotic modulus. Asymptotic modulus of a compact is an empirical index showing solidity and ability of compressed powder to sustain unrelaxed stresses. The asymptotic modulus is given as follows:

$$E_A = \frac{F_0}{A\varepsilon}\left(1 - \frac{1}{k_2}\right) \tag{2.34}$$

where: E_A = asymptotic modulus (Pa);

A = cell cross sectional area (m^2); and

ε = strain.

This equation was used by Tabil and Sokhansanj (1997) and Shaw and co-workers (2005) to determine asymptotic modulus of biomaterials.

2.4.5 Water hydration capacity

Water hydration capacity (WHC) is interchangeable with water holding capacity, water binding, and water absorption in literatures. Water hydration capacity is an index showing the maximum amount of water that protein materials can take up and hold in the food formulation (Quinn and Paton 1979). Research has shown that the WHC by protein depends on various parameters including size, shape, conformational characteristics, hydrophilic-hydrophobic balance of amino acids in the protein molecules, lipids and carbohydrates associated with the proteins, thermodynamic properties of the system (such as energy of bonding, interfacial tension, etc.), physicochemical environment (such as pH, ionic strength, etc.), and solubility of protein molecules (Han and Khan 1990b). Han and Khan (1990b) found that starch-rich and protein-rich fractions of air-classified chickpea grain had lower WHC compared to the corresponding values of navy bean and pinto bean. They attributed this phenomenon to the relatively high fat content of chickpea grain.

2.4.6 Emulsion capacity and stability

Emulsions play an important role in foods such as cream, mayonnaise, sausage, and baked stuff. Emulsion has been defined as a mixture of two liquids which can not normally combine smoothly and make a uniform liquid. In other words, an emulsion is a heterogeneous structure consisting two phases: one immiscible liquid, and another phase which can be liquid or air; in most cases, it is a liquid. In an emulsion structure, the immiscible phase is dispersed in another phase. This structure has low stability, which can be improved by surface-active agents, called emulsifier (deMan 1990). Emulsion capacity and stability are indexes used to evaluate the ability of materials in making a stable emulsion

as used by Johnson and Brekke (1983), Han and Khan (1990b), and Sánchez-Vioque and co-workers (1999).

2.5 Summary

Previous studies have shown that legumes are good source of starch and protein. These components can be separated from legumes using either dry processing (e.g. air classification) or wet processing technique. Application aspects of air classification for legumes have been studied by many researchers. These studies have shown that air classification is not an effective technique for starch-protein separation from chickpea. Wet processing has been also been reported for starch-protein separation from legumes. Wet processing results in more purified starch and protein fractions than dry processing. There are different methods under wet processing; the most common and effective method is isoelectric precipitation. This method was used by many researchers to separate components such as starch, protein, and fibre from legumes. Centrifugation, hydrocyclone, filtration, and sieving were combined with isoelectric precipitation to increase the purity of each fraction. No work has been done on starch-protein separation from chickpea using isoelectric precipitation method resulting in high separation efficiency. Moreover, most of the researchers used centrifugation rather than hydrocyclone process in separating starch and protein fractions during wet processing. The hydrocyclone is flexible to be employed in different situations and means. It is also can be used in different degrees of purification as a continuous process and its installation and maintenance are low.

Starch and protein fractions are intended to be used as ingredient in food processing and non-food products, as well as for some special purpose in some industries, such as

cosmetic and pharmaceutical industries. Therefore, knowledge on the chemical, physical, and functional properties of obtained products (ingredients) is very helpful and necessary for consumers in selecting these ingredients (fractionated materials) according to the required characteristics. It also allows for better prediction of the ability of these materials (starch fraction or protein fraction) in processing and improvement of the final products made from these materials. In addition, the obtained information from fractionated products may be used in processing, storage, and design.

3. MATERIALS AND METHODS

To improve starch-protein fractionation from chickpea flour, some critical chemical, physical, and functional properties affecting separation were determined. Using a series of processes, an integrated starch-protein fractionation was developed. Selected physical and functional properties beneficial for future utilization of chickpea flour and starch and protein fractions were measured.

3.1 Materials

Commercial dehulled split desi chickpea (dhal) from the crop harvested in the fall of 2003 was obtained from Canadian Select Grains in Eston, Saskatchewan, Canada. The split chickpea grain was stored in a walk-in cooler maintained at a temperature of 2 ± 2°C. It was then ground using a pin-mill (GM 280/S-D, Condux werk, Hannau, Wolfgang, Germany) to obtain chickpea flour. The pin-mill had two discs, one had 86 pins rotating at 8034 rpm, and the other had 108 pins and was stationary.

3.2 Analytical methods

The moisture content of whole and defatted chickpea flour was determined according to AOAC method 925.10 (AOAC 2002). The moisture content of aqueous media was measured using the method described by Egan and co-workers (1981) for determining

moisture content of syrup and condensed milk. For this purpose, the vacuum oven was set at 70˚C with a vacuum gage pressure of 3.33 kPa. The protein content was measured by AACC method 46-30 (AACC 2000) using LECO Model FP-528 Nitrogen/Protein Determinator (LECO Corporation, St. Joseph, MI). A factor of 6.25 was used to convert nitrogen to protein content. The starch content was determined using the method described by Holm and co-workers (1986). Ash, total dietary fibre, and crude fat contents were measured according standard methods 08-16, 32-05, and 30-25 of the AACC (2000), respectively. To measure crude fat, the Goldfish (Labconco Corp., Kansas City, MO) apparatus and *n*-hexane was used. All analytical experiments were conducted in triplicates.

3.3 Surface charge

Zeta potential is used as an index of the surface charge of particles. The zeta potential of chickpea flour and protein fraction was measured using Malvern Instruments ZetaSizer Model NanoZS (Malvern Instruments Ltd., Malvern, Worcestershire UK) as used by Hammer and co-workers (1999). This experiment was conducted by initially preparing a slurry of the sample in deionized water at concentration of 1.0 and 0.1 mg/mL for chickpea flour and protein fraction, respectively. The measurement was conducted at the unaltered pH of the slurry and in pH range of 2.0 to 10.0. To determine the relationship between zeta potential and pH, the following model was proposed:

$$ZP = a \ln(pH) + b \tag{3.1}$$

where: ZP = zeta potential;

pH = pH value of slurry; and

a, b = constants of the model.

3.4 Particle size distribution

Particle size distribution of the samples was determined based on laser beam diffraction pattern of particles, using the Malvern Mastersizer Long Bench Particle Size Analyzer (Malvern Instruments Ltd., Malvern, Worcestershire, UK). The Mastersizer was connected to a PC equipped with Malvern software (Malvern Mastersizer 1994). Wet feeding methods were used to subject the samples to laser beam. In the laser diffraction technique, the background measurement is subtracted from the scattering pattern with the sample present to show the information on particles. The correct amount of sample has to be passed through the laser light to obtain the correct measurement. The Mastersizer measures the correct concentration of sample by measuring the amount of laser light that has been lost by passing it through the sample. This is called "obscuration" and is expressed as a percentage. In other words, obscuration is a measure of the proportion of laser light lost due to the introduction of the sample within the analyzer (Malvern Instruments 1997).

In this study, particle size of chickpea flour, starch and protein fractions, and overflow and underflow fractions, resulting from hydrocyclone under different inlet pressure and liquid media, was determined. The particle size of chickpea flour and protein fraction was determined in isopropyl alcohol and that of starch fraction, overflow, and underflow was measured in deionized water at obscuration of 15% in five replicates. The laser diffraction technique determines the mean volume or volume equivalent mean of particles. This is identical to the weight equivalent mean if the density was constant (Rawle Year Unknown). Geometric mean diameter (GMD) and geometric standard deviation of particle diameter (S_{gw}) were determined using ASAE standard S319.3 (ASAE 2004) with the

assumption that the particle density of each sample was identical and that the size of particles is normally distributed.

To estimate the cumulative undersize fraction, the following model was used:

$$y = a\left[1 - \exp\left(-bx\right)\right] \tag{3.2}$$

where: y = undersize fraction (% volume);

x = particle size (μm); and

a, b = constants of the model.

This equation was used by Edwards and Hamson (1990) to show the behaviour of a series of data increasing to a limit which equals to constant a of the model. In this study, the undersize fraction was increased up to 100% which was the limit. SAS NLIN procedure (Statistical Analysis System, Cary, NC) was employed to estimate the constants of model and fit the model to experimental data.

3.5 Size and form factor of starch granules

Major and minor diameters, perimeter, projected area and form factor of starch granules were determined using the scanning electron microscope (SEM) image and personal computer equipped with Matrox Inspector 2.0 software (Matrox Electronic System Ltd., Montreal, QC). Chickpea flour and starch fraction particles were fixed with double-coated tape onto circular aluminum studs. Since these samples were not conductive, the surfaces of the samples were coated with approximately 10 Å of gold. The size and shape of starch granules were observed under the Philips Model 505 SEM (Philips, Netherlands) and the representative pictures were taken on the Polaroid 665 (Polaroid Corp., Cambridge, MA). Images obtained from the SEM were introduced to the Matrox Inspector software. This

software can remove the overlapping objects in the image followed by reconstructing the object to the original surface and perimeter, and calculating parameters. Average diameter and form factor of starch granules were calculated according to the method of Davydova and co-researchers (1995). The average diameter of granules was determined using the following equation:

$$\overline{D} = \frac{1}{n}\sum_{n} D_n \tag{3.3}$$

where: $\overline{D}$ = the average size of starch granules; and

D_n = the diameter of a circle with the same area as the area of granule number n. The form factor of starch granules was determined by these equations:

$$F = \frac{4\ \pi\ S_i}{P_i^2} \tag{3.4}$$

$$\overline{F} = \frac{1}{n}\sum_{n} F_n \tag{3.5}$$

where: F = form factor;

S_i = area of granule image (μm^2);

P_i = perimeter of the granule image (μm); and

$\overline{F}$ = average form factor.

The area of captured granule image, S, is the number of pixels in a desired image accounted by software, converting to square micrometer after calibration. This area does not include any hole in the image. The F value for spherical or circular object is 1.0.

3.6 Determination of starch-protein interactive force

The magnitude of starch-protein adhesive force was measured using the 4200 ITC (Calorimetry Sciences Corp. Lindon, UT). To measure interactive force between starch and

protein, starch fraction and non-denatured protein fraction were used. The energy released or absorbed during titration of one of the samples into the other was measured. The starch and protein were fractionated by increasing pH of chickpea slurry to 9.0 and passing it through the hydrocyclone. Then the starch and protein fractions were freeze dried. The pH of the protein fraction was not reduced to its isoelectric point to prevent protein denaturation. Solutions of starch (5 g starch/L solution) and protein (1 g protein/L solution) in water were made and pH was adjusted to 9.0. A buffer was also prepared from double-distilled water with pH adjusted to 9.0. Using burette syringe, 10 μL of one solution containing either protein solution or buffer was injected to the sample cell assembly having either starch or protein solution. Contents in the cell were stirred with the stirrer motor set at 400 rpm. The heat quantities resulting from each injection were measured by the ITC as summarized in Table 3.1. Each experiment resulted in 20 peaks; the area under each peak was measured as released heat using BindWorks version 3.0.78 software (Calorimetry Sciences Corp., Lindon, UT), the isothermal titration calorimeter data analysis program.

As shown in Table 3.1, titration 1 contains heat resulting from starch dilution, protein dilution, buffer dilution, and mechanical mixing. Equation 2.1 was used to determine the interactive force between starch and protein.

3.7 Nitrogen solubility index of chickpea flour

The nitrogen solubility index (NSI) of chickpea flour was determined according to AACC approved method 46-23 (AACC 2000) in duplicates at pH range of 2.0 to 10.0 with 1-unit increment. The nitrogen content was measured using LECO Model FP-528 Nitrogen/Protein Determinator (LECO Corporation, St. Joseph, MI).

Table 3.1 Heat effect measurements of protein and starch.

Titration number	Location of sample and buffer		Heat effect
	Burette	Cell	
1	Protein solution	Starch solution	A + B + C + D
2	Buffer	Starch solution	C + D
3	Buffer	Protein solution	B + D
4	Buffer	Buffer	D

A = Heat of starch-protein interaction, B = Heat of starch dilution, C = Heat of protein dilution, D = Heat of buffer dilution and mechanical mixing

3.8 Description of proposed integrated separation

Starch granules and protein particles are different in size. Since the separation in hydrocyclone is a particle-size dependent process, a hydrocyclone was employed to separate these components. To do so, a series of experiments were conducted to reach the optimum separation efficiencies at acceptable starch and protein contents.

3.8.1 Hydrocyclone set-up

A hydrocyclone (Figure 3.1) included a 10-mm hydrocyclone (Dorrclone, GL&V Canada Inc., Orillia, ON) connected to a positive displacement pump (Model 4100C, Hypro Inc., St. Paul, MI) running at 1950 rpm. The pump was supplied by a feed tank. The schematic of the hydrocyclone system is presented in Figure 3.2. The Dorrclone unit consisted of four 10-mm hydrocyclones operating in parallel. Three of these hydrocyclones were removed and the vacant ports were plugged using rubber stoppers. Using only one hydrocyclone reduced the feed requirements and increased operating pressure, making the unit suitable for lab-scale trials. A by-pass valve, located between the pump and feed tank, was employed to circulate the slurry, keep flour particles in suspension form and help to control pressure. A valve was

located before cyclone to control inlet pressure. The overflow and underflow valves were kept fully-opened during the test.

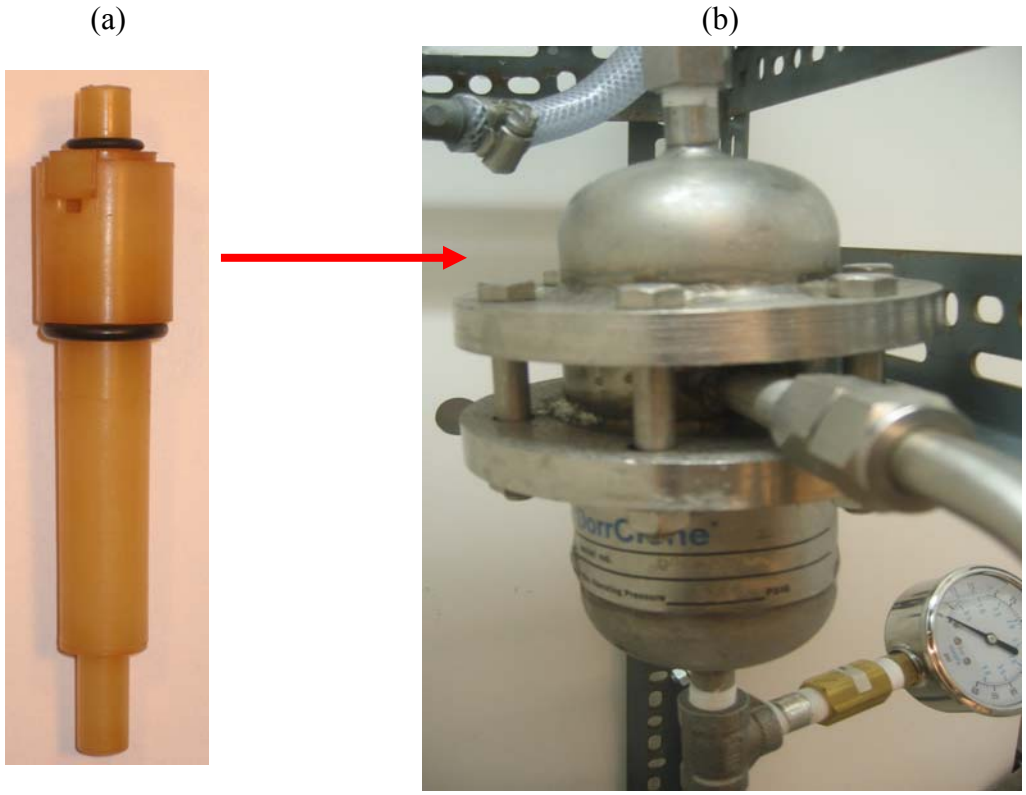

Figure 3.1 10-mm hydrocyclone (a) and Dorrclone unit (b).

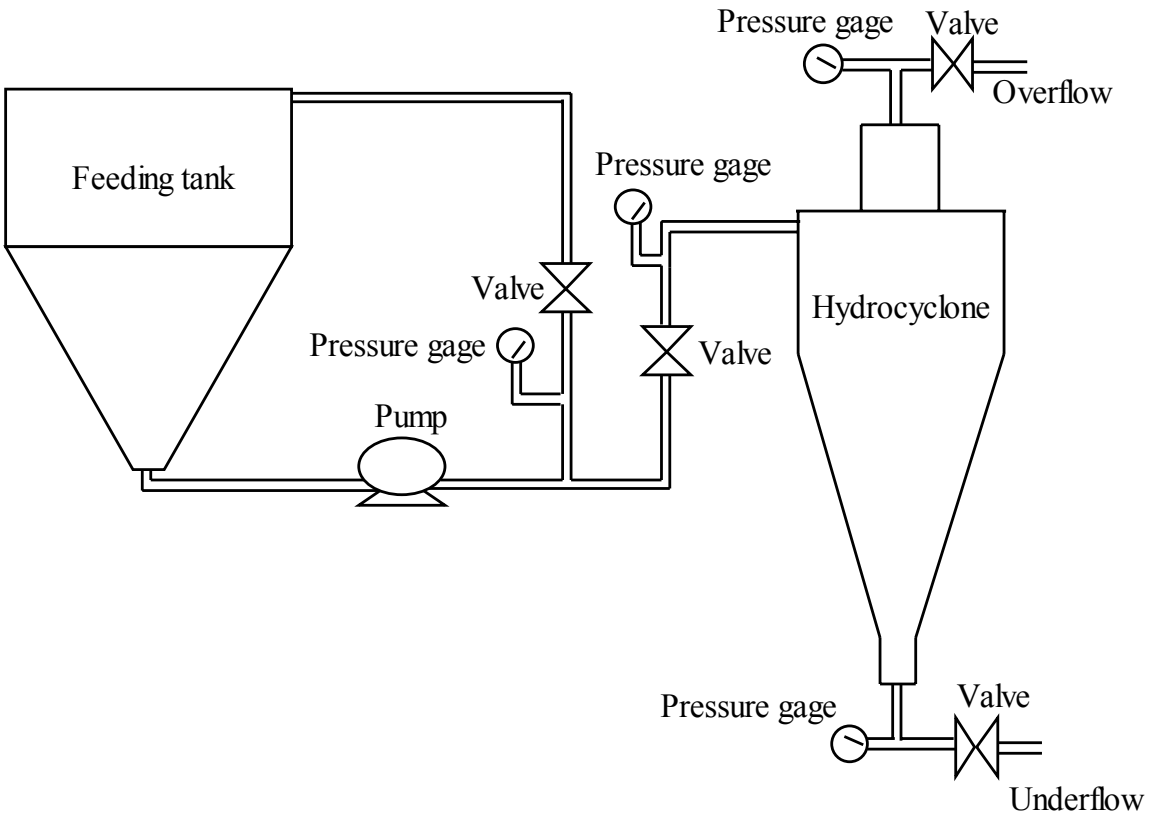

Figure 3.2 Schematic of the hydrocyclone system.

3.8.2 Hydrocyclone process

A slurry was made from whole or defatted chickpea flour and an medium, either isopropyl alcohol or deionized water at desired concentration. The measured pH of the slurry was 6.6. To obtain a slurry pH of 9.0, 10 *M* NaOH solution was used. In the case of isopropyl alcohol media, the pH adjustment was not performed. The slurry was stirred for one hour using a mixer (Model 17105, OMNI-MIXER, Sorvall Inc., Newtown, CT) employing shear force. The slurry was covered and left overnight followed by mixing for one hour. The slurry was transferred to the feed tank of the hydrocyclone system and pumped to the hydrocyclone. The slurry was circulated through the by-pass pipe so that flour particles, including starch granules and protein particles, continue to be suspended while the inlet valve was closed.

When the system stabilized, the inlet valve was opened and the inlet pressure was adjusted to desired value using the by-pass and inlet valves. Both the overflow and underflow valves were kept fully-opened during the test. The samples from the overflow and underflow were collected in glass jars at the same time to determine their starch and protein contents.

3.8.3 Inlet pressure

Inlet pressure is the back pressure at the cyclone entrance. Since there was no information about the effect of inlet pressure on starch-protein separation in the literature, three levels of inlet pressure were selected, namely 827, 689, and 552 kPa (120, 100, and 80 psi, respectively). The overflow valve was kept fully-opened during operation to maintain a pressure drop, which is the pressure difference between the inlet and overflow pressures, equal to inlet pressure at each inlet pressure operation.

3.8.4 Double-pass hydrocyclone process

The double-pass hydrocyclone process is shown schematically in Figure 3.3. This process was used in some aspects of experiments to figure out the effect of single- and double-pass process on starch-protein separation and also used to determine the effect of defatting and pH adjustment on starch-protein separation. The slurry was passed through the hydrocyclone resulting in first-pass overflow (O1) and underflow (U1). O1 and U1 were separately passed through the hydrocyclone to obtain second-pass overflow (OO1) and underflow (UU1) products.

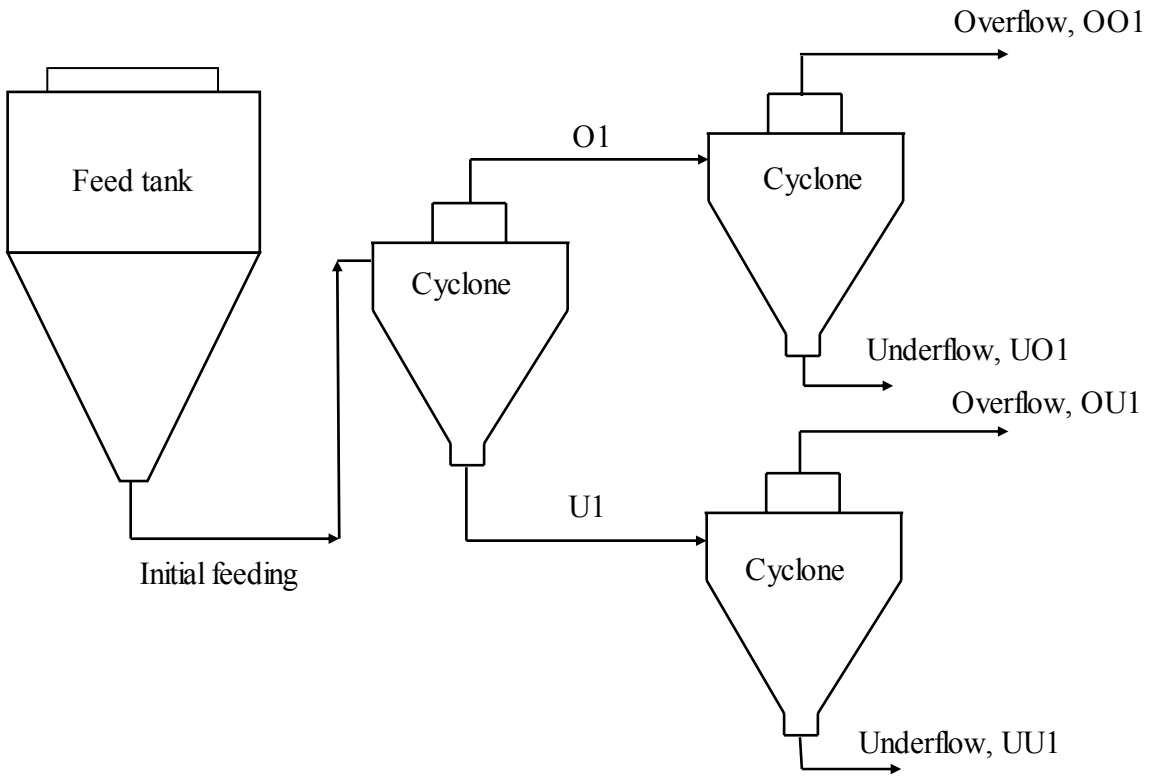

Figure 3.3 Schematic of the double-pass process.

3.8.5 Medium

To select a suitable medium for making a slurry, ACS grade isopropyl alcohol (EMD, Gibbstown, NJ) containing 99.5% and deionized water were used. Isopropyl alcohol was used to dissolve fat of chickpea flour in the solvent medium and reduce the stickiness between particles including starch and protein particles. Deionized water was employed using defatted chickpea flour to eliminate the effect of fat. Since chickpea flour has low fat content compared to oilseed grains, such as soybean, it is not economical to add a unit

operation as defatting of chickpea flour. Therefore, an experiment was conducted to improve starch-protein separation with the presence of fat in the whole chickpea flour.

3.8.6 pH adjustment of slurry

Globulins (legumin and vicilin) constitute the majority of chickpea storage proteins followed by glutelins and albumins. Chickpea proteins have the highest solubility at pH 9.0. In order to transfer the chickpea protein to the soluble phase and overflow during the hydrocyclone process, the initial slurry was adjusted to pH 9.0. The starch content of the underflow and the protein content of the overflow resulting from the slurry at pH 9.0 were compared with those derived from the slurry at the original pH (pH 6.6).

3.8.7 Defatting of chickpea flour

A portion of whole chickpea flour, resulting from pin-milling, was defatted by ACS-grade isopropyl alcohol (EMD, Gibbstown, NJ) using Soxhlet extraction system. The remaining alcohol in the sample was evaporated by placing the sample in the fume hood. Whole chickpea flour and defatted chickpea flour were used in experiments.

3.8.8 Separation process of starch and protein

Schematic separation of starch and protein is shown in Figure 3.4. This procedure, called process 1, was a modified method from Sumner and co-worker's (1981) and Liu and Hung's (1998) method. In this method, a slurry containing deionized water and dehulled chickpea flour at concentration 5% (w/w) was made. To disperse protein particles in the water and

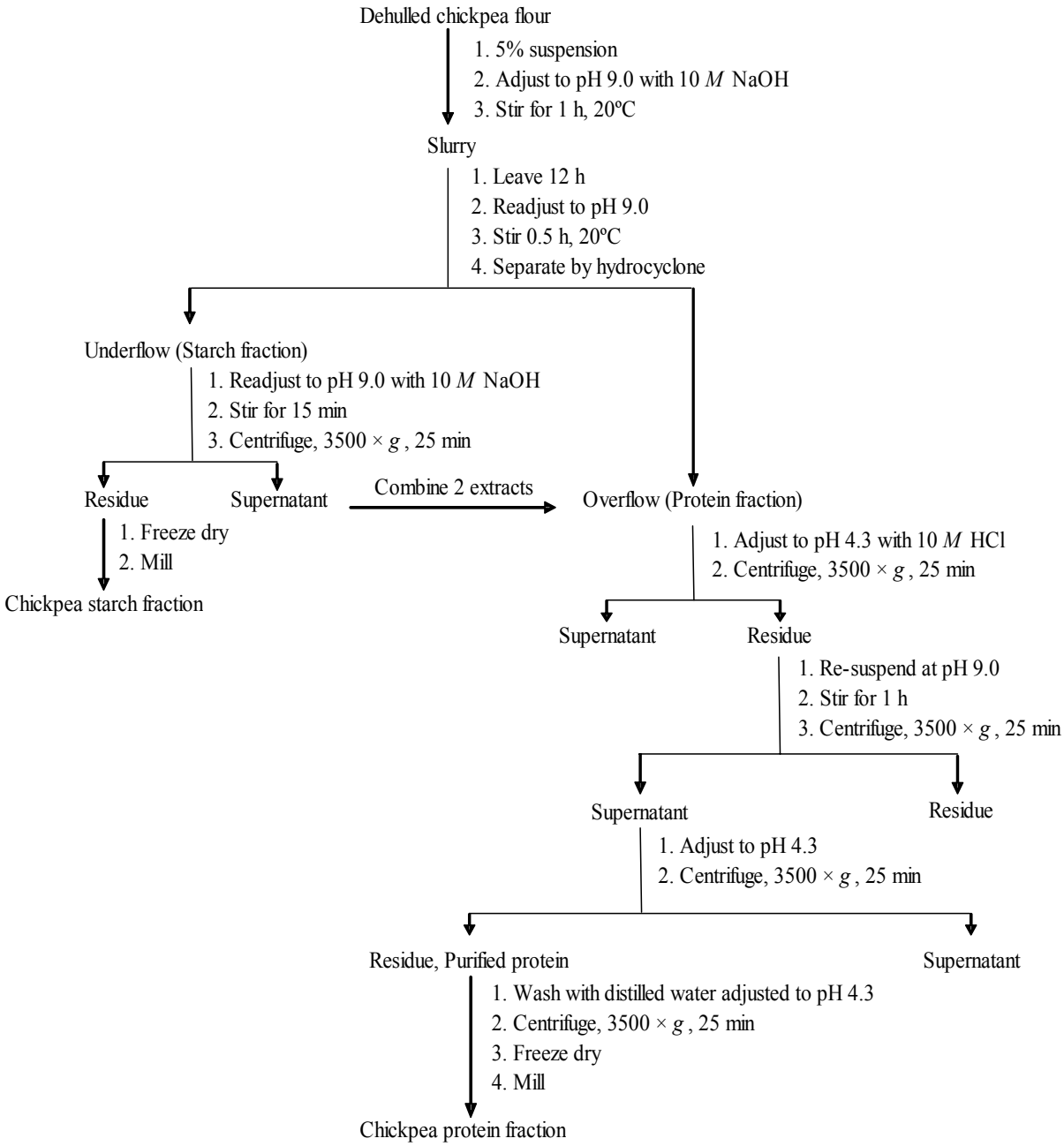

Figure 3.4 Schematic diagram of starch and protein fractionation using process 1.

transfer them to the continuous phase, the pH of the slurry was increased to 9.0 using 10 *M* NaOH. Since pin-milling of chickpea grains is not able to break starch and protein bonds, the slurry was stirred for one hour at 20°C using a mixer (Model 17105, OMNI-MIXER, Sorvall Inc., Newtown, CT). The shear force imparted by the mixer improved separation of protein particles from starch granules. The slurry was left overnight to make sure all particles have been hydrated. Protein particles acted as buffer and were able to diminish the effect of alkaline medium. The pH of slurry after being left overnight reduced to pH 7.5 to 8.0. Thus, the pH was readjusted to 9.0 and stirred for one hour at 20°C. Then, the slurry was transferred to the feed tank of the hydrocyclone system and run through the by-pass pipe (Figure 3.2) while the inlet valve was closed. When the system stabilized, the inlet valve was opened gradually; the overflow and underflow valves were kept fully-opened. The inlet pressure was adjusted to 827 kPa. During the process, the by-pass valve was not completely closed to prevent precipitation of particles in the slurry and provide uniform slurry during the operation. The hydrocyclone process resulted in underflow and overflow fractions. Since starch granules are larger and heavier than protein particles, they were collected in the underflow; protein particles were collected in the overflow. However, the underflow and overflow were still contaminated with protein and starch, respectively. More processing was required to purify these fractions. The underflow fraction was adjusted to pH 9.0 to disperse the remaining protein in the continuous phase followed by stirring for 15 min at 20°C and centrifugation (Allegra 21 Series Centrifuge, Beckman Coulter, Inc., Fullerton, CA, USA) at 3500 × *g* for 25 min. The precipitate was freeze dried (Labconco freeze dryer, Model 79480, Labconco Corp., Kansas City, MO, USA) and milled using a Wiley mill (Model 4, Thomas Wiley Mill, Thomas Scientific, Swedesboro, NJ) equipped with a mesh

opening of 2 mm. The overflow pH was adjusted to 4.3 to precipitate the proteins at the isoelectric pH; passed through the centrifuge which resulted in supernatant and precipitate containing high concentration of protein. The precipitate pH was increased to 9.0 to disperse proteins, then stirred for one hour at 20°C, and centrifuged. The supernatant containing high protein content was re-adjusted to pH 4.3 to precipitate proteins followed by centrifugation. The precipitate containing high protein content was washed using deionized water, adjusted to pH 4.3, centrifuged and freeze dried. The dried protein fraction was ground in the Wiley mill using mesh opening of 2 mm.

To compare the performance of process 1, a separation procedure, referred to as process 2, was conducted based upon the method reported by Sosulski and Sosulski (1986) (Figure 3.5). A slurry of 20% dehulled chickpea flour was made; its pH was adjusted to 9.0 using 10 *M* NaOH. The slurry was stirred for one hour using the OMNI-mixer followed by centrifugation at 3500 × *g* for 25 min. The precipitate contained high starch fraction although it was still contaminated with cell wall material. To remove cell wall material from starch fraction, the precipitate was passed through 200-mesh sieve and was washed using deionized water three times. In order to increase the starch purity of filtrate, it was reprocessed by pH readjustment, centrifugation, and sieving. The filtrate and residual materials resulting from sieving were freeze dried and milled as chickpea starch and cell wall fractions, respectively.

The supernatant from the second stage of the process was added to the first one. To precipitate protein particles, the pH was decreased to 4.3 using 10 *M* HCl; then the protein fraction was centrifuged at 3500 × *g* for 25 min, which resulted in supernatant and residual.

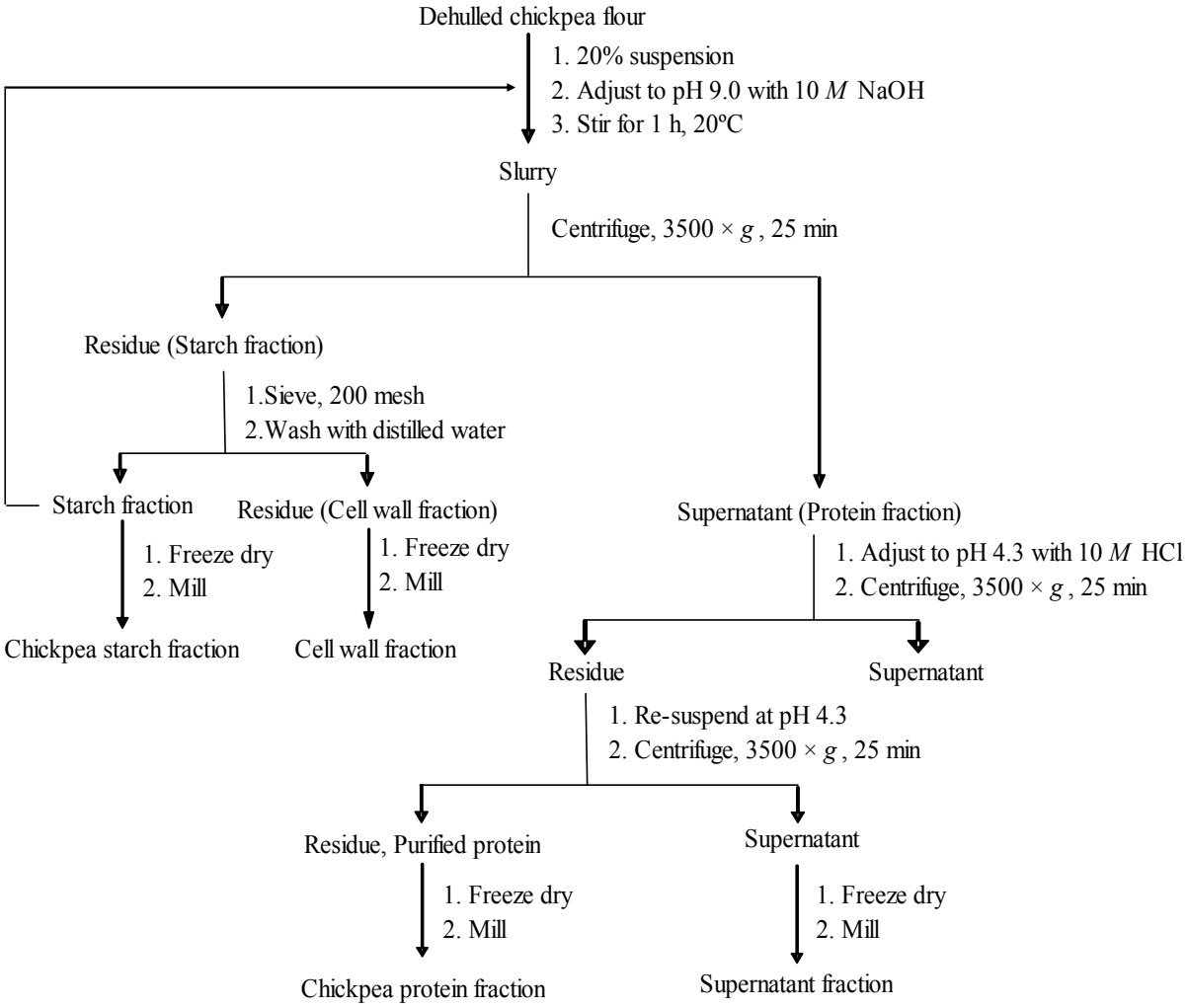

Figure 3.5 Schematic diagram of starch and protein fractionation using process 2.

The residual was re-suspended at pH 4.3 and re-centrifuged. Both residual and supernatant were freeze dried and milled as chickpea protein and supernatant fractions, respectively.

3.8.9 Separation efficiency

Starch and protein separation efficiencies were calculated according to the method used by Tyler and co-workers (1981) with some modification for dilute materials. The following equation was used to calculate starch or protein separation efficiency:

$$SE = \frac{TS_P \times C_P}{TS_F \times C_F} \times 100 \tag{3.6}$$

where: SE = separation efficiency (%);

TS_P = total solid of product (kg);

C_P = component content in the product (% d.b.);

TS_F = total solid of feed material (kg); and

C_F = component content in the feed material (% d.b.).

3.8.10 Calculation of centrifugal and drag forces

Centrifugal force is an outward direction force moving large particles to underflow fraction (Svarovsky 1990; Bradley 1965). The tangential velocity of the particle was determined using the following equation:

$$Q = \frac{\mathrm{V}}{t} = \frac{A_i \; l}{t} = A_i \; v \tag{3.7}$$

where: Q = volume flow rate (m^3/s);

V = volume of fluid (m^3);

t = time (s);

A_i = cross-sectional area of inlet (m^2);

l = length traveled by fluid (m); and

v = tangential velocity of the particle (m/s).

Therefore, using the cross-sectional area of the hydrocyclone inlet (4×10^{-6} m^2) and volume flow rate, the tangential velocity of particle was calculated. Then, the centrifugal acceleration and centrifugal force were calculated using Equations 2.2 and 2.3, respectively. The *g*-force was determined by Equation 2.4.

Drag force results in an inward radial direction of the moving fluid (Svarovsky 1990; Bradley 1965). With the assumption that the particles, starch and protein, are spherical, the drag force was calculated using Equation 2.8. To determine the projected (frontal) area, the geometric mean diameter resulting from size measurement of the particles in the overflow and underflow was used.

Generally, the relative velocity between the fluid and particle can be found by trial and error by guessing Reynolds number range and applying Equations 2.10, 2.12, and 2.14. Then, the Reynolds number is recalculated using Equation 2.7 by the velocity resulting from calculation to check whether the right Reynolds number range had been used.

3.9 Measurement of physical and functional properties of chickpea flour and starch and protein fractions

Some physical and functional properties of chickpea flour and starch and protein fractions were measured. These properties will be beneficial for future uses of these materials in food and feed processing and other industrial applications and also could extend the utilization of products.

3.9.1 Bulk density

Bulk density was measured in five replicates using a 0.5-L cylindrical container filled using a funnel, with its discharge opening located 55 mm above the top edge of the container. Since the powder in the funnel bridged, it was stirred with a thin glass bar to provide continuous flow of the funnel discharge. The funnel was removed from top of the container and the powder on the container was leveled by rolling a round stainless steel bar across the container in two perpendicular directions. Then, the container was weighed. The bulk density was calculated using the following equation:

$$\rho_b = \frac{m}{V_c} \tag{3.8}$$

where: ρ_b = bulk density (kg/m^3);

m = mass of sample in the cylinder (kg); and

V_c = volume of cylinder (m^3).

3.9.2 Particle density

A gas pycnometer (Multi Pycnometer Model MVP-2, Quantachrome Corp., Boynton Beach, FL) was employed to measure the solid volume of particles in a sample. The corresponding mass of the sample was also measured. The measurement was conducted in five replicates and particle density was calculated using the following equation:

$$\rho_t = \frac{m}{V_s} \tag{3.9}$$

where: ρ_t = particle density (kg/m^3);

m = mass of sample in the cylinder (kg); and

V_s = volume of solid (m^3).

To measure the volume of solid in the gas pycnometer, the gas was pressurized in the reference volume to about 17 psi (P_1) and then the gas was allowed into the sample cell to reach a constant pressure (P_2). The following equation was used to determine volume of solid:

$$V_s = V_{cell} - V_R\left[\frac{P_1}{P_2} - 1\right] \tag{3.10}$$

where: V_s = volume of solid (cm^3);

V_{cell} = volume of the cell (cm^3);

V_R = reference volume for the large cell (cm^3);

P_1 = pressure reading after pressurizing the reference volume (psi); and

P_2 = pressure reading after including volume of the cell (psi).

3.9.3 Porosity

As proposed by Mohsenin (1986) and Fang and co-workers (2000), the porosity was determined from bulk density and particle density using the following equation:

$$\varepsilon = \left(1 - \frac{\rho_b}{\rho_t}\right) \times 100 \tag{3.11}$$

where: ε = porosity (%);

ρ_b = bulk density (kg/m^3); and

ρ_t = particle density (kg/m^3).

Since porosity was calculated using bulk density and particle density values resulting from measurement, the calculated error is the root of the individual errors (Equation 3.12). This kind of error calculation was discussed by Ma and co-workers (1998) for determination of error of secondary quantities.

$$\Delta\varepsilon = 100 \times \sqrt{\left(\frac{\partial\varepsilon}{\partial\rho_b}\Delta\rho_b\right)^2 + \left(\frac{\partial\varepsilon}{\partial\rho_t}\Delta\rho_t\right)^2} \tag{3.12}$$

where: $\Delta\varepsilon$ = error of porosity;

$\Delta\rho_b$ = error of bulk density; and

$\Delta\rho_t$ = error of particle density.

In the current study, each value in Equation 3.12 is given by:

$$\frac{\partial\varepsilon}{\partial\rho_b}\Delta\rho_b = -\frac{1}{\rho_t}\Delta\rho_b \tag{3.13}$$

$$\frac{\partial\varepsilon}{\partial\rho_t}\Delta\rho_t = \frac{\rho_b}{\rho_t^2}\Delta\rho_t \tag{3.14}$$

Therefore, the error of porosity is obtained by substituting Equations 3.13 and 3.14 into Equation 3.12:

$$\Delta\varepsilon = \sqrt{\left(-\frac{1}{\rho_t}\Delta\rho_b\right)^2 + \left(\frac{\rho_b}{\rho_t^2}\Delta\rho_b\right)^2} \tag{3.15}$$

3.9.4 Colour measurement

The samples' colour was measured using a HunterLab spectrocolorimeter (Hunter Associates Laboratory, Inc., Reston, VA) using a 1.27 cm-area view and a 2.54 cm-port size. About 50 g of sample was placed in a 5.5 cm petri dish and covered with its lid. The petri dish was tapped to fill the empty spaces and to prevent the passing of light through the sample. Five readings per sample were taken by rotating the sample, to compensate irregular sample surface. Colour was expressed in terms of Hunter **L**, **a**, and **b** values (Dobrzanski and Rybczynski 2002).

3.9.5 Thermal conductivity determination

The effective thermal conductivity was measured using the line heat source method. A thermal conductivity probe was assembled using a brass cylinder with 89.82 mm in length and 1.57 mm in diameter. The schematic of probe assembled in this study is shown in Figure 3.6. A single insulated constantan wire with diameter of 0.13 mm was passed through whole length of cylinder as a heater until it appeared at the tip. The tip was plugged and the bare constantan wire was soldered to the tip; however, the opposite end of the wire was attached to the positive wire of the power source. Another power wire (negative polarity) was soldered to the outer layer of cylinder, where the constantan wire had been attached. A T-type (constantan and copper) thermocouple with diameter of 0.13 mm was inserted halfway into the cylinder. The remaining space in the cylinder was filled with high thermal conductivity paste (Wakefield Thermal Solutions, Inc., Pelham, NH). A 2-cm heat shrink was connected to the end of cylinder to keep the heater wire and thermocouple stable and in place. Thermal conductivity of deionized water containing agar (1% w/v) (Iwabuchi et al. 1999) was measured, in three replicates, at temperatures of –18, 4, 22, and 40°C and compared with values reported in references to calculate for error percentage as explained by Fontana and co-researchers (2001). Agar forms a gel in water medium and it was used to minimize natural heat convection in water (Iwabuchi et al. 1999). Thermal properties of agar gel and water are almost the same.

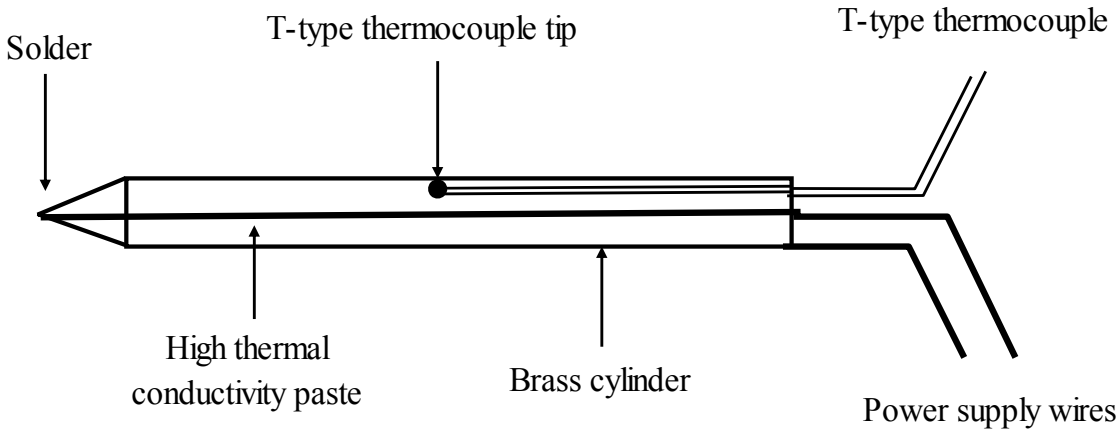

Figure 3.6 Schematic of thermal conductivity probe.

The schematic of the set-up used for thermal conductivity measurement is presented in Figure 3.7. The specimen's thermal conductivity was measured for about 1 min using the probe; time and temperature were recorded in 0.25 s intervals using a Campbell data logger (Model CR10X, Campbell Scientific, Inc. Logan, UT). Data was transferred to a laptop computer. The power supply provided a constant current of 0.600 A. The specific resistance of heater-wire was measured to be 51.21 Ω/m. The thermal conductivity value was calculated using maximum slope method (Wang and Hayakawa 1993). Local slope was calculated between each 20-data-sequence of logarithm value of time (ln t) and probe temperature differences using linear regression analysis. The maximum slope was substituted in Equation 2.18 to calculate the thermal conductivity value as used by Drouzas and co-workers (1991), Singh and Goswami (2000), and Yang and co-workers (2002).

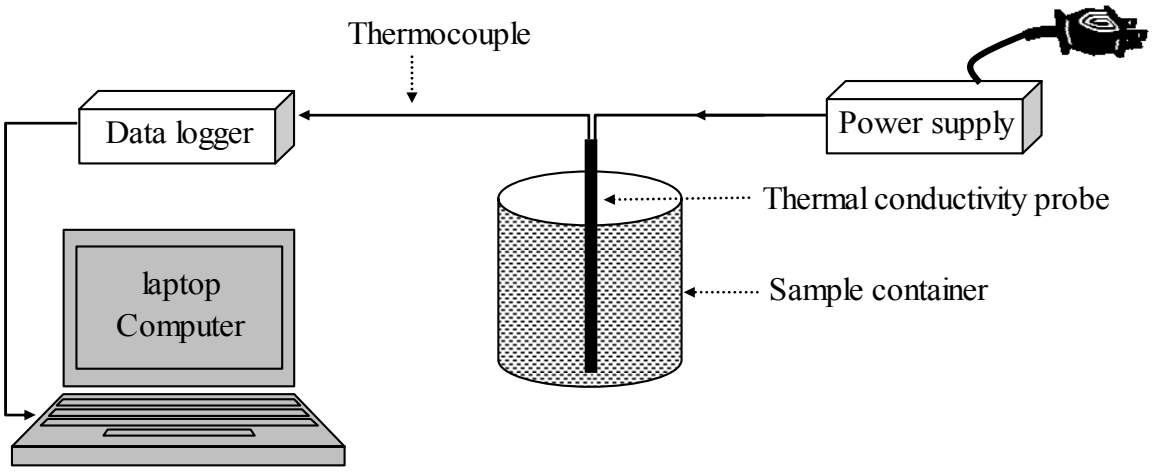

Figure 3.7 Schematic set up for thermal conductivity measurement.

This study was conducted in a combination of four temperatures (–18, 4, 22, and 40°C) and three levels of bulk density (from 335.06 to 504.12 kg/m^3) in three replicates. Thermal conductivity of chickpea flour and starch and protein fractions was measured at moisture content of 9.6, 7.8, and 2.2% w.b., respectively, which were in equilibrium with laboratory environment. Therefore, a completely randomized experimental design with factorial treatment resulted in 12 treatments. A 10-min interval was permitted between tests so that the probe reached a stable temperature. To provide three bulk density levels of a sample, a 0.5-L cylindrical container was used and filled by three methods:

- by spoon;
- by funnel, with its discharge opening located 55 mm above the top edge of the container; and
- by tapping of container which has been filled by funnel.

Since the powder in the funnel bridged, it was stirred with a thin glass bar to provide continuous flow of the sample to the container. The funnel was removed from top of the

container and the powder on the container was leveled by rolling a steel bar across the container in two perpendicular directions. To prevent change in moisture content of samples at different treatments, the cylinder container was covered with air-tight plastic bag.

The Statistical Analysis System (SAS 2003) was used for analysis of variance (ANOVA) and regression of the experimental data. SAS REG procedure was employed to determine the parameters of the applicable model. The general form of relationship between thermal conductivity, temperature, and bulk density is as follows:

$$k = aT + b\rho_b + c \tag{3.16}$$

where: k = thermal conductivity (W m^{-1} °C^{-1});

ρ_b = bulk density (kg/m^3);

T = temperature (°C); and

a, b, c = constants of the model.

3.9.6 Determination of specific heat and phase transition

The specific heat of chickpea flour and starch and protein fractions was measured using DSC at moisture content between 0.5 to 30.0% w.b. The moisture content of sample at 0.5% w.b. was achieved by drying it in a vacuum oven. Sample moisture content at other levels was adjusted by spraying calculated amount of water. The required amount of water was determined using mass balance. The sample was kept in an air-tight bag at 4°C for one week to allow for moisture equilibration. The specific heat of the samples was determined by DSC 2910 (TA Instruments, New Castle, DE) using a liquid nitrogen cooling accessory. The instrument was calibrated for specific heat measurement using a standard sample of sapphire. The reference for specific heat values of sapphire was obtained from the

manufacturer. The specific heat measurement was performed at a heating rate of 5°C/min over a temperature range of –20 to 280°C and sensitivity of 0.003 mW. Specific heat of samples was determined at temperatures of –18, 4, 22, and 40°C with precision of 0.05 kJ kg^{-1} $°C^{-1}$. The value of specific heat capacity was calculated by TA Instruments analysis software (TA Instruments, New Castle, DE) using heat flow and heating rate information (Equations 2.21 and 2.22). Using SAS REG procedure, the following model was fitted to data to find the relationship between specific heat, moisture content, and temperature:

$$c_p = aW_w + bT + c \tag{3.17}$$

where: c_p = specific heat (kJ kg^{-1} $°C^{-1}$);

W_w = moisture content (% w.b.);

T = temperature (°C); and

a, b, c = constants of the model.

Thermal transitions of starch fraction were characterized by peak gelatinization temperature (T_p) and width of the peak (ΔT); those of protein fraction were described by peak denaturation/aggregation or decomposition temperature (T_d). The ΔH_p and ΔH_d were the enthalpy of starch gelatinization and enthalpy of protein denaturation/aggregation or decomposition, respectively. The enthalpy values were obtained from the DSC thermogram by integrating the area under each peak in the heating curve using Universal Analysis 2000 software (TA Instruments, New Castle, DE). The peaks were identified through deviation of plot from baseline to a maximum or minimum point.

3.9.7 Thermal diffusivity estimation

Thermal diffusivity was calculated using indirect method (Equation 2.25) as reported by Drouzas and co-workers (1991) and Yang and co-workers (2002). Since thermal diffusivity was calculated as a secondary quantity, the error of measurement ($\Delta\alpha$) was calculated as shown below (Ma et al. 1998):

$$\Delta\alpha = \sqrt{\left(\frac{\partial\alpha}{\partial k}\Delta k\right)^2 + \left(\frac{\partial\alpha}{\partial\rho_b}\Delta\rho_b\right)^2 + \left(\frac{\partial\alpha}{\partial c_p}\Delta c_p\right)^2} \tag{3.18}$$

where: Δk = error of thermal conductivity; and

$\Delta\rho_b$ = error of bulk density; and

Δc_p = error of specific heat.

Using Equation 2.25, each value in Equation 3.18 is as follows:

$$\frac{\partial\alpha}{\partial k}\Delta k = \frac{1}{\rho_b c_p}\Delta k \tag{3.19}$$

$$\frac{\partial\alpha}{\partial\rho_b}\Delta\rho_b = -\frac{k}{{\rho_b}^2 c_p}\Delta\rho_b \tag{3.20}$$

$$\frac{\partial\alpha}{\partial c_p}\Delta c_p = -\frac{k}{\rho_b {c_p}^2}\Delta c_p \tag{3.21}$$

Therefore, substitution of Equations 3.19, 3.20, and 3.21 into Equation 3.18 yields:

$$\Delta\alpha = \sqrt{\left(\frac{1}{\rho_b c_p}\Delta k\right)^2 + \left(-\frac{k}{{\rho_b}^2 c_p}\Delta\rho_b\right)^2 + \left(-\frac{k}{\rho_b {c_p}^2}\Delta c_p\right)^2} \tag{3.22}$$

To find the relationship between thermal diffusivity, temperature, and bulk density, the following polynomial linear model was fitted to experimental data using SAS REG procedure:

$$\alpha = aT + b\rho_b + c \tag{3.23}$$

where: α = thermal diffusivity (m^2/s);

T = temperature (°C);

ρ_b = bulk density (kg/m^3); and

a, b, c = constants of the model.

3.9.8 Angle of internal friction and cohesion

A Wykeham Farrance shear box apparatus (Wykeham Farrance International Ltd., Slough, UK) equipped with a shear box measuring 100 mm square and motor assembly (Mani et al. 2004a) was used to determine the angle/coefficient of internal friction and cohesion of chickpea flour and starch and protein fractions. Both lower and top boxes of the apparatus were filled with sample using a funnel positioned 55 mm above the top edge of the box. The lower box moved at a constant speed of 0.4 mm/min. Shear stress at four different normal loads (200, 400, 600, and 800 N) were measured with the setup shown in Figure 3.8. The test was conducted in three replicates, as explained by Peleg (1977), Duffy and Puri (1996), and Tabil and Sokhansanj (1997). Equation 3.24 shows the relationship between shear stress and normal stress as used by Peleg and co-workers (1973), Chancellor (1994), Duffy and Puri (1996), and Puchalski and Brusewitz (1996). Regression analysis was conducted to calculate the angle and coefficient of internal friction and cohesion.

$$\tau = C_c + \tan\phi_i \ \sigma \tag{3.24}$$

where: τ = shear stress (Pa);

C_c = cohesion (Pa);

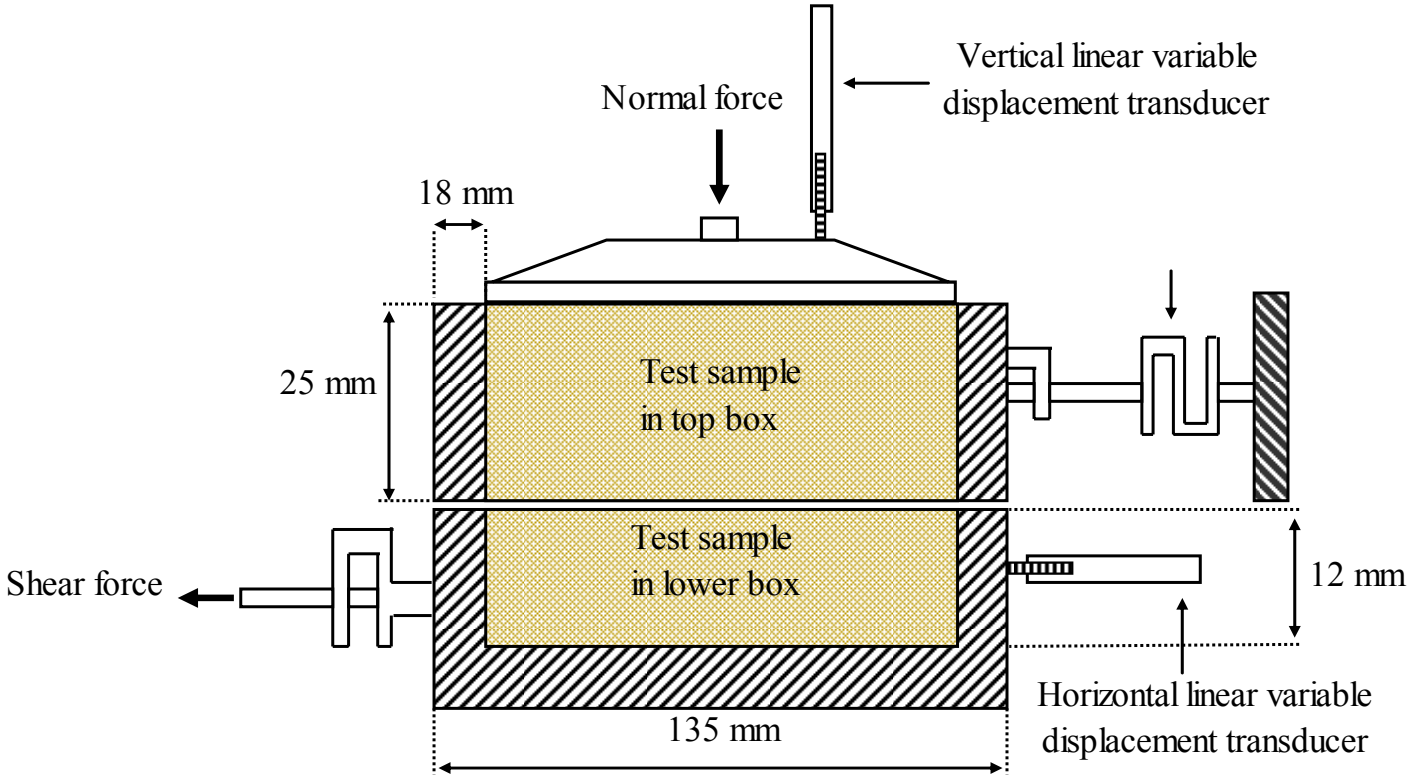

Figure 3.8 Schematic of shear box apparatus.

ϕ_i = angle of internal friction; and

σ = normal stress (Pa).

3.9.9 Angle of external friction and adhesion

Similar to the measurement of internal friction, a Wykeham Farrance shear box apparatus with a 100-mm^2 shear box (Figure 3.8) was used to determine shear stress at four different normal loads (200, 400, 600, and 800 N) on four test sheet materials: polished steel, concrete (plastic smooth finish), Teflon, and polypropylene. To measure the coefficient of external friction between sample particles and a test sheet material, the lower box was occupied by test sheet material and the top box by the sample in such a way that the sample slid and moved on the test sheet material (Puchalski and Brusewitz 1996; Chancellor 1994; Zhang and Kushwaha 1993). Other adjustments were similar to internal friction measurement. The test was carried out in three replicates. Equation 3.25 was used to calculate the angle and coefficient of external friction and adhesion.

$$\tau = C_a + \tan\phi_e \ \sigma \tag{3.25}$$

where: τ = shear stress (Pa);

C_a = adhesion (Pa);

ϕ_e = angle of external friction; and

σ = normal stress (Pa).

3.9.10 Compressibility and stress relaxation tests

A cylindrical die with 25.00 mm inside diameter and 37.60 mm in height was used in this test. A 24.91 mm diameter flat-end plunger was used to compress the sample in the die

using Instron Model 1011 testing machine (Instron Corp., Canton, MA) equipped with a 5000 N load cell. Crosshead speed of the Instron tester was set at 30 mm/min. Samples weighing 6.22 to 7.72 g, weighed to the nearest 0.01 g were filled in the die. A sample was subjected to uniaxial compression test at preset load of 500, 1000, 2000, 3000, and 4000 N where the force-deformation data was recorded as shown in Figure 3.9. Using the inner area of the cylindrical die and the distance between the plunger end and the bottom of the die, the volume and bulk density of the compressed sample was calculated at each data point. Once the preset loads were reached, the plunger remained in place for 5 min and the relaxation mode was started; the force-time data was recorded. This test was conducted in three replicates. Equations 2.28 - 2.32 were fitted to the experimental data.

The force-relaxation curves, obtained in the relaxation data, were normalized using Equation 2.33. Empirical constant, k_2, resulting from normalization was used to calculate for asymptotic modulus using Equation 2.34. The following equation shows the general relationship between asymptotic modulus and initial stress:

$$E_A = a\,\sigma_0 + b \tag{3.26}$$

where: E_A = asymptotic modulus (MPa);

σ_0 = initial stress (MPa); and

a, b = constants of the model.

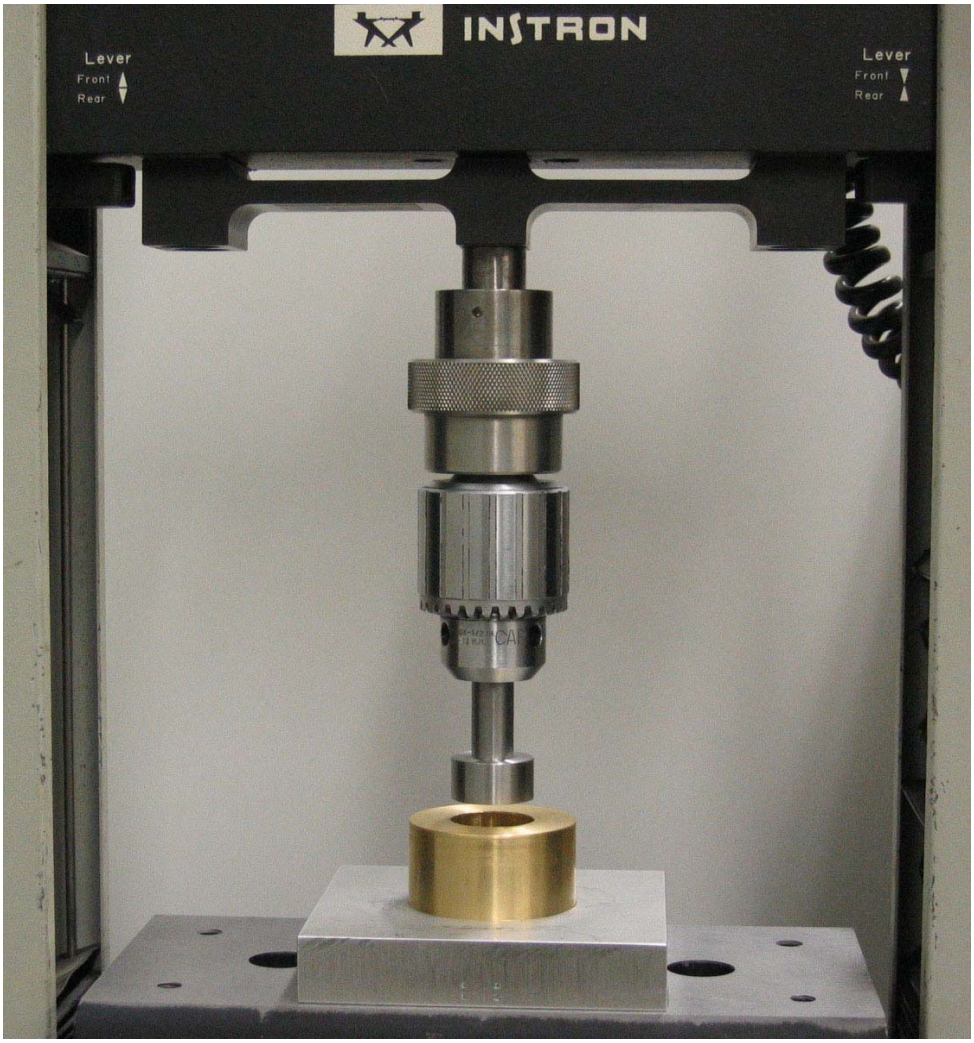

Figure 3.9 Cylindrical die, plunger and set up of uniaxial compression test.

3.9.11 Functional properties

The WHC was determined in triplicates according to AACC approved method 56-30 (2000) and that reported by Quinn and Paton (1979).

The emulsion capacity was determined according to the method of Beuchat (1977) as modified by Sathe and Salunkhe (1981) and Han and Khan (1990b) in triplicates. A 2-g sample (dry basis) was blended in a 10-speed Osterizer blender (Oster 6640 blender, Miami, FL) at the lowest speed with 100 mL double-distilled water for 30 s. Canola oil (Sunfresh

Ltd., Toronto, ON) was added to the blended sample at a rate of 0.5 mL/s until the emulsion reached the breakpoint defined as the decrease in resistance to blending. Adding oil beyond the breakpoint results in appearance of small drops of oils on the surface. The volume (mL) of oil added up to this point per unit weight of sample (g) was reported as emulsion capacity (mL/g).

The emulsion stability was determined by measuring the percentage of water retained in the emulsion after centrifugation, according to the method of Johnson and Brekke (1983) as modified by Han and Khan (1990b). This test was conducted in triplicates. The amount of sample required to make an emulsion with 15 mL oil was calculated from emulsion capacity. The sample was diluted with 15 mL double-distilled water at pH 7.0. A 15-mL canola oil was added gradually to sample solution and an emulsion was made using Ultra-Turrax T25 mixer (Janke & Kunkel, IKA-Labrotechnik T25, Germany) for 1 min at a speed of 24000 rpm. The emulsion was placed in a calibrated centrifuge tube and the total volume was recorded. The emulsion was stressed by centrifuging at 141 × *g* for 3 min. The volume of released water was measured. The emulsion stability was expressed as water retained in the emulsion after centrifugation and obtained using the following equation:

$$\text{Water retained } \% = \frac{V_w - V_r}{V_w} \times 100 \tag{3.27}$$

where: V_w = total volume of water in the emulsion (mL); and

V_r = volume of released water from emulsion (mL).

The foaming capacity and stability were measured according to Bencini (1986) as modified by Han and Khan (1990b) in triplicates. To measure foaming capacity and stability, a slurry of 3% (w/v dry basis) sample in double-distilled water was made and pH was adjusted to 7.0 using 0.1 *N* NaOH. The slurry was whipped for 5 min using a 10-speed

Osterizer blender (Oster 6640 blender, Miami, FL) at the highest speed. The whipped sampled was poured into a 250-mL graduated cylinder; whole volume and foam volume were measured at time 0, 5, 15, 30, 45, 60, 90, 120, and 180 min. Foam volume at interval times was recorded as foaming stability. The specific volume was calculated using the following equation (Han and Khan 1990b):

$$\text{Specific volume} = \frac{v_f}{W} \tag{3.28}$$

where: v_f = foam volume (mL); and

W = weight of sample (g).

Foaming capacity was described as volume increase using the following equation (Han and Khan 1990b; Bencini 1986):

$$\text{Volume increase } \% = \frac{V_f - V_i}{V_i} \times 100 \tag{3.29}$$

where: V_f= whole volume after whipping (mL); and

V_i = whole volume before whipping (mL).

3.10 Statistical analysis

The hydrocyclone process in each experiment was conducted in three trials and sample was collected. The Statistical Analysis System (SAS 2003) was used for statistical analysis including analysis of variance. Duncan's multiple range test and t-test were also employed to compare means, where appropriate. A completely randomized experimental design with factorial treatment structure was used for thermal conductivity, specific heat, and thermal diffusivity measurements. Thermal conductivity and thermal diffusivity were measured using two factors: temperature and bulk density. The analysis of variance was implemented to analyze data of thermal conductivity measurement. Specific heat was measured using a

factorial experimental design; the factors were temperature and moisture content. SAS REG and NLIN procedures were used to estimate the parameters of linear and non-linear models, respectively, from the experimental data.

4. RESULTS

In Chapter 3, experiments to study chemical, physical, and functional properties affecting starch-protein separation, as well as those which would benefit future utilization, were explained. Techniques and methods used in starch-protein separation from chickpea flour were also described. In the current chapter, values for chemical, physical, and functional properties affecting starch-protein separation are presented. The results obtained from starch-protein separation using a hydrocyclone are then shown. Finally, the physical and functional properties, which would be useful for future utilization and design of equipment and processes involving chickpea flour and its fractions, are presented.

4.1 Chemical composition of chickpea flour

The chemical composition of pin-milled chickpea flour is presented in Table 4.1. Starch was the major constituent followed by protein. Starch and total dietary fibre contents had higher standard deviations compared to other components. These high values were related to the respective methods of measurement.

Table 4.1 Chemical composition of pin-milled chickpea flour.

Chemical composition	Quantity* (% d.b.)
Starch	48.0 ± 0.3†
Protein	26.3 ± 0.1
Fat	6.0 ± 0.1
TDF	11.0 ± 1.0
Ash	2.4 ± 0.1

* Values are averages of three replicates.

† Value following the mean is standard error.

TDF: Total dietary fibre

4.2 Surface charge of chickpea flour

The zeta potential, as measured, is an index showing the surface charge of chickpea flour. Chickpea flour slurry had an initial pH of 6.5 with a zeta potential of –16.5 ± 0.6 mV before titration. Titration of slurry in the pH range from 2.0 to 10.0 resulted in changes in the zeta potential (Figure 4.1). By increasing the pH from 4.3 to 10.0, the zeta potential of chickpea flour decreased from 0.0 to –21.6 mV. Therefore, the isoelectric point of chickpea flour was approximately pH 4.3. These results showed that chickpea flour had a negative charge. As the pH increased from 2.0 to 10.0, the zeta potential decreased from positive to negative values, passing through the isoelectric point (zeta potential = 0).

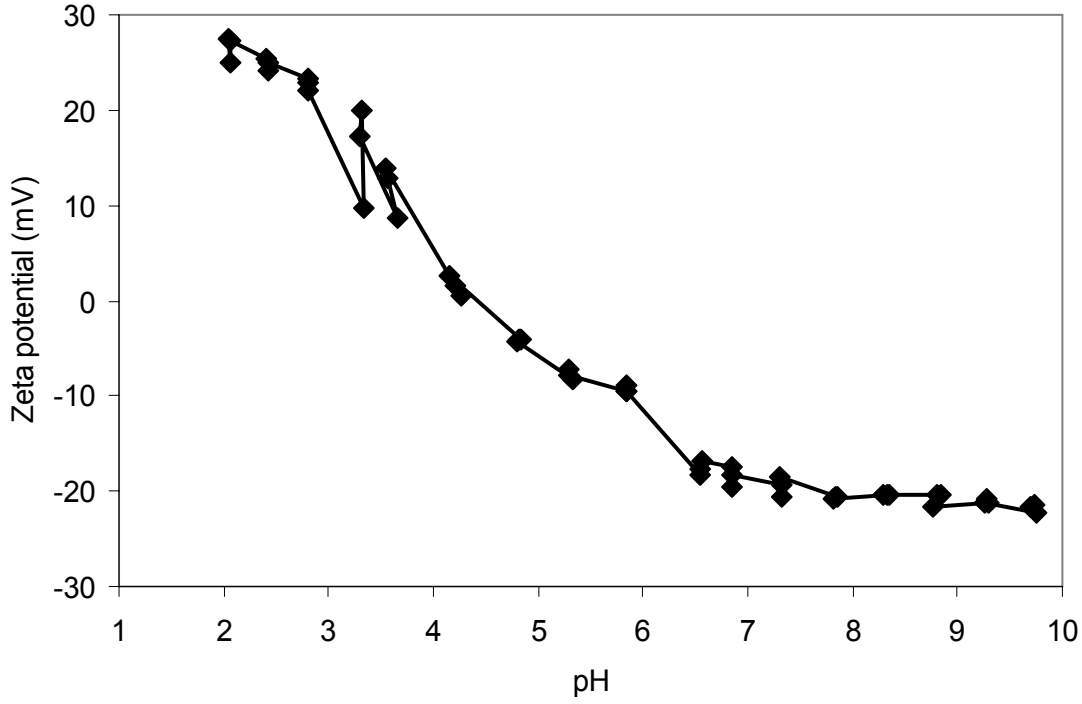

Figure 4.1 Experimental values of the zeta potential versus pH changes in chickpea flour (each data point was obtained from non-replicated experiment).

4.3 Particle size distribution of chickpea flour

Figure 4.2 shows a typical particle size distribution chart of chickpea flour. Table 4.2 shows the geometric mean diameter and geometric standard deviation of chickpea flour. The geometric standard deviation was high. This was due to the presence of particles with different compositions and sizes resulting from pin-milling. Particles from cell wall material were large. However, protein particles were small. Therefore, a wide variation in particle size was obtained from pin-milling chickpea into flour.

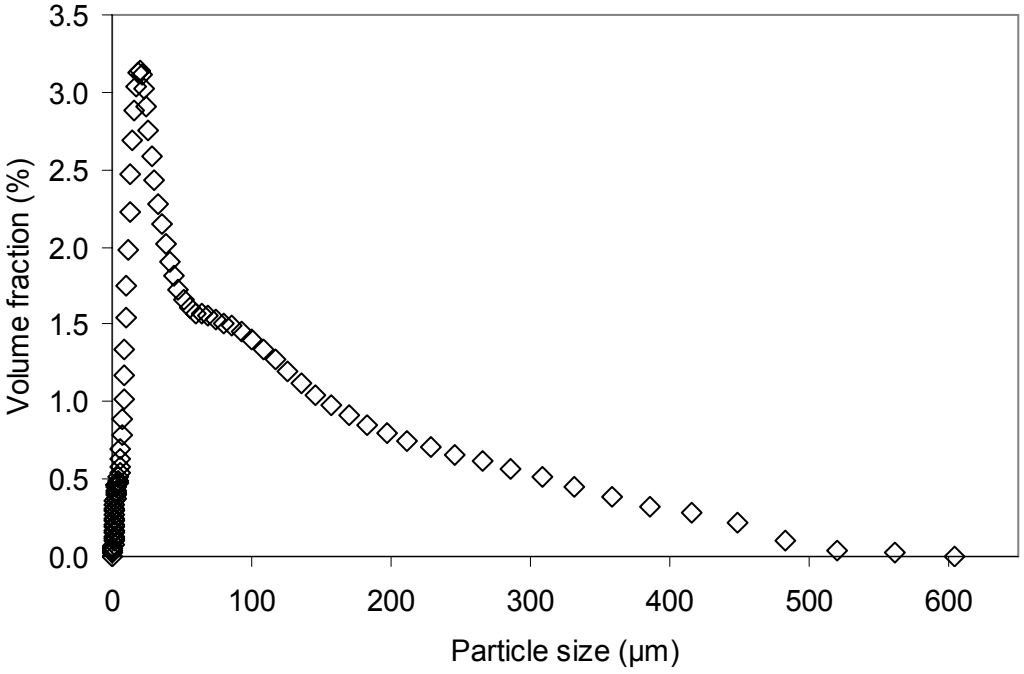

Figure 4.2 Typical particle size distribution of chickpea flour.

Table 4.2 Geometric mean diameter of chickpea flour.

Characteristic*	Chickpea flour
GMD (µm)	25.56
S_{gw} (µm)	37.64

* Values are averages of five replicates.

GMD: Geometric mean diameter

S_{gw}: Geometric standard deviation of particle diameter

4.4 Geometric size and form factor of starch granules

Figure 4.3 is a scanning electron micrograph of chickpea flour. The aggregates of protein bodies, agglomerates of starch and proteinaceous materials, fragments of cell wall material, and starch granules adhering to fine protein particles are detectable in this photograph. In order to incorporate an image into Matrox Inspector, a digital file of the image was produced using a scanner. Using Matrox Inspector software, the major diameter, minor diameter, perimeter, and projected area values and distributions of starch granules were determined, and a form factor distribution was calculated (Equation 3.4) (Table 4.3). Table 4.4 summarizes the statistical parameters of the geometric properties of starch granules. The size of starch granules ranged from 7.18 to 27.97 μm, and the

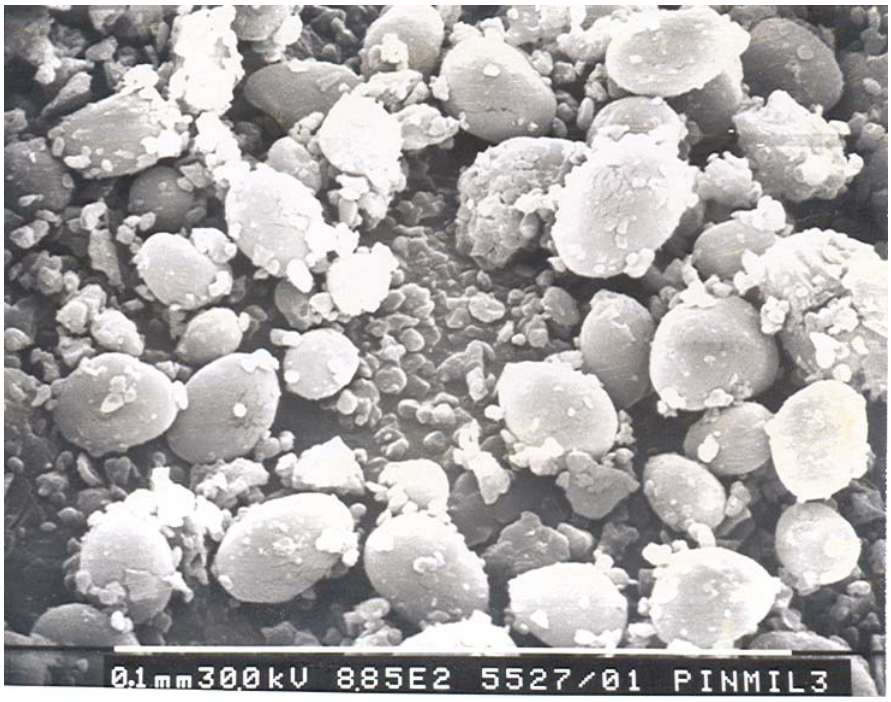

Figure 4.3 Scanning electron micrograph of chickpea flour.

Table 4.3 Distribution of dimensions, projected perimeter, projected area, and form factor of starch granules.

Major diameter		Minor diameter		Perimeter		Projected area		Form factor	
Range (μm)	Frequency	Range (μm)	Frequency	Range (μm)	Frequency	Range (μm^2)	Frequency	Range	Frequency
≤ 7	0	≤ 7	0	≤ 25	0	≤40	0	≤ 0.73	0
7 – 9	1	7 – 9	6	25 – 35	4	40 – 80	4	0.73 – 0.75	1
9 – 11	1	9 – 11	4	35 – 45	9	80 – 120	8	0.75 – 0.77	2
11 – 13	4	11 – 13	8	45 – 55	10	120 – 160	4	0.77 – 0.79	5
13 – 15	5	13 – 15	15	55 – 65	14	160 – 200	7	0.79 – 0.81	6
15 – 17	8	15 – 17	7	65 – 75	12	200 – 240	10	0.81 – 0.83	11
17 – 19	7	17 – 19	10	75 – 85	2	240 – 280	4	0.83 – 0.85	13
19 – 21	5	19 – 21	1			280 – 320	8	0.85 – 0.87	12
21 – 23	10					320 – 360	4	0.87 – 0.89	1
23 – 25	5					360 – 400	0		
25 – 27	4					400 – 440	2		
27 – 29	1								

Table 4.4 Statistical parameters* of starch granules.

Statistical parameter	Diameter (μm)		Perimeter (μm)	Projected area (μm^2)	Form factor
	Major	Minor			
Maximum	27.97	20.98	80.60	427.90	0.88
Minimum	8.22	7.18	25.36	44.08	0.74
Mean	18.92	13.81	55.02	209.66	0.83
S.D.	4.80	3.25	13.33	92.79	0.03
U.L.C.I.	20.27	14.72	58.77	235.76	0.83
L.L.C.I.	17.57	12.89	51.27	183.56	0.82

* Values are averages of five replicates.

S.D. = Standard deviation

U.L.C.I. = Upper limit confidence interval

L.L.C.I. = Lower limit confidence interval

majority of starch granules had a major diameter between 21 and 23 μm and a minor diameter between 13 and 15 μm. The majority of starch granules had perimeters of 55 and 65 μm and projected areas of 200 and 240 μm^2.

4.5 Calculated starch-protein interactive force

Figure 4.4 shows calorimetric titration of starch with protein particles of chickpea flour using the ITC. The area under each peak represents the heat released after each injection in to the ITC. In order to eliminate the heating effect of dilution, which is generated by adding the buffer and the effect of mechanical mixing, the area under the peaks shown in Figures 4.5 and 4.6 was subtracted from the area under the peaks presented in Figure 4.4. However, the area under the peaks of Figure 4.7 was added to value above, which is explained in Equation 2.1. All titrations revealed a major exothermic peak. The resultant

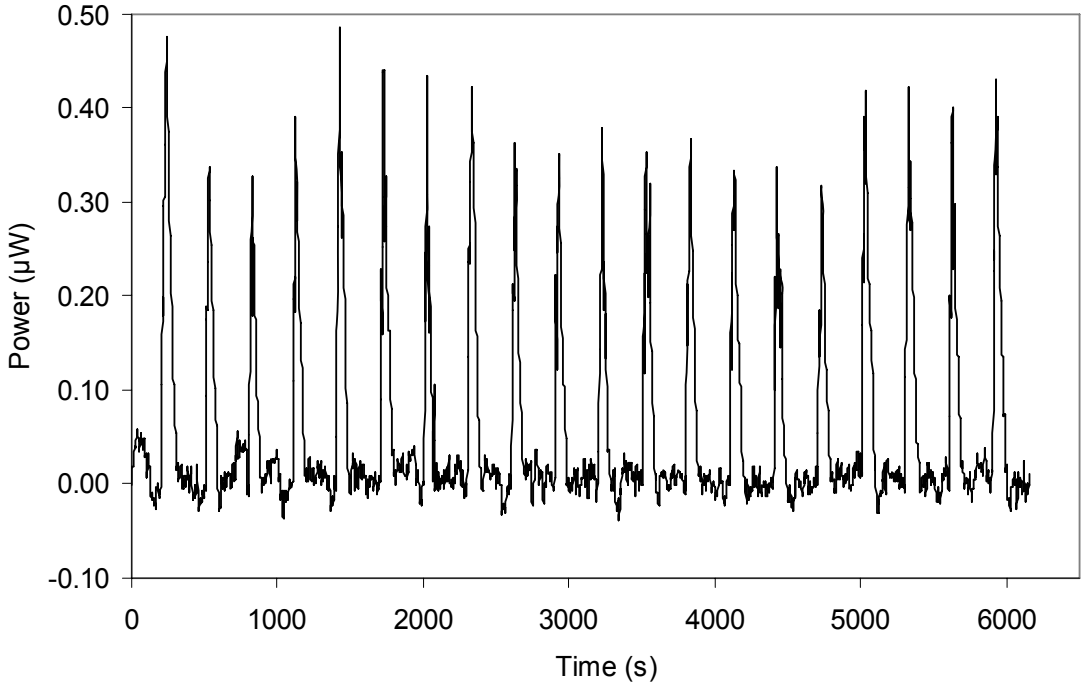

Figure 4.4 Calorimetric titration of starch with protein.

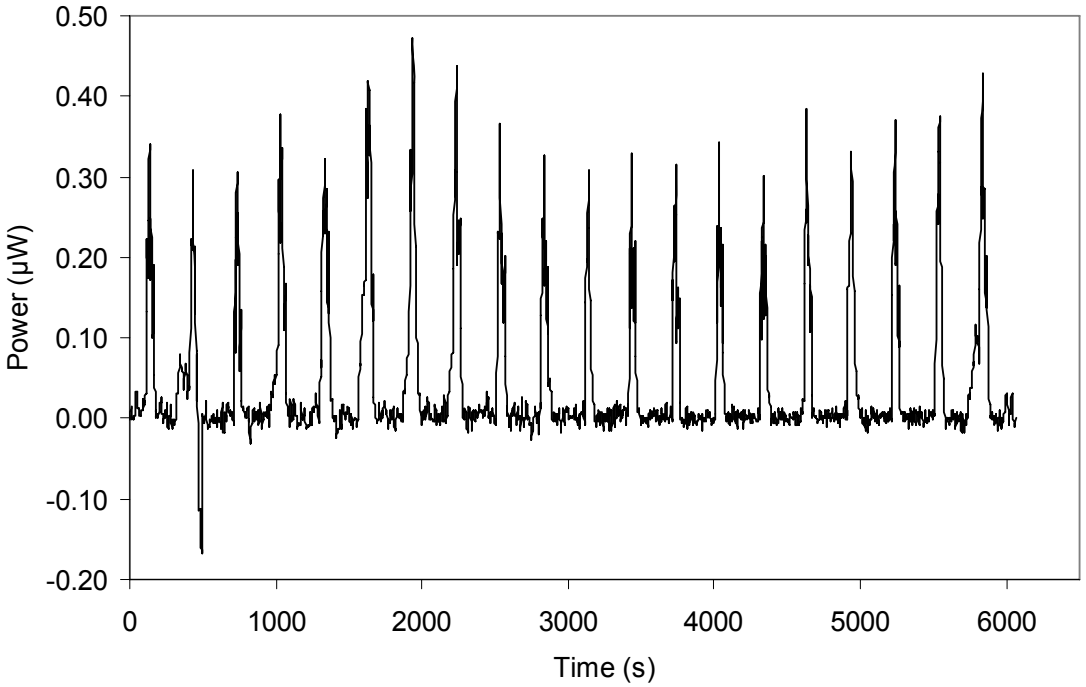

Figure 4.5 Calorimetric titration of starch with double-distilled water adjusted to pH 9.0.

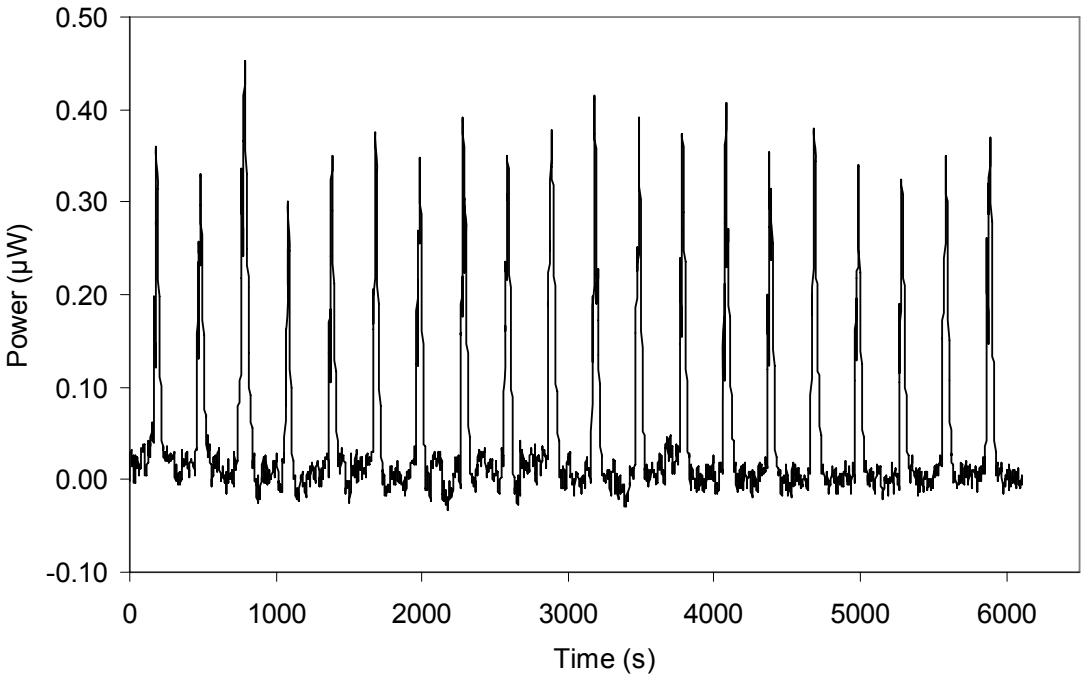

Figure 4.6 Calorimetric titration of protein with double-distilled water adjusted to pH 9.0.

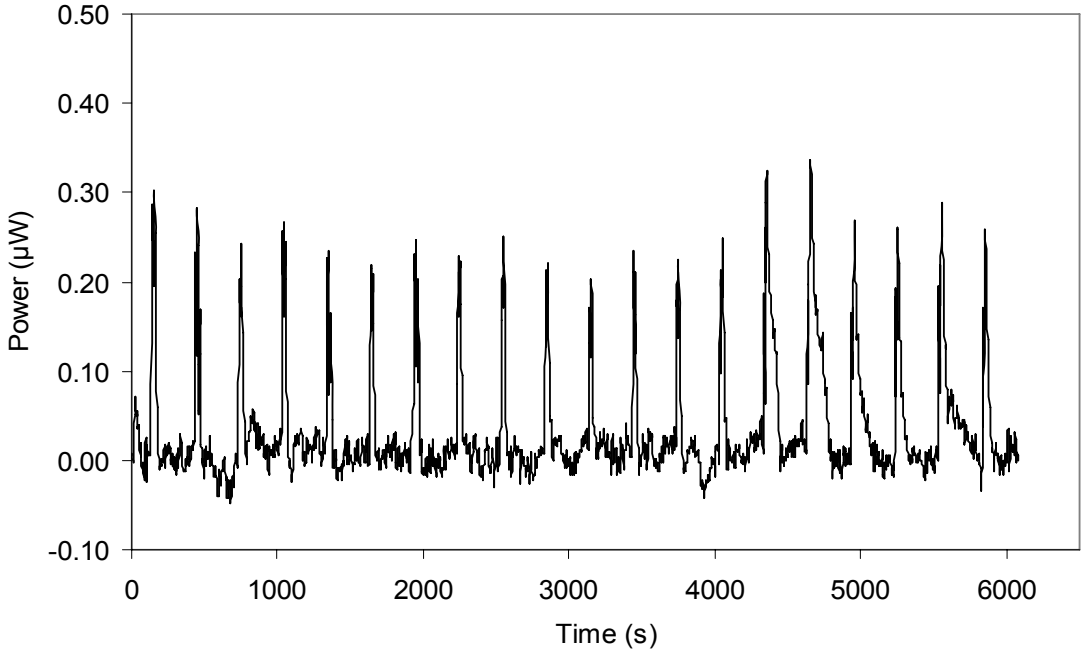

Figure 4.7 Calorimetric titration of double-distilled water with double-distilled water adjusted to pH 9.0.

heat reaction between starch and protein was not significant and was approximately zero indicating that there was no chemical interaction between starch granules and protein particles.

4.6 Measured nitrogen solubility index

Figure 4.8 presents the NSI of chickpea flour. The pH-solubility profile of chickpea flour shows that its protein had minimum solubility at a pH of 4.3 (21% nitrogen solubility). The curve shows that the minimum nitrogen solubility was in the pH range of 4.3 to 4.5, which is the isoelectric region.

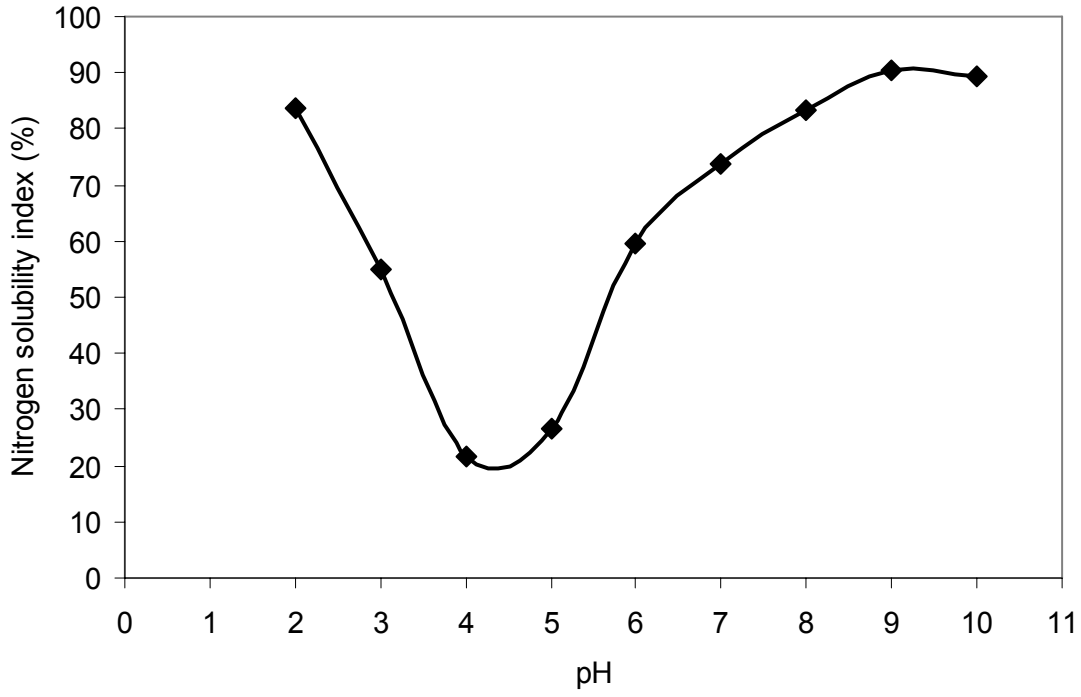

Figure 4.8 Nitrogen solubility profile of chickpea flour.

4.7 Starch-protein separation from chickpea flour

Presented in this section are the results of experiments conducted to establish an integrated starch-protein fractionation using a hydrocyclone.

4.7.1 Effect of inlet pressure at the hydrocyclone

Since chickpea flour has a relatively high fat content that affects starch-protein separation, 99.5% isopropyl alcohol was used as fat solvent and medium. The slurry was made at 2.5% (w/v) of chickpea flour in isopropyl alcohol. The slurry was passed through the hydrocyclone at three inlet pressures, 827, 689, and 552 kPa. Both the overflow and underflow valves were kept fully-opened during the operation. Table 4.5 shows the starch and protein contents of the overflow and underflow resulting from hydrocyclone operation. Decreasing the inlet pressure from 827 kPa to 552 kPa did not make a significant difference ($P > 0.05$) in the underflow starch contents. However, it reduced the overflow protein content from 52.9% to 44.2%. At an inlet pressure of 827 kPa, the protein content of the overflow fraction was enriched to twice that of chickpea flour. Table 4.6 shows starch and protein separation efficiencies at three inlet pressures. Both starch and protein separation efficiencies dropped with a reduction in inlet pressure. The high value of standard error for starch and protein separation efficiencies was related to fluctuation in hydrocyclone operation, and also the standard error of the method used to measure starch content.

Table 4.5 Starch and protein contents (% d.b.)* at constant feed concentration of 2.5% (w/v) and different inlet pressures in isopropyl alcohol medium.

Inlet pressure (kPa)	Overflow		Underflow	
	Starch	Protein†	Starch	Protein
827	21.7 a	52.9 a	51.4 a	20.2 b
689	10.4 b	46.2 b	49.3 a	25.2 a
552	8.6 c	44.2 b	52.4 a	26.1 a

* Values are averages of three replicates.

† % N × 6.25

a-c: Values in the same column followed by common letter are not significantly different at 5% level.

Starch content of chickpea flour = 48.0% d.b.

Protein content of chickpea flour = 26.3% d.b.

Table 4.6 Starch and protein separation efficiencies achieved at a constant feed concentration of 2.5% (w/v) and different inlet pressures in isopropyl alcohol medium.

Inlet pressure (kPa)	Starch separation efficiency* (%)	Protein separation efficiency* (%)
827	76.3 ± 2.1†	72.2 ± 0.9
689	62.3 ± 1.8	70.8 ± 1.1
552	61.4 ± 1.7	69.3 ± 0.9

* Values are averages of three replicates.

† Value following the mean is standard error.

4.7.2 Single- and double-pass processes

An experiment was conducted to determine the effect of single- and double-pass processes on starch-protein separation using the hydrocyclone. The double-pass process was carried out as shown in Figure 3.3. The slurry at an initial feed concentration of 2.5% (w/v) chickpea flour in isopropyl alcohol was passed through the hydrocyclone at an inlet pressure of 827 kPa, resulting in first-pass overflow (O1) and underflow (U1). O1 and U1 were separately passed through the hydrocyclone to obtain second-pass overflows (OO1 and OU1) and underflows (UU1 and UO1). Table 4.7 presents the starch and protein contents of underflow and overflow resulting from single- and double-pass processes. The effect of the double-pass hydrocyclone process on the starch content of the underflows (U1, UU1, and UO1) was significant ($P < 0.05$). UU1 had higher starch content than U1, although it still had relatively low purity. The double-pass hydrocyclone process did not increase the protein contents of the overflows (O1, OO1 and OU1) significantly ($P > 0.05$). OO1 had the highest protein content and its protein content was enriched to 56.0%, which was 2.1 times of that of chickpea flour. However, protein purity of OO1 was still relatively low.

Table 4.7 shows the starch and protein separation efficiencies. The values were calculated with respect to the starch and protein contents of chickpea flour. The starch separation efficiency of U1 was 72.1%. It shows that in the single-pass hydrocyclone process, three-quarters of the starch was collected in the underflow. In the double-pass hydrocyclone process, 51.7% of the starch was collected in UU1. The protein separation efficiency of O1 was 72.7% and the double-pass hydrocyclone process reduced this value. Increasing the number of passes in the hydrocyclone using isopropyl alcohol as a medium

increased the desired component in the undesired fraction (i.e. protein to the underflow and starch to the overflow).

Table 4.7 Starch and protein contents and corresponding separation efficiencies of single- and double-pass processes in isopropyl alcohol medium*.

Fraction	Starch (% d.b.)	Protein† (% d.b.)	Starch separation efficiency (%)	Protein separation efficiency (%)
Overflow				
O1	21.3 a	54.6 a	_	72.7 ± 0.8
OO1	5.6 c	56.0 a	_	28.3 ± 0.6
OU1	16.9 b	49.8 b	_	42.0 ± 0.7
Underflow				
U1	51.8 b	21.1 b	72.1 ± 1.9	_
UU1	55.2 a	14.3 c	51.7 ± 1.4	_
UO1	35.3 c	38.7 a	13.0 ± 0.6	_

* Values are averages of three replicates.

† % N × 6.25

a-c: Values in the same column followed by common letter are not significantly different at 5% level.

Starch content of chickpea flour = 48.0% d.b.

Protein content of chickpea flour = 26.3% d.b.

O1 = Overflow of the first-pass, OO1 = Overflow of the second-pass of O1, U1 = Underflow of the first-pass, UU1 = Underflow of the second-pass of U1, OU1 = Overflow of the second-pass of U1, UO1 = Underflow of the second-pass of O1

4.7.3 Performance comparison of two media in the separation process

Using isopropyl alcohol resulted in poor separation of starch and protein in the hydrocyclone operation and low starch and protein contents in the underflow and overflow, respectively, although it is an excellent medium for dissolving the fat in chickpea into the continuous phase. Overall, isopropyl alcohol did not exhibit the characteristics of a good medium. To confirm this, single-pass experiments were run in the hydrocyclone employing chickpea flour slurried with isopropyl alcohol or with deionized water at an inlet pressure of 827 kPa and three levels of feed concentration (0.5, 1.0 and 1.5% (w/v)). Whole chickpea flour was used in isopropyl alcohol. Defatted chickpea flour was used in deionized water.

Table 4.8 shows the starch and protein contents of the overflows and underflows resulting from the three different feed concentrations and two media. Comparison of the underflow starch contents and the overflow protein contents confirmed that at all feed concentrations, the starch and protein contents resulting from the water medium were consistently higher than those resulting from isopropyl alcohol. The underflow starch contents using water were 1.3 to 1.4 times higher than the corresponding feed concentration in isopropyl alcohol medium. Likewise, the protein content of the overflows obtained using water as medium was 1.9 to 2.1 times that of the corresponding feed concentration with isopropyl alcohol as medium. With water as medium at a feed concentration of 1.5%, the starch content in the underflow was 73.1% and the protein content in the overflow was 81.5%. However, the underflow and overflow fractions were still contaminated with protein and starch, respectively. The effect of feed concentration in the range of 0.5 to 1.5% (w/v) was not significant ($P > 0.05$) with respect to the underflow starch content or the overflow

protein content with isopropyl alcohol as medium. The overflow protein content in water medium increased significantly ($P < 0.05$) with feed concentration.

Starch separation efficiency (Table 4.9) in water medium was greater than that in isopropyl alcohol. However, protein separation efficiency in water medium was lower than that in isopropyl alcohol. In both media, the starch and protein separation efficiencies decreased as the feed concentration increased.

Table 4.8 Starch and protein contents* of single-pass hydrocyclone process in isopropyl alcohol and deionized water media.

Feed concentration (% w/v)	Overflow		Underflow	
	Starch (% d.b.)	Protein† (% d.b.)	Starch (% d.b.)	Protein (% d.b.)
Whole chickpea flour in isopropyl alcohol				
0.5	11.8 a	37.0 a	54.0 a	25.7 a
1.0	11.1 a	38.1 a	52.7 a	25.4 a
1.5	10.8 a	38.2 a	52.0 a	25.2 a
Defatted chickpea flour in deionized water				
0.5	9.4 a	71.7 c	73.4 a	24.3 a
1.0	8.3 a	76.1 b	69.1 a	21.5 b
1.5	8.2 a	81.5 a	73.1 a	19.9 c

* Values are averages of three replicates.

† % N × 6.25

a-c: Values in the same column followed by common letter are not significantly different at 5% level.

Starch content of chickpea flour = 48.0% d.b.

Protein content of chickpea flour = 26.3% d.b.

Starch content of defatted chickpea flour = 51.0% d.b.

Protein content of defatted chickpea flour = 27.9% d.b.

Table 4.9 Starch and protein separation efficiencies* achieved in single-passes processes in isopropyl alcohol and deionized water media.

Feed concentration (% w/v)	Starch separation efficiency (%)	Protein separation efficiency (%)
Whole chickpea flour in isopropyl alcohol		
0.5	76.4 ± 1.4†	79.8 ± 0.6
1.0	71.7 ± 1.1	76.9 ± 0.8
1.5	72.8 ± 1.3	74.5 ± 0.9
Defatted chickpea flour in deionized water		
0.5	97.8 ± 0.8	73.3 ± 0.9
1.0	97.7 ± 0.8	73.0 ± 0.6
1.5	96.3 ± 1.1	70.4 ± 0.7

* Values are averages of three replicates.

† Value following the mean is standard error.

4.7.4 Effect of inlet pressure and medium on particle size separation

Table 4.10 shows the geometric mean diameter of the overflow and underflow fractions at three different inlet pressures in isopropyl alcohol and deionized water. In both media, the small particles, having geometric mean diameters of 12.10 μm or lower, were separated in the overflow, and larger particles were collected in the underflow. Geometric standard deviation was high in all fractions, especially in underflow fractions. The geometric mean diameter of the underflow fraction in deionized water was greater than that in isopropyl alcohol. The geometric mean diameters of the overflows in isopropyl alcohol were not markedly different than those in deionized water. In each medium, a decrease in the inlet

pressure increased the geometric mean diameter of particles collected in the overflow and underflow.

Table 4.10 Geometric mean diameter* of the overflow and underflow fractions at three different inlet pressures in isopropyl alcohol and deionized water media.

Inlet pressure (kPa)	Overflow		Underflow	
	GMD (μm)	S_{gw} (μm)	GMD (μm)	S_{gw} (μm)
Isopropyl alcohol				
827	4.89	4.89	17.09	21.89
689	9.80	5.02	18.11	22.45
552	10.90	5.12	21.12	24.02
Deionized water				
827	5.30	6.12	26.27	41.40
689	10.71	29.20	27.97	44.05
552	12.10	31.18	31.28	51.90

* Values are averages of five replicates.

GMD: Geometric mean diameter

S_{gw}: Geometric standard deviation of particle diameter

4.7.5 Defatting and pH adjustment of feed material

Experiments were conducted to investigate the effect of defatting of chickpea flour and slurry pH on starch-protein separation using the hydrocyclone. Slurries were made using flour (whole chickpea flour or defatted chickpea flour) and deionized water at a concentration of 1.5% (w/w). The slurry was fed through the hydrocyclone at pH 6.6, the initial pH of the slurry, or at pH 9.0 using a double-pass hydrocyclone process with an inlet pressure of 827 kPa, as shown in Figure 3.3. O1 and U1 were separately passed through the

hydrocyclone to obtain second-pass overflow (OO1) and underflow (UU1) products. OO1 was left overnight to obtain sediment (SE) and supernatant (SU). SU was poured to another container and the protein contents of both SE and SU were determined.

The starch contents of the overflows and the underflows are presented in Table 4.11. The effect of the double-pass hydrocyclone process on the starch content of the underflows (U1, UU1, and UO1) was significant for both defatted and whole chickpea flour at both pH levels. UU1 had significantly higher ($P < 0.05$) starch content (1.2 to 1.4 times) than U1. The starch content of UU1 from whole flour was 86.6 and 90.9% at pH 6.6 and 9.0, respectively. Statistical analysis (t-test) between UU1 at two pH levels showed that starch content was significantly higher ($P < 0.05$) at pH 9.0 than at pH 6.6.

For defatted flour, the starch content of UU1 at pH 9.0 (99.7%) was significantly higher (t-test, $P < 0.05$) than that at pH 6.6 (93.1%). Among all applied conditions, 99.7% starch was obtained from defatted flour at a slurry pH of 9.0.

Table 4.11 shows the starch separation efficiency values in the underflows. The starch separation efficiencies of the double-pass hydrocyclone process were calculated with respect to the starch content of chickpea flour. The lowest starch separation efficiency was from underflow products resulting from UO1.

Table 4.11 Starch content of the overflow and underflow and starch separation efficiency using different feed materials and pH values in the water medium.

Fraction		Starch content[a] (% d.b.)		Starch separation efficiency[a] (%)	
		pH 6.6	pH 9.0	pH 6.6	pH 9.0
Whole flour[b]					
Overflow	O1	3.4 b	3.5 b	_	_
	OO1	1.9 c	1.9 c	_	_
	OU1	5.2 a	5.5 a	_	_
Underflow	U1	63.2 b	67.1 b	93.8 ± 2.4[d]	97.2 ± 0.6
	UU1	86.6 a	90.9 a	93.2 ± 0.8	93.9 ± 1.2
	UO1	5.8 c	3.6 c	1.1 ± 0.1	1.2 ± 0.1
Defatted flour[c]					
Overflow	O1	7.6 a	0.7 a	_	_
	OO1	1.1 b	0.6 a	_	_
	OU1	1.1 b	1.1 a	_	_
Underflow	U1	77.8 b	79.9 b	96.8 ± 0.4	96.7 ± 1.6
	UU1	93.1 a	99.7 a	96.7 ± 0.3	96.6 ± 0.2
	UO1	14.7 c	0.8 c	3.3 ± 0.1	0.2 ± 0.1

[a] Values are averages of three replicates.

[b] Whole flour starch content = 48.0% d.b.

[c] Defatted flour starch content = 51.0% d.b.

[d] Value following the mean is standard error.

O1 = Overflow of the first-pass, OO1 = Overflow of the second-pass of O1, U1 = Underflow of the first-pass, UU1 = Underflow of the second-pass of U1, OU1 = Overflow of the second-pass of U1, UO1 = Underflow of the second-pass of O1

a-c: values in the same column in each group of flour followed by common letter are not significantly different at 5% level.

Table 4.12 shows the protein content of the overflows and the underflows. For the whole flour and defatted flour, O1 had higher protein content than U1 at both pH levels. Sediments (SEs) of the overflow and the underflow were markedly different in protein content at both pH levels. Although high pH improved the protein contents of the overflow SEs, as well as those of the SUs, the effect of increased pH was not statistically (t-test) significant ($P > 0.05$). The protein contents of SEs from OO1 were 2.5 to 2.7 times that of the whole flour; whereas, they were 3.5 times that of the defatted flour. UO1 was still high in protein, which may be due to the agglomeration of starch granules and proteinaceous material. The effect of defatting on the protein contents of the overflow SEs was significant ($P < 0.05$), which is desirable since protein is concentrated in the SEs. However, it was not significant ($P > 0.05$) for the overflow SUs. Using the double-pass hydrocyclone process, protein contents of the overflow products (OO1 and OU1), where proteins are expected to accumulate, did not increase because the protein particles were still dispersed in the media. Adjusting the pH of the overflow to isoelectric point (pH 4.3) may have improved protein separation and increased protein content.

Table 4.13 shows the protein separation efficiency values. For both whole flour and defatted flour, higher pH improved the protein separation efficiencies due to the higher solubility of chickpea protein at pH 9.0 than at pH 6.6.

Table 4.12 Protein content[a] (% d.b.) of sediment and supernatant of the overflow and underflow using different feed materials and pH values in the water medium.

Fraction		pH 6.6		pH 9.0	
		SE	SU	SE	SU
Whole flour[b]					
Overflow	O1	66.9 a	69.6 a	68.4 b	67.0 a
	OO1	68.5 a	64.1 a	70.3 a	68.3 a
	OU1	64.0 b	72.1 a	65.7 c	65.7 a
Underflow	U1	8.0 b	34.1 b	7.0 b	22.4 b
	UU1	7.0 b	31.5 c	5.4 c	20.1 c
	UO1	52.3 a	67.1 a	53.2 a	55.3 a
Defatted flour[c]					
Overflow	O1	72.8 c	68.1 a	92.5 b	63.5 ab
	OO1	97.8 a	82.4 a	98.9 a	66.1 a
	OU1	88.3 b	72.7 a	88.3 c	59.1 b
Underflow	U1	18.5 b	67.1 a	16.6 b	61.1 a
	UU1	12.0 c	65.6 a	11.1 c	60.4 a
	UO1	58.1 a	69.6 a	90.1 a	60.5 a

[a] Values are averages of three replicates.

[b] Whole flour protein content = 26.26% d.b.

[c] Defatted flour protein content = 27.90% d.b.

SE = Sediment, SU = Supernatant

O1 = Overflow of the first-pass, OO1 = Overflow of the second-pass of O1, U1 = Underflow of the first-pass, UU1 = Underflow of the second-pass of U1, OU1 = Overflow of the second-pass of U1, UO1 = Underflow of the second-pass of O1

a-c: values in the same column in each group of flour followed by common letter are not significantly different at 5% level.

Table 4.13 Protein separation efficiency* (%) achieved in the overflows using different feed materials in the water medium.

Feed material		pH 6.6	pH 9.0
Whole flour			
Overflow	O1	65.7 ± 1.2†	70.1 ± 1.1
	OO1	31.9 ± 0.5	35.1 ± 0.9
	OU1	13.2 ± 0.2	11.4 ± 0.2
Defatted flour			
Overflow	O1	67.5 ± 0.8	83.1 ± 0.9
	OO1	50.2 ± 0.3	43.1 ± 0.7
	OU1	29.1 ± 0.2	29.0 ± 0.3

* Values are averages of three replicates.

† Value following the mean is standard error.

O1 = Overflow of the first-pass, OO1 = Overflow of the second-pass of O1, U1 = Underflow of the first-pass, UU1 = Underflow of the second-pass of U1, OU1 = Overflow of the second-pass of U1, UO1 = Underflow of the second-pass of O1

4.7.6 Higher feed concentrations

The overflow and underflow fractions should be dried for utilization; drying of fractions requires energy, which is costly. Therefore, at higher concentration, less water would need to be evaporated, and less energy would be required. An experiment was conducted to determine the optimal feed concentration, in terms of the starch and protein contents and their separation efficiencies in the underflow and overflow, respectively. Since the objective was to find the highest feed concentrations, this experiment was initiated at a feed concentration of 20.0% (w/w). The pump was not able to run properly at 20.0% (w/w) feed concentration because of the high viscosity of the slurry. Therefore, the experiment was resumed at a feed concentration of 15.0% (w/w). Table 4.14 shows the starch and protein

contents of the overflow and underflow at five feed concentrations at pH 9.0 using the hydrocyclone. The effect of feed concentration was significant ($P < 0.05$) with respect to starch and protein contents. The starch content in the underflow and the protein content in the overflow decreased with increasing feed concentration. Table 4.15 shows the separation efficiencies at each feed concentration. Increasing the feed concentration reduced separation efficiencies. The pump was able to feed the slurry properly at a feed concentration of 5%. A feed concentration of 5.0% (w/w) resulted in 95.2% starch separation efficiency and 68.7% protein separation efficiency. This means that at 5% (w/w) feed concentration, 95.2% of the starch component was collected in the underflow from chickpea flour, and 68.7% of the protein was retained in the overflow. The starch fraction, containing 66.7% starch, was still contaminated with other components such as protein (3.8%). The relatively low level protein in the overflow (76.1%) would have been due in part, to accumulation of lipid components in the overflow.

Table 4.14 Starch and protein contents* (% d.b.) of the overflow and underflow at pH 9.0 using different feed concentrations.

Feed concentration (% w/w)	Overflow		Underflow	
	Starch	Protein	Starch	Protein
1.5	3.5 e	81.9 a	68.2 a	3.5 c
3.0	4.1 d	80.2 b	66.3 b	3.6 c
5.0	4.9 c	76.1 c	66.7 b	3.8 c
10.0	7.0 b	74.4 d	64.0 c	5.3 b
15.0	7.7 a	70.3 e	61.9 d	7.3 a

* Values are averages of three replicates.

a-e: Values in the same column followed by common letter are not significantly different at 5% level.

Table 4.15 Starch and protein separation efficiencies of the overflow and underflow using different feed concentrations.

Feed concentration (% w/w)	Starch separation efficiency* (%)	Protein separation efficiency* (%)
1.5	98.4 ± 1.0†	70.0 ± 0.7
3.0	97.3 ± 1.2	69.1 ± 0.3
5.0	95.2 ± 1.3	68.7 ± 0.4
10.0	88.7 ± 0.9	63.7 ± 1.0
15.0	85.9 ± 1.1	60.2 ± 0.5

* Values are averages of three replicates.

† Value following the mean is standard error.

4.7.7 Centrifugal force in the hydrocyclone in two different media

The hydrocyclone was run at a feed concentration of 1.5% (w/v) chickpea flour in two media, isopropyl alcohol or deionized water, and three inlet pressures, 827, 689, and 552 kPa. This test was conducted in triplicates. Using the cross-sectional area of the hydrocyclone inlet (4×10^{-6} m^2), the volume flow rate, tangential velocity, centrifugal acceleration, centrifugal force, and *g*-force were determined, as summarized in Table 4.16. In each medium, volume flow rate, tangential velocity of particles, centrifugal acceleration, and *g*-force decreased with a decrease in inlet pressure. However, the centrifugal force increased with a decrease in inlet pressure. Comparing the two media showed that at a given inlet pressure, the volume flow rate, tangential velocity, and centrifugal acceleration for the isopropyl alcohol medium were greater than those for deionized water. Conversely, the centrifugal force in deionized water was higher than that in isopropyl alcohol.

Table 4.16 Hydrodynamic characteristics and centrifugal force in the hydrocyclone at three different inlet pressures in isopropyl alcohol and deionized water media.

Inlet pressure (kPa)	Q ($\times 10^{-4}$ m^3/s)	v (m/s)	a_c ($\times 10^4$ m/s^2)	F_c ($\times 10^{-6}$ N)	g-force ($\times g$)
Isopropyl alcohol					
827	1.05	26.2	13.7	0.54	14000
689	0.96	24.0	11.5	0.54	11800
552	0.90	22.6	10.2	0.76	10400
Deionized water					
827	0.86	21.5	9.23	1.32	9400
689	0.79	19.8	7.84	1.35	8000
552	0.74	18.6	6.92	1.67	7000

Q = volume flow rate

v = tangential velocity of the particle

a_c = centrifugal acceleration

F_c = centrifugal force

4.7.8 Drag force in the hydrocyclone under two different media

The drag force acting on the overflow particles, in the same experiment as described in the previous section, was determined. To calculate the drag force, it was assumed that all particles were spherical and having particle diameters equal to the geometric mean diameter. The Reynolds number and relative velocity of particles were calculated in isopropyl alcohol having a density of 785 kg/m^3 and viscosity of 0.00243 Pa s at 20°C and also in deionized water with a density of 998 kg/m^3 and viscosity of 0.00099 Pa s at 20°C. With the assumption that the Reynolds number of particle was less than 2, the relative velocity between the fluid and particle was calculated and summarized in Table 4.17. Then the corresponding Reynolds number of particle was recalculated to check if the Reynolds

number was indeed less than 2. The drag coefficient and, consequently, the drag force of the hydrocyclone separation, were calculated, as summarized in Table 4.17.

The Reynolds number increased with a decrease in inlet pressure in isopropyl alcohol and deionized water. However, the drag coefficient was reduced. The Reynolds number in isopropyl alcohol was lower than that in deionized water at a given inlet pressure. Reynolds number of particle in isopropyl alcohol was one-fourth that in deionized water. However, the drag coefficient of particles in isopropyl alcohol was greater than that in deionized water ranging from 3.8 to 4.1 times that of deionized water. The drag force applied to the overflow fraction in isopropyl alcohol was about twice the drag force in deionized water.

Table 4.17 Drag force calculation of the hydrocyclone overflow at three different inlet pressures in isopropyl alcohol and deionized water media.

Inlet pressure (kPa)	u (m/s)	Re_p	C_D	F_D ($\times 10^{-8}$ N)
Isopropyl alcohol				
827	0.038	0.06	403	0.42
689	0.128	0.40	59	2.87
552	0.140	0.49	49	3.50
Deionized water				
827	0.042	0.23	106	0.21
689	0.147	1.58	15	1.47
552	0.165	2.00	12	1.87

u = relative velocity between the fluid and particle

Re_p = Reynolds number of particle

C_D = drag coefficient

F_D = drag force

4.7.9 Particle size distribution of the overflow and underflow fractions

Figures 4.9 and 4.10 show the typical particle size distribution charts of the overflow and underflow fractions, respectively. Table 4.18 shows the geometric mean diameters of the overflow and underflow fractions resulting from hydrocyclone operating at a feed concentration of 5% and an inlet pressure of 827 kPa. The geometric mean diameter of the overflow (5.30 μm) was lower than that of the underflow (26.27 μm). The overflow fraction had lower geometric standard deviation than the underflow.

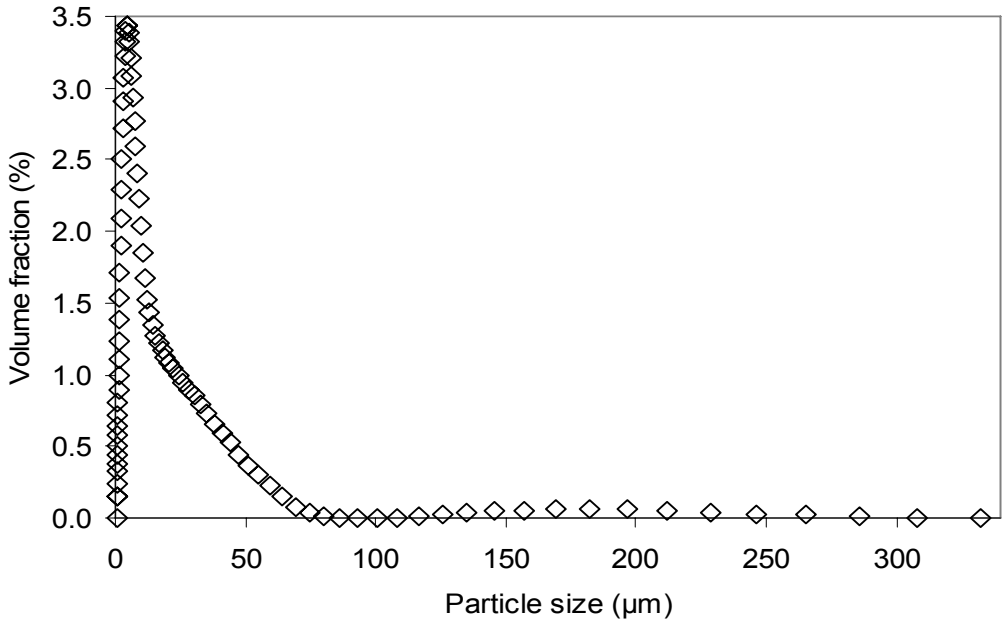

Figure 4.9 Typical particle size distribution of the overflow fraction.

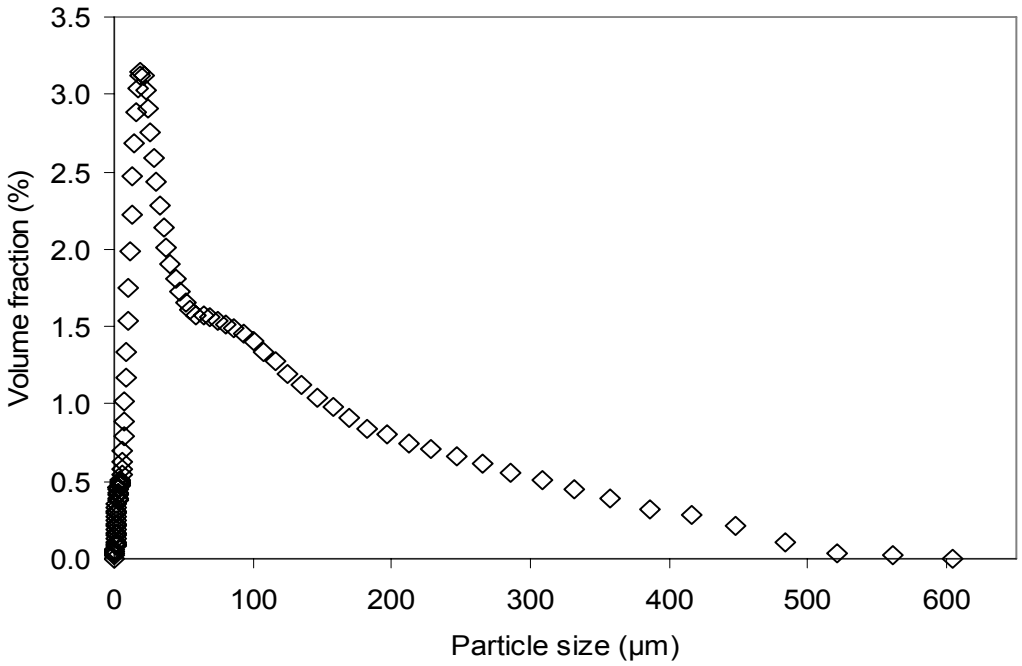

Figure 4.10 Typical particle size distribution of the underflow fraction.

Table 4.18 Geometric mean diameter* of the overflow and underflow fractions.

Characteristic	Overflow	Underflow
GMD (µm)	5.30	26.27
S_{gw} (µm)	6.12	41.40

* Values are averages of five replicates.

GMD: Geometric mean diameter

S_{gw}: Geometric standard deviation of particle diameter

4.7.10 Integrated separation process

To increase starch and protein contents in the underflow and overflow, respectively, and to remove contaminating components from each fraction, the slurry pH was increased to separate starch fraction using a hydrocyclone. The pH was then decreased to separate the

protein fraction by employing a centrifuge. Two separation processes (processes 1 and 2) were performed for comparison. The schematic diagram of isolating starch and protein in process 1, using a hydrocyclone and centrifuge, is shown in Figure 3.4. The fraction yield of each product was measured based on the recovery percentage of each fraction. Because of unavoidable losses of particles during the process, the yield of supernatant fraction was calculated as the difference between the dry weights of chickpea flour and the recovered fractions.

Table 4.19 presents the fraction yields and chemical compositions of starch, protein and supernatant fractions obtained from separation process 1. Starch and protein contents were enriched to 1.5 and 3.1 times, respectively, the initial levels in chickpea flour. In terms of fraction yield, the starch fraction had the highest value, as it was the major constituent of chickpea flour (Table 4.1). Figure 4.11 shows a scanning electron micrograph of chickpea starch. In terms of shape and size, starch granules were heterogeneous with shape from round to oval and size from small to large. Granules were smooth with no evidence of fissures. The fraction compositions in Table 4.19 demonstrate that most of the fat was fractionated into the protein and supernatant fractions. The fat contents of the protein and supernatant fractions were 1.6 and 5.2 times that of chickpea flour, respectively. However; dietary fibre was fractionated with the starch fraction because of the large particle size of cell wall material and the residual hull from dehulling. The protein content of the supernatant fraction was relatively high (13.0%).

Separation process 2 (Figure 3.5) was conducted to compare results with process 1. In process 2, hydrocyclone was not used and separation was conducted using a centrifuge. A sieving step was also added to remove cell wall material and other fibre components from

Table 4.19 Fraction yield and chemical compositions[a] of fractions resulting from processing of chickpea flour[b] using separation processes 1 and 2.

Fraction	Fraction yield (% d.b.)	Chemical composition of fraction (% d.b.)				
		Starch	Protein	Fat	TDF	Ash
Separation process 1						
Starch fraction	64.8 ± 1.1[c]	75.0 ± 2.2	2.1 ± 0.9	0.3 ± 0.1	14.4 ± 1.0	1.6 ± 0.1
Protein fraction	28.6 ± 0.9	0.9 ± 0.1	81.9 ± 0.4	9.5 ± 0.1	1.5 ± 0.1	5.0 ± 0.1
Supernatant fraction	6.6 ± 0.7	0.4 ± 0.0	13.0 ± 0.3	31.1 ± 0.1	0.5 ± 0.1	14.2 ± 0.1
Separation process 2						
Starch fraction	62.2 ± 0.9	78.3 ± 1.6	2.9 ± 0.1	0.9 ± 0.1	7.6 ± 0.1	1.9 ± 0.1
Protein fraction	27.7 ± 0.8	0.4 ± 0.1	80.2 ± 0.5	12.2 ± 0.2	0.8 ± 0.1	4.0 ± 0.1
Cell wall fraction	7.2 ± 0.4	6.6 ± 0.2	2.3 ± 0.1	1.5 ± 0.2	69.4 ± 1.9	0.6 ± 0.1
Supernatant fraction	2.9 ± 0.2	3.2 ± 0.1	25.8 ± 0.3	26.3 ± 0.3	0.2 ± 0.1	18.1 ± 0.1

[a] Values are averages of three replicates.

[b] Chemical composition of chickpea flour was as follows: starch = 48.0% d.b., protein = 26.3% d.b., fat = 6.0% d.b., TDF = 11.0% d.b., and ash = 2.4% d.b.

[c] Value following the mean is standard error.

TDF: Total dietary fibre

Figure 4.11 Scanning electron micrograph of starch fraction.

the starch fraction. Thus, another fraction, the cell wall fraction, was obtained from process 2. Table 4.19 shows the fraction yield and chemical composition of fractions resulting from separation process 2. Since the residual from the first centrifugation was passed through the sieve, the cell wall fraction was derived from sieving and this process resulted in a lower yield of the starch fraction compared to process 1. The starch content of the starch fraction in process 2 was higher (78.3%) than that in process 1 (75.0%).

Table 4.20 presents starch and protein separation efficiencies for separation processes 1 and 2. The starch separation efficiencies did not show a marked difference, although that of process 1 was a little higher. Process 2 had lower starch and protein separation efficiencies although the starch fraction resulting from process 2 had a higher starch content than that from process 1.

Table 4.20 Starch and protein separation efficiencies achieved in separation processes 1 and 2.

Process type	Starch separation efficiency* (%)	Protein separation efficiency* (%)
Separation process 1	99.7 ± 0.1†	89.3 ± 0.7
Separation process 2	99.3 ± 0.1	84.6 ± 0.1

* Values are averages of three replicates.

† Value following the mean is standard error.

4.8 Physical and functional properties of chickpea flour and fractionated starch and protein

This section presents results of experiments conducted to determine the physical and functional properties useful for future product applications and extending to possible utilization of the fractions in different industries.

4.8.1 Surface charge of fractionated products

The zeta potential of fractionated products was measured as an indicator of the surface charge. In spite of frequent attempts, including re-milling and changing the medium, the starch fraction simply agglomerated too much to be measured. The protein fraction slurry had an initial pH of 5.9 with a zeta potential of –5.3 ± 0.6 mV before titration. Titration of the slurry from pH of 2.0 to 10.0 resulted in a change in the zeta potential (Figure 4.12). The zeta potential decreased from 0.0 to –18.0 mV when the pH increased from 4.8 to 10.0 and then increased to 25.4 mV at pH of 2.1.

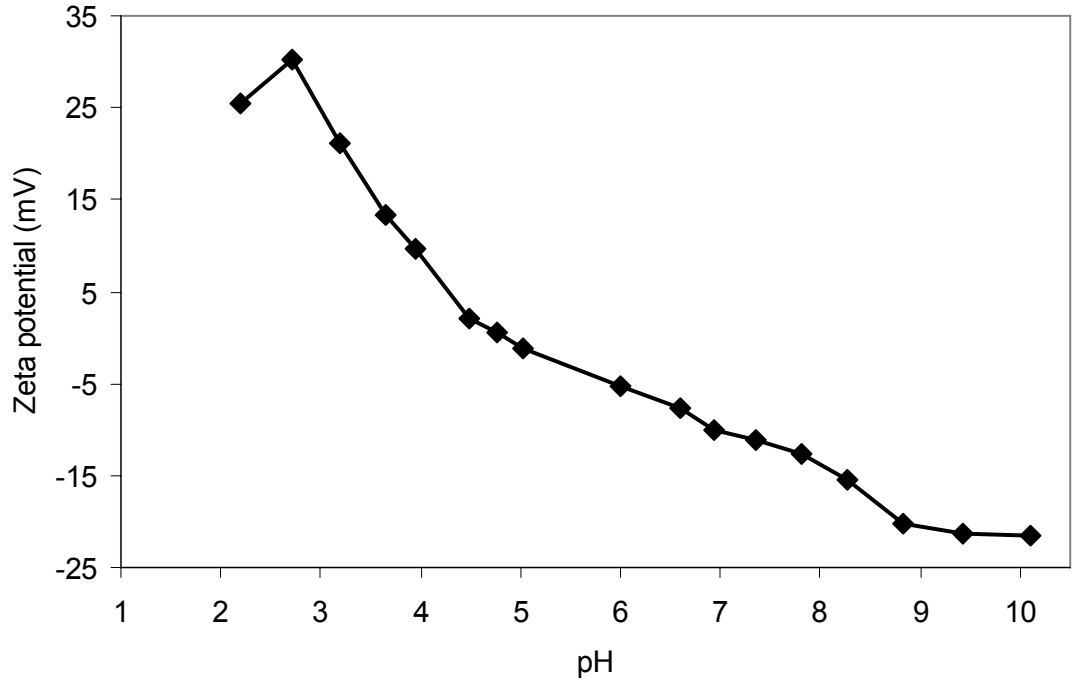

Figure 4.12 Experimental values of the zeta potential versus pH changes in protein fraction (each data point was obtained from non-replicated experiment).

4.8.2 Density, porosity, and colour

Table 4.21 lists the bulk density, particle density, porosity, and colour parameters of chickpea flour and starch and protein fractions at moisture contents which were in equilibrium with the laboratory environment. Chickpea flour had a higher bulk density and lower porosity than starch or protein fraction. In terms of colour, starch fraction was the lightest (Hunter **L**) and protein fraction was the darkest. Protein fraction had the most redness (Hunter **a**) and starch fraction had the lowest redness. Protein fraction had the highest yellowness (Hunter **b**) followed by chickpea flour.

Table 4.21 Bulk density, particle density, porosity, and colour parameters of chickpea flour and starch and protein fractions.

Characteristic[a]	Chickpea flour	Starch fraction	Protein fraction
Bulk density (kg/m^3)	416.49 ± 2.58[b]	346.68 ± 1.41	335.06 ± 1.32
Particle density (kg/m^3)	1457.60 ± 7.11	1508.24 ± 5.09	1289.65 ± 2.05
Porosity (%)	71.43 ± 0.23[c]	77.01 ± 0.13	74.02 ± 0.11
Moisture content (% d.b.)	10.6 ± 0.0	8.4 ± 0.0	2.3 ± 0.0
Colour			
L[d]	85.51 ± 0.00	89.69 ± 0.00	67.58 ± 0.01
a[e]	1.32 ± 0.00	0.11 ± 0.01	4.18 ± 0.01
b[f]	17.98 ± 0.00	6.43 ± 0.01	18.94 ± 0.02

[a] Values are averages of five replicates except moisture content values which are averages of three replicates.

[b] Value following the mean is standard error.

[c] Standard error for porosity was calculated using Equation 3.15.

[d] Hunter **L** is 100 for white and zero for black.

[e] Hunter **a** is positive for redness, zero for grey, and negative for greenness.

[f] Hunter **b** is positive for yellowness and negative for blueness.

4.8.3 Thermal properties of chickpea flour and fractionated products

This section presents the results of experiments performed to determine the thermal properties of chickpea flour and starch and protein fractions.

4.8.3.1 Thermal conductivity values

Table 4.22 shows the physical characteristics of the chickpea flour and starch and protein fractions used in thermal conductivity measurements. Protein fraction showed the highest geometric mean diameter and the lowest particle density. The bulk density increased as the porosity decreased for all samples as the air spaces between particles diminished. Chickpea

flour had the lowest porosity at a bulk density of 504.12 kg/m^3. However, starch fraction had the highest porosity at a bulk density of 346.68 kg/m^3. Protein fraction had the lowest moisture content among samples.

Table 4.23 shows the thermal conductivity of distilled water containing agar (1% w/v) and error values. In the temperature range of 4 to 40°C, both measured and reference thermal conductivity increased as the temperature increased. At a temperature below freezing, –18°C, the thermal conductivity value was approximately 4 times the values at temperature above freezing. Regression analysis between the measured thermal conductivity and reference values of distilled water resulted in an equation with a coefficient of determination (R^2) of 1.00:

$$k_c = 0.9792k_m + 0.0114 \quad (4.1)$$

where: k_c = corrected thermal conductivity; and

k_m = measured thermal conductivity.

Since the slope of the linear regression was very close to 1.00 and the intercept was very low, the probe was suitable for the measurement of thermal conductivity. Furthermore, since the regression equation resulted in a slope very close to 1.00 and high R^2, the measured thermal conductivity values were used in this study.

Table 4.22 Bulk density, particle density, and porosity of chickpea flour and starch and protein fractions.

Sample	GMD (μm)	Moisture content[a] (% w.b.)	Particle density[b] (kg/m^3)	Bulk density[b] (kg/m^3)	Porosity[b] (%)
Chickpea flour	25.56	9.6	1457.60 ± 7.11[c]	416.49 ± 2.58	71.43 ± 0.23[d]
				456.02 ± 2.38	68.71 ± 0.22
				504.12 ± 2.21	65.41 ± 0.23
Starch fraction	55.44	7.8	1508.24 ± 5.09	346.68 ± 1.41	77.01 ± 0.13
				387.05 ± 1.23	74.34 ± 0.12
				427.10 ± 1.64	71.68 ± 0.14
Protein fraction	316.59	2.2	1289.65 ± 2.05	335.06 ± 1.32	74.02 ± 0.11
				375.12 ± 1.26	70.91 ± 0.11
				414.98 ± 1.82	67.82 ± 0.15

GMD = geometric mean diameter

[a] Values are averages of three replicates.

[b] Values are averages of five replicates.

[c] Value following the mean is standard error.

[d] Standard error for porosity was calculated using Equation 3.15.

Table 4.23 Thermal conductivity of distilled water containing agar (1% w/v) at different temperatures.

Temperature (°C)	Measured k* (W m^{-1} °C^{-1})	Reference k (W m^{-1} °C^{-1})	Reference	Error (%)
–18	2.4803 ± 0.38†	2.440	Mohsenin 1980	1.65
4	0.5756 ± 0.01	0.568	Singh and Heldman 2001	1.34
22	0.6079 ± 0.01	0.597	Singh and Heldman 2001	1.82
40	0.6176 ± 0.01	0.633	Singh and Heldman 2001	2.44

k: Thermal conductivity

* Values are averages of three replicates.

† Value following the mean is standard error.

Table 4.24 shows the thermal conductivity of chickpea flour and starch and protein fractions at moisture contents of 9.6, 7.8, and 2.2% w.b., respectively, which were in equilibrium with the laboratory environment. The thermal conductivities of samples increased with temperature at a given bulk density and increased with bulk density at a given temperature. For chickpea flour, the highest thermal conductivity (0.1058 W m^{-1} °C^{-1}) was measured at the highest temperature (40°C) and bulk density (504.12 kg/m^3). Conversely, the lowest thermal conductivity (0.0739 W m^{-1} °C^{-1}) was measured at the lowest temperature (–18°C) and bulk density (416.49 kg/m^3).

Table 4.24 Thermal conductivity of chickpea flour and starch and protein fractions in different temperatures and bulk densities.

Temperature (°C)	Chickpea flour		Starch fraction		Protein fraction	
	ρ_b (kg/m^3)	Mean* (W m^{-1} °C^{-1})	ρ_b (kg/m^3)	Mean* (W m^{-1} °C^{-1})	ρ_b (kg/m^3)	Mean* (W m^{-1} °C^{-1})
−18	416.49	0.0739 ± 0.0007†	346.68	0.0688 ± 0.0018	335.06	0.0643 ± 0.0021
	456.02	0.0807 ± 0.0011	387.05	0.0717 ± 0.0005	375.12	0.0701 ± 0.0012
	504.12	0.0843 ± 0.0025	427.10	0.0720 ± 0.0016	414.98	0.0716 ± 0.0037
4	416.49	0.0839 ± 0.0016	346.68	0.0733 ± 0.0002	335.06	0.0682 ± 0.0030
	456.02	0.0896 ± 0.0023	387.05	0.0780 ± 0.0022	375.12	0.0715 ± 0.0014
	504.12	0.0978 ± 0.0120	427.10	0.0789 ± 0.0031	414.98	0.0716 ± 0.0012
22	416.49	0.0846 ± 0.0013	346.68	0.0751 ± 0.0046	335.06	0.0707 ± 0.0005
	456.02	0.0933 ± 0.0034	387.05	0.0810 ± 0.0022	375.12	0.0722 ± 0.0010
	504.12	0.0986 ± 0.0041	427.10	0.0837 ± 0.0049	414.98	0.0755 ± 0.0012
40	416.49	0.0921 ± 0.0007	346.68	0.0896 ± 0.0094	335.06	0.0752 ± 0.0040
	456.02	0.0998 ± 0.0054	387.05	0.0915 ± 0.0031	375.12	0.0767 ± 0.0009
	504.12	0.1058 ± 0.0009	427.10	0.0919 ± 0.0053	414.98	0.0787 ± 0.0020

ρ_b: bulk density

* Values are averages of three replicates.

† Value following the mean is standard error.

As Table 4.25 demonstrates for chickpea flour, the effects of temperature and bulk density were significant ($P < 0.00$) on thermal conductivity, whereas their interaction did not show a significant difference. For starch fraction, ANOVA results demonstrated that the effect of temperature on thermal conductivity was significant, although the effect of bulk density and the interaction effect of temperature and bulk density were not significant. In the case of protein fraction, the effects of temperature and bulk density were significant ($P < 0.00$ and $P < 0.03$, respectively), whereas their interaction was not.

Table 4.25 Analysis of variance results of thermal conductivity of chickpea flour and starch and protein fractions.

Source of variation	Chickpea flour		Starch fraction		Protein fraction	
	df*	Probability	df	Probability	df	Probability
Temperature	3	0.00	3	0.00	3	0.00
Bulk density	2	0.00	2	0.23	2	0.03
Interaction	6	1.00	6	0.99	6	0.91
Error	12		12		12	
Total	23		23		23	

* Degree of freedom

4.8.3.2 Specific heat values

The specific heat of chickpea flour and starch and protein fractions was determined at four temperature and moisture content levels (Table 4.26). In the majority of the conditions, the specific heat increased with moisture content and temperature. The specific heat values of chickpea flour and starch and protein fractions were in the range of 1.158 - 1.786, 0.718 - 1.837, and 0.816 - 2.206 kJ kg^{-1} $°C^{-1}$, respectively.

Table 4.26 Specific heat (kJ kg^{-1} $°C^{-1}$) of chickpea flour and starch and protein fractions (data were obtained from non-replicated experiment).

Sample	Moisture content (% w.b.)	Temperature (°C)			
		–18	4	22	40
Chickpea flour	0.5	1.158	1.190	1.239	1.307
	9.6	1.276	1.273	1.299	1.337
	20.0	1.228	1.343	1.427	1.527
	30.0	1.649	1.698	1.734	1.786
Starch fraction	0.5	0.718	0.820	0.900	0.993
	7.8	0.924	1.002	1.101	1.183
	20.0	1.117	1.166	1.194	1.242
	30.0	1.384	1.537	1.686	1.837
Protein fraction	0.5	0.816	0.879	0.975	1.032
	2.2	1.135	1.256	1.344	1.431
	10.0	1.111	1.242	1.344	1.487
	20.0	1.573	1.659	1.721	1.796
	30.0	1.759	1.928	2.066	2.206

Figures 4.13 and 4.14 show the trends of the specific heat values of samples as a function of moisture content and temperature, respectively. Specific heat increased linearly with increases in temperature and moisture content, with R^2 ranging between 0.87 and 1.00.

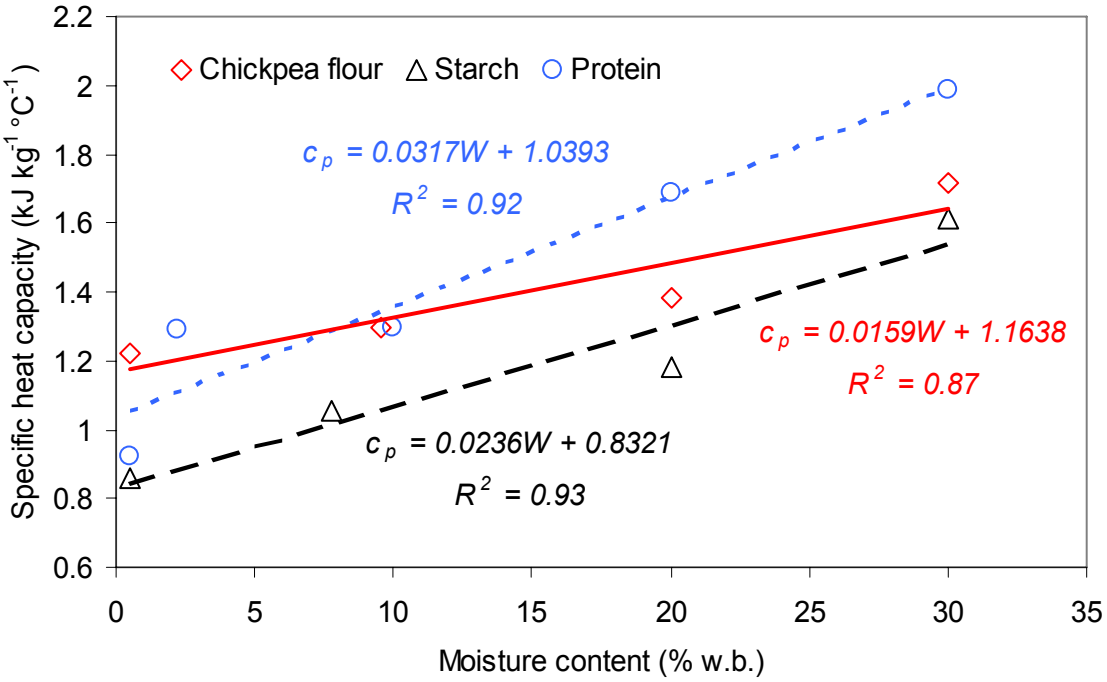

Figure 4.13 Change of specific heat with moisture content.

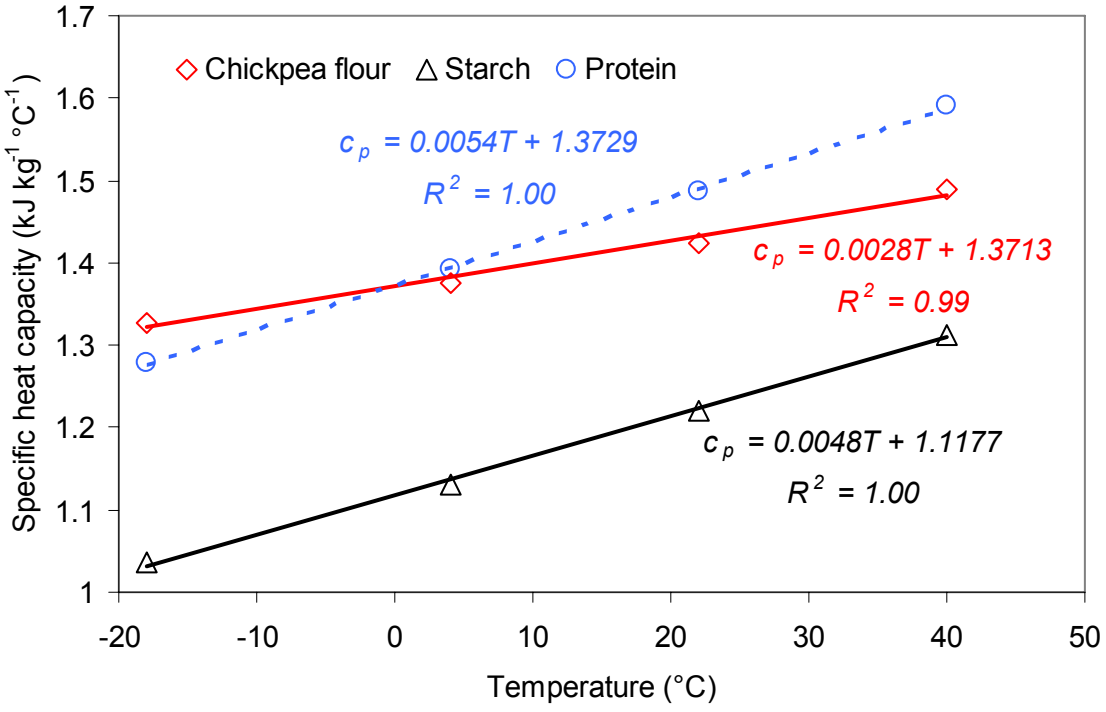

Figure 4.14 Change of specific heat with temperature.

4.8.3.3 Estimated thermal diffusivity values

Table 4.27 shows the thermal diffusivity values of chickpea flour and starch and protein fractions at four temperatures (–18, 4, 22, and 40°C) and three different bulk densities, with the corresponding error estimates calculated using Equation 3.22. Thermal diffusivity values for chickpea flour and starch and protein fractions were calculated at moisture contents of 9.6, 7.8, and 2.2% w.b., respectively. Thermal diffusivity did not show any specific trend with temperature. However, it decreased with an increase in bulk density. Starch fraction had a higher thermal diffusivity than did either chickpea flour or protein fraction.

4.8.3.4 Phase transition thermograms

The DSC thermograms of chickpea flour at three different moisture contents are depicted in Figure 4.15. Chickpea flour showed a major endothermic gelatinization peak which differed with moisture content. The DSC characteristics of chickpea flour have been summarized in Table 4.28. In general, as moisture content increased, the T_p and ΔT decreased and ΔH_p increased. By increasing moisture content, the tailing shoulder of the endothermic peak decreased; and hence, the ΔT decreased. The DSC thermogram of chickpea flour at a moisture content of 9.6% w.b. showed a minor endothermic peak at 109°C; this peak likely was associated with denaturation/aggregation temperature of protein in chickpea flour.

Table 4.27 Thermal diffusivity* of chickpea flour and starch and protein fractions at different temperatures and bulk densities.

Temperature (°C)	Chickpea flour		Starch fraction		Protein fraction	
	ρ_b (kg/m^3)	α ($\times 10^{-7}$ m^2/s)	ρ_b (kg/m^3)	α ($\times 10^{-7}$ m^2/s)	ρ_b (kg/m^3)	α ($\times 10^{-7}$ m^2/s)
–18	416.49	1.391 ± 0.057†	346.68	2.148 ± 0.129	335.06	1.691 ± 0.093
	456.02	1.387 ± 0.058	387.05	2.005 ± 0.110	375.12	1.646 ± 0.078
	504.12	1.311 ± 0.064	427.10	1.824 ± 0.107	414.98	1.520 ± 0.104
4	416.49	1.582 ± 0.070	346.68	2.110 ± 0.106	335.06	1.621 ± 0.097
	456.02	1.543 ± 0.073	387.05	2.011 ± 0.115	375.12	1.518 ± 0.068
	504.12	1.524 ± 0.196	427.10	1.843 ± 0.117	414.98	1.374 ± 0.059
22	416.49	1.564 ± 0.065	346.68	1.967 ± 0.150	335.06	1.570 ± 0.060
	456.02	1.575 ± 0.084	387.05	1.900 ± 0.101	375.12	1.432 ± 0.057
	504.12	1.506 ± 0.086	427.10	1.779 ± 0.132	414.98	1.354 ± 0.055
40	416.49	1.654 ± 0.064	346.68	2.185 ± 0.247	335.06	1.568 ± 0.100
	456.02	1.637 ± 0.108	387.05	1.998 ± 0.109	375.12	1.429 ± 0.053
	504.12	1.570 ± 0.061	427.10	1.819 ± 0.130	414.98	1.325 ± 0.058

ρ_b: bulk density

α: thermal diffusivity

* Values are averages of three estimates.

† Value following the mean is standard error.

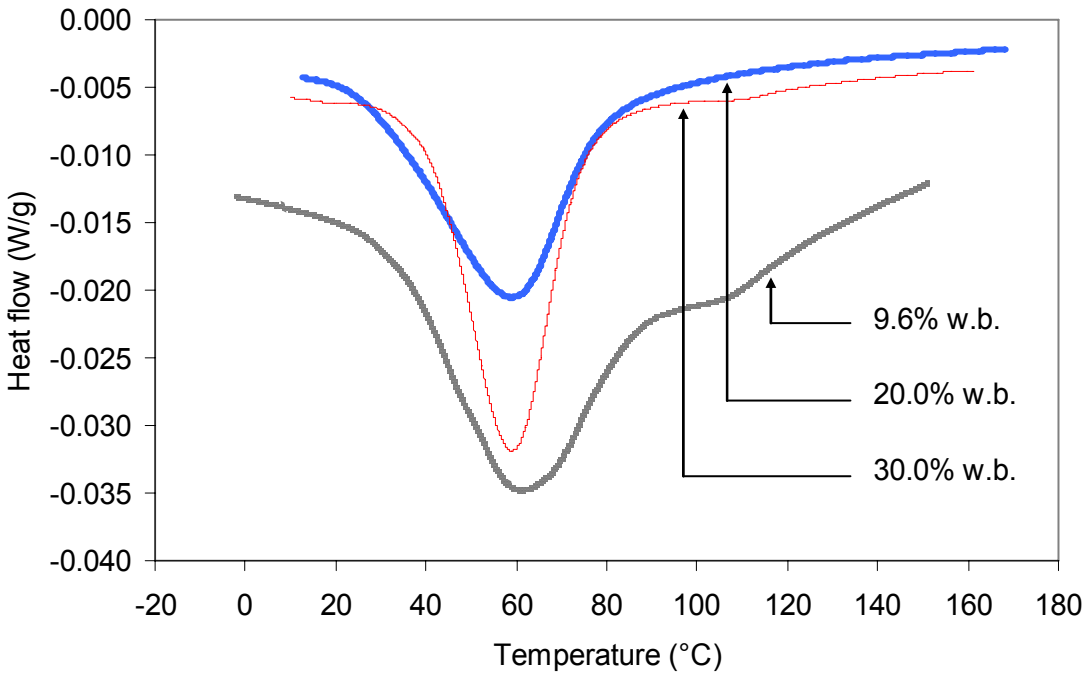

Figure 4.15 DSC thermograms of chickpea flour at three moisture contents (each data point was obtained from non-replicated experiment).

Figure 4.16 displays the DSC thermograms of starch fraction at three moisture contents. The glass transition phase was not observed at these moisture contents and no T_g was detected. The DSC thermograms presented a major endothermic peak at all three moisture contents; these peaks were associated with gelatinization of starch granules. As moisture content increased, the T_p decreased. T_p was between 67 and 68°C (Table 4.28), somewhat higher than for chickpea flour. The tailing shoulder was reduced with an increase in moisture content.

Figure 4.17 shows DSC thermograms of protein fraction at four moisture contents. Since all samples were low in starch content, none of them showed a T_p peak. Samples at all moisture contents presented a major endothermic peak over a temperature range of 144 to 182°C. As the moisture content increased, the tailing shoulder decreased and a peak with

higher resolution was obtained. The ΔH associated with denaturation and decomposition ranged from 20.1 to 388.0 J/g.

Table 4.28 DSC characteristics of chickpea flour and starch and protein fractions (data were obtained from non-replicated experiment).

Sample	W_w (% w.b.)	T_p (°C)	ΔT (°C)	ΔH_p (J/g)	T_d (°C)	ΔH_d (J/g)
Chickpea flour	9.6	63	62	6.0	109	2.1
	20.0	61	61	6.9	_	_
	30.0	60	57	7.2	_	_
Starch fraction	7.8	68	70	13.9	_	_
	20.0	67	58	14.6	_	_
	30.0	67	52	15.0	_	_
Protein fraction	2.2	_	_	_	182	20.1
	10.0	_	_	_	158	28.0
	20.0	_	_	_	144	223.2
	30.0	_	_	_	157	388.0

W_w: moisture content (wet basis)

T_p: peak gelatinization temperature

ΔT: width of the peak gelatinization temperature

ΔH_p: enthalpy of starch gelatinization

T_d: peak denaturation/aggregation or decomposition temperature

ΔH_d: enthalpy of denaturation/aggregation or decomposition of protein

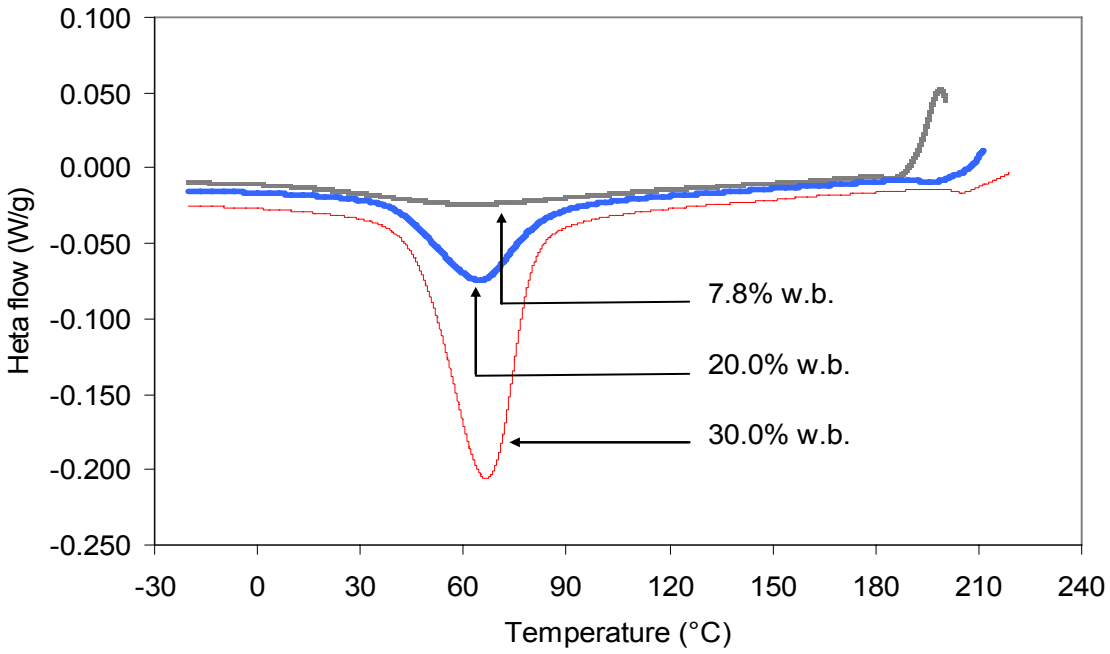

Figure 4.16 DSC thermograms of starch fraction at three moisture contents (each data point was obtained from non-replicated experiment).

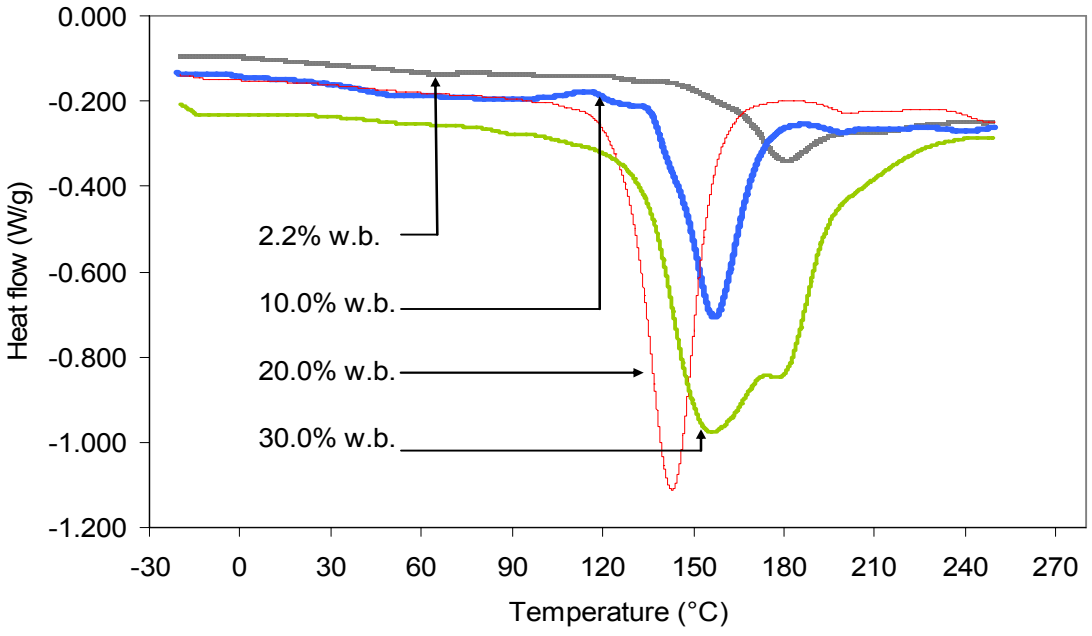

Figure 4.17 DSC thermograms of protein fraction at four moisture contents (each data point was obtained from non-replicated experiment).

4.8.4 Frictional properties

Presented in this section are results of experiments involving measurement of internal and external frictional properties of chickpea flour and starch and protein fractions.

4.8.4.1 Internal friction

Coefficient of friction, angle of internal friction, and cohesion values of chickpea flour and starch and protein fractions were determined at a moisture content in equilibrium with the surrounding atmosphere at a temperature of 22°C. The moisture content of chickpea flour and starch and protein fractions was 10.6, 8.4, and 2.3% d.b., respectively. Chickpea flour showed the highest coefficient of internal friction and angle of internal friction among samples (Table 4.29). Figure 4.18 shows the relationship between normal stress and shear stress of the experimental samples. The relationship was expressed in terms of Equation 3.24. Equation 3.24 confirmed the linear relationship between shear stress and normal stress with coefficient of internal friction as the slope and cohesion (shear stress at zero normal stress) as the intercept. Values for cohesion of the three powder samples are also listed in Table 4.29. Starch fraction had the highest cohesion among three powder samples.

Table 4.29 Coefficient of internal friction, angle of internal friction and cohesion of chickpea flour and starch and protein fractions*.

Sample	W_d (% d.b.)	μ_i	ϕ_i (Degree)	Cohesion		
				Estimate (kPa)	R^2	SEE
Chickpea flour	10.6	0.68	34.26	3.46	1.00	0.73
Starch fraction	8.4	0.63	32.01	7.11	0.99	1.83
Protein fraction	2.3	0.64	32.44	3.22	1.00	1.35

* Values are averages of three replicates.

W_d: moisture content

μ_i: coefficient of internal friction

ϕ_i : angle of internal friction

SEE: standard error of estimate

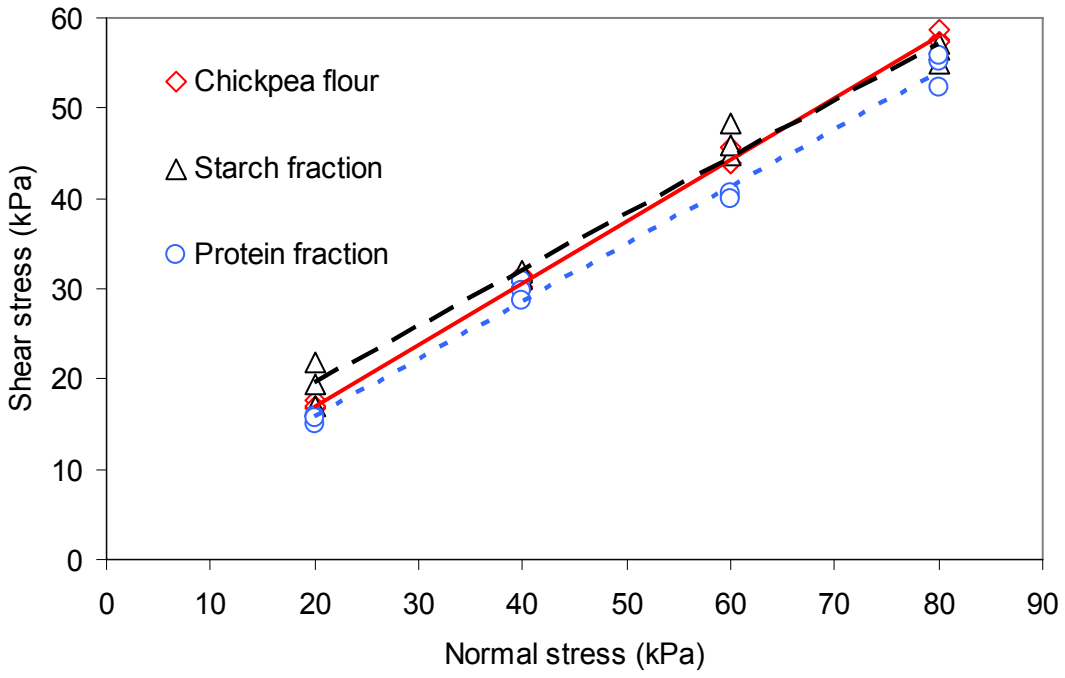

Figure 4.18 Normal stress-shear stress plot for internal friction measurement of chickpea flour and starch and protein fractions.

4.8.4.2 External friction

The coefficient of external friction values, angle of external friction, and adhesion of chickpea flour and starch and protein fractions on polished steel, concrete (plastic smooth finish), Teflon, and polypropylene are presented in Table 4.30. The test was conducted for each sample, like the internal friction test, at a moisture content in equilibrium with the surrounding atmosphere at a temperature of 22°C. Figures 4.19, 4.20, and 4.21 show the relationship between normal stress and shear stress for chickpea flour and starch and protein fractions, respectively. The relationship between normal stress and shear stress for all three samples was expressed in terms of Equation 3.25, which fitted to the data very well. In all three samples, the highest coefficient of external friction and angle of external friction were obtained from concrete, and the lowest from polypropylene. Starch fraction had a lower coefficient of external friction and angle of external friction on steel, Teflon, and polypropylene than did chickpea flour and protein fraction.

The lowest adhesion was obtained on a polypropylene surface. All three samples had the highest adhesion on a concrete surface, followed by Teflon and steel surfaces. The protein fraction showed the lowest adhesion value (0.00 kPa) on a steel surface.

Table 4.30 Coefficient of external friction, angle of external friction and adhesion of chickpea flour and starch and protein fractions on different friction surfaces*.

Sample	Friction surface	μ_e	ϕ_e	Adhesion		
			(Degree)	Estimate (kPa)	R^2	SEE
Chickpea flour	Steel	0.387	21.18	2.59	0.98	1.48
	Concrete	0.615	31.59	4.34	1.00	1.06
	Teflon	0.381	20.83	3.68	0.99	0.70
	Polypropylene	0.304	16.89	1.82	1.00	0.38
Starch fraction	Steel	0.305	16.95	3.40	0.99	0.58
	Concrete	0.690	34.61	3.13	0.99	1.76
	Teflon	0.296	16.49	3.29	1.00	0.33
	Polypropylene	0.278	15.52	1.36	0.99	0.53
Protein fraction	Steel	0.378	20.73	0.00	1.00	1.12
	Concrete	0.628	32.11	1.49	1.00	0.99
	Teflon	0.417	22.65	0.57	1.00	0.48
	Polypropylene	0.343	18.95	0.46	1.00	0.57

* Values are averages of three replicates.

μ_e: coefficient of external friction

ϕ_e: angle of external friction

SEE: standard error of estimate

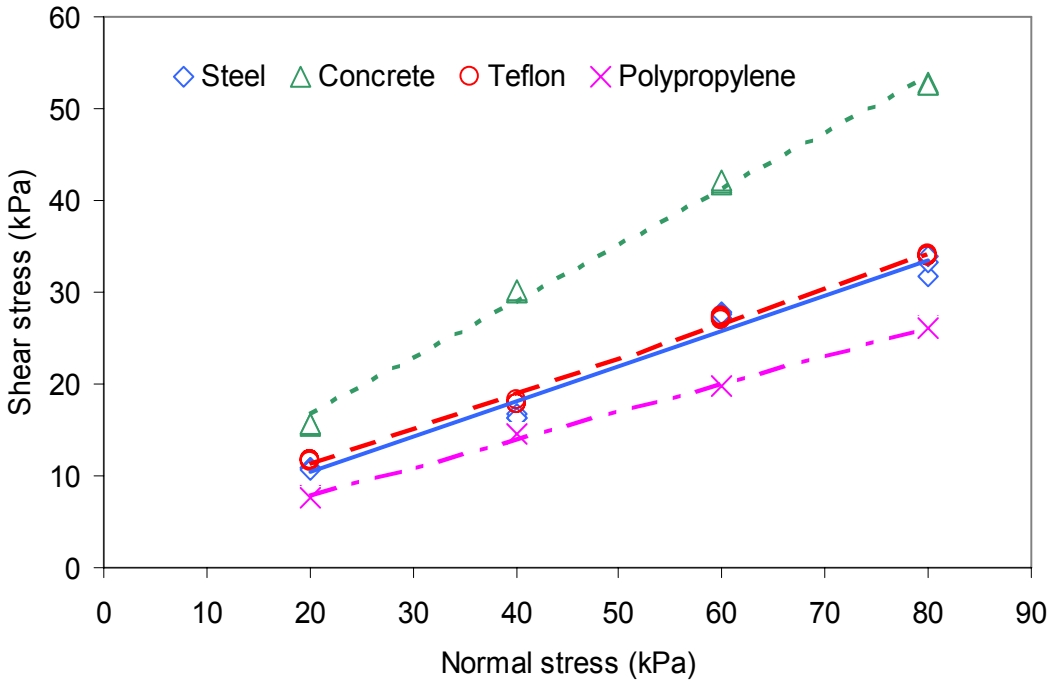

Figure 4.19 Normal stress-shear stress plot for chickpea flour on different friction surfaces.

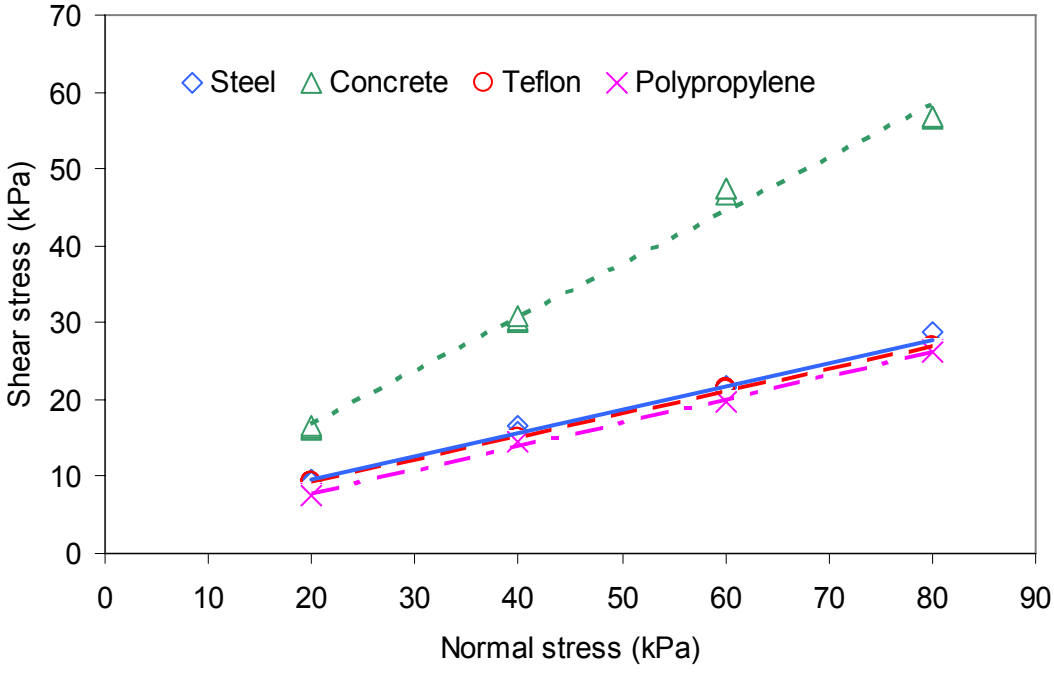

Figure 4.20 Normal stress-shear stress plot for starch fraction on different friction surfaces.

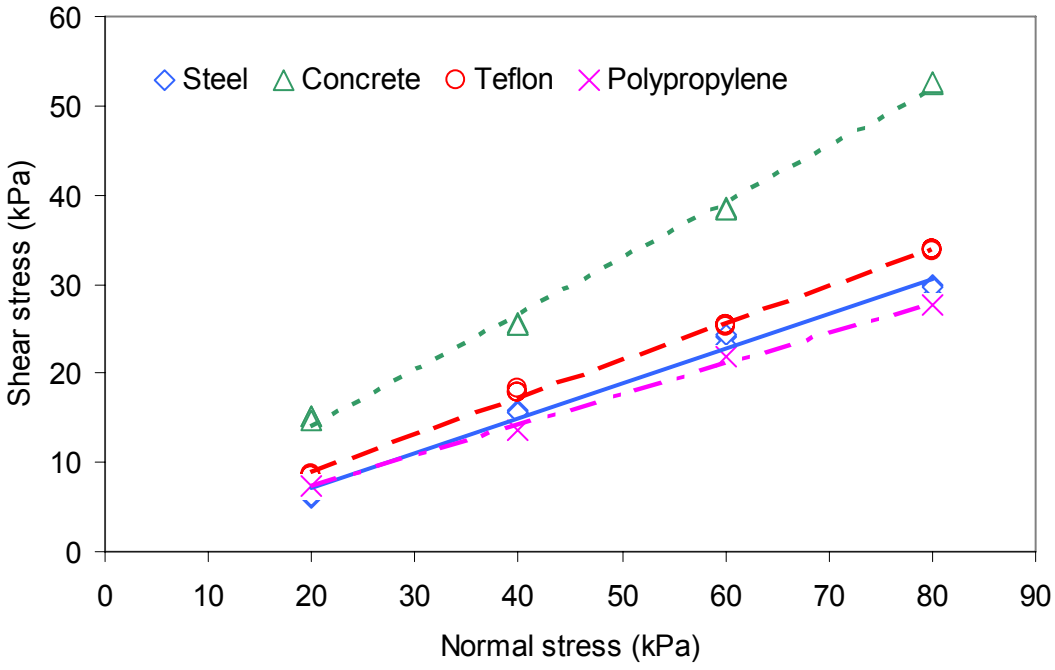

Figure 4.21 Normal stress-shear stress plot for protein fraction on different friction surfaces.

4.8.5 Compressibility and stress relaxation behaviour

Figure 4.22 shows a typical force-time relationship during compression of chickpea flour and starch and protein fractions. The actual compressive force was slightly higher than preset compression loads due to the inertia of the plunger of the Instron testing machine (that could not be stopped instantaneously). The curves were similar in deformation and relaxation and the required time to reach the preset load (4000 N) was similar for all test samples. Table 4.31 shows the results of compression models fitted to the experimental data. Using SAS, the linear regression was used to determine the constants of linear models including the Walker, Jones, and Barbosa-Cánovas and co-workers models; PROC NLIN was used to determine the constants of the Cooper and Eaton, and Kawakita and Lüdde

models. In terms of R^2, all five models showed a good fit. However, the Kawakita and Lüdde model had a higher standard error of estimate, for all three samples, than did the other models indicating that this model did not fit as well with the experimental data. Among all models, the Cooper and Eaton model had the best fit with the experimental data, with a high R^2 (ranging from 0.97 to 0.99) and a very low standard error of estimate for all three samples.

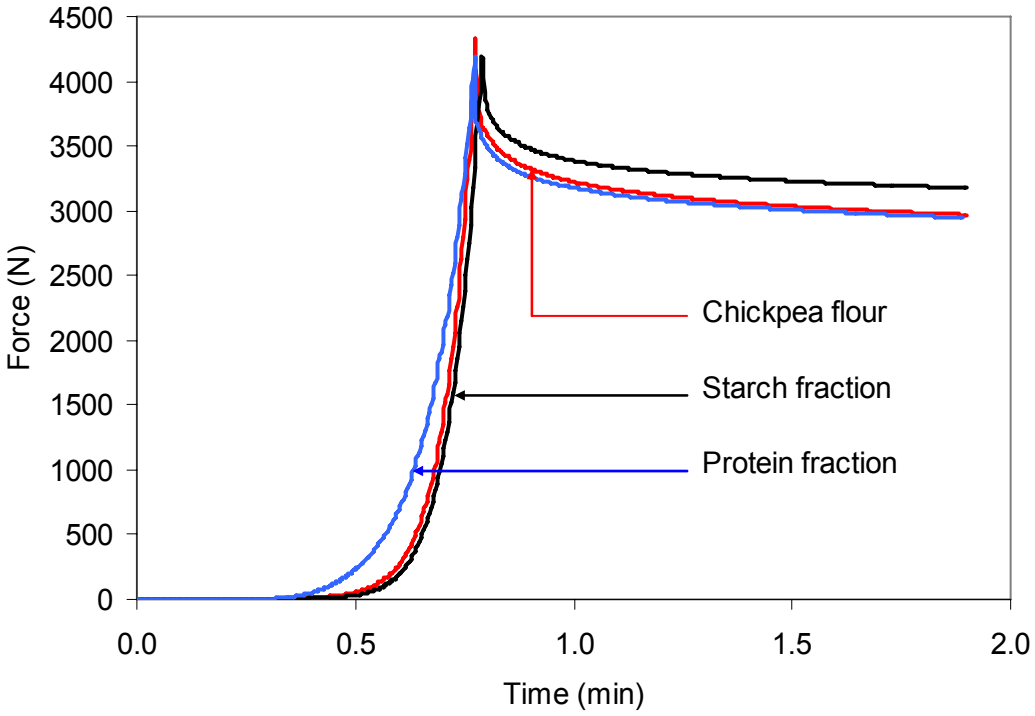

Figure 4.22 Typical force-time relationship during compression test of chickpea flour and starch and protein fractions.

Table 4.31 Constants and statistical parameters of compression models.

Walker model: $\frac{V}{V_0} = a \ \ln P + b$

	a (compressibility)	b	R^2	SEE*
Chickpea flour	-9.15×10^{-3}	3.51	0.96	0.46×10^{-2}
Starch fraction	-1.08×10^{-2}	4.34	0.94	0.73×10^{-2}
Protein fraction	-8.68×10^{-3}	3.84	0.97	0.42×10^{-2}

Jones model: $\ln \rho_b = a \ \ln P + b$

	a (compressibility)	b	R^2	SEE
Chickpea flour	2.68×10^{-3}	– 0.88	0.96	0.13×10^{-2}
Starch fraction	2.55×10^{-3}	– 1.06	0.94	0.17×10^{-2}
Protein fraction	2.32×10^{-3}	– 1.09	0.97	0.11×10^{-2}

Barbosa-Cánovas and co-workers model: $\frac{\rho - \rho_0}{\rho_0} = a \log \sigma + b$

	a (compressibility)	b	R^2	SEE
Chickpea flour	6.26×10^{-3}	– 0.02	0.96	0.13×10^{-2}
Starch fraction	5.95×10^{-3}	– 0.01	0.94	0.17×10^{-2}
Protein fraction	5.41×10^{-3}	– 0.01	0.92	0.11×10^{-2}

Cooper and Eaton model: $\frac{V_0 - V}{V_0 - V_s} = a_1 \exp\left(\frac{-k_1}{P}\right) + a_2 \exp\left(\frac{-k_2}{P}\right)$

	a_1	a_2	k_1 (MPa)	k_2 (MPa)	R^2	SEE
Chickpea flour	0.022	0.012	4617.10	349369.00	0.99	0.12×10^{-2}
Starch fraction	0.021	0.010	3630.40	448156.00	0.98	0.14×10^{-2}
Protein fraction	0.017	0.015	2863.50	655996.00	0.97	0.14×10^{-2}

Kawakita and Lüdde model: $\frac{P}{C} = \frac{1}{ab} + \frac{P}{a}$

	a	b	R^2	SEE
Chickpea flour	0.02	-1.33×10^{73}	1.00	7.74×10^{4}
Starch fraction	0.02	-2.41×10^{74}	1.00	7.59×10^{4}
Protein fraction	0.07	-5.34×10^{36}	1.00	1.58×10^{6}

* SEE: standard error of estimate

Figure 4.23 shows typical force-time relationships representing the deformation and relaxation phases during compression of test samples at preset compression loads of 500, 1000, 2000, 3000, and 4000 N. Similar to the compressibility test, the actual compressive force was slightly higher than the preset compression loads. The deformation portion of the curve had a similar shape and trend for all preset loads. At the beginning of the test, the compression was small, with the compressive force increasing rapidly thereafter.

Table 4.32 represents the maximum compressive pressure and asymptotic modulus of chickpea flour and starch and protein fractions at preset compression loads. Starch fraction showed the highest asymptotic modulus at all preset loads, except at 500 N. Chickpea flour had the lowest asymptotic modulus at all preset loads. The trend for the

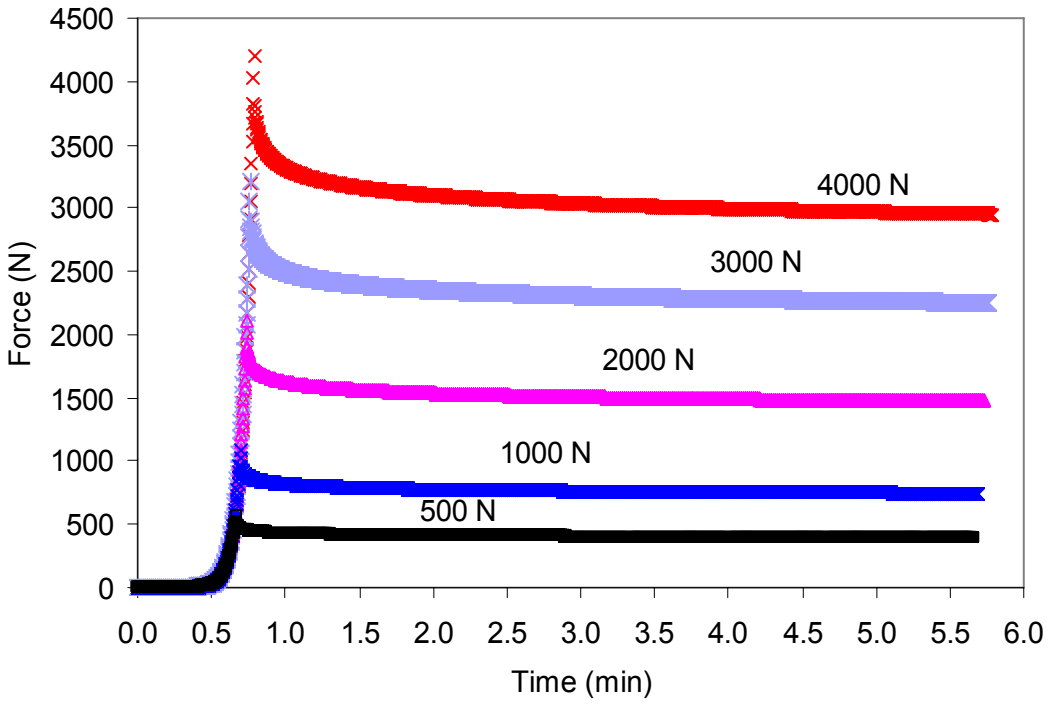

Figure 4.23 Typical force-time relationship during compression and relaxation of starch fraction powder at different setpoint compression forces.

increase in asymptotic modulus versus the maximum compressive pressure is presented in Figure 4.24. Starch fraction had a higher asymptotic modulus than did the other samples. When the asymptotic modulus values were compared to the corresponding physical properties (Table 4.21), the maximum and minimum asymptotic modulus values corresponded to the highest and lowest initial sample porosities, respectively.

Table 4.32 Maximum compressive load and asymptotic modulus at different applied loads.

Sample	Load (N)	Maximum compressive pressure† (MPa)	Asymptotic modulus† (MPa)
Chickpea flour	500	1.11 ± 0.01*	27.72 ± 0.17
	1000	2.19 ± 0.03	52.44 ± 1.36
	2000	4.37 ± 0.05	105.40 ± 2.69
	3000	6.47 ± 0.04	160.88 ± 2.47
	4000	8.71 ± 0.08	224.29 ± 2.56
Starch fraction	500	1.11 ± 0.01	36.34 ± 0.82
	1000	2.21 ± 0.02	66.61 ± 1.76
	2000	4.42 ± 0.03	128.84 ± 1.22
	3000	6.51 ± 0.02	188.52 ± 2.52
	4000	8.58 ± 0.09	242.80 ± 2.77
Protein fraction	500	1.07 ± 0.00	37.23 ± 0.20
	1000	2.14 ± 0.01	65.60 ± 0.70
	2000	4.24 ± 0.03	120.74 ± 1.64
	3000	6.35 ± 0.03	169.18 ± 0.78
	4000	8.54 ± 0.04	230.01 ± 2.94

† Values are averages of three replicates.

* Value following the mean is standard error.

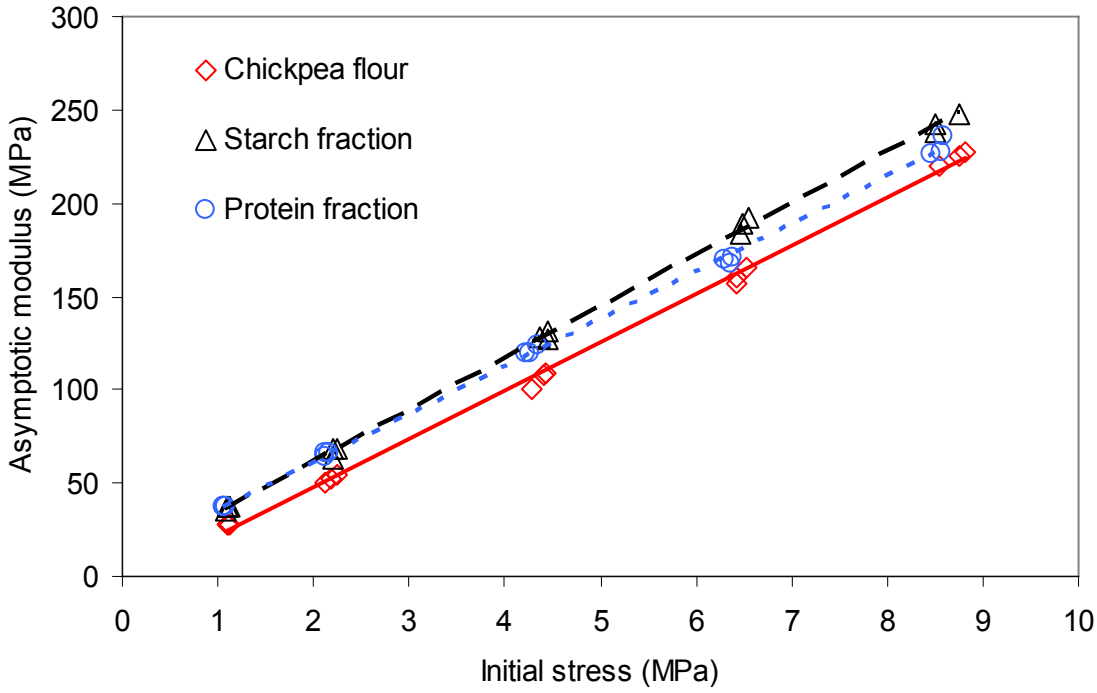

Figure 4.24 Relationship between maximum compressive pressure (initial stress) and asymptotic modulus of compressed chickpea flour and starch and protein fractions.

4.8.6 Water hydration capacity, emulsion capacity, and emulsion stability

The WHC, emulsion capacity, and emulsion stability of chickpea flour and starch and protein fractions are presented in Table 4.33. In terms of WHC, starch fraction showed the highest value, followed by chickpea flour. In terms of emulsion capacity and stability, chickpea flour had the highest emulsion capacity and, therefore, was able to absorb more oil droplets in an emulsion than were starch and protein fractions. In contrast, protein fraction showed the highest emulsion stability hence a lower percentage of water was released from the emulsion of protein fraction. Chickpea flour had lower emulsion stability than either starch or protein fraction; hence emulsion of chickpea flour released more water when stressed by centrifugation.

Table 4.33 WHC, emulsion capacity, and emulsion stability values*.

Sample	WHC† (mL/g)	Emulsion capacity (mL/g)	Emulsion stability (%)
Chickpea flour	0.93 ± 0.01 ‡	40.60 ± 0.35	44.22 ± 0.57
Starch fraction	1.32 ± 0.01	0.50 ± 0.0	74.42 ± 0.59
Protein fraction	0.91 ± 0.01	0.58 ± 0.02	93.78 ± 0.45

* Values are averages of three replicates.

† Water hydration capacity

‡ Value following the mean is standard error.

4.8.7 Foaming capacity and stability

Table 4.34 shows the foaming capacity (specific volume and volume increase of foam after whipping) of chickpea flour and the protein fraction. The starch fraction was not able to generate stable foam during whipping. The protein fraction had lower specific volume and volume increase than did chickpea flour since the protein fraction had a higher lipid content.

The foaming stability of chickpea flour and protein fraction is presented in Figures 4.25 and 4.26, respectively. In both samples, the volume of foam decreased exponentially with time. The foam volume of protein fraction diminished with a steeper slope than did that of chickpea flour. There was no marked difference in the final volume of the two samples.

Table 4.34 Specific volume and foaming capacity of chickpea flour and protein fraction.

Sample	Specific volume* (mL/g)	Volume increase* (%)
Chickpea flour	12.78 ± 0.11†	30.00 ± 3.06
Protein fraction	12.22 ± 0.59	21.67 ± 1.16

* Values are averages of three replicates.

† Value following the mean is standard error.

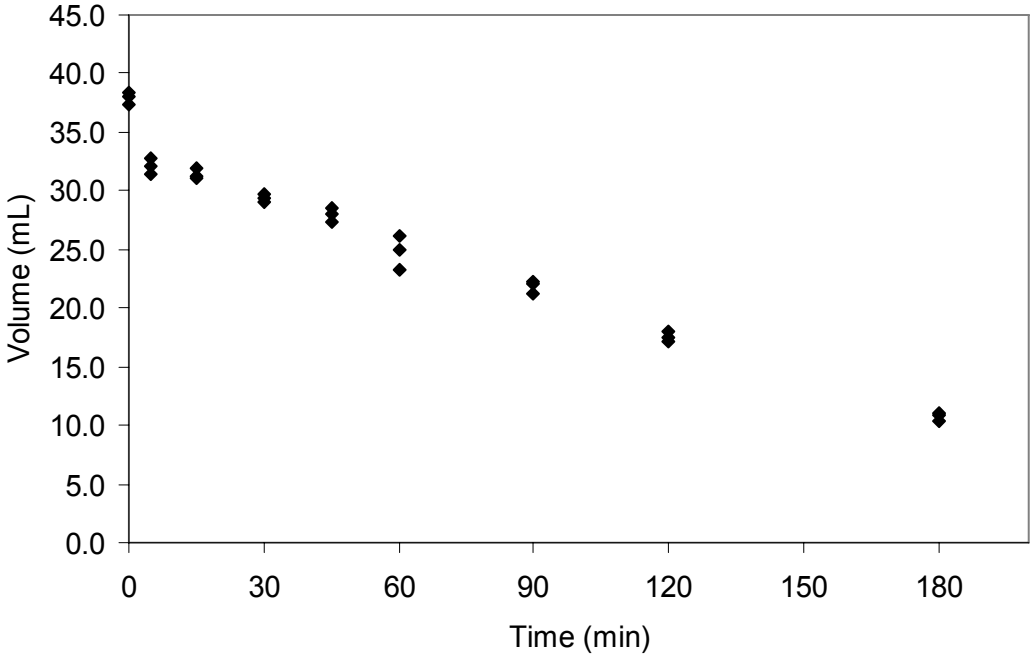

Figure 4.25 Experimental values of the foaming stability of chickpea flour versus time.

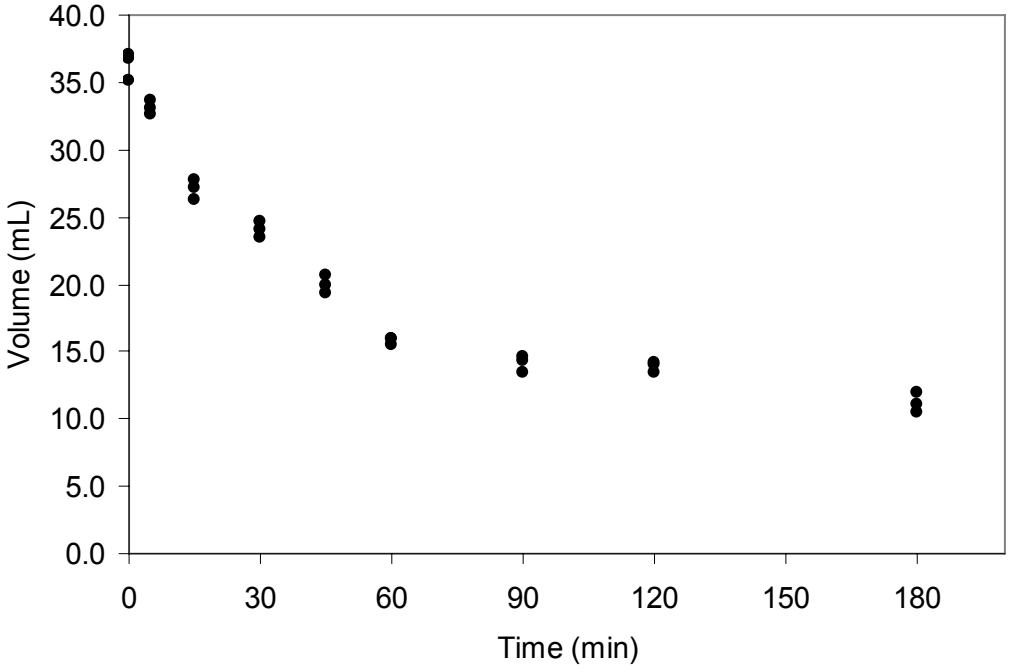

Figure 4.26 Experimental values of the foaming stability of protein fraction versus time.

5. DISCUSSION

Knowledge of chemical, physical, and functional properties of chickpea flour is important in understanding the starch-protein separation process. This study shows factors affecting starch-protein separation from chickpea flour and factors involved in the hydrocyclone operation. The effect of two different media on the hydrocyclone performance is discussed in this chapter. Towards the end, the physical and functional properties of chickpea flour and fractionated products relevant to future utilization are discussed.

5.1 Comparison of chickpea flour composition with literature values

The chemical composition of pin-milled chickpea flour is comparable to values reported by other researchers (Jood et al. 1998; Sosulski et al. 1987; Han and Khan 1990a; Sokhansanj and Patil 2003). The starch content obtained (Table 4.1) was lower than the values reported by Sosulski and co-workers (1987) (52.5% d.b.), Jood and co-workers (1998) (from 55 to 58% d.b.), and Sokhansanj and Patil (2003) (60.6% d.b.). Protein content was higher than the value obtained by Sosulski and co-researchers (1987) (17.7% d.b.). It was in the same range reported by Jood and co-workers (1998) (from 24.59 to 27.32% d.b.) and Sokhansanj and Patil (2003) (from 14.9 to 29.6% d.b.). The fat content of chickpea flour was lower than the value reported by Sosulski and co-workers (1987) (7.2% d.b.) and was greater than the value reported by Jood and co-workers (1998) (between 4.16 and 5.66% d.b.) and

Sokhansanj and Patil (2003) (5.0% d.b.). Total dietary fibre content was lower than the value reported by Han and Khan (1990a) (15.4% d.b.). The differences can be attributed to the differences in the cultivars studied, and environmental effects on a particular cultivar. The relatively high total dietary fibre content of dehulled chickpea flour (11.0% d.b.) was undesirable since fine fibre and cell wall material tend to co-settle with the starch fraction and reduces its purity (Ratnayake et al. 2002).

5.2 Equation for surface charge of chickpea flour

Chickpea flour slurry was negatively charged (–16.5 ± 0.6 mV) showing that the negatively charged (acidic) amino acids dominated the positively charged (basic) amino acids (Nelson and Cox 2005). Titration of chickpea flour slurry (Figure 4.1) showed that its isoelectric point was at pH 4.3, which is the most unstable pH for protein particles in slurry. The following model (Equation 5.1) characterized the relationship between the zeta potential and pH. The R^2 of 0.96 and standard error of estimate of 3.48 showing good fit to data (Figure 5.1).

$$ZP = -36.22 \ \ln(\text{pH}) + 55.49 \tag{5.1}$$

where ZP is zeta potential. The negative sign of the first-order coefficient in the proposed model also confirmed that the zeta potential was inversely proportional to pH.

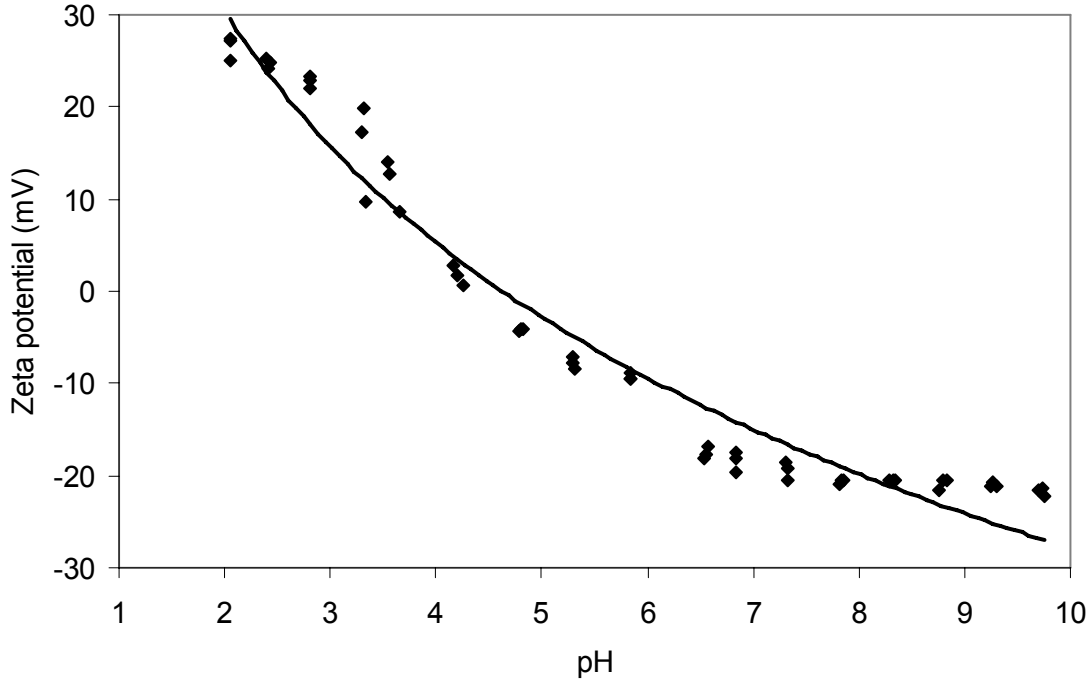

Figure 5.1 Relationship between the zeta potential and pH in chickpea flour slurry.

This study also confirmed the pH range (4.3 to 4.5) obtained for the NSI of chickpea flour (Figure 4.8). This pH range was used by other researchers in isolating protein from pulse grains (Sánchez-Vioque et al. 1999; Tian et al. 1999; Sosulski and Sosulski 1986; Sumner et al. 1981). The maximum protein solubility was obtained at pH 9.0 (90% nitrogen solubility). A similar value was reported by Bencini (1986) for chickpea flour. Since pulse protein has the highest solubility at pH 9.0, this pH was used by other researchers for dispersing of protein and separation of protein and starch (Sosulski and Sosulski 1986; Sumner et al. 1981). The NSI trend obtained was similar to those reported by Anderson and Romo (1976), Reichert and Youngs (1978), Han and Khan (1990b), and Sánchez-Vioque and co-workers (1999) for chickpea flour, as well as Thompson (1977) for mung bean, Beuchat (1977) for peanut flour, and Johnson and Brekke (1983) for peas.

5.3 Discussion on particle size distribution of chickpea flour

The particle size distribution of feed material, i.e. chickpea flour, affects separation efficiency (Jones and McGinnis 1991). A large particle size, i.e. greater than 100 to 150 μm, increases the chance of presence of aggregated starch-protein; whereby, protein particles are collected in the starch fraction and the protein yield is reduced (Owusu-Ansah and Mc Curdy 1991).

Figure 5.2 shows the particle size distribution of chickpea flour expressed as volume fraction and cumulative undersize percentage. The model describing the relationship between particle size and cumulative undersize is presented by the following equation:

$$y = 98.26\left[1 - \exp\left(-2.53\times10^{-2}\,x\right)\right] \tag{5.2}$$

where: y = cumulative undersize fraction (% volume); and

x = particle size (μm).

This model fitted to the data very well with R^2 of 0.99 and standard error of estimate of 3.61. The proposed model overestimated the undersize fraction in the particle size range from 70 to 210 μm and from 330 μm and higher. Figure 5.2 shows that pin-milled chickpea flour had a cut-size, defined as the particle size at 50% cumulative undersize (Svarovsky 1984), of less than 40 μm and had a geometric mean diameter of 25.56 μm. However, more than 30% of particles had particle sizes greater than 100 μm. Large particles are due to the presence of agglomerated protein particles and starch granules, remaining hull, and cell wall material. These particles in the flour reduce the yield of the overflow fraction and the purity of the starch fraction. The yield of the overflow would improve if chickpea were dehulled completely.

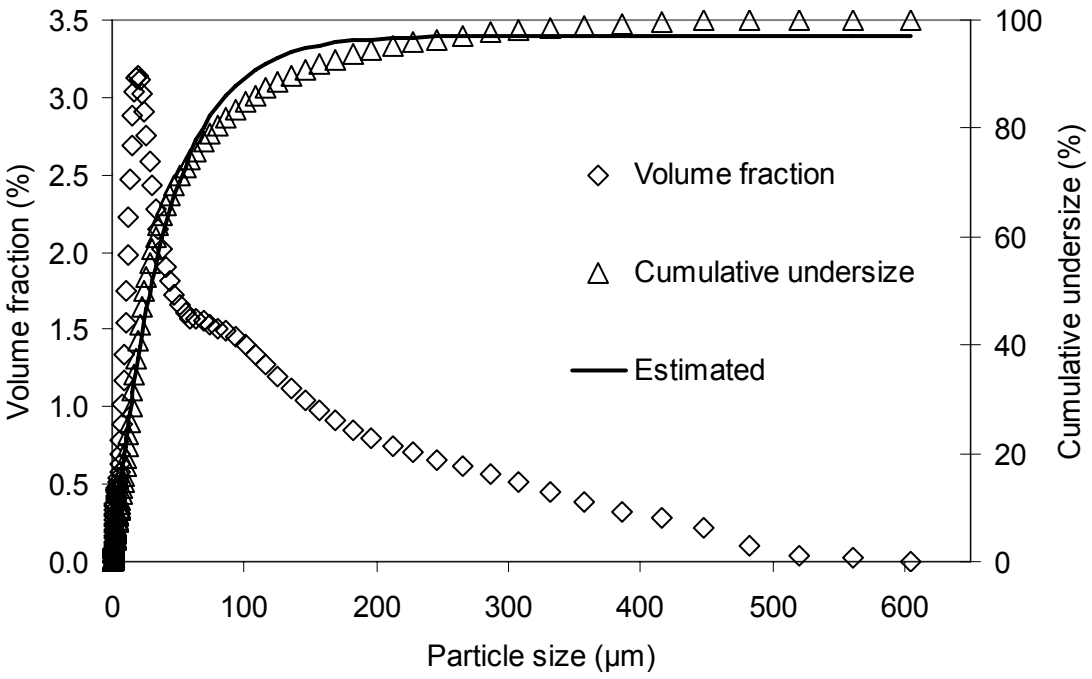

Figure 5.2 Relation ship between particle size and volume fraction and cumulative undersize of chickpea flour.

5.4 Comparison of geometric size and form factor of starch granules with literature values

Values obtained in the current study for the size and form factor of starch granules are similar to those obtained by Davydova and co-workers (1995) for pea starch. The size of starch granules (between 13.81 and 18.92 µm) was lower than values reported by Davydova and co-workers (1995) for pea starch granules (between 22 and 30 µm). Both major and minor starch granule diameters were in the range reported by Hoover and Sosulski (1991) for chickpea starch granules (8-54 µm). Comparison of mean values (Table 4.4) with literature values shows that the major and minor diameters were smaller than those of pinto bean, navy bean, and field pea (Gujska et al. 1994). The high value of form factor, i.e. close to 1.0, reinforced the assumption in future calculations that all particles were spherical. A

form factor of 1.0 was not observed, showing that none of the starch granules was a perfect sphere or circular object. However, Davydova and co-workers (1995) reported that pea starch granules had form factors ranging from 0.2 to 1.0 and reported a lower mean form factor (0.74 to 0.78) than was observed in this study (0.83).

5.5 Discussion on starch-protein interactive force

The results of ITC revealed that there was no significant chemical interactive force between starch granules and protein particles in the chickpea flour. However, it is likely that physical forces, such as electrostatic force, may exist. This result also confirmed that application of physical force, such as gravity and centrifugal force, could separate starch granules and protein particles.

5.6 Discussion on starch-protein separation from chickpea flour

Starch granules differ from protein particles in terms of particle size. Therefore, a hydrocyclone was employed to separate starch and protein from chickpea flour as used by Vose (1980) for field pea and horsebean and by Singh and Eckhoff (1995) for corn. Since chickpea grain has a relatively high fat content compared to other starchy legumes, the separation was initiated using isopropyl alcohol, a good fat solvent, as medium to reduce the stickiness of particles. Thus, the effect of high fat content was decreased.

5.6.1 Effect of inlet pressure

As Table 4.5 shows, hydrocyclone operation at a high inlet pressure led to a significant ($P < 0.05$) increase in the protein content of the overflow fraction, although it did not make a

significant difference in the starch content of the underflow fraction. Furthermore, a high inlet pressure increased both starch and protein separation efficiencies (Table 4.6). This result was in agreement with Svarovsky (1984) who stated that increasing the pressure drop improved the separation in the hydrocyclone. The effect of high inlet pressure on separation efficiency was also attributed to the shear force applied to chickpea flour particles. At high inlet pressure, the shear force would break down the starch-protein bond and remove protein particles from starch granule surfaces.

Table 4.10 presents the geometric mean diameter of the overflow and underflow fractions at three different inlet pressures using two media. These results confirm that the current hydrocyclone and set-up was able to separate particles based on their particle size as small particles were collected in the overflow and large ones were separated into the underflow. Additionally, in each medium, the geometric mean diameter of the overflow and underflow decreased with an increase in inlet pressure. This result shows that low inlet pressure did not provide enough shear force to break up agglomerated particles, which resulted in lower starch and protein separation efficiencies. Again it seems that the higher inlet pressure provided more shear force, improving segregation of flour particles, principally starch granules and protein particles. Thus, starch granules and protein particles could be separated with higher efficiency at higher inlet pressures.

The medium also had a marked effect on geometric mean diameter. At a given inlet pressure, isopropyl alcohol resulted in a smaller geometric mean diameter in the overflow and underflow fractions than was the case with deionized water. This phenomenon was attributed to the solubility of fat in isopropyl alcohol. By dissolving the lipid in chickpea flour in isopropyl alcohol, chickpea flour particles segregated more easily and particle

stickiness was reduced markedly. Therefore, the overflow and underflow fractions had lower geometric mean diameters in isopropyl alcohol than in deionized water.

5.6.2 Comparison between single- and double-pass processes

The double-pass hydrocyclone process in this study increased significantly the starch content in the underflow, but did not significantly increase the protein content in the overflow (Table 4.7), over that of the single-pass process. However, this kind of process reduced the starch and protein separation efficiencies (Table 4.7). Using a double-pass hydrocyclone process led to re-splitting of the overflow (O1) and underflow (U1) to a new series of overflows (OO1 and OU1) and underflows (UU1 and UO1). Accordingly, some starch granules in U1 went to the overflow and a portion of protein particles in O1 went to the underflow. Strictly speaking, increasing the number of hydrocyclone passes increased starch and protein contents in the underflow and overflow, respectively with some starch lost to the overflow and some protein lost to the underflow.

5.6.3 Effect of two media in the separation process

Tables 4.8 and 4.9 show the performance of the two media (isopropyl alcohol and water) in the hydroclone separation process. Isopropyl alcohol was not effective in starch-protein separation in the hydrocyclone. This medium resulted in a lower starch content in the underflow and a lower protein content in the overflow than was the case with deionized water. This problem was attributed to a difference in the flow resistance of isopropyl alcohol and deionized water. Isopropyl alcohol has lower density and higher viscosity than deionized water. Therefore, separation forces applied to the particles in isopropyl alcohol

were different than those applied in deionized water. The fluid pressure, which causes rotational motion and flow resistance (Bradley 1965), plays an important role on particle separation in the hydrocyclone. As the flow resistance of the cyclone increases, the solid recovery improves (Svarovsky 1984). When a particle along with the fluid enters into the hydrocyclone centrifugal field, two forces are applied to the particle and fluid. Centrifugal force having outward radial direction results in the underflow fraction; and drag force having inward radial direction results in the overflow fraction.

Table 4.16 presents some hydrodynamic characteristics and centrifugal force applied to the underflow particles using isopropyl alcohol and deionized water. Comparison of each characteristic in the two media shows that the inlet pressure was directly proportional to the volume flow rate, tangential velocity of particle, centrifugal acceleration, and *g*-force. The centrifugal force is a function of the centrifugal acceleration and particle mass (Equations 2.2 and 2.3). The expectation was that the centrifugal force increases with an increase in inlet pressure and centrifugal acceleration. This expectation would have been borne out if the particle mass had been identical at all inlet pressures. In reality, as inlet pressure was increased, the size of particles gathered in the overflow and the underflow decreased, as discussed earlier. Thus, the mass of particles gathered decreased with an increase in inlet pressure and a decrease in particle size since particle density was constant. Consequently, the centrifugal force decreased with an increase of inlet pressure and was inversely proportional to the inlet pressure.

At a given inlet pressure, the slurry in isopropyl alcohol had higher tangential velocity, centrifugal acceleration, and *g*-force. The high value of *g*-force was due to higher tangential velocity in isopropyl alcohol compared to deionized water. However, the

centrifugal force in isopropyl alcohol was lower than in deionized water. The starch-protein separation process in isopropyl alcohol resulted in smaller particle size than in deionized water, as already discussed. Therefore, the particle mass in isopropyl alcohol was lower than that in deionized water. Thus, the centrifugal force applied to the particles in isopropyl alcohol was lower than that in deionized water. The *g*-force calculated in this study ranged from 7,000 to 14,000 × *g*, which was in the range reported by Rushton and co-workers (1996). They stated that a hydrocyclone provides high *g*-force, ranging from 800 × *g* in a large diameter hydrocyclone, to 50,000 × *g* in a small diameter hydrocyclone. Grady and co-workers (Year Unknown) also reported *g*-force values as high as 10,000 × *g* for a 10-mm hydrocyclone, the same hydrocyclone diameter as employed in the current study. The *g*-force in this work was high and comparable to values reported in literature.

Protein particles are small particles and reach equilibrium radial orbit at a smaller radius. Therefore, they tend to move to the overflow by drag force (Svarovsky 1990; Svarovsky 1984). Table 4.17 shows the estimated drag force and related values acting on overflow particles using isopropyl alcohol and deionized water. Comparison of summarized values for each medium demonstrates that inlet pressure was inversely proportional to the relative velocity between the fluid and particle and the Reynolds number of the particle. However, the drag coefficient directly increased with inlet pressure. Reynolds number of particle was also inversely proportional to drag coefficient. This phenomenon was in agreement with the well-established curve showing the relationship between Reynolds number of a spherical particle and drag coefficient (McCabe et al. 2005; Rushton et al. 1996; McCabe et al. 1993; McCabe and Smith 1976). The estimates also agreed with the trend of the drag coefficient decreasing with an increase in Reynolds number of particle (Svarovsky

1990; Svarovsky 1984). The Reynolds numbers of particles in this study were low (less than 2) as explained by Svarovsky (1984) for such a hydrocyclone where used for separation of fine particles. The highest drag force was obtained at the lowest inlet pressure in each medium. Decreasing the inlet pressure reduced starch and protein separation efficiencies, as discussed before. Therefore, the low separation efficiency at low inlet pressure corresponded to the presence of a high drag force in the hydroclone. The drag force in the hydrocyclone resulted in the overflow fraction (Svarovsky 1990; Bradley 1965). It seems that a high drag force which is greater than the force required to move just fine particles, i.e. protein particles, to the overflow, resulted in the moving of some of the coarse particles, i.e. starch granules, to the overflow. As a result, not only is the overflow contaminated with starch granules, but the yield and starch content of the underflow is reduced as well.

Comparison of the two media at a given inlet pressure shows that deionized water had a higher relative velocity between the fluid and particle and a higher Reynolds number of particle than did isopropyl alcohol. The high value of Reynolds number was due to the higher density and lower viscosity of deionized water compared to isopropyl alcohol. The hydrocyclone performance is highly affected by fluid viscosity (Bradley 1965). The values of drag coefficient and drag force in isopropyl alcohol were greater than those in deionized water. Thus, in isopropyl alcohol, a higher drag force was applied to particles which moved them to the overflow fraction. This higher force caused the transfer of some starch granules to the overflow and resulted in the reduction of starch separation efficiency. Although isopropyl alcohol is an excellent solvent for fat, it was not able to efficiently separate starch and protein particles in the hydrocyclone. Furthermore, according to the residence time theory, particles in a high-viscosity fluid have a small chance to reach the inner

hydrocyclone wall. However, the same particles in a low-viscosity fluid can reach the inner hydrocyclone wall faster and have more chance to move to the underflow (Svarovsky 1990; Svarovsky 1984).

As Equation 2.8 shows, the value of drag force is a function of drag coefficient, fluid density, projected area of the particle, and relative velocity between the fluid and particle. The drag coefficient is affected by fluid density and viscosity, which are also affected by fluid temperature (Equation 2.9 - 2.14). Increasing temperature from 10°C to higher values results in decreasing fluid density and viscosity in both isopropyl alcohol and deionized water. Since viscosity (denominator of Equation 2.7) decreases at a greater rate than density (numerator of Equation 2.7), the Reynolds number increases as fluid temperature increases. By increasing the Reynolds number, the drag coefficient decreases (Equations 2.9 and 2.11). Additionally, the value of relative velocity between the fluid and the particle is affected by fluid density and viscosity (Equation 2.10). Therefore, the relative velocity decreases with an increase in fluid temperature. The overall effect of increasing temperature would be a decrease in drag force and a resultant increase in starch separation efficiency and a decrease in protein separation efficiency. Operation of the hydrocyclone with isopropyl alcohol at higher temperatures was not attempted in this study due to the enhanced risk of fire or explosion with our system.

5.6.4 Effect of defatting and pH adjustment of feed material on separation

Table 4.11 shows the effect of slurry pH and defatting of chickpea flour on starch content and starch separation efficiency. High slurry pH increased the starch content of underflow products. Since at pH 9.0 (maximum NSI) the protein particles were better dispersed in the

aqueous medium than at pH 6.6, most of the protein moved into the overflow. This phenomenon resulted in less protein contamination in the underflow. The small amount of starch in the overflows (O1, OO1, and OU1) was likely associated with damaged starch granules resulting from pin-milling (Tyler et al. 1981). Defatting of chickpea flour also increased the starch content of the underflows significantly. The high fat content of chickpea flour increases the tendency of particles to agglomerate, thus affecting separation (Han and Khan 1990a). Apparently, defatting of chickpea flour reduced the agglomeration between particles resulting in a higher efficiency of separation. The starch contents obtained in the current study were similar to those reported by Vose (1980) for field pea and horsebean employing a high pH (pH 8.5) and a series of three hydrocyclones, where a starch fraction of as high as 99% starch was obtained. Employing high slurry pH (pH 10.2 for field pea and pH 9.6 for fababean) but using centrifugation, Sosulski and Sosulski (1986) obtained a starch fraction with a starch content as high as 94% from field pea and fababean, which was lower than value obtained in this study. The starch separation efficiencies of U1 and UU1 ranged between 93.2 and 97.2% and these values were similar to those reported by Tyler and co-workers (1981) in air classification of legumes. However, values from this study were higher than those reported by Sosulski and Sosulski (1986) who employed high pH and centrifugation in separating starch from field pea and fababean flours (76-79%).

The effect of slurry pH and defatting of chickpea flour on starch content and starch separation efficiency is shown in Table 4.11. High pH, i.e. pH 9.0, did not significantly affect the protein content of the SUs of the overflows. However, separation at pH 9.0 improved protein separation efficiency. Defatting of chickpea flour significantly increased the protein content of overflow SEs, whereas it did not have any significant effect on the

protein content of the overflow SUs. Defatting of chickpea flour increased protein separation efficiency. This improvement was attributed to the easier separation of particles in chickpea flour devoid of fat. The protein separation efficiencies in this study were similar to those reported by Sosulski and Sosulski (1986) for field pea and fababean using high pH and centrifugation (72-74%).

5.6.5 Effect of higher feed concentration

Table 4.15 shows the separation efficiencies at five feed concentrations. Increasing feed concentration decreased the starch and protein separation efficiencies. This result confirmed those of Svarovsky (1984) who reported that the separation efficiency drops as the feed concentration increases. Typically, the separation of a starch fraction from legume seeds is difficult because of the presence of insoluble flocculent protein and fine fibre diminishing sedimentation, co-settling with the starch fraction and resulting in a brownish deposit (Ratnayake et al. 2002; Hoover and Sosulski 1991). Therefore, the low starch content of the underflow can be attributed to the presence of insoluble protein, fine fibre, and cell wall material. Furthermore, some proteins, especially albumins, are soluble even at pH 4.3 (Sánchez-Vioque et al. 1999). Thus, they are not recovered, resulting in a lower protein content in the protein fraction and a reduction in protein separation efficiency. This study demonstrated that a feed concentration of 5% was the most efficient since a chickpea flour slurry at this concentration was pumpable through the hydrocyclone. This feed concentration also resulted in acceptable separation efficiencies. At this feed concentration, the starch content of the starch fraction and the protein content of the protein fraction were enriched to 1.4 and 2.9 times, respectively, those of chickpea flour.

5.6.6 Discussion on particle size distribution of the overflow and underflow fractions

Chickpea flour with a particle geometric mean diameter of 25.56 μm was fractionated into the overflow and underflow fractions having geometric mean diameters of 26.27 and 5.30 μm, respectively. This distribution confirmed that the hydrocyclone separated fractions on the basis of their particle sizes. Therefore, large particles, including starch granules, were collected in the underflow, whereas small particles, including protein particles, were collected in the overflow. The relationships between particle size and cumulative undersize of the overflow and underflow are presented as Equations 5.3 and 5.4, respectively:

$$y = 99.49\left[1 - \exp\left(-1.27 \times 10^{-1} x\right)\right] \tag{5.3}$$

$$y = 97.18\left[1 - \exp\left(-2.52 \times 10^{-2} x\right)\right] \tag{5.4}$$

where: y = undersize fraction (% volume); and

x = particle size (μm).

The model fitted to experimental data very well (Figures 5.3 and 5.4) with R^2 of 0.99 and standard errors of estimate of 4.51 and 3.21 for the overflow and underflow, respectively. The proposed model overestimated the undersize fraction of the underflow in the particle size range from 60 to 230 μm and from 330 μm and higher. In the experimental data, the undersize fraction of the overflow increased with greater slope than did that of the underflow fraction. The proposed model confirmed this trend, as the absolute value of parameter of the independent variable in the overflow was larger than that in the underflow.

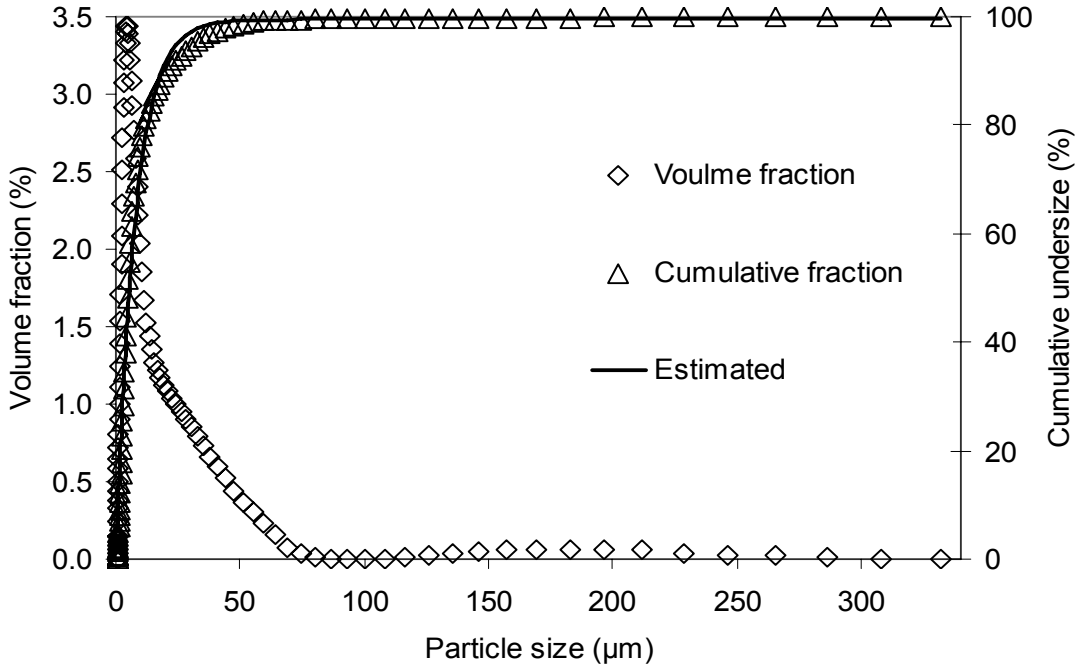

Figure 5.3 Relationship between particle size and volume fraction and cumulative undersize of the overflow fraction.

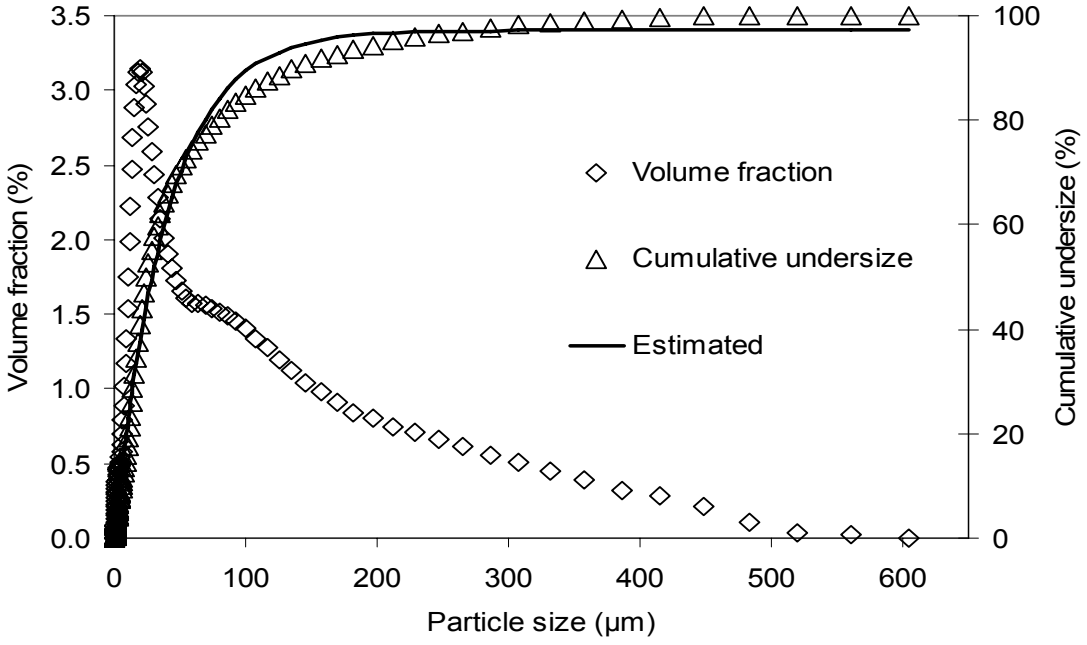

Figure 5.4 Relationship between particle size and volume fraction and cumulative undersize of the underflow fraction.

5.6.7 Discussion on integrated separation process

Table 4.19 shows the yield and chemical composition of fractions resulting from integrated separation process 1. The yield of the starch fraction in this study was lower than the value reported for air classification of pin-milled chickpea flour (91.5%) and other legumes (Sosulski et al. 1987). This may be due to losses of some starch granules into the overflow fraction. The presence of protein in the starch fraction was most likely due to the remaining protein that could not be separated from starch granules during pin-milling (Han and Khan 1990a). The majority of the total dietary fibre (cell wall material and the residual hulls from dehulling) was collected in the starch fraction fraction, because fibre has a relatively large particle size. This high concentration of total dietary fibre was in agreement with the study reported by Ratnayake and co-researchers (2002). In this study, comparison of scanning electron micrographs of chickpea flour (Figure 4.3) and fractionated starch (Figure 4.11) showed that the separation process reduced aggregation of proteinaceous materials and starch granules. The starch fraction had a lower percentage of protein particles than did chickpea flour.

The yield of the protein fraction in this work was higher than the yield of the fine friction, i.e. the protein-rich fraction, reported in the air classification of pin-milled chickpea flour (8.5%). However, it was close to values reported for lentil, field bean, and cowpea (from 24.1 to 27.6%) (Sosulski et al. 1987). The presence of starch in the protein fraction was associated with damaged starch granules resulting from pin-milling. Damaged starch granules, having smaller particle sizes than undamaged ones, are separated with the protein fraction. Most of the fat was fractionated with the protein fraction and supernatant fraction. Fat contents in the protein fraction and the supernatant fraction were 1.6 and 5.2 times,

respectively, that of chickpea flour. This was attributed to the presence of lipid complexed with protein particles in the overflow. This result agreed with the study reported by Sosulski and co-workers (1987) and Han and Khan (1990a) stating that majority of the fat is concentrated in the fine fraction during air classification, i.e. protein-rich fraction.

The high protein content of the supernatant fraction was attributed to the protein which was solubilized during extraction. Some proteins, especially albumins, are grouped as highly soluble proteins (Sánchez-Vioque et al. 1999). Thus, during the process, they are lost and the protein separation efficiency of the protein fraction is reduced. The high amount of ash in the protein fraction and supernatant fraction was due to the reaction between sodium hydroxide and hydrochloric acid which yielded sodium chloride and water.

Table 4.19 presents the yield and chemical composition of fractions resulting from separation process 2. The main differences between separation processes 1 and 2 were: a) the lower yield of the starch fraction in process 2; and b) having one more fraction in process 2, namely, the cell wall fraction. By removing the cell wall material from the starch fraction, the starch content of the starch fraction rose to 78.3% (d.b.) and the total dietary fibre content decreased to 0.8% (d.b.). The starch separation efficiency in process 1 was slightly higher than that in process 2 (Table 4.20). This was due to the sieving step in process 2. Some starch granules remained on the sieve with the cell wall fraction, thus reducing the starch content and yield of the starch fraction. The starch contents of both separation processes in this study were lower than values reported by Sosulski and Sosulski (1986) in wet processing of field pea (83.2%) and faba bean (77.3%). The low starch content may be associated with the presence of insoluble flocculent proteins, fine fibre (Ratnayake et al. 2002) and cell wall material, as well as the relatively high fat content of chickpea flour

which reduces separation efficiency. Although Sosulski and Sosulski (1986) reported a higher starch content in their study, the starch separation efficiencies that were obtained were lower than those obtained in this study. Sosulski and Sosulski (1986) recovered 79.2 and 76.2% of the starch component from field pea and faba bean, respectively. The starch separation efficiencies of the current study were similar to the values reported by Tyler and co-workers (1981) for air classification of field pea and lima bean.

The protein fraction in separation process 2 was also contaminated with starch, which may be due to damaged starch granules resulting from pin milling. The protein contents of protein fractions resulting from processes 1 and 2 were not markedly different. Comparison of protein separation efficiencies, in Table 4.20, reveals that process 1 had a higher value, along with a higher standard error. The higher standard error for protein separation efficiency was associated with sampling error, protein measurement error, and fluctuation of hydrocyclone operation. The protein separation efficiencies in this study were in the same range as reported by Tyler and co-workers (1981) for the dry processing of mungbean, lentil, Great Northern bean, and faba bean. The protein contents of both processes were similar to values reported by Sánchez-Vioque and co-workers (1999), and were higher than values determined by Tian and co-workers (1999). Sánchez-Vioque and co-workers (1999) reported 80.9% (d.b.) protein content resulting from chickpea flour, and Tian and co-workers (1999) produced protein isolate from field pea containing 77.1% (d.b.) protein and 14.5% (d.b.) carbohydrate. Nevertheless, values resulting from the current study were less than those obtained from wet processing of field pea and faba bean (87.7 and 94.1%, respectively) as reported by Sosulski and Sosulski (1986). This variation was due to

the difference in chemical composition, fat content, between chickpea grain and field pea and faba bean grains.

Although high in total dietary fibre, the cell wall fraction from sieving in process 2 still contained starch. This confirmed that chickpea flour contained cell wall material having a relatively large particle size, i.e. greater than 200-mesh sieve.

In the supernatant fraction of process 2, the high ash content was due to the presence of sodium chloride resulting from reaction between sodium hydroxide and hydrochloric acid used in dispersing and precipitating protein, respectively.

From all of the above, it is concluded that application of separation process 2 did not result in any marked difference in the starch and protein contents of the protein fraction. Comparison of the yields and chemical compositions of fractions of processes 1 and 2 demonstrates that since the slurry was fractionated into four fractions in process 2 (instead of three as in process 1), the yield of starch, protein, and supernatant, as well as separation efficiencies of starch and protein, were lower. However, the sieving step in process 2 reduced the total dietary fibre in the starch fraction markedly as the total dietary fibre was collected in a separate cell wall fraction. This result shows that complete dehulling of chickpea (i.e. no hull remaining in the dehulled chickpea grain), followed by sieving during the process (process 2) would reduce the amount cell wall material collected in the starch fraction and increase its starch content.

5.7 Discussion on physical and functional properties of chickpea flour and starch and protein fractions

The physical and functional properties of chickpea flour and fractionated products are important in the design of specific process equipment and the prediction of product behaviour during storage and during different unit operations (Mohsenin 1986). These properties are discussed in this section.

5.7.1 Factors affecting surface charge of fractionated products

Isolated protein had a negative zeta potential (–5.3 ± 0.6 mV) before titration, indicating that acidic amino acids dominated the basic amino acids. The model below (Equation 5.5), describing the relationship between the zeta potential and pH, had a R^2 of 0.97 and a standard error of estimate of 3.39 (Figure 5.5), showing a good fit to data.

$$ZP = -35.24\ \ln(\text{pH}) + 58.26 \tag{5.5}$$

where ZP is zeta potential. The proposed model and figure confirm that the zeta potential was inversely proportional to pH.

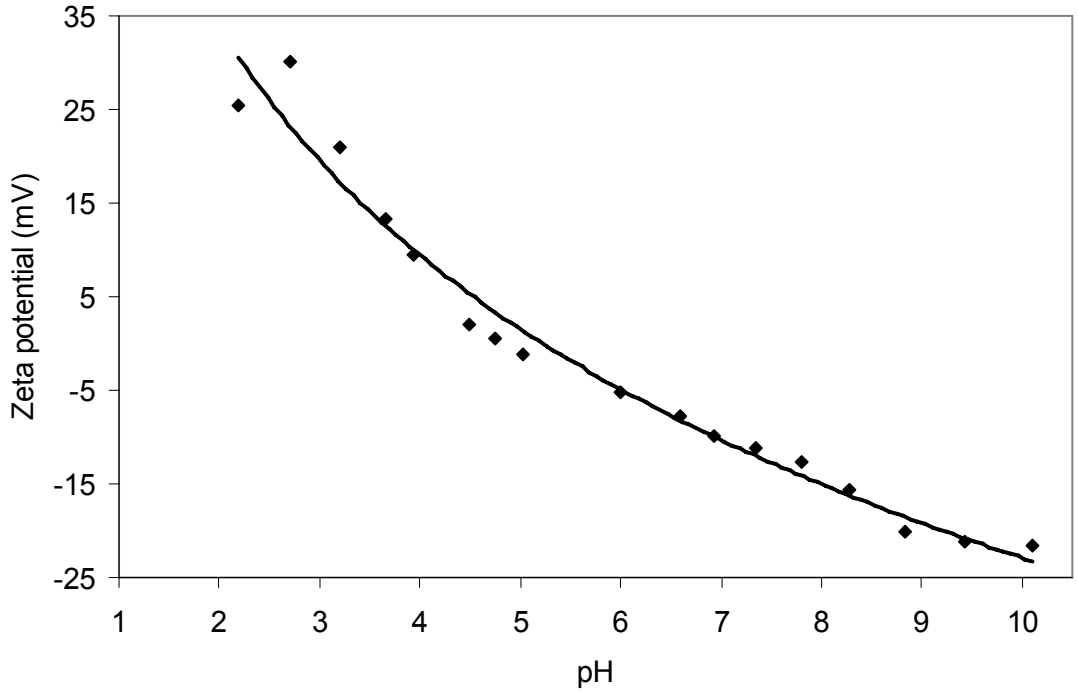

Figure 5.5 Relationship between the zeta potential and pH in protein fraction.

5.7.2 Factors affecting density, porosity, and colour

As presented in Table 4.21, chickpea flour had the highest bulk density and the lowest porosity among samples. Therefore, chickpea flour contained less air space between its particles compared to the starch and protein fractions. Freeze drying of the starch and protein fractions resulted in the evaporation of water, leaving the dried material with substantial porosity. The starch fraction had the highest porosity. Milling the freeze dried fractions to a finer granularity would have increased their bulk densities.

In terms of colour, the **L** value (lightness) of chickpea flour was lower, and its **a** value (redness) was higher, than values reported by Han and Khan (1990a) for chickpea. However, the **b** value (yellowness) was in the same range. The yellowness of starch fraction, although low, was related to the presence of insoluble flocculent proteins and fine fibre

which had co-settled with starch fraction and increased its yellowness and brownness (Ratnayake et al. 2002).

5.7.3 Effect of temperature and bulk density on thermal conductivity

Studies have shown that thermal conductivity changes with moisture content (Fang et al. 2000). Therefore, reporting of sample moisture content is required for future comparisons. Protein fraction had the lowest moisture content among the samples (Table 4.22). This is due to the chemical composition of protein fraction containing less hygroscopic components, such as carbohydrates, than did chickpea flour and starch fraction. In addition, protein fraction was obtained by the isoelectric precipitation method where proteins are agglomerated at the isoelectric point. Therefore, the water solubility of the protein is diminished and its ability to absorb water is reduced.

The thermal conductivity of chickpea flour in this study (Table 4.24) was close to values reported by Saravacos and Maroulis (2001) for soy flour, which was from 0.106 to 0.650 W m^{-1} $°C^{-1}$ at moisture contents of 0 to 64% d.b. and temperatures between 20 and 60°C. The thermal conductivity values of starch fraction in this study were similar to values reported by Saravacos and Maroulis (2001) for potato starch, which were from 0.061 to 2.100 W m^{-1} $°C^{-1}$ at moisture contents of 0 to 2400% d.b. and temperatures from –42 to 120°C.

The influence of temperature on thermal conductivity was due to higher atomic activity at higher temperatures. At higher temperature, there is higher atomic activity and the material has greater ability to transfer heat energy. Thus, it has higher thermal conductivity. The direct linear relationship between bulk density and thermal conductivity can be

attributed to the presence of pores and air pockets among powder particles. Since air has relatively low thermal conductivity, higher porosity (lower bulk density) would result in lower thermal conductivity. Since chickpea flour had lower porosity than starch and protein fractions (Table 4.22), its thermal conductivity was higher.

The effect of temperature on the thermal conductivity of the samples in this study was similar to the results reported by Drouzas and Saravacos (1988) and Fang and co-workers (2000) for granular starch, and Lan and co-workers (2000) for tapioca starch. Lan and co-researchers (2000) reported an increase in thermal conductivity from 0.077 to 0.090 W m^{-1} $°C^{-1}$ when the temperature was increased from 25 to 75°C. The value reported at 75°C was lower than value determined in the current study at 40°C, due to differences in the bulk density of samples. Moreover, the trend for the effect of bulk density on thermal conductivity was similar to the results of studies reported by Drouzas and Saravacos (1988) and Fang and co-workers (2000) for granular starch. Drouzas and Saravacos (1988) reported a linear increase in thermal conductivity from 0.065 to 0.220 W m^{-1} $°C^{-1}$ when bulk density increased from 500 to 800 kg/m^3 for granular starch materials.

Using the SAS REG procedure, multiple regression analysis was run to determine the relationship between the thermal conductivity of each sample and its bulk density and temperature (Table 5.1). The models had low standard error of estimate and high R^2, showing a good fit to the experimental data. The models obtained for all samples had positive coefficients for temperature and bulk density showing that thermal conductivity increased with both bulk density and temperature. Figures 5.6, 5.7, and 5.8 depict the prediction model for the effect of moisture content and temperature on the thermal conductivity of chickpea flour and starch and protein fractions, respectively. The responses

surface graphs reveal that thermal conductivity increases with an increase in bulk density or temperature or both.

Table 5.1 Relationship between thermal conductivity value and bulk density and temperature values.

Sample	Thermal conductivity equation†	R^2	SEE*
Chickpea flour	$k = 3.18\times10^{-4}\,T + 1.47\times10^{-4}\,\rho_b + 0.0189$	0.95	0.002
Starch fraction	$k = 3.29\times10^{-4}\,T + 6.13\times10^{-5}\,\rho_b + 0.0520$	0.91	0.003
Protein fraction	$k = 1.39\times10^{-4}\,T + 5.89\times10^{-5}\,\rho_b + 0.0484$	0.90	0.001

† k = thermal conductivity (W m^{-1} °C^{-1}), T = temperature (°C), ρ_b = bulk density (kg/m^3)

* SEE: standard error of estimate

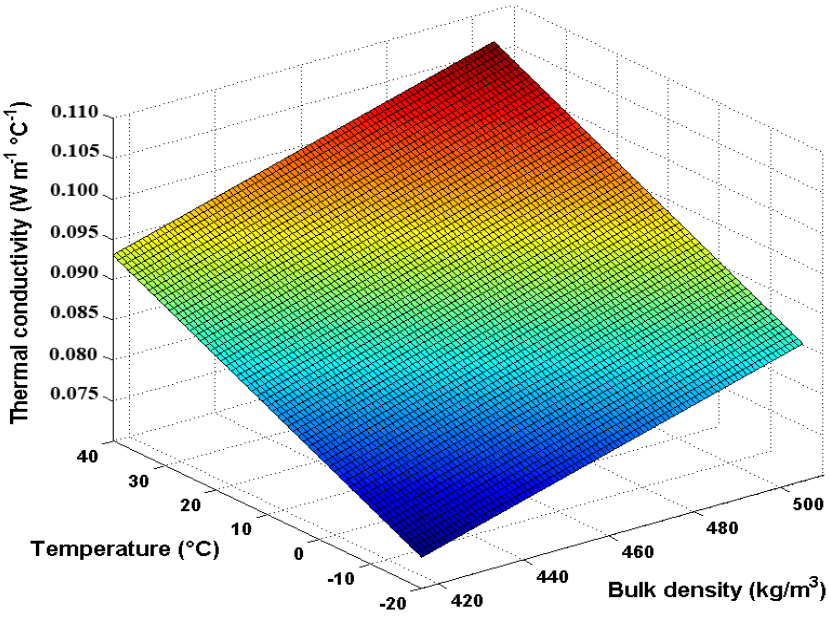

Figure 5.6 Relationship between thermal conductivity and bulk density and temperature of chickpea flour.

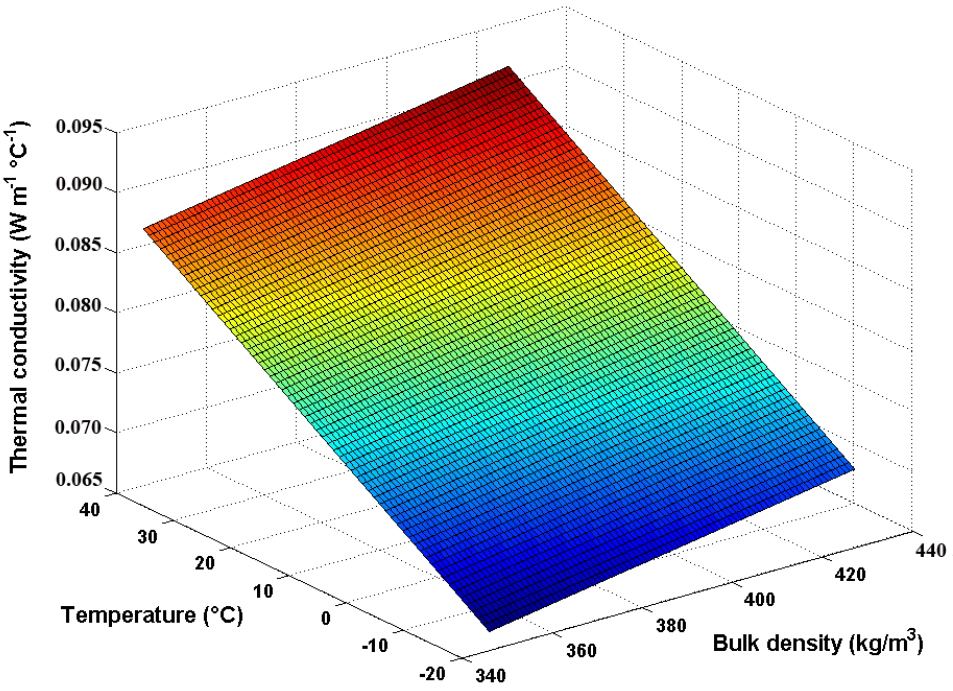

Figure 5.7 Relationship between thermal conductivity and bulk density and temperature of starch fraction.

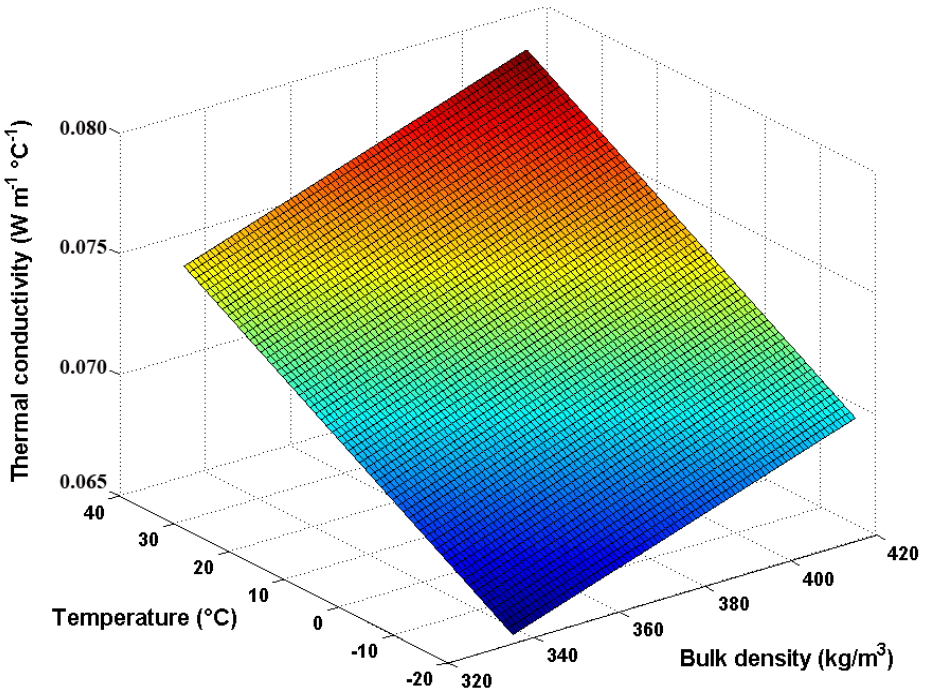

Figure 5.8 Relationship between thermal conductivity and bulk density and temperature of protein fraction.

5.7.4 Effect of temperature and moisture content on specific heat

The specific heat of samples was affected by their chemical composition. The trend of increasing specific heat with an increase in moisture content or temperature in all three samples was in agreement with a study conducted on tapioca starch by Lan and co-workers (2000) where the specific heat rose from 0.337 to 0.459 kJ kg^{-1} $°C^{-1}$ at temperatures ranging between 25 and 75°C. Furthermore, this study agreed with results reported by Drouzas and co-workers (1991) and Sweat (1995) who reported that the specific heat of granular corn starch linearly increased from 1.260 to 1.800 kJ kg^{-1} $°C^{-1}$ as the moisture content increased from 0 to 30% d.b.

Since the specific heat of samples increased linearly with both moisture content and temperature (Figures 4.13 and 4.14) at high R^2, the polynomial linear model was used to find a prediction model for specific heat. Table 5.2 shows multiple regression models expressing the relationship between the moisture content and temperature of a sample and the corresponding specific heat. These models were obtained using SAS REG procedure. Figures 5.9, 5.10, and 5.11 indicate changes in the specific heat of chickpea flour and starch and protein fractions, respectively, with variations in moisture content and temperature using the prediction polynomial linear models. The surface responses reveal that as the moisture content and temperature increase, the specific heat also increases. In all three samples, the coefficients of moisture content and temperature were positive, indicating that the specific heat was directly proportional to moisture content and temperature.

Table 5.2 Relationship between specific heat value and moisture content and temperature values.

Sample	Specific heat equation†	R^2	SEE*
Chickpea flour	$c_p = 0.016\ W_w + 0.003\ T + 1.131$	0.86	0.085
Starch fraction	$c_p = 0.024\ W_w + 0.005\ T + 0.775$	0.92	0.096
Protein fraction	$c_p = 0.032\ W_w + 0.005\ T + 0.975$	0.92	0.119

† c_p =specific heat (kJ kg^{-1} °C^{-1}), W_w = moisture content (% w.b.), T = temperature (°C)

* SEE: standard error of estimate

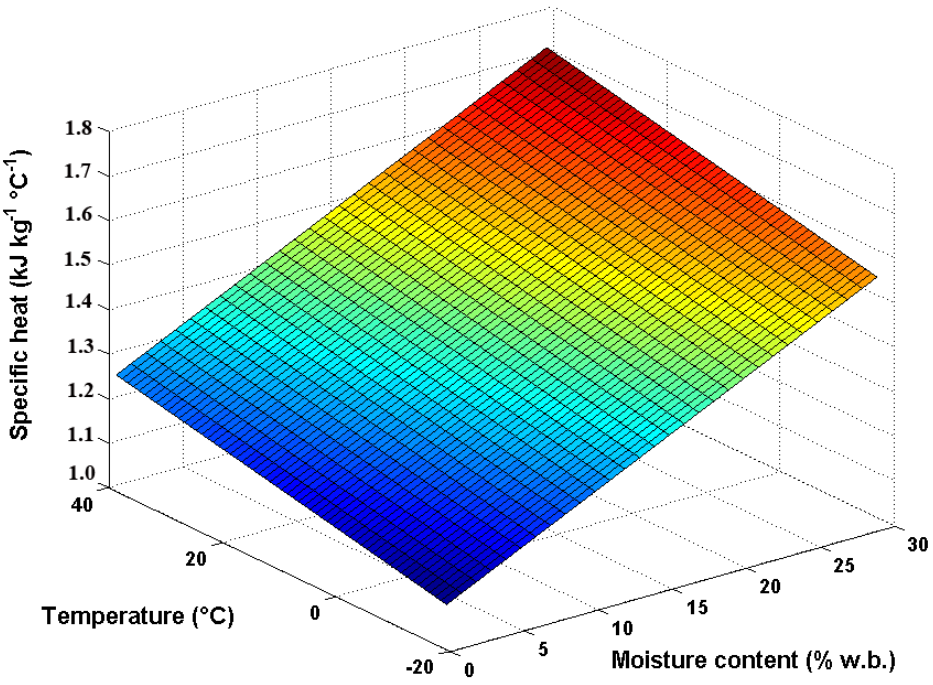

Figure 5.9 Prediction model for the effect of moisture content and temperature on specific heat of chickpea flour.

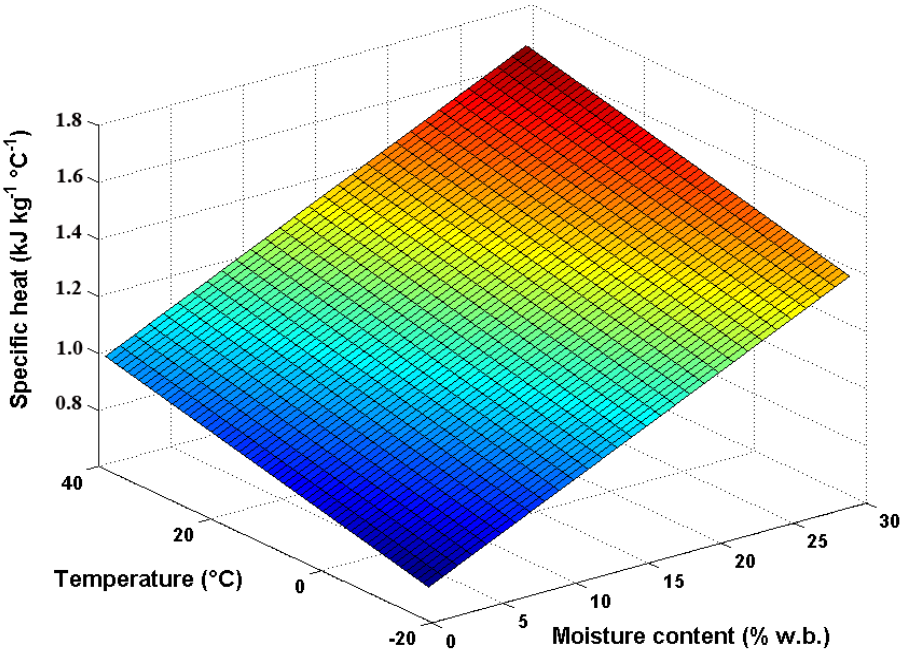

Figure 5.10 Prediction model for the effect of moisture content and temperature on specific heat of starch fraction.

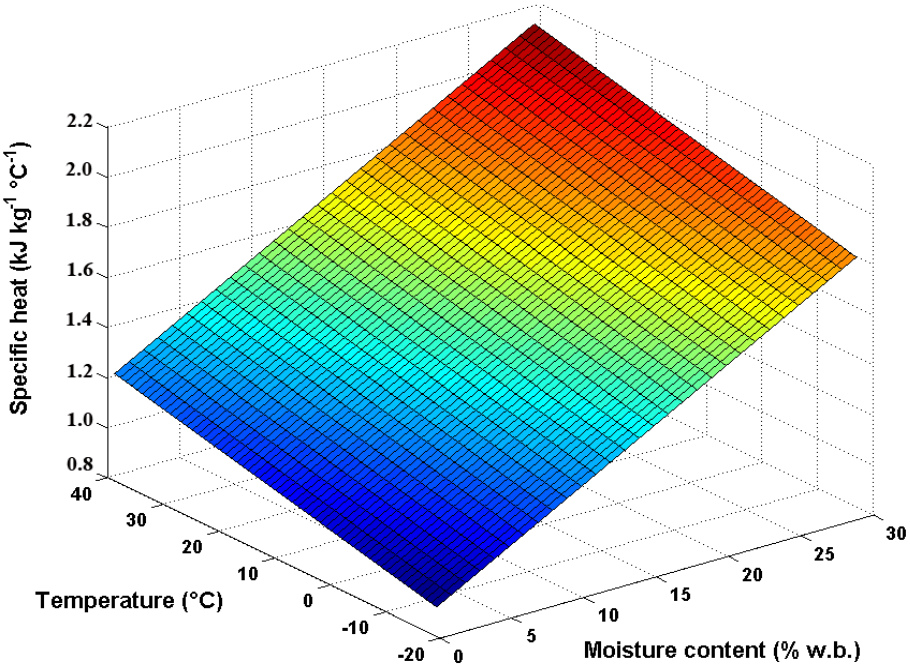

Figure 5.11 Prediction model for the effect of moisture content and temperature on specific heat of protein fraction.

5.7.5 Factors affecting estimated thermal diffusivity

Thermal diffusivity did not show any particular trend with temperature. This was in agreement with the study conducted by Lan and co-researchers (2000) who reported that the thermal diffusivity of tapioca starch dropped from 2.6×10^{-7} to 2.4×10^{-7} m^2/s when the temperature was increased from 25 to 50°C, and then increased to 2.7×10^{-7} m^2/s when temperature was increased to 75°C. Thermal diffusivity decreased with an increase in bulk density. By increasing bulk density, pores and air pockets within and among powder particles were reduced and the thermal conductivity value increased (numerator of Equation 2.25). Meanwhile, the bulk density value (denominator of Equation 2.25) increased at a greater rate, which resulted in the increase of thermal diffusivity. Starch fraction had a higher thermal diffusivity than did either chickpea flour or protein fraction. This higher value was due to the low specific heat of starch fraction, showing that it has a greater tendency to conduct heat than to store it, as compared to the other two materials.

To determine the relationship between thermal diffusivity and temperature and bulk density, the SAS REG procedure was employed. Table 5.3 shows the multiple linear regression models for chickpea flour and starch and protein fractions. For the three samples, the coefficient of bulk density was negative, indicating that thermal diffusivity decreases with increase of bulk density. Figures 5.12, 5.13, and 5.14 represent the variations of thermal diffusivity with temperature and bulk density using the polynomial linear models.

Table 5.3 Relationship between thermal diffusivity value and temperature and bulk density values.

Sample	Thermal diffusivity equation†	R^2	SEE*
Chickpea flour	$\alpha = 4.095\times10^{-10}\ T - 8.165\times10^{-11}\ \rho_b + 1.845\times10^{-7}$	0.85	4.572×10^{-9}
Starch fraction	$\alpha = -4.534\times10^{-11}\ T - 3.553\times10^{-10}\ \rho_b + 3.346\times10^{-7}$	0.81	6.473×10^{-9}
Protein fraction	$\alpha = -3.108\times10^{-10}\ T - 2.743\times10^{-10}\ \rho_b + 2.570\times10^{-7}$	0.94	3.391×10^{-9}

† α = thermal diffusivity (m^2/s), T = temperature (°C), ρ_b = bulk density (kg/m^3)

* SEE: standard error of estimate

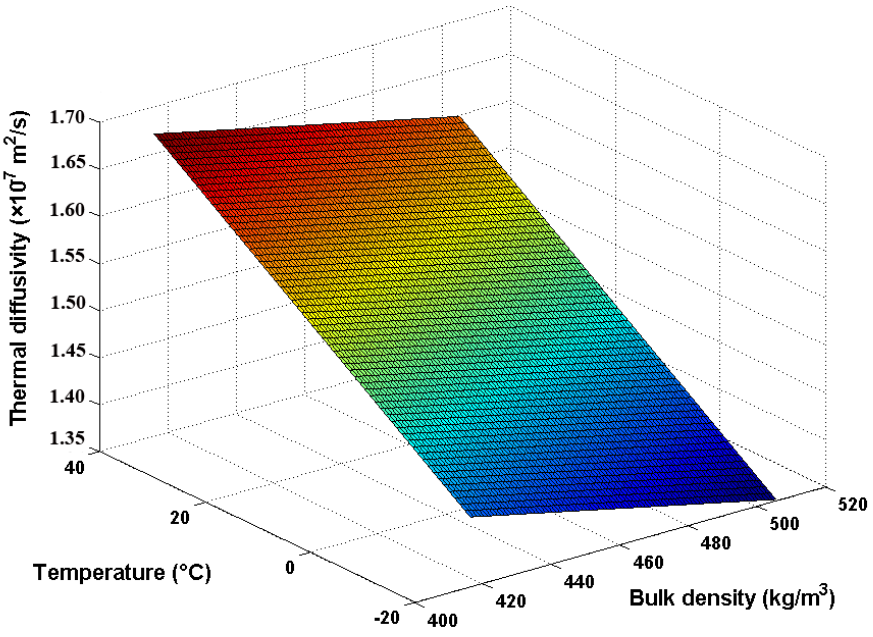

Figure 5.12 Prediction model for the effect temperature and bulk density on thermal diffusivity of chickpea flour.

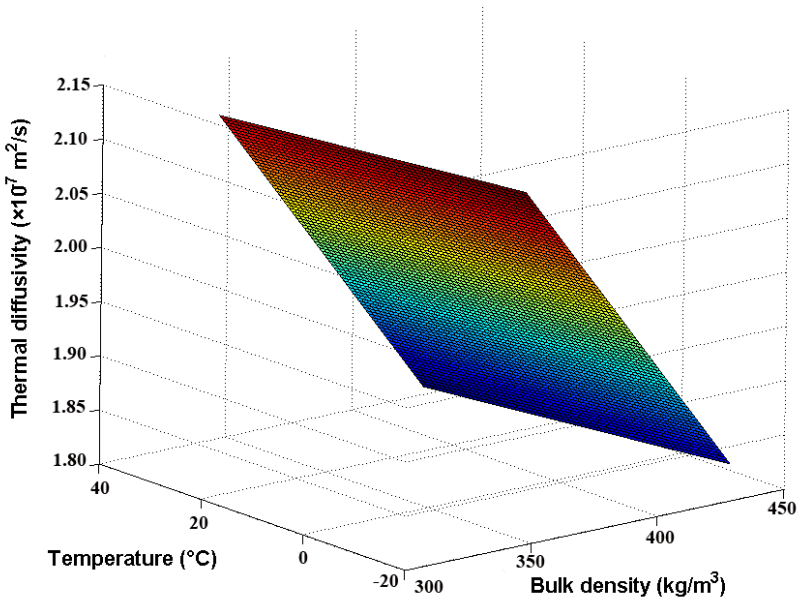

Figure 5.13 Prediction model for the effect temperature and bulk density on thermal diffusivity of starch fraction.

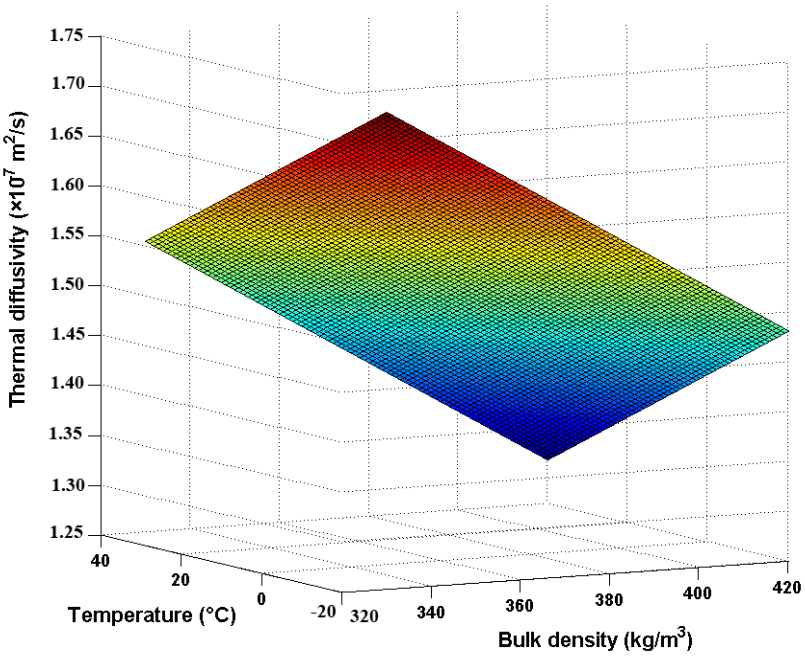

Figure 5.14 Prediction model for the effect temperature and bulk density on thermal diffusivity of protein fraction.

5.7.6 Phase transitions

In chickpea flour, the T_p ranged from 60 to 63°C, and this trend was similar to the study reported by Donovan (1979) for potato starch and by Kerr and co-researchers (2000) for cowpea flour. The variation in the tailing shoulder of the endothermic peak and ΔT with a change of moisture content was also observed by Donovan (1979) for potato starch. The ΔH_p, associated with the enthalpy of gelatinization, ranged from 6.0 to 7.2 J/g. The trend of increasing ΔH_p agreed with Kerr and co-researchers (2000) who worked on cowpea flour. The magnitude of ΔH_p obtained in the current study was similar to the value reported by Kosson and co-workers (1994) for SS Alaska variety of smooth pea (6.3 J/g) at a moisture content of 9.0% w.b. However, the ΔH_p was somewhat lower than values reported by Sosulski and co-workers (1985) for eight legumes. The minor endothermic peak at 109°C, which is presumably the denaturation/aggregation temperature, was similar to T_d reported by Sosulski and co-workers (1985) for pin-milled legumes which ranged from 81 to 98°C; however, they did not report T_d for pin-milled cowpea.

For starch fraction, the values of T_p were similar to those reported for lentil starch (65°C) by Sosulski and co-workers (1985) and smooth pea starch (60 to 63°C) by Davydova and co-workers (1995). The area under the endothermic peaks, ΔH_p, increased with moisture content and ranged from 13.9 to 15.0 J/s, since more starch granules are gelatinized at higher moisture contents. Thus, more heat energy was required for gelatinization at higher moisture contents. The ΔH_p values were similar to values reported by Davydova and co-workers (1995) for smooth pea. The T_d was not observed at these moisture content levels, similar to some legumes (field pea and lentil) in the study conducted by Sosulski and co-workers (1985).

For the protein fraction, the T_p peak was not observed at any moisture levels; similar results were reported by Sosulski and co-workers (1985) for air-classified protein fractions from lentil, field pea, faba bean, and lima bean. However, major endothermic peaks were observed in the temperature range of 144 to 182°C, similar to the decomposition temperature reported for wheat flour by Teunou and Fitzpatrick (1999). Presumably, the high value for ΔH was due to the decomposition of chickpea protein at these relatively high temperatures.

5.7.7 Factors affecting internal friction

In chickpea flour, the high value for the coefficient of internal friction and angle of internal friction among samples (Table 4.29) was related to chickpea flour particle size since particle size distribution affects angle of internal friction (Teunou et al. 1999). Powder samples cannot flow if their particle size is less than 120 μm, even if they are dry (Peleg 1977). The angle of internal friction of starch and protein fractions was close to that of wheat flour (32°) (Teunou et al. 1999). However, the angle of internal friction of chickpea flour was similar to that of soy bean flour (34.3°) and was less than that of potato starch (36.8°) (Peleg et al. 1973). This result shows that particles of starch and protein fractions would slide over each other and make angles of 32.01 and 32.44° with the horizontal, respectively. These values are employed in designing equipment used in storage and transfer, such as calculating pressures applied by the material to the bin wall.

Starch fraction had the highest cohesion, higher than values reported for corn starch (Peleg et al. 1973). Powders with high cohesion have low flowability. This may be due to the presence of water molecules, resulting in a liquid bridge between particles which would

lead to flow difficulty. In powders with high cohesion, this phenomenon leads to agglomeration (Teunou et al. 1999; Peleg 1977). Comparison of values in this study with other materials shows that cohesion of all three samples was greater than that of sugar (1.6 kPa) at a moisture content of 0.3% d.b. However, the values in this study were lower than those reported for sugar (from 9.1 to 13.3 kPa) at a moisture content of 3.3% d.b. (Duffy and Puri 1996). The cohesion values of potato starch and soy flour were 0.2 and 0.1 kPa, respectively (Peleg et al. 1973), lower than the values obtained in this study.

5.7.8 Factors affecting external friction

Starch fraction had a lower coefficient of external friction and angle of external friction on steel, Teflon and polypropylene than did chickpea flour and protein fraction (Table 4.30). This characteristic was related to the low fat content of starch fraction. However, chickpea flour had a higher adhesion than starch and protein fractions on concrete, Teflon and polypropylene. Transferring oils, fats and waxes from the sample to the friction surface leads to an increase in friction (Mohsenin 1986). The oil, fat and wax films between the sample and the friction surface provided a sticky surface and inhibited the sliding of sample particles on the surface. Besides the presence of fat in the flour, another important reason was the fineness of chickpea flour particles. Since chickpea flour had a smaller particle size, it had closer contact with the friction surfaces which resulted in higher adhesion.

The lowest adhesion was obtained on the polypropylene surface. All three samples had the highest adhesion on the concrete surface, followed by the Teflon and steel surfaces. This is attributed to differences in the surface roughness of the plates (steel, concrete, Teflon and polypropylene) as explained by Mohsenin (1986). Protein fraction showed the lowest

adhesion value on the steel surface. This may be attributed to measurement error and to the presence of other forces, such as electrostatic force, aside from frictional force during measurement.

The angle of external friction on steel obtained in the current study was lower than values reported by Duffy and Puri (1996) for sugar. It was reported that sugar at moisture contents of 0.3 and 3.3% d.b. had angles of external friction of 31.0° and 24.2°, respectively, on steel, and 32.2° and 29.2°, respectively, on aluminum. All of these values were greater than those determined on steel in this study.

5.7.9 Compressibility and stress relaxation

Adapa and co-researchers (2002), Mani and co-workers (2004b), and Shaw and co-workers (2005) reported that the Cooper and Eaton model fitted to the experimental data for ground biomaterials, which was in agreement with the current study. Also, the Walker (Equation 2.28), Jones (Equation 2.29), and Barbosa-Cánovas and co-workers (Equation 2.30) models resulted in high R^2 and low standard error of estimate, an indication of good fit to the experimental data.

The slope value in the Walker and Jones models, as well as in the Barbosa-Cánovas and co-workers model, represents compressibility (Kaletunc and Breslauer 2003; Tabil and Sokhansanj 1997). Compressibility is an index showing the flowability of powders. Powder with high compressibility has low flowability. The Jones and the Barbosa-Cánovas and co-workers models did not show any marked difference in compressibility among samples. However, the Walker model showed that starch fraction had the highest compressibility and protein fraction, the lowest. The Cooper and Eaton model showed that a_1 was larger than a_2

for all test samples. This means the particles of the samples underwent particle rearrangement during compression. High compressibility values (Table 4.31) corresponded with high porosity (Table 4.21).

Figure 4.23 shows the typical force-time relationship for compression of samples at different preset loads. In the first stage, particles move and voids are filled with particles of identical size or smaller (Kaletunc and Breslauer 2003). In the second stage, the smaller voids are filled by particles that have undergone elastic deformation, plastic deformation and/or fragmentation (Kaletunc and Breslauer 2003; Tabil and Sokhansanj 1997).

Linear regression was used to determine the constants of a linear model between asymptotic modulus (E_A) and maximum compressive pressure (σ_0) (Table 5.4). The model obtained for starch fraction showed that its asymptotic modulus increased with initial stress faster than did those of chickpea flour or protein fraction. Thus, starch fraction has higher solidity and a greater tendency to sustain unrelaxed stresses.

Table 5.4 Relationship between asymptotic modulus and maximum compressive pressure.

Sample	Asymptotic modulus equation†	R^2	SEE*
Chickpea flour	$E_A = 25.847\ \sigma_0 - 3.9214$	1.00	3.35
Starch fraction	$E_A = 27.782\ \sigma_0 - 5.7967$	1.00	2.50
Protein fraction	$E_A = 25.533\ \sigma_0 - 10.322$	1.00	2.64

† E_A = asymptotic modulus (MPa), σ_0 = initial stress (MPa)

* SEE: standard error of estimate

5.7.10 Factors affecting water hydration capacity, emulsion capacity, and emulsion stability

Starch fraction exhibited the highest WHC, followed by chickpea flour. This trend was due to the lower lipid content of starch fraction compared to chickpea flour and protein fraction (Han and Khan 1990b). Since lipids are hydrophobic components, they reduce the WHC.

The emulsion capacity of chickpea flour obtained in this study was higher than those of the starch and protein fractions, and was similar to that reported by Han and Khan (1990b) for chickpea flour (42.81 mL/g). Chickpea flour had lower emulsion stability than did the fractioned products, showing that a higher percentage of water was released from chickpea flour during centrifugation. This study showed that separation of starch and protein by increasing pH and then reducing pH to the isoelectric point (process 1) can change the emulsification ability (both capacity and stability) of components. This change was related to the solubility of components. Proteins near their isoelectric point are poor emulsifying agents. Increasing the net charge of the proteins (keeping them away from their isoelectric point) increases their solubility and emulsion ability (Christen and Smith 2000).

5.7.11 Factors affecting foaming capacity and stability

Generally, foam is similar to an emulsion. However, it contains two distinct phases. The liquid or solid comprises the continuous phase, and the gas constitutes the dispersed phase. During foaming, the foaming agent migrates to and adsorbs, and spreads at the air/water interface to make a cohesive layer around air bubbles (Christen and Smith 2000).

The specific volume for chickpea flour was greater than the value reported by Han and Khan (1990b) for chickpea flour. This difference was attributed to the higher lipid

content of the chickpea flour (7.1% d.b.) used in the previous study, as foaming capacity improves with a reduction in lipid content (Bencini 1986).

Protein fraction had higher a fat content than did chickpea flour. Therefore, specific volume and volume increase for protein fraction were lower than for chickpea flour. Lipids reduce foaming ability (Christen and Smith 2000). In protein fraction, specific volume was lower and volume increase was greater than values reported by Han and Khan (1990b) for air-classified chickpea protein. This difference was attributed to the chemical treatment applied in the current study. These treatments denatured proteins and changed their structure and functional properties. However, the volume increase in protein fraction was less than values reported by Bencini (1986) for chickpea flour and defatted chickpea flour. This difference may be due to the difference in the chemical composition of the flour, i.e. the higher protein content and lower lipid content increased foam capacity.

In order to estimate the foaming stability of chickpea flour and protein fraction, the following model was proposed and fitted to the measured data:

$$V = a + b\exp(-ct) \tag{5.6}$$

where: V = foam volume (mL);

t = time (min); and

a, b, c = constants of the model.

Constant c shows the slope of decrease of V to a final limit. The SAS NLIN procedure was used to calculate constants of model and to fit the model to the experimental data. Table 5.5 presents the foaming stability equation and the statistical parameters of the fitted model for chickpea flour and protein fraction. The model fitted the experimental data very well with high R^2 and low standard errors of estimate. The absolute value of constant c for protein

fraction (0.025) was greater than the value for chickpea flour (0.004). This difference confirms that the foaming volume of protein fraction diminished faster than that of chickpea flour, as mentioned earlier and shown in Figures 4.25 and 4.26.

Table 5.5 Relationship between foaming stability and time.

Sample	Foaming stability equation†	R^2	SEE*
Chickpea flour	$V = -14.07 + 49.17 \exp(-0.004\, t)$	0.97	1.47
Protein fraction	$V = 11.61 + 24.36 \exp(-0.025\, t)$	0.99	1.03

† V = volume (mL), t = time (min)

* SEE: standard error of estimate

5.8 Potential utilization of chickpea starch and protein

Chickpea protein is higher in lysine, but lower in tryptophan and sulfur-containing amino acids, than is cereal protein. Thus, a combination of chickpea protein, or some other legume protein, and cereal protein would provide a good balance of essential amino acids (Swanson 1990; Chavan et al. 1986). Chickpea protein has a high biological value and protein quality compared to other legumes (Chavan et al. 1986). Utilization of chickpea protein in the manufacture of cereal-based food products, such as breakfast foods, bread, cookies, and snacks, could improve both the quality and the nutritional value of these products. In addition, application of chickpea protein in some processed meat products, such as hamburger and sausages, potentially could reduce the prices of these products.

Starch is the most abundant component in many legume seeds, including chickpea. The starch fractions from different species and different cultivars may vary in composition, physical properties, and functional properties (Ratnayake et al. 2001). Chickpea starch obtained in this study has the potential to be used in different industries such as food (baby

foods, sausages, snacks, sauces, low fat foods, soft drinks, and ice cream), animal feed (feed pellets), hygiene (diapers), pharmaceuticals (tablets), paper (corrugated paper), cosmetics, and textiles (International Starch Institute 2003). The properties of the final product, including food and feed products, are not characterized only by starch. The processing conditions and the effects of other ingredients are crucial determinants of the characteristics of the end product. The chickpea starch obtained in this study had high WHC but was not able to make a stable foam. It could be used as a binder for wafers and ice cream cones or as a coating and glazing agent for nut meats and candies (Liu 2005). Chickpea starch had a higher asymptotic modulus than did chickpea flour, as it was able to sustain unrelaxed stress. Thus, it could be used effectively as a binder in feed pellets. Chickpea starch also could be used as an ingredient in starch-filled polyethylene film. The presence of large starch granules in chickpea starch could improve the light transmittance of the film, as discussed by Lim and co-workers (1992) for potato starch.

In terms of composition, chickpea starch had a lower starch content (75.0% d.b.) than did Nastar (99% d.b.), a commercial pea starch produced by Cosucra (Fontenoy, Belgium), and Accu-Gel (95% d.b.), a commercial pea starch produced by Nutri-Pea Limited (Portage la Prairie, MB). The residual protein and ash contents of chickpea starch (2.1 and 1.6% d.b., respectively) were higher than those of Nastar (less than 0.5 and 0.2% d.b., respectively) and Accu-Gel (1.0% d.b. and less than 0.2% d.b., respectively) (Cosucra 2007a; Nutri-Pea Limited 2007). Chickpea starch also had a lower starch content than did air-classified pea starch, i.e. Starlite (84% d.b.), produced by Parrheim Foods (Saskatoon, SK), but was lower in protein and ash than Starlite (6% and less than 2% d.b., respectively) (Parrheim Foods 2007a).

Chickpea protein had a lower protein content (81.9% d.b.) than did Pisane (90.0% d.b.), a commercial pea protein isolate produced by Cosucra, but was similar in protein content to Propulse (82.0% d.b.), a pea protein isolate produced by Nutri-Pea Limited. The fat content of chickpea protein (9.5% d.b.) was higher than that of Pisane (1.5% d.b.) and Propulse (3.0% d.b.). The ash content of chickpea protein (%5.0 d.b.) was similar to that of Pisane (6.0% d.b.) and Propulse (less than 4.0% d.b.) (Cosucra 2007b; Nutri-Pea Limited 2006). Chickpea protein had higher protein and fat contents than did air-classified protein, i.e. Prestige (50% and less than 6% d.b., respectively), produced by Parrheim Foods (Parrheim Foods 2007b).

In terms of functional properties, the WHC of chickpea protein (0.91 mL/g) was markedly lower than that of Pisane (7.08 mL/g) and Propulse (4.43 mL/g). It also was lower than that of soybean protein concentrate (2.5 to 3.9 mL/g), soybean protein isolate (4.10 mL/g), and winged bean protein isolate (5.00 mL/g) (Pokatong 1994; Onuma Okezie and Bello 1988). The emulsion capacities of Pisane and Propulse were reported as 2.57 and 1.29 g oil/g, respectively, equivalent to 2.86 and 1.43 mL/g, respectively, if the density of oil is assumed to be 0.9 g/cm^3. The emulsion capacity of chickpea protein was 0.58 mL/g, significantly lower than that of Pisane and Propulse (Soral-Śmietana et al. 1998). It also was lower than that of soybean protein concentrate (from 83.5 to 247.5 mL/g as determined by Pokatong (1994)), soybean protein isolate (12.90 mL/g as reported by Onuma Okezie and Bello (1988) and 379.4 mL/g as determined by Rawung (1995) (different method for assessing emulsion capacity were employed by these authors), and winged bean protein isolate (8.00 mL/g). The foaming capacity of chickpea protein (21.67%) was poorer than that of soybean protein concentrate (from 116 to 199% as determined by Pokatong (1994)),

soybean protein isolate (84.00% as reported by Onuma Okezie and Bello (1988) and 250% as determined by Rawung (1995), and winged bean protein isolate (82.00%) (Onuma Okezie and Bello 1988).

In summary, chickpea starch had lower purity than did commercial products prepared from pea. Chickpea protein had a similar or slightly lower protein content compared to commercial pea protein isolates. However, chickpea protein was higher in protein than air-classified pea protein. Chickpea protein had poorer functional properties than did corresponding products obtained from other legumes. The poor functionality of chickpea protein reflected its relatively high fat content in addition to its relatively low degree of purity. This was the case for Propulse relative to Pisane. It appears that the chickpea protein produced in this study because of relatively low purity and functionality, would not perform well in application using soy protein isolate. Neutralization of protein fraction, preceding freeze drying, could have improved the solubility of the protein fraction.

6. SUMMARY AND CONCLUSIONS

6.1 Summary

The Canadian pulse crop (pea, lentil, bean, and chickpea), the majority of which is produced in the province of Saskatchewan, is mostly exported without any significant degree of processing or fractionation. Fractionation of pulses, including chickpea, may be one way to enhance their economic value and increase domestic consumption.

In this study, separation of starch and protein from chickpea flour was carried out using a hydrocyclone in two media, isopropyl alcohol and deionized water. Different operating parameters, including inlet pressure, feed concentration, defatting of flour, and pH, were examined in an effort to obtain fractions with high starch and protein contents and high separation efficiency. Furthermore, the chemical, physical, and functional properties of chickpea flour and starch and protein fractions were examined.

The chemical interactive force between starch and protein was determined for the first time. The particle size distributions of chickpea flour, overflow, and underflow fractions were characterized using an exponential model. A polynomial linear model was fitted to experimental data for thermal conductivity, specific heat, and thermal diffusivity. Phase transitions of samples were determined at different moisture contents. Frictional properties of samples, including external friction on different test sheet materials and internal friction, were determined. Samples were subjected to compression testing and

empirical compression models were fitted to data. A linear model was fitted to asymptotic modulus data. The functional properties of chickpea starch and protein were investigated.

6.2 Conclusions

Based on the results of experiments and the analysis of data, the following conclusions were reached.

6.2.1 Starch-protein separation from chickpea flour using a hydrocyclone

1. Starch and protein separation efficiencies were improved by increasing the inlet pressure of the hydrocyclone.
2. At the highest inlet pressure (827 kPa) using deionized water, particles having a geometric mean diameter of 5.30 μm were separated in the overflow fraction, and particles with a geometric mean diameter of 26.27 μm were shifted to the underflow fraction.
3. Hydrocyclone operation using isopropyl alcohol resulted in a lower Reynolds number of particles and a higher drag force than did deionized water. Therefore, protein separation efficiency in isopropyl alcohol was slightly higher than that in deionized water. Additionally, isopropyl alcohol resulted in lower centrifugal force than did deionized water. Therefore, starch separation efficiency in isopropyl alcohol was lower than that in deionized water. Isopropyl alcohol was not a good medium in a hydrocyclone to separate starch and protein. This comparison was a contribution to knowledge.
4. Increasing the number of passes through the hydrocyclone, i.e. single- pass to double-pass, significantly increased the starch content of the underflow but did not significantly

affect the protein content of the overflow. The separation efficiencies of both starch and protein decreased in the double-pass process.

5. The use of pH 9.0 and defatting of chickpea flour improved the starch content of the overflow resulting from the second-pass of the first overflow. Defatting of chickpea flour enhanced the protein contents of the overflow sediments. The use of pH 9.0 did not significantly affect the protein content of the supernatants of the overflows. These results were published in the Journal of Food Engineering (Emami et al. 2007).
6. A feed concentration of 5% (w/w) chickpea flour in deionized water was optimal for starch-protein separation using the hydroclone. The optimal inlet pressure was 827 kPa. Chickpea starch and protein were obtained at high separation efficiencies (99.7 and 89.3%, respectively) although their purities were lower than those of commercial starch and protein products from field pea. Nevertheless, this study resulted in relatively higher purity in starch and protein fractions (75.0% d.b. starch and 81.9% d.b. protein, respectively) compared to previous studies conducted on fractionation of chickpea.

6.2.2 Physical properties of chickpea flour and starch and protein fractions

1. There was no chemical interaction between starch and protein particles in the chickpea flour as shown by calorimetric titration using isothermal titration calorimeter. Therefore, observed interactions (by scanning electron microscopy) between starch granules and protein particles in chickpea must have been due to physical interaction. Hence, starch-protein separation could be effected by employing physical force, e.g. centrifugal force.

2. Chickpea flour was fractionated into overflow (smaller particle size) and underflow (larger particle size) streams. The undersize fraction percentage of each sample was modeled using an exponential model.
3. Chickpea starch and protein had higher porosity than did chickpea flour. With respect to colour, chickpea starch was lighter (higher **L** value) and chickpea protein was more red (higher **a** value) and more yellow (higher **b** value) than chickpea flour.
4. The zeta potential of chickpea flour before titration, at a concentration of 1.0 mg/mL and initial pH of 6.5, was –16.5 ± 0.6 mV. The isoelectric pH of chickpea flour was between 4.3 and 4.5. The zeta potential of protein fraction, at a concentration of 0.1 mg/mL and an initial pH of 5.9, was –5.3 ± 0.6 mV.
5. The thermal conductivity of chickpea flour and starch and protein fractions increased linearly with temperature and bulk density.
6. The specific heat of chickpea flour and starch, and protein fractions increased linearly with temperature and moisture content.
7. The thermal diffusivity of chickpea flour and starch and protein fractions decreased with bulk density. However, thermal diffusivity did not show a specific trend with temperature. Chickpea starch had a higher thermal diffusivity than did chickpea flour and protein due to its lower specific heat. Therefore, chickpea starch would have a greater tendency to conduct heat rather than store it, compared to its starch and protein fractions. The results of studies on the thermal properties of chickpea flour and starch and protein fractions were published in Transactions of the ASABE (Emami et al. 2007).
8. The DSC thermograms of chickpea flour and starch and protein fractions showed a major endothermic peak at all moisture contents. By increasing the moisture content of

chickpea flour and starch, the peak gelatinization temperature and tailing shoulder decreased and the enthalpy of starch gelatinization increased.

9. Chickpea flour exhibited the highest coefficient of internal friction. Starch exhibited the highest cohesion.
10. All samples exhibited the highest coefficient of external friction on a concrete surface. The lowest coefficient of external friction was observed on a polypropylene surface for all samples.
11. Chickpea flour and protein fraction exhibited the highest adhesion on a concrete surface, whereas starch exhibited the highest adhesion on a polished steel surface.
12. All empirical compression models showed a good fit to measured data, with the exception of the Kawakita and Lüdde model. The particles in all three samples were under rearrangement during compression rather than deformation. The starch fraction had the highest compressibility. The results of studies on the friction and compression characteristics of chickpea flour and its components were published in Powder Technology (Emami and Tabil 2007).

6.2.3 Functional properties of chickpea flour and starch and protein fractions

1. The nitrogen solubility of chickpea flour was lowest at pH 4.3 - 4.5, and highest at pH 9.0.
2. Chickpea starch had the highest water hydration capacity compared to chickpea flour and protein. The high water hydration capacity of starch fraction was related to its low fat content.

3. Separation of starch and protein by increasing the pH during extraction and subsequently reducing the pH to the isoelectric point (process 1) altered the emulsification ability (both stability and capacity) of chickpea starch and protein.
4. The foaming capacity of samples corresponded to their emulsion capacities. Chickpea flour had the highest foaming capacity and emulsion capacity. The relatively low purity of chickpea starch and protein contributed to their relatively poor functionality. In particular, the relatively high fat content of chickpea protein would have negatively impacted its foaming and emulsifying characteristics.

7. RECOMMENDATIONS FOR FUTURE RESEARCH

The following are suggestions for future study and research which can be conducted as a result of this research:

1. There is a need to separate starch and protein from chickpea flour using a series of hydrocyclones. The starch and protein separation efficiencies in each hydrocyclone should be measured. If separation efficiency in any overflow or underflow fraction is low, this fraction should be recycled back to the feed tank of the previous stage or the initial feed tank.
2. Studies should be performed to reduce production of foam during hydrocyclone operation. Using a high-speed mixer improves the starch-protein separation by exerting shear force. This shear force removes protein particles from the surface of starch granules. Meanwhile, operation of the mixer increases foam on the surface of the slurry and causes difficulty in hydrocyclone operation. There is a need to study the performance of different commercial antifoam products in the starch-protein separation process. However, the antifoam may be collected in the overflow and would result in a protein fraction with poor functional properties.
3. To increase the utilization of fractionated products in different industries, more study is required to improve functional properties of starch and protein fractions.

4. There is a need to study the factors affecting agglomeration of dried protein fraction to improve its functional properties.
5. Studies are needed on the utilization of starch and protein fractions in various industries, e.g. food and feed, hygiene, pharmaceuticals, and paper.
6. Studies should be conducted on starch-protein separation from field pea and lentil using the same technique.
7. Application of starch fraction in fermentation industries, such as biofuel industries, should be studied since this industry is growing very fast. Application of starch fraction in fermentation reactions, e.g. bioethanol production, could increase starch loading for ethanol fermentation.

REFERENCES

AACC. 2000. Method 08-16-ash in soy flour, Method 32-05-total dietary fiber, Method 30-25-crude fat in wheat, corn, and soy flour, feed, and mixed feeds, Method 56-30-water hydration capacity of protein materials, Method 46-23-nitrogen solubility index, Method 46-30-crude protein-combustion method. St. Paul, MN: American Association of Cereal Chemists.

AAFC. 2005. Canada: Pulse Special Crops Supply and Disposition. http://www.agr.gc.ca/mad-dam/e/sd2e /2005e / jun2005sc_e.htm#download (2005/07/29).

Adapa, P.K., L.G. Tabil, G.J. Schoenau, B. Crerar and S. Sokhansanj. 2002. Compression characteristics of fractionated alfalfa grinds. *Powder Handling and Processing* 14(4): 252-259.

Alagusundaram, K., D.S. Jayas, W.E. Muir and N.D.J. White. 1991. Thermal conductivity of bulk barley, lentil, and peas. *Transactions of the ASAE* 34(4): 1784-1788.

Alonso, M. and E.J. Finn. 1980. *Fundamental University Physics*, 2nd edition. Reading, MA: Addison-Wesley Publishing Company.

Anderson, C.G. and C.R. Romo. 1976. Influence of extraction medium pH on the protein content of some legume starches. *Journal of Food Technology* 11(6): 647-654.

Anon. 2005. Manual: Hydrocyclone. http://www.tkk.fi/Units/ChemEng/kurssit/kem 42122/ohjeet/13-ohje-en.pdf (2006/08/25).

AOAC. 2002. AOAC method 925.10 – solids (total) and moisture in flour. Gaithersburg, MD: AOAC International.

ASAE. 2004. ASAE S319.3: Method of determining and expressing fineness of feed materials by sieving. In *ASAE Standards 2004*, 578-581. St. Joseph, MI: ASAE.

Banks, W. and C.T. Greenwood. 1975. *Starch and Its Components*. Edinburg, NY: Edinburgh University Press.

Barbosa-Cánovas, G.V., J. Malavé and M. Peleg. 1987. Density and compressibility of selected food powders mixtures. *Journal of Food Process Engineering* 10(1): 1-19.

Bencini, M.C. 1986. Functional properties of drum-dried chickpea (*Cicer arietinum* L.) flours. *Journal of Food Science* 51(6): 1518-1526.

Beuchat, L.R. 1977. Functional and electrophoretic characteristics of succinylated peanut flour protein. *Journal of Agricultural and Food Chemistry* 25(2): 258-261.

Biliaderis, C.G., D.R. Grant and J.R. Vose. 1981. Structural characterization of legume starches. I. studies on amylose, amylopectin, and beta-limit dextrins. *Cereal Chemistry* 58(6): 496-502.

Bishnoi, S. and N. Khetarpaul. 1993. Variability in physico-chemical properties and nutrient composition of different pea cultivars. *Food Chemistry* 47(4): 371-373.

Bradley, D. 1965. *The Hydrocyclone*, 1st edition. London, UK: Pergamon Press.

Chancellor, W.J. 1994. Friction between soil and equipment materials - a review. In *1994 ASAE Summer Meeting*. ASAE Paper No. 94-1034. St. Joseph, MI.: ASAE.

Chavan, J.K., S.S. Kadam and D.K. Salunkhe. 1986. Biotechemistry and technology of chickpea (*Cicer arietinum* L.) seeds. *CRC Critical Reviews in Food Science and Nutrition* 25(2): 107-158.

Cheftel, J.C., J.L. Cuq and D. Lorient. 1985. Amino acids, peptides, and proteins. In *Food Chemistry*, 2nd edition, ed. O.R. Fennema, 245-369. New York, NY: Marcel Dekker, Inc.

Cheremisinoff, P.N. 1995. *Processing Engineering Handbook Series-Solid/liquid*. Lancaster, PA: Technomic Publishing Co., Inc.

Christen, G.L. and J.S. Smith. 2000. *Food Chemistry: Principles and Applications*. West Sacramento, CA: Science Technology System.

Clemente, A., J. Vioque, R. Sanchez-Vioque, J. Pedroche, J. Bautista and F. Millan. 2000. Factors affecting the in vitro protein digestibility of chickpea albumins. *Journal of the Science of Food and Agriculture* 80(1): 79-84.

Colonna, P., A. Buleon, M. LeMaguer and C. Mercier. 1982. *Pisum sativum* and *Vicia faba* carbohydrates: Part IV-granular structure of wrinkled pea starch. *Carbohydrate Polymers* 2(1): 43-59.

Colonna, P., J. Gueguen and C. Mercier. 1981. Pilot scale preparation of starch and cell-wall material from *Pisum sativum* and *Vicia faba*. *Sciences Des Aliments* 1(3): 415-426.

Cooper, A. and C.M. Johnson. 1994. Isothermal titration microcalorimetry. In *Microscopy, Optical Spectroscopy, and Macroscopic Techniques*, Vol 22, ed. C. Jones, B. Mulloy and A.H. Thomas, 137-150. Totowa, NJ: Humana Press, Inc.

Cooper, A.R. and L.E. Eaton. 1962. Compaction behavior of several ceramic powders. *Journal of the American Ceramic Society* 45(3): 97-101.

Cosucra. 2007a. Specification sheet of *Nastar*. Fontenoy, Belgium: Cosucra Groupe Warcoing.

Cosucra. 2007b. Specification sheet of *Pisane F9*. Fontenoy, Belgium: Cosucra Groupe Warcoing.

Davydova, N.I., S.P. Leont'ev, Y.V. Genin, A.Y. Sasov and T.Y. Bogracheva. 1995. Some physico-chemical properties of smooth pea starches. *Carbohydrate Polymers* 27(2): 109-115.

Day, R.W., C.N. Grichar and T.H. Bier. 1997. Hydrocyclone separation. In *Handbook of Separation Techniques for Chemical Engineers*, ed. P.A. Schweitzer, 4.161- 4.168. New York, NY: McGraw-Hill.

deMan, J.M. 1990. *Principles of Food Chemistry*, 2nd edition. New York, NY: Van Nostrand Reinhold.

Differential Scanning Calorimetry. 1997. http://www.psrc.usm.edu/macrog/dsc.htm (2005/12/30).

Dobrzanski, B.J. and R. Rybczynski. 2002. Colour as a quality factor of fruits and vegetables. In *Physical Methods in Agriculture: Approach to Precision and Quality*, ed. J. Blahovec and M. Kutílek, 375-398. New York, NY: Kluwer Academic / Plenum Publishers.

Donovan, J.W. 1979. Phase transitions of the starch-water system. *Biopolymers* 18: 263-275.

Drouzas, A.E. and G.D. Saravacos. 1988. Effective thermal conductivity of granular starch materials. *Journal of Food Science* 53(6): 1795-1799.

Drouzas, A.E., Z.B. Maroulis, V.T. Karathanos and G.D. Saravacos. 1991. Direct and indirect determination of the effective thermal diffusivity of granular starch. *Journal of Food Engineering* 13(2): 91-101.

Duffy, S.P. and V.M. Puri. 1996. Flowability parameters and flow functions for confectionary sugar and detergent powder at two moisture contents. *American Society of Agricultural Engineering* 12(5): 601-606.

Earle, R.L. 1983. *Unit Operations in Food Processing*, 2nd edition. Oxford, UK: Pergamon Press.

Edwards, D. and M. Hamson. 1990. *Guide to Mathematical Modelling*. Boca Raton, FL: CRC Press.

Egan, H., R.S. Kirk and R. Sawyer. 1981. *Pearson's Chemical Analysis of Foods*, 8th edition. Essex, UK: Longman Scientific & Technical.

Emami, S. and L. Tabil. 2007. Friction and compression characteristics of chickpea flour and components. *Powder Technology* 175: 14-21 available at http://dx.doi.org/10.1016/j.powtec.2006.12.021.

Emami, S., L. G. Tabil, R. T. Tyler and W. J. Crerar. 2007. Starch-protein separation from chickpea flour using a hydrocyclone. *Journal of Food Engineering* 82(4): 460-465 available at http://dx.doi.org/10.1016/j.jfoodeng.2007.03.002.

Emami, S., L.G. Tabil and R.T. Tyler. 2007. Thermal properties of chickpea flour, isolated chickpea starch, and isolated chickpea protein. *Transactions of the ASABE* 50(2): 597-604.

Fang, Q., Y. Lan, M.F. Kocher and M.A. Hanna. 2000. Thermal conductivity of granular rice starches. *International Journal of Food Properties* 3(2): 283-293.

FAO. 2006. FAOSTAT statistical database. Food and Agriculture Organization of United Nations. http:/faostat.fao.org/faostat/form?collection=Production.Crops.Primary&Domain=Production&servlet=1&hasbulk=0&version=ext&language=EN (2005/07/29).

Fontana, A.J., B. Wacker, C.S. Campbell and G.S. Campbell. 2001. Simultaneous thermal conductivity, thermal resistivity, and thermal diffusivity measurement of selected foods and soils. In *2001 ASAE Annual International Meeting*. ASAE Paper No. 01-6101. St. Joseph, MI.: ASAE.

Gardner, H.K.J., R.J.S. Hron and H.L.E. Vix. 1976. Removal of pigment glands (gossypol) from cottonseed. *Cereal Chemistry* 53(4): 549-560.

Grady, S., G.D. Wesson, M.M. Abdullah and E.E. Kalu. Year Unknown. Small diameter hydrocyclone separation efficiency estimation using computational fluid dynamics. http://ipec.utulsa.edu/Conf2003/Abstracts/grady.html (2006/09/23).

Gujska, E., W.D. Reinhard and K. Khan. 1994. Physicochemical properties of field pea, pinto and navy bean starches. *Journal of Food Science* 59(3): 634-636.

Hammer, A., C. Grüttner and R. Schumann. 1999. The effect of electrostatic charge of food particles on capture efficiency by *Oxyrrhis marina* dujardin (dinoflagellate). *Protist* 150(4): 375-382.

Han, J. and K. Khan. 1990a. Physicochemical studies of pin-milled and air-classified dry edible bean fractions. *Cereal Chemistry* 67(4): 384-390.

Han, J. and K. Khan. 1990b. Functional properties of pin-milled and air-classified dry edible bean fractions. *Cereal Chemistry* 67(4): 390-394.

Holm, J., A.D. Björck and N.-G. Asp. 1986. A rapid method for the analysis of starch. *Starch* 38(7): 224-226.

Hooper, F.C. and F.R. Lepper. 1950. Transient heat flow apparatus for the determination of thermal conductivities. *Heating, Piping, and Air Conditioning* 22: 129-134.

Hoover, R. and F.W. Sosulski. 1991. Composition, structure, functionality, and chemical modification of legume starches: a review. *Canadian Journal of Physiology and Pharmacology* 69(1): 79-91.

International Starch Institute. 2003. Tapioca Starch Applications. http://www.starch.dk/isi /applic/applic.htm (2006/04/22).

Iwabuchi, K., T. Kimura and L. Otten. 1999. Effect of volumetric water content on thermal properties of dairy cattle feces mixed with sawdust. *Bioresource Technology* 70(3): 293-297.

Jaya, T.V. and L.V. Venkataraman. 1979. Effect of germination on the supplementary value of chickpea and greengram protein to those of rice and wheat. *Nutrition Reports International* 19(6): 777-783.

Jenike, A.W. 1967. Storage and flow of solids. Bulletin No. 123. Salt Lake City, UT: University of Utah.

Johnson, E.A. and C.J. Brekke. 1983. Functional properties of acylated pea protein isolates. *Journal of Food Science* 48(3): 722-725.

Johnson, L.A. 1997. Theoretical, comparative, and historical analysis of alternative technologies for oilseed extraction. In *Technology and Solvents for Extracting Oilseeds and Nonpetroleum Oils*, ed. P.J. Wan and P.J. Wakelyn, 4-47. Champaign, IL: AOCS Press.

Jones, J.D. and D.S. McGinnis. 1991. Separation of oilseed components in solvent phase. United States Patent 5035910.

Jones, W.D. 1960. *Fundamental Principles of Powder Metallurgy*. London, UK: Edward Arnold Publisher Ltd.

Jood, S., S. Bishnoi and A. Sharma. 1998. Chemical analysis and physico-chemical properties of chickpea and lentil cultivars. *Nahrung* 42(2): 71-74.

Kaletunc, G. and K.J. Breslauer. 2003. *Characterization of Cereal and Flours-Properties, Analysis, and Applications*. New York, NY: Marcel Dekker, Inc.

Kawakita, K. and K.H. Lüdde. 1971. Some considerations on powder compression equations. *Powder Technology* 4(2): 61-68.

Kerr, W.L., C.D.W. Ward, K.H. McWatters and A.V.A. Resurreccion. 2000. Effect of milling and particle size on functionality and physicochemical properties of cowpea flour. *Cereal Chemistry* 77(2): 213-219.

Kosson, R., Z. Czuchajowska and Y. Pomeranz. 1994. Smooth and wrinkled peas. 1. general physical and chemical characteristics. *Journal of Agricultural and Food Chemistry* 42(1): 91-95.

Krokida, M.K., Z.B. Maroulis and M.S. Rahman. 2001. A structural generic model to predict the effective thermal conductivity of granular materials. *Drying Technology* 19(9): 2277-2290.

Kurien, P.P. 1987. Post-harvest technology of chickpea. In *The Chickpea*, ed. M.C. Saxena and K.B. Singh, 369-381. Wallingford, UK: CAB International.

Lan, Y., Q. Fang, M.F. Kocher and M.A. Hanna. 2000. Thermal properties of tapioca starch. *International Journal of Food Properties* 3(1): 105-116.

Lim, S.T., J.L. Jane, S. Rajagopalan and P.A. Seib. 1992. Effect of starch granule size on physical properties of starch-filled polyethylene film. *Biotechnology Progress* 8(1): 51-57.

Lineback, D.R. and C.H. Ke. 1975. Starches and low-molecular-weight carbohydrates from chick pea and horse bean flours. *Cereal Chemistry* 52(3): 334-347.

Liu, L.H. and T.V. Hung. 1998. Flow properties of chickpea proteins. *Journal of Food Science* 63(2): 229-233.

Liu, Q. 2005. Understanding starches and their role in foods. In *Food Carbohydrates: Chemistry, Physical Properties, and Applications*, ed. S.W. Cui, 309-355. Boca Raton, FL: CRS Press-Taylor & Francis Group.

Ma, L., D.C. Davis, L.G. Obaldo and G.V. Barbosa-Cánovas. 1998. *Engineering Properties of Food and Other Biological Materials*. St. Joseph, MI: ASAE.

Mahadevappa, V.G. and P.L. Raina. 1978. Nature of some Indian legume lipids. *Journal of Agricultural and Food Chemistry* 26(5): 1241-1243.

Makhmudov, A. 1980. Increased nutritive value of the national grades of bread baked in Central Asia republics. *Voprosy Pitaniia* (6): 64-66.

Malvern Instruments. 1997. *Getting Started*. Malvern, Worcestershire, UK: Malvern Instruments Ltd.

Malvern Instruments. 2005a. Zeta potential - an introduction in 30 minutes. *Zetasizer Nano Series Technical Note*. Malvern, Worcestershire, UK: Malvern Instruments Ltd.

Malvern Instruments. 2005b. Automated protein characterization with the MPT-2 autotitrator. *Zetasizer Nano Application Note*. Malvern, Worcestershire, UK: Malvern Instruments Ltd.

Malvern Instruments. 2005c. The measurement of zeta potential using an autotitrator: effect of conductivity. *Application Note*. Malvern, Worcestershire, UK: Malvern Instruments Ltd.

Malvern Mastersizer. 1994. *Mastersizer Series Software Suite*. Ver. 2.19. Malvern, Worcestershire, UK: Malvern Instruments Ltd.

Mani, S., L.G. Tabil and S. Sokhansanj. 2004a. Mechanical properties of corn stover grind. *Transactions of the ASAE* 47(6): 1983-1990.

Mani, S., L.G. Tabil and S. Sokhansanj. 2004b. Evaluation of compaction equations applied to four biomass species. *Canadian Biosystems Engineering* 46(3): 55-61.

McCabe, W.L. and J.C. Smith. 1976. *Unit Operations of Chemical Engineering*, 3rd edition. New York, NY: McGraw-Hill.

McCabe, W.L., J.C. Smith and P. Harriott. 1993. *Unit Operations of Chemical Engineering*, 5th edition. New York, NY: McGraw-Hill.

McCabe, W.L., J.C. Smith and P. Harriott. 2005. *Unit Operations of Chemical Engineering*, 7th edition. New York, NY: McGraw-Hill.

Menkov, N.D. 2000. Moisture sorption isotherms of chickpea seeds at several temperatures. *Journal of Food Engineering* 45(4): 189-194.

MicroCal. 2005. Ultrasensitive Calorimetry for the Life Science. http://www. microcalorimetry .com/index.php?id=13 (2006/01/22).

Mohsenin, N.N. 1980. *Thermal Properties of Foods and Agricultural Materials*. New York, NY: Gordon and Breach Science Publisher.

Mohsenin, N.N. 1986. *Physical Properties of Plant and Animal Materials : Structure, Physical Characteristics and Mechanical Properties*, 2nd edition. New York, NY: Gordon and Breach Science Publishers.

Moreyra, R. and M. Peleg. 1981. Effect of equilibrium water activity on the bulk properties of selected food powders. *Journal of Food Science* 46(6): 1918-1922.

Murata, S., A. Tagawa and S. Ishibashi. 1987. The effect of moisture content and temperature on specific heat of cereal grains measured by DSC. *Journal of the Japanese Society of Agricultural Machinery* 46(6): 547-554.

Murray, E.D., C.D. Myers and L.D. Barker. 1979. Protein product and process for preparing same. United States Patent 4169090.

Nelson, D.L. and M.M. Cox. 2005. *Lehninger Principles of Biochemistry*, 4th edition. New York, NY: W.H. Freeman and Company.

Nesvadba, P. 1982. Methods for the measurement of thermal conductivity and diffusivity of foodstuffs. *Journal of Food Engineering* 1(2): 93-113.

Nix, G.H., G.W. Lowery, R.I. Vachon and G.E. Tanger. 1967. Direct determination of thermal diffusivity and conductivity with a refined line-source technique. In *Progress*

in Aeronautics and Astronautic: Thermophysics of Spacecraft and Planetary Bodies 20: 865-878. New York, NY: Academic Press.

Nutri-Pea Limited. 2006. Specification sheet of *Propulse- pea protein*. Portage la Prairie, Manitoba, Canada: Nutri-Pea Limited.

Nutri-Pea Limited. 2007. Specification sheet of A*ccu-Gel-native pea starch*. Portage la Prairie, Manitoba, Canada: Nutri-Pea Limited.

Onuma Okezie, B. and A.B. Bello. 1988. Physicochemical and functional properties of winged bean flour and isolate compared with soy isolate. *Journal of Food Science* 53(2): 450-454.

Opoku, A., L.G. Tabil, B. Crerar and M.D. Shaw. 2006. Thermal conductivity and thermal diffusivity of timothy hay. *Canadian Biosystems Engineering* 48(3): 1-7.

Owusu-Ansah, Y.J. and S.M. Mc Curdy. 1991. Pea proteins: a review of chemistry, technology of production, and utilization. *Food Reviews International* 7(1): 103-134.

Parrheim Foods. 2007a. Specification sheet of *Starlite.* Saskatoon, SK, Canada: Parrheim Foods-A Division of Parrish and Heimbecker.

Parrheim Foods. 2007b. Specification sheet of *Prestige protein.* Saskatoon, SK, Canada: Parrheim Foods-A Division of Parrish and Heimbecker.

Peleg, M. 1977. Flowability of food powders and methods for its evaluation - a review. *Journal of Food Process and Engineering* 1(4): 303-328.

Peleg, M. 1979. Characterization of the stress relaxation curves of solid foods. *Journal of Food Science* 44(1): 277-281.

Peleg, M. and R. Moreyra. 1979. Effect of moisture on the stress relaxation pattern of compacted powders. *Powder Technology* 23(2): 277-279.

Peleg, M., C.H. Mannheim and N. Passy. 1973. Flow properties of some food powders. *Journal of Food Science* 38(6): 959-964.

Pierce, M.M., C.S. Raman and B.T. Nall. 1999. Isothermal titration calorimetry of protein-protein interactions. *Methods* 19(2): 213-221.

Pokatong, W.D.R. 1994. Effect of processing method on the composition and functionality of protein concentrates prepared from air-classified pea protein and soy flour. Unpublished M.Sc. thesis. Saskatoon, SK: Department of Applied Microbiology and Food Science, University of Saskatchewan.

Puchalski, C. and G.H. Brusewitz. 1996. Coefficient of friction of watermelon. *Transactions of the ASAE* 39(2): 589-594.

Quinn, J.R. and D. Paton. 1979. A practical measurement of water hydration capacity of protein materials. *Cereal Chemistry* 56(1): 38-40.

Rackis, J.J., D.J. Sessa and D.H. Honig. 1979. Flavor problems of vegetable food proteins. *Journal of the American Oil Chemists' Society* 56(3): 262-271.

Rahman, S. 1995. *Food Properties Handbook*. Boca Raton, FL: CRC Press.

Ratnayake, W.S., R. Hoover and T. Warkentin. 2002. Pea starch: composition, structure and properties - a review. *Starch* 54(6): 217-234.

Ratnayake, W.S., R. Hoover, F. Shahidi, C. Perera and J. Jane. 2001. Composition, molecular structure, and physicochomical properties of starches from four field pea (*Pisum sativum* L.) cultivars. *Food Chemistry* 74(2): 189-202.

Rawle, A. Year Unknown. Basic principles of particle size analysis. Malvern, UK: Malvern Instruments Ltd.

Rawung, D. 1995. Recovery of protein from pea and soybean whey by heat precipitation, ultrafiltration and ion exchange. Unpublished M.Sc. thesis. Saskatoon, SK: Department of Applied Microbiology and Food Science, University of Saskatchewan.

Reichert, R.D. 1982. Air classification of peas (*Pisum sativum*) varying widely in protein content. *Journal of Food Science* 47(4): 1263-1267, 1271.

Reichert, R.D. and C.G. Youngs. 1978. Nature of residual protein associated with starch fractions from air-classified field peas. *Cereal Chemistry* 55(4): 469-480.

Ridlehuber, J.M. and H.K. Gardner Jr. 1974. Production of food-grade cottonseed protein by the liquid cyclone process. *Journal of the American Oil Chemists' Society* 51(4): 153-157.

Rushton, A., A.S. Ward and R.G. Holdich. 1996. *Solid-Liquid Filtration and Separation Technology*. New York, NY: VCH Publishers, Inc.

Salunkhe, D.K., S.S. Kadam and J.K. Chavan. 1985. *Postharvest Biotechnology of Food Legumes*. Boca Raton, FL: CRC Press.

Sánchez-Vioque, R., A. Clemente, J. Vioque, J. Bautista and F. Millán. 1999. Protein isolates from chickpea (*Cicer arietinum* L.): chemical composition, functional properties and protein characterization. *Food Chemistry* 64(2): 237-243.

Saravacos, G.D. and Z.B. Maroulis. 2001. *Transport Properties of Foods*. New York, NY: Marcel Dekker, Inc.

SAS. 2003. *SAS User's Guide: Statistics*. Ver. 9.1. Cary, NC: Statistical Analysis System, Inc.

Saskatchewan Agriculture and Food. 2005. 2004 special crop reports. http://www.agr.gov.sk.ca/DOCS/crops/special_crops/production_information/specialtycroprpt2004.pdf (2005/07/29).

Saskpulse. 2005. Introduction. http://www.saskpulse.com/library/ppm/history.pdf (2005/07/29).

Sathe, S.K. and D.K. Salunkhe. 1981. Investigations on winged bean [*Psophocarpus tetragonolobus* (L.) DC] proteins and antinutritional factors. *Journal of Food Science* 46(5): 1389-1393.

Scoville, E. and M. Peleg. 1981. Evaluation of the effects of liquid bridges on the bulk properties of model powders. *Journal of Food Science* 46(1): 174-177.

Shaw, M.D., L.G. Tabil, A. Opoku and W.J. Crerar. 2005. Compression studies of peat moss, wheat straw, oat hulls and flax shives. In *2005 North Central ASAE/CSAE Conference.* ASAE/CSAE Paper No. SD05-604. St. Joseph, MI.: ASAE.

Singh, K.K. and T.K. Goswami. 2000. Thermal properties of cumin seed. *Journal of Food Engineering* 45(4): 181-187.

Singh, N. and S.R. Eckhoff. 1995. Hydrocyclone procedure for starch-protein separation in laboratory wet milling. *Cereal Chemistry* 72(4): 344-348.

Singh, R.P. and D.R. Heldman. 2001. *Introduction to Food Engineering*, 3rd edition. San Diego, CA: Academic Press.

Sokhansanj, S. and R.T. Patil. 2003. Dehulling and splitting pulses. In *Handbook of Postharvest Technology: Cereals, Fruits, Vegetables, Tea, and Spices*, ed. A. Chakraverty, A.S. Mujumdar, G.S.V. Raghavan and H.S. Ramaswamy, 397-426. New York, NY: Marcel Dekker, Inc.

Soral-Śmietana, M., A. Świgoń, R. Amarowicz and L. Sijtsma. 1998. Chemical composition, microstructure and physico-chemical characteristics of two commercial pea protein isolates. *Polish Journal of Food and Nutrition Sciences* 7/48(2): 193-200.

Sosulski, F. and R. Zadernowski. 1981. Fractionation of rapeseed meal into flour and hull components. *Journal of the American Oil Chemists' Society* 58(2): 96-98.

Sosulski, F.W. and K. Sosulski. 1986. Composition and functionality of protein, starch, and fiber from wet and dry processing of grain legumes. In *ACS Symposium Series, 312*, 176-189. Washington, DC: American Chemical Society.

Sosulski, F.W. and R. Zadernowski. 1980. Dehulling of rapeseed or mustard defatted meals. Canadian Patent 1089849.

Sosulski, F.W., A.F. Walker, P. Fedec and R.T. Tyler. 1987. Comparison of air classifiers for separation of protein and starch in pin-milled legume flours. *Lebensmittel-Wissenschaft und –Technology* (*Food Science and Technology*) 20(5): 221-225.

Sosulski, F.W., R. Hoover, R.T. Tyler, E.D. Murray and S.D. Arntfield. 1985. Differential scanning calorimetry of air-classified starch and protein fractions from eight legume species. *Starch* 37(8): 257-262.

Statie, E., M. Salcudean, I. Gartshore and E. Bibeau. 2002. A computational study of particle separation in hydrocyclones. *Journal of Pulp and Paper Science* 28(3): 84-92.

Sumner, A.K., M.A. Nielsen and C.G. Youngs. 1981. Production and evaluation of pea protein isolate. *Journal of Food Science* 46(2): 364-366, 372.

Svarovsky, L. 1984. *Hydrocyclones*. Lancaster, PA: Technomic Publishing Co., Inc.

Svarovsky, L. 1990. Hydrocyclones. In *Solid-Liquid Separation*, 3rd edition, ed. L. Svarovsky, 202-250. London, UK: Butterworths.

Swanson, B.G. 1990. Pea and lentil protein extraction and functionality. *Journal of the American Oil Chemists' Society* 67(5): 276-280.

Sweat, V.E. 1995. Thermal propertied of foods. In *Engineering Properties of Foods*, 2nd edition, ed. M.A. Rao and S.S.H. Rizvi, 99-138. New York, NY: Marcel Dekker, Inc.

Tabil, L.G. and S. Sokhansanj. 1997. Bulk properties of alfalfa grind in relation to its compaction characteristics. *Applied Engineering in Agriculture* 13(4): 499-505.

Tabil, L.G., S. Sokhansanj and R.T. Tyler. 1995. Processing of pulses. In *Proceedings of the Pulse Cleaning and Processing Workshop.* Saskatoon, SK: Department of Agricultural and Bioresource Engineering and the Extension Division, University of Saskatchewan.

Teunou, E. and J.J. Fitzpatrick. 1999. Effect of relative humidity and temperature on food powder flowability. *Journal of Food Engineering* 42(2):109-116.

Teunou, E., J.J. Fitzpatrick and E.C. Synnott. 1999. Characterisation of food powder flowability. *Journal of Food Engineering* 39(1): 31-37.

Thompson, L.U. 1977. Preparation and evaluation of mung bean protein isolates. *Journal of Food Science* 42(1): 202-206.

Tian, S., W.S.A. Kyle and D.M. Small. 1999. Pilot scale isolation of proteins from field peas (*Pisum sativum* L.) for use as food ingredients. *International Journal of Food Science and Technology* 34(1): 33-39.

Tyler, R.T. 1984. Impact milling quality of grain legumes. *Journal of Food Science* 49(3): 925-930.

Tyler, R.T., C.G. Youngs and F.W. Sosulski. 1981. Air classification of legumes. I. separation efficiency, yield, and composition of the starch and protein fractions. *Cereal Chemistry* 58(2): 144-147.

Valdebouze, P., E. Bergeron, T. Gaborit and J. Delort-laval. 1980. Content and distribution of trypsin inhibitors and hemagglutinins in some legume seeds. *Canadian Journal of Plant Science* 60(2): 695-701.

Van der Held, E.F.M. and F.G. Van Drunen. 1949. A method of measuring thermal conductivity of liquids. *Physica* 15(10): 865-881.

Vasanthan, T. and R. Hoover. 1992. Effect of defatting on starch structure and physicochemical properties. *Food Chemistry* 45(5): 337-347.

Vose, J.R. 1977. Functional characteristics of an intermediate amylase starch from smoth-seeded field peas compared with corn and wheat starches. *Cereal Chemistry* 54(5): 1141-1151.

Vose, J.R. 1980. Production and functionality of starches and protein isolates from legume seeds (field peas and horsebeans). *Cereal Chemistry* 57(6): 406-410.

Walker, E.E. 1923. The properties of powders-Part VI: The compressibility of powders. *Transitions of the Faraday Society* 19(1): 73-82.

Wan, P.J., J. Green, C.M. Cater and K.F. Mattil. 1979. Factors influencing the color of cottonseed protein products. *Journal of Food Science* 44(2): 475-479.

Wang, J. and K. Hayakawa. 1993. Maximum slope method for evaluating thermal conductivity probe data. *Journal of Food Science* 58(6): 1340-1345.

Watson, P.J. and P.A. Tuzinski. 1989. *Study of Zeta Potential for Material Particles in Chemical Additive Solutions*. United States Bureau of Mines Information Circular. Washington, DC: United States Bureau of Mines, Department of Interior.

Widmann, G. and R. Reissen. 1987. *Thermal Analysis: Terms, Methods and Applications.* Heidelberg, Germany: Verlag GmbH.

Yang, W., S. Sokhansanj, J. Tang and P. Winter. 2002. Determination of thermal conductivity, specific heat and thermal diffusivity of borage seeds. *Biosystems Engineering* 82(2): 169-176.

Zeleznak, K.J. and R.C. Hoseney. 1987. The glass transition in starch. *Cereal Chemistry* 64(2): 121-124.

Zhang, J. and R.L. Kushwaha. 1993. Effect of relative humidity and temperature on grain-metal friction. *Canadian Agricultural Engineering* 35(1): 41-44.

APPENDIXES

LIST OF APPENDIXES

Appendix A

Statistical analysis of starch and protein contents at different inlet pressures in isopropyl alcohol medium

A.1 Statistical analysis of the overflow starch content at different inlet pressures

The SAS System
The GLM Procedure

Class Level Information

Class	Levels	Values
Pressure	3	552 689 827

Number of observations 9

The SAS System
The GLM Procedure

Dependent Variable: Overflow Starch

Source	DF	Sum of Squares	Mean Square	F Value	Pr > F
Model	2	301.9088889	150.9544444	1306.34	<.0001
Error	6	0.6933333	0.1155556		
Corrected Total	8	302.6022222			

R-Square	Coeff Var	Root MSE	Overflow Starch Mean
0.997709	2.509772	0.339935	13.54444

Source	DF	Type III SS	Mean Square	F Value	Pr > F
Pressure	2	301.9088889	150.9544444	1306.34	<.0001

The SAS System
The GLM Procedure

Duncan's Multiple Range Test for Overflow Starch

Alpha	0.05
Error Degrees of Freedom	6
Error Mean Square	0.115556

Number of Means	2	3
Critical Range	.6792	.7039

Means with the same letter are not significantly different.

Duncan Grouping	Mean	N	Pressure
A	21.6667	3	827
B	10.4000	3	689
C	8.5667	3	552

A.2 Statistical analysis of the overflow protein content at different inlet pressures

The SAS System
The GLM Procedure

Class Level Information

Class	Levels	Values
Pressure	3	552 689 827

Number of observations 9

The SAS System
The GLM Procedure

Dependent Variable: Overflow Protein

Source	DF	Sum of Squares	Mean Square	F Value	Pr > F
Model	2	124.8955556	62.4477778	5.72	0.0407
Error	6	65.4733333	10.9122222		
Corrected Total	8	190.3688889			

R-Square	Coeff Var	Root MSE	Overflow Protein Mean
0.656071	6.912413	3.303365	47.78889

Source	DF	Type III SS	Mean Square	F Value	Pr > F
Pressure	2	124.8955556	62.4477778	5.72	0.0407

The SAS System
The GLM Procedure

Duncan's Multiple Range Test for Overflow Protein

Alpha	0.05
Error Degrees of Freedom	6
Error Mean Square	10.91222

Number of Means	2	3
Critical Range	6.600	6.840

Means with the same letter are not significantly different.

Duncan Grouping	Mean	N	Pressure
A	52.933	3	827
B	46.200	3	689
B			
B	44.233	3	552

A.3 Statistical analysis of the underflow starch content at different inlet pressures

The SAS System
The GLM Procedure

Class Level Information

Class	Levels	Values
Pressure	3	552 689 827

Number of observations 9

The SAS System
The GLM Procedure

Dependent Variable: Underflow Starch

Source	DF	Sum of Squares	Mean Square	F Value	Pr > F
Model	2	14.33555556	7.16777778	1.75	0.2520
Error	6	24.58000000	4.09666667		
Corrected Total	8	38.91555556			

R-Square	Coeff Var	Root MSE	Underflow Starch Mean
0.368376	3.966943	2.024022	51.02222

Source	DF	Type III SS	Mean Square	F Value	Pr > F
Pressure	2	14.33555556	7.16777778	1.75	0.2520

The SAS System
The GLM Procedure

Duncan's Multiple Range Test for Underflow Starch

Alpha	0.05
Error Degrees of Freedom	6
Error Mean Square	4.096667

Number of Means	2	3
Critical Range	4.044	4.191

Means with the same letter are not significantly different.

Duncan Grouping	Mean	N	Pressure
A	52.367	3	552
A			
A	51.367	3	827
A			
A	49.333	3	689

A.4 Statistical analysis of the underflow protein content at different inlet pressures

The SAS System
The GLM Procedure

Class Level Information

Class	Levels	Values
Pressure	3	552 689 827

Number of observations 9

The SAS System
The GLM Procedure

Dependent Variable: Underflow Protein

Source	DF	Sum of Squares	Mean Square	F Value	Pr > F
Model	2	60.08222222	30.04111111	18.70	0.0026
Error	6	9.64000000	1.60666667		
Corrected Total	8	69.72222222			

R-Square	Coeff Var	Root MSE	Underflow Protein Mean
0.861737	5.315886	1.267544	23.84444

Source	DF	Type III SS	Mean Square	F Value	Pr > F
Pressure	2	60.08222222	30.04111111	18.70	0.0026

The SAS System
The GLM Procedure
Duncan's Multiple Range Test for Underflow Protein

Alpha	0.05
Error Degrees of Freedom	6
Error Mean Square	1.606667

Number of Means	2	3
Critical Range	2.532	2.625

Means with the same letter are not significantly different.

Duncan Grouping	Mean	N	Pressure
A	26.133	3	552
A			
A	25.167	3	689
B	20.233	3	827

Appendix B

Statistical analysis of starch and protein contents of single- and double-pass processes in isopropyl alcohol medium

B.1 Statistical analysis of the overflow starch content using single- and double-pass processes

The SAS System
The GLM Procedure

Class Level Information

Class	Levels	Values
Fraction	3	O1 OO1 OU1

Number of observations 9

The SAS System
The GLM Procedure

Dependent Variable: Overflow Starch

Source	DF	Sum of Squares	Mean Square	F Value	Pr > F
Model	2	392.6288889	196.3144444	1840.45	<.0001
Error	6	0.6400000	0.1066667		
Corrected Total	8	393.2688889			

R-Square	Coeff Var	Root MSE	Overflow Starch Mean
0.998373	2.235276	0.326599	14.61111

Source	DF	Type III SS	Mean Square	F Value	Pr > F
Fraction	2	392.6288889	196.3144444	1840.45	<.0001

The SAS System
The GLM Procedure

Duncan's Multiple Range Test for Overflow Starch

Alpha	0.05
Error Degrees of Freedom	6
Error Mean Square	0.106667

Number of Means	2	3
Critical Range	.6525	.6763

Means with the same letter are not significantly different.

Duncan Grouping	Mean	N	Fraction
A	21.3333	3	O1
B	16.8667	3	OU1
C	5.6333	3	OO1

B.2 Statistical analysis of the overflow protein content using single- and double-pass processes

The SAS System
The GLM Procedure

Class Level Information

Class	Levels	Values
Fraction	3	O1 OO1 OU1

Number of observations 9

The SAS System
The GLM Procedure

Dependent Variable: Overflow Protein

Source	DF	Sum of Squares	Mean Square	F Value	Pr > F
Model	2	64.46222222	32.23111111	6.82	0.0285
Error	6	28.36000000	4.72666667		
Corrected Total	8	92.82222222			

R-Square	Coeff Var	Root MSE	Overflow Protein Mean
0.694470	4.067098	2.174090	53.45556

Source	DF	Type III SS	Mean Square	F Value	Pr > F
Fraction	2	64.46222222	32.23111111	6.82	0.0285

The SAS System
The GLM Procedure

Duncan's Multiple Range Test for Overflow Protein

Alpha	0.05
Error Degrees of Freedom	6
Error Mean Square	4.726667

Number of Means	2	3
Critical Range	4.344	4.502

Means with the same letter are not significantly different.

Duncan Grouping	Mean	N	Fraction
A	56.033	3	OO1
A			
A	54.567	3	O1
B	49.767	3	OU1

B.3 Statistical analysis of the underflow starch content using single- and double-pass processes

The SAS System
The GLM Procedure

Class Level Information

Class	Levels	Values
Fraction	3	U1 UO1 UU1

Number of observations 9

The SAS System
The GLM Procedure

Dependent Variable: Underflow Starch

Source	DF	Sum of Squares	Mean Square	F Value	Pr > F
Model	2	678.2688889	339.1344444	327.49	<.0001
Error	6	6.2133333	1.0355556		
Corrected Total	8	684.4822222			

R-Square	Coeff Var	Root MSE	Underflow Starch Mean
0.990923	2.144370	1.017623	47.45556

Source	DF	Type III SS	Mean Square	F Value	Pr > F
Fraction	2	678.2688889	339.1344444	327.49	<.0001

The SAS
The GLM Procedure

Duncan's Multiple Range Test for Underflow Starch

Alpha	0.05
Error Degrees of Freedom	6
Error Mean Square	1.035556

Number of Means	2	3
Critical Range	2.033	2.107

Means with the same letter are not significantly different.

Duncan Grouping	Mean	N	Fraction
A	55.2000	3	UU1
B	51.8333	3	U1
C	35.3333	3	UO1

B.4 Statistical analysis of the underflow protein content using single- and double-pass processes

The SAS System
The GLM Procedure

Class Level Information

Class	Levels	Values
Fraction	3	U1 UO1 UU1

Number of observations 9

The SAS System
The GLM Procedure

Dependent Variable: Underflow Protein

Source	DF	Sum of Squares	Mean Square	F Value	Pr > F
Model	2	947.8466667	473.9233333	726.63	<.0001
Error	6	3.9133333	0.6522222		
Corrected Total	8	951.7600000			

R-Square	Coeff Var	Root MSE	Underflow Protein Mean
0.995888	3.269647	0.807603	24.70000

Source	DF	Type III SS	Mean Square	F Value	Pr > F
Fraction	2	947.8466667	473.9233333	726.63	<.0001

The SAS System
The GLM Procedure

Duncan's Multiple Range Test for Underflow Protein

Alpha	0.05
Error Degrees of Freedom	6
Error Mean Square	0.652222

Number of Means	2	3
Critical Range	1.614	1.672

Means with the same letter are not significantly different.

Duncan Grouping	Mean	N	Fraction
A	38.6667	3	UO1
B	21.1333	3	U1
C	14.3000	3	UU1

Appendix C

Statistical analysis of starch and protein contents of single-pass hydrocyclone process in isopropyl alcohol and deionized water media

C.1 Statistical analysis of the overflow starch content at three feed concentrations in isopropyl alcohol

The SAS System
The GLM Procedure

Class Level Information

Class	Levels	Values
Concentration	3	AL-0.5 AL-1.0 AL-1.5

Number of observations 9

The SAS System
The GLM Procedure

Dependent Variable: Overflow Starch

Source	DF	Sum of Squares	Mean Square	F Value	Pr > F
Model	2	1.81555556	0.90777778	2.81	0.1378
Error	6	1.94000000	0.32333333		
Corrected Total	8	3.75555556			

R-Square	Coeff Var	Root MSE	Overflow Starch Mean
0.483432	5.066947	0.568624	11.22222

Source	DF	Type III SS	Mean Square	F Value	Pr > F
Concentration	2	1.81555556	0.90777778	2.81	0.1378

The SAS System
The GLM Procedure

Duncan's Multiple Range Test for Overflow Starch

Alpha	0.05
Error Degrees of Freedom	6
Error Mean Square	0.323333

Number of Means	2	3
Critical Range	1.136	1.177

Means with the same letter are not significantly different.

Duncan Grouping	Mean	N	Concentration
A	11.8333	3	AL-0.5
A			
A	11.0667	3	AL-1.0
A			
A	10.7667	3	AL-1.5

C.2 Statistical analysis of the overflow protein content at three feed concentrations in isopropyl alcohol

The SAS System
The GLM Procedure

Class Level Information

Class	Levels	Values
Concentration	3	AL-0.5 AL-1.0 AL-1.5

Number of observations 9

The SAS System
The GLM Procedure

Dependent Variable: Overflow Protein

Source	DF	Sum of Squares	Mean Square	F Value	Pr > F
Model	2	2.66000000	1.33000000	0.83	0.4801
Error	6	9.60000000	1.60000000		
Corrected Total	8	12.26000000			

R-Square	Coeff Var	Root MSE	Overflow Protein Mean
0.216966	3.349279	1.264911	37.76667

Source	DF	Type III SS	Mean Square	F Value	Pr > F
Concentration	2	2.66000000	1.33000000	0.83	0.4801

The SAS System
The GLM Procedure

Duncan's Multiple Range Test for Overflow Protein

Alpha	0.05
Error Degrees of Freedom	6
Error Mean Square	1.6

Number of Means	2	3
Critical Range	2.527	2.619

Means with the same letter are not significantly different.

Duncan Grouping	Mean	N	Concentration
A	38.200	3	AL-1.5
A			
A	38.100	3	AL-1.0
A			
A	37.000	3	AL-0.5

C.3 Statistical analysis of the underflow starch content at three feed concentrations in isopropyl alcohol

The SAS System
The GLM Procedure

Class Level Information

Class	Levels	Values
Concentration	3	AL-0.5 AL-1.0 AL-1.5

Number of observations 9

The SAS System
The GLM Procedure

Dependent Variable: Underflow Starch

Source	DF	Sum of Squares	Mean Square	F Value	Pr > F
Model	2	6.54888889	3.27444444	0.96	0.4350
Error	6	20.48000000	3.41333333		
Corrected Total	8	27.02888889			

R-Square	Coeff Var	Root MSE	Underflow Starch Mean
0.242292	3.491745	1.847521	52.91111

Source	DF	Type III SS	Mean Square	F Value	Pr > F
Concentration	2	6.54888889	3.27444444	0.96	0.4350

The SAS System
The GLM Procedure

Duncan's Multiple Range Test for Underflow Starch

Alpha	0.05
Error Degrees of Freedom	6
Error Mean Square	3.413333

Number of Means	2	3
Critical Range	3.691	3.826

Means with the same letter are not significantly different.

Duncan Grouping	Mean	N	Concentration
A	54.033	3	AL-0.5
A			
A	52.733	3	AL-1.0
A			
A	51.967	3	AL-1.5

C.4 Statistical analysis of the underflow starch content at three feed concentrations in isopropyl alcohol

The SAS System
The GLM Procedure

Class Level Information

Class	Levels	Values
Concentration	3	AL-0.5 AL-1.0 AL-1.5

Number of observations 9

The SAS System
The GLM Procedure

Dependent Variable: Underflow Protein

Source	DF	Sum of Squares	Mean Square	F Value	Pr > F
Model	2	0.43555556	0.21777778	1.32	0.3339
Error	6	0.98666667	0.16444444		
Corrected Total	8	1.42222222			

R-Square	Coeff Var	Root MSE	Underflow Protein Mean
0.306250	1.593737	0.405518	25.44444

Source	DF	Type III SS	Mean Square	F Value	Pr > F
Concentration	2	0.43555556	0.21777778	1.32	0.3339

The SAS System
The GLM Procedure

Duncan's Multiple Range Test for Underflow Protein

Alpha	0.05
Error Degrees of Freedom	6
Error Mean Square	0.164444

Number of Means	2	3
Critical Range	.8102	.8397

Means with the same letter are not significantly different.

Duncan Grouping	Mean	N	Concentration
A	25.7333	3	AL-0.5
A			
A	25.4000	3	AL-1.0
A			
A	25.2000	3	AL-1.5

C.5 Statistical analysis of the overflow starch content at three feed concentrations in deionized water

The SAS System
The GLM Procedure

Class Level Information

Class	Levels	Values
Concentration	3	W-0.5 W-1.0 W-1.5

Number of observations 9

The SAS System
The GLM Procedure

Dependent Variable: Overflow Protein

Source	DF	Sum of Squares	Mean Square	F Value	Pr > F
Model	2	2.84222222	1.42111111	1.10	0.3913
Error	6	7.74000000	1.29000000		
Corrected Total	8	10.58222222			

R-Square	Coeff Var	Root MSE	Overflow Protein Mean
0.268585	13.13886	1.135782	8.644444

Source	DF	Type III SS	Mean Square	F Value	Pr > F
Concentration	2	2.84222222	1.42111111	1.10	0.3913

The SAS System
The GLM Procedure

Duncan's Multiple Range Test for Overflow Protein

Alpha	0.05
Error Degrees of Freedom	6
Error Mean Square	1.29

Number of Means	2	3
Critical Range	2.269	2.352

Means with the same letter are not significantly different.

Duncan Grouping	Mean	N	Concentration
A	9.4333	3	W-0.5
A			
A	8.3333	3	W-1.0
A			
A	8.1667	3	W-1.5

C.6 Statistical analysis of the overflow protein content at three feed concentrations in deionized water

The SAS System
The GLM Procedure

Class Level Information

Class	Levels	Values
Concentration	3	W-0.5 W-1.0 W-1.5

Number of observations 9

The SAS System
The GLM Procedure

Dependent Variable: Overflow Protein

Source	DF	Sum of Squares	Mean Square	F Value	Pr > F
Model	2	142.6755556	71.3377778	47.14	0.0002
Error	6	9.0800000	1.5133333		
Corrected Total	8	151.7555556			

R-Square	Coeff Var	Root MSE	Overflow Protein Mean
0.940167	1.609710	1.230176	76.42222

Source	DF	Type III SS	Mean Square	F Value	Pr > F
Concentration	2	142.6755556	71.3377778	47.14	0.0002

The SAS System
The GLM Procedure

Duncan's Multiple Range Test for Overflow Protein

Alpha	0.05
Error Degrees of Freedom	6
Error Mean Square	1.513333

Number of Means	2	3
Critical Range	2.458	2.547

Means with the same letter are not significantly different.

Duncan Grouping	Mean	N	Concentration
A	81.467	3	W-1.5
B	76.067	3	W-1.0
C	71.733	3	W-0.5

C.7 Statistical analysis of the underflow starch content at three feed concentrations in deionized water

The SAS System
The GLM Procedure

Class Level Information

Class	Levels	Values
Consentration	3	W-0.5 W-1.0 W-1.5

Number of observations 9

The SAS System
The GLM Procedure

Dependent Variable: Underflow Starch

Source	DF	Sum of Squares	Mean Square	F Value	Pr > F
Model	2	35.69555556	17.84777778	2.88	0.1328
Error	6	37.18000000	6.19666667		
Corrected Total	8	72.87555556			

R-Square	Coeff Var	Root MSE	Underflow Starch Mean
0.489815	3.463255	2.489310	71.87778

Source	DF	Type III SS	Mean Square	F Value	Pr > F
Concentration	2	35.69555556	17.84777778	2.88	0.1328

The SAS System
The GLM Procedure

Duncan's Multiple Range Test for Underflow Starch

Alpha	0.05
Error Degrees of Freedom	6
Error Mean Square	6.196667

Number of Means	2	3
Critical Range	4.973	5.154

Means with the same letter are not significantly different.

Duncan Grouping	Mean	N	Concentration
A	73.433	3	W-0.5
A			
A	73.133	3	W-1.5
A			
A	69.067	3	W-1.0

C.8 Statistical analysis of the underflow starch content at three feed concentrations in deionized water

The SAS System
The GLM Procedure

Class Level Information

Class	Levels	Values
Concentration	3	W-0.5 W-1.0 W-1.5

Number of observations 9

The SAS System
The GLM Procedure

Dependent Variable: Underflow Protein

Source	DF	Sum of Squares	Mean Square	F Value	Pr > F
Model	2	28.96888889	14.48444444	47.23	0.0002
Error	6	1.84000000	0.30666667		
Corrected Total	8	30.80888889			

R-Square	Coeff Var	Root MSE	Underflow Protein Mean
0.940277	2.529936	0.553775	21.88889

Source	DF	Type III SS	Mean Square	F Value	Pr > F
Concentration	2	28.96888889	14.48444444	47.23	0.0002

The SAS System
The GLM Procedure

Duncan's Multiple Range Test for Underflow Protein

Alpha	0.05
Error Degrees of Freedom	6
Error Mean Square	0.306667

Number of Means	2	3
Critical Range	1.106	1.147

Means with the same letter are not significantly different.

Duncan Grouping	Mean	N	Concentration
A	24.2667	3	W-0.5
B	21.4667	3	W-1.0
C	19.9333	3	W-1.5

Appendix D

Statistical analysis of starch and protein contents of the overflow and underflow using different feed materials and pH values in the water medium

D.1 Statistical analysis of the overflow starch content using whole chickpea flour at pH 6.6

The SAS System
The GLM Procedure

Class Level Information

Class	Levels	Values
Fraction	3	O1 OO1 OU1

Number of observations 9

The SAS System
The GLM Procedure

Dependent Variable: Overflow Starch

Source	DF	Sum of Squares	Mean Square	F Value	Pr > F
Model	2	16.36222222	8.18111111	28.65	0.0009
Error	6	1.71333333	0.28555556		
Corrected Total	8	18.07555556			

R-Square	Coeff Var	Root MSE	Overflow Starch Mean
0.905213	15.36539	0.534374	3.477778

Source	DF	Type III SS	Mean Square	F Value	Pr > F
Fraction	2	16.36222222	8.18111111	28.65	0.0009

The SAS System
The GLM Procedure

Duncan's Multiple Range Test for Overflow Starch

Alpha	0.05
Error Degrees of Freedom	6
Error Mean Square	0.285556

Number of Means	2	3
Critical Range	1.068	1.106

Means with the same letter are not significantly different.

Duncan Grouping	Mean	N	Fraction
A	5.1667	3	OU1
B	3.4000	3	O1
C	1.8667	3	OO1

D.2 Statistical analysis of the overflow starch content using whole chickpea flour at pH 9.0

The SAS System
The GLM Procedure

Class Level Information

Class	Levels	Values
Fraction	3	O1 OO1 OU1

Number of observations 9

The SAS System
The GLM Procedure

Dependent Variable: Overflow Starch

Source	DF	Sum of Squares	Mean Square	F Value	Pr > F
Model	2	19.89555556	9.94777778	40.15	0.0003
Error	6	1.48666667	0.24777778		
Corrected Total	8	21.38222222			

R-Square	Coeff Var	Root MSE	Overflow Starch Mean
0.930472	13.65840	0.497773	3.644444

Source	DF	Type III SS	Mean Square	F Value	Pr > F
Fraction	2	19.89555556	9.94777778	40.15	0.0003

The SAS System
The GLM Procedure

Duncan's Multiple Range Test for Overflow Starch

Alpha	0.05
Error Degrees of Freedom	6
Error Mean Square	0.247778

Number of Means	2	3
Critical Range	0.994	1.031

Means with the same letter are not significantly different.

Duncan Grouping	Mean	N	Fraction
A	5.5333	3	OU1
B	3.5000	3	O1
C	1.9000	3	OO1

D.3 Statistical analysis of the underflow starch content using whole chickpea flour at pH 6.6

The SAS System
The GLM Procedure

Class Level Information

Class	Levels	Values
Fraction	3	U1 UO1 UU1

Number of observations 9

The SAS System
The GLM Procedure

Dependent Variable: Underflow Starch

Source	DF	Sum of Squares	Mean Square	F Value	Pr > F
Model	2	10373.22889	5186.61444	678.19	<.0001
Error	6	45.88667	7.64778		
Corrected Total	8	10419.11556			

R-Square	Coeff Var	Root MSE	Underflow Starch Mean
0.995596	5.330725	2.765462	51.87778

Source	DF	Type III SS	Mean Square	F Value	Pr > F
Fraction	2	10373.22889	5186.61444	678.19	<.0001

The SAS System
The GLM Procedure

Duncan's Multiple Range Test for Underflow Starch

Alpha	0.05
Error Degrees of Freedom	6
Error Mean Square	7.647778

Number of Means	2	3
Critical Range	5.525	5.726

Means with the same letter are not significantly different.

Duncan Grouping	Mean	N	Fraction
A	86.600	3	UU1
B	63.233	3	U1
C	5.800	3	UO1

D.4 Statistical analysis of the underflow starch content using whole chickpea flour at pH 9.0

The SAS System
The GLM Procedure

Class Level Information

Class	Levels	Values
Fraction	3	U1 UO1 UU1

Number of observations 9

The SAS System
The GLM Procedure

Dependent Variable: Underflow Starch

Source	DF	Sum of Squares	Mean Square	F Value	Pr > F
Model	2	12199.88222	6099.94111	5140.40	<.0001
Error	6	7.12000	1.18667		
Corrected Total	8	12207.00222			

R-Square	Coeff Var	Root MSE	Underflow Starch Mean
0.999417	2.022711	1.089342	53.85556

Source	DF	Type III SS	Mean Square	F Value	Pr > F
Fraction	2	12199.88222	6099.94111	5140.40	<.0001

The SAS System
The GLM Procedure

Duncan's Multiple Range Test for Underflow Starch

Alpha	0.05
Error Degrees of Freedom	6
Error Mean Square	1.186667

Number of Means	2	3
Critical Range	2.176	2.256

Means with the same letter are not significantly different.

Duncan Grouping	Mean	N	Fraction
A	90.8667	3	UU1
B	67.0667	3	U1
C	3.6333	3	UO1

D.5 Statistical analysis of the overflow starch content using defatted chickpea flour at pH 6.6

The SAS System
The GLM Procedure

Class Level Information

Class	Levels	Values
Fraction	3	O1 OO1 OU1

Number of observations 9

The SAS System
The GLM Procedure

Dependent Variable: Overflow Starch

Source	DF	Sum of Squares	Mean Square	F Value	Pr > F
Model	2	83.63555556	41.81777778	31.23	0.0007
Error	6	8.03333333	1.33888889		
Corrected Total	8	91.66888889			

R-Square	Coeff Var	Root MSE	Overflow Starch Mean
0.912366	35.18221	1.157104	3.288889

Source	DF	Type III SS	Mean Square	F Value	Pr > F
Fraction	2	83.63555556	41.81777778	31.23	0.0007

The SAS System
The GLM Procedure

Duncan's Multiple Range Test for Overflow Starch

Alpha	0.05
Error Degrees of Freedom	6
Error Mean Square	1.338889

Number of Means	2	3
Critical Range	2.312	2.396

Means with the same letter are not significantly different.

Duncan Grouping	Mean	N	Fraction
A	7.6000	3	O1
B	1.1333	3	OO1
B			
B	1.1333	3	OU1

D.6 Statistical analysis of the overflow starch content using defatted chickpea flour at pH 9.0

The SAS System
The GLM Procedure

Class Level Information

Class	Levels	Values
Fraction	3	O1 OO1 OU1

Number of observations 9

The SAS System
The GLM Procedure

Dependent Variable: Overflow Starch

Source	DF	Sum of Squares	Mean Square	F Value	Pr > F
Model	2	0.46888889	0.23444444	2.43	0.1691
Error	6	0.58000000	0.09666667		
Corrected Total	8	1.04888889			

R-Square	Coeff Var	Root MSE	Overflow Starch Mean
0.447034	38.33169	0.310913	0.811111

Source	DF	Type III SS	Mean Square	F Value	Pr > F
Fraction	2	0.46888889	0.23444444	2.43	0.1691

The SAS System
The GLM Procedure

Duncan's Multiple Range Test for Overflow Starch

Alpha	0.05
Error Degrees of Freedom	6
Error Mean Square	0.096667

Number of Means	2	3
Critical Range	.6212	.6438

Means with the same letter are not significantly different.

Duncan Grouping	Mean	N	Fraction
A	1.1333	3	OU1
A			
A	0.6667	3	O1
A			
A	0.6333	3	OO1

D.7 Statistical analysis of the underflow starch content using defatted chickpea flour at pH 6.6

The SAS System
The GLM Procedure

Class Level Information

Class	Levels	Values
Fraction	3	U1 UO1 UU1

Number of observations 9

The SAS System
The GLM Procedure

Dependent Variable: Underflow Starch

Source	DF	Sum of Squares	Mean Square	F Value	Pr > F
Model	2	10371.69556	5185.84778	839.44	<.0001
Error	6	37.06667	6.17778		
Corrected Total	8	10408.76222			

R-Square	Coeff Var	Root MSE	Underflow Starch Mean
0.996439	4.018254	2.485514	61.85556

Source	DF	Type III SS	Mean Square	F Value	Pr > F
Fraction	2	10371.69556	5185.84778	839.44	<.0001

The SAS System
The GLM Procedure

Duncan's Multiple Range Test for Underflow Starch

Alpha	0.05
Error Degrees of Freedom	6
Error Mean Square	6.177778

Number of Means	2	3
Critical Range	4.966	5.147

Means with the same letter are not significantly different.

Duncan Grouping	Mean	N	Fraction
A	93.100	3	UU1
B	77.800	3	U1
C	14.667	3	UO1

D.8 Statistical analysis of the underflow starch content using defatted chickpea flour at pH 9.0

The SAS System
The GLM Procedure

Class Level Information

Class	Levels	Values
Fraction	3	U1 UO1 UU1

Number of observations 9

The SAS System
The GLM Procedure

Dependent Variable: Underflow Starch

Source	DF	Sum of Squares	Mean Square	F Value	Pr > F
Model	2	16406.33556	8203.16778	7259.44	<.0001
Error	6	6.78000	1.13000		
Corrected Total	8	16413.11556			

R-Square	Coeff Var	Root MSE	Underflow Starch Mean
0.999587	1.768089	1.063015	60.12222

Source	DF	Type III SS	Mean Square	F Value	Pr > F
Fraction	2	16406.33556	8203.16778	7259.44	<.0001

The SAS System
The GLM Procedure

Duncan's Multiple Range Test for Underflow Starch

Alpha	0.05
Error Degrees of Freedom	6
Error Mean Square	1.13

Number of Means	2	3
Critical Range	2.124	2.201

Means with the same letter are not significantly different.

Duncan Grouping	Mean	N	Fraction
A	99.6667	3	UU1
B	79.8667	3	U1
C	0.8333	3	UO1

D.9 Statistical analysis of protein content of the overflow sediment using whole chickpea flour at pH 6.6

The SAS System
The GLM Procedure

Class Level Information

Class	Levels	Values
Fraction	3	O1,SE OO1,SE OU1,SE

Number of observations 9

The SAS System
The GLM Procedure

Dependent Variable: Overflow Protein

Source	DF	Sum of Squares	Mean Square	F Value	Pr > F
Model	2	30.72888889	15.36444444	38.52	0.0004
Error	6	2.39333333	0.39888889		
Corrected Total	8	33.12222222			

R-Square	Coeff Var	Root MSE	Overflow Protein Mean
0.927742	0.950533	0.631577	66.44444

Source	DF	Type III SS	Mean Square	F Value	Pr > F
Fraction	2	30.72888889	15.36444444	38.52	0.0004

The SAS System
The GLM Procedure

Duncan's Multiple Range Test for Overflow Protein

Alpha	0.05
Error Degrees of Freedom	6
Error Mean Square	0.398889

Number of Means	2	3
Critical Range	1.262	1.308

Means with the same letter are not significantly different.

Duncan Grouping	Mean	N	Fraction
A	68.4667	3	OO1,SE
B	66.8667	3	O1,SE
C	64.0000	3	OU1,SE

D.10 Statistical analysis of protein content of the overflow supernatant using whole chickpea flour at pH 6.6

The SAS System
The GLM Procedure

Class Level Information

Class	Levels	Values
Fraction	3	O1,SU OO1,SU OU1,SU

Number of observations 9

The SAS System
The GLM Procedure

Dependent Variable: Overflow Protein

Source	DF	Sum of Squares	Mean Square	F Value	Pr > F
Model	2	101.4022222	50.7011111	2.42	0.1694
Error	6	125.6333333	20.9388889		
Corrected Total	8	227.0355556			

R-Square	Coeff Var	Root MSE	Overflow Protein Mean
0.446636	6.668253	4.575903	68.62222

Source	DF	Type III SS	Mean Square	F Value	Pr > F
Fraction	2	101.4022222	50.7011111	2.42	0.1694

The SAS System
The GLM Procedure

Duncan's Multiple Range Test for Overflow Protein

Alpha	0.05
Error Degrees of Freedom	6
Error Mean Square	20.93889

Number of Means	2	3
Critical Range	9.142	9.475

Means with the same letter are not significantly different.

Duncan Grouping	Mean	N	Fraction
A	72.133	3	OU1,SU
A			
A	69.633	3	O1,SU
A			
A	64.100	3	OO1,SU

D.11 Statistical analysis of protein content of the overflow sediment using whole chickpea flour at pH 9.0

The SAS System
The GLM Procedure

Class Level Information

Class	Levels	Values
Fraction	3	O1,SE OO1,SE OU1,SE

Number of observations 9

The SAS System
The GLM Procedure

Dependent Variable: Overflow Protein

Source	DF	Sum of Squares	Mean Square	F Value	Pr > F
Model	2	31.62888889	15.81444444	18.95	0.0026
Error	6	5.00666667	0.83444444		
Corrected Total	8	36.63555556			

R-Square	Coeff Var	Root MSE	Overflow Protein Mean
0.863339	1.340942	0.913479	68.12222

Source	DF	Type III SS	Mean Square	F Value	Pr > F
Fraction	2	31.62888889	15.81444444	18.95	0.0026

The SAS System
The GLM Procedure

Duncan's Multiple Range Test for Overflow Protein

Alpha	0.05
Error Degrees of Freedom	6
Error Mean Square	0.834444

Number of Means	2	3
Critical Range	1.825	1.891

Means with the same letter are not significantly different.

Duncan Grouping	Mean	N	Fraction
A	70.2667	3	OO1,SE
B	68.4000	3	O1,SE
C	65.7000	3	OU1,SE

D.12 Statistical analysis of protein content of the overflow supernatant using whole chickpea flour at pH 9.0

The SAS System
The GLM Procedure

Class Level Information

Class	Levels	Values
Fraction	3	O1,SU OO1,SU OU1,SU

Number of observations 9

The SAS System
The GLM Procedure

Dependent Variable: Overflow Protein

Source	DF	Sum of Squares	Mean Square	F Value	Pr > F
Model	2	10.66888889	5.33444444	0.53	0.6160
Error	6	60.86000000	10.14333333		
Corrected Total	8	71.52888889			

R-Square	Coeff Var	Root MSE	Overflow Protein Mean
0.149155	4.752734	3.184860	67.01111

Source	DF	Type III SS	Mean Square	F Value	Pr > F
Fraction	2	10.66888889	5.33444444	0.53	0.6160

The SAS System
The GLM Procedure

Duncan's Multiple Range Test for Overflow Protein

Alpha	0.05
Error Degrees of Freedom	6
Error Mean Square	10.14333

Number of Means	2	3
Critical Range	6.363	6.595

Means with the same letter are not significantly different.

Duncan Grouping	Mean	N	Fraction
A	68.333	3	OO1,SU
A			
A	67.033	3	O1,SU
A			
A	65.667	3	OU1,SU

D.13 Statistical analysis of protein content of the underflow sediment using whole chickpea flour at pH 6.6

The SAS System
The GLM Procedure

Class Level Information

Class	Levels	Values
Fraction	3	U1,SE UO1,SE UU1,SE

Number of observations 9

The SAS System
The GLM Procedure

Dependent Variable: Underflow Protein

Source	DF	Sum of Squares	Mean Square	F Value	Pr > F
Model	2	4018.468889	2009.234444	2550.51	<.0001
Error	6	4.726667	0.787778		
Corrected Total	8	4023.195556			

R-Square	Coeff Var	Root MSE	Underflow Protein Mean
0.998825	3.958432	0.887568	22.42222

Source	DF	Type III SS	Mean Square	F Value	Pr > F
Fraction	2	4018.468889	2009.234444	2550.51	<.0001

The SAS System
The GLM Procedure

Duncan's Multiple Range Test for Underflow Protein

Alpha	0.05
Error Degrees of Freedom	6
Error Mean Square	0.787778

Number of Means	2	3
Critical Range	1.773	1.838

Means with the same letter are not significantly different.

Duncan Grouping	Mean	N	Fraction
A	52.3000	3	UO1,SE
B	7.9667	3	U1,SE
B			
B	7.0000	3	UU1,SE

D.14 Statistical analysis of protein content of the underflow supernatant using whole chickpea flour at pH 6.6

The SAS System
The GLM Procedure

Class Level Information

Class	Levels	Values
Fraction	3	U1,SU UO1,SU UU1,SU

Number of observations 9

The SAS System
The GLM Procedure

Dependent Variable: Underflow Protein

Source	DF	Sum of Squares	Mean Square	F Value	Pr > F
Model	2	2367.695556	1183.847778	991.13	<.0001
Error	6	7.166667	1.194444		
Corrected Total	8	2374.862222			

R-Square	Coeff Var	Root MSE	Underflow Protein Mean
0.996982	2.470155	1.092906	44.24444

Source	DF	Type III SS	Mean Square	F Value	Pr > F
Fraction	2	2367.695556	1183.847778	991.13	<.0001

The SAS System
The GLM Procedure

Duncan's Multiple Range Test for Underflow Protein

Alpha	0.05
Error Degrees of Freedom	6
Error Mean Square	1.194444

Number of Means	2	3
Critical Range	2.184	2.263

Means with the same letter are not significantly different.

Duncan Grouping	Mean	N	Fraction
A	67.1333	3	UO1,SU
B	34.1000	3	U1,SU
C	31.5000	3	UU1,SU

D.15 Statistical analysis of protein content of the underflow sediment using whole chickpea flour at pH 9.0

The SAS System
The GLM Procedure

Class Level Information

Class	Levels	Values
Fraction	3	U1,SE UO1,SE UU1,SE

Number of observations 9

The SAS System
The GLM Procedure

Dependent Variable: Underflow Protein

Source	DF	Sum of Squares	Mean Square	F Value	Pr > F
Model	2	4412.606667	2206.303333	29201.1	<.0001
Error	6	0.453333	0.075556		
Corrected Total	8	4413.060000			

R-Square	Coeff Var	Root MSE	Underflow Protein Mean
0.999897	1.257044	0.274874	21.86667

Source	DF	Type III SS	Mean Square	F Value	Pr > F
Fraction	2	4412.606667	2206.303333	29201.1	<.0001

The SAS System
The GLM Procedure

Duncan's Multiple Range Test for Underflow Protein

Alpha	0.05
Error Degrees of Freedom	6
Error Mean Square	0.075556

Number of Means	2	3
Critical Range	.5492	.5692

Means with the same letter are not significantly different.

Duncan Grouping	Mean	N	Fraction
A	53.1667	3	UO1,SE
B	7.0333	3	U1,SE
C	5.4000	3	UU1,SE

D.16 Statistical analysis of protein content of the underflow supernatant using whole chickpea flour at pH 9.0

The SAS System
The GLM Procedure

Class Level Information

Class	Levels	Values
Fraction	3	U1,SU UO1,SU UU1,SU

Number of observations 9

The SAS System
The GLM Procedure

Dependent Variable: Underflow Protein

Source	DF	Sum of Squares	Mean Square	F Value	Pr > F
Model	2	2324.242222	1162.121111	945.67	<.0001
Error	6	7.373333	1.228889		
Corrected Total	8	2331.615556			

R-Square	Coeff Var	Root MSE	Underflow Protein Mean
0.996838	3.402788	1.108553	32.57778

Source	DF	Type III SS	Mean Square	F Value	Pr > F
Fraction	2	2324.242222	1162.121111	945.67	<.0001

The SAS System
The GLM Procedure

Duncan's Multiple Range Test for Underflow Protein

Alpha	0.05
Error Degrees of Freedom	6
Error Mean Square	1.228889

Number of Means	2	3
Critical Range	2.215	2.295

Means with the same letter are not significantly different.

Duncan Grouping	Mean	N	Fraction
A	55.2667	3	UO1,SU
B	22.3667	3	U1,SU
C	20.1000	3	UU1,SU

D.17 Statistical analysis of protein content of the overflow sediment using defatted chickpea flour at pH 6.6

The SAS System
The GLM Procedure

Class Level Information

Class	Levels	Values
Fraction	3	O1,SE OO1,SE OU1,SE

Number of observations 9

The SAS System
The GLM Procedure

Dependent Variable: Overflow Protein

Source	DF	Sum of Squares	Mean Square	F Value	Pr > F
Model	2	913.9488889	456.9744444	83.85	<.0001
Error	6	32.7000000	5.4500000		
Corrected Total	8	946.6488889			

R-Square	Coeff Var	Root MSE	Overflow Protein Mean
0.965457	2.711060	2.334524	86.11111

Source	DF	Type III SS	Mean Square	F Value	Pr > F
Fraction	2	913.9488889	456.9744444	83.85	<.0001

The SAS System
The GLM Procedure

Duncan's Multiple Range Test for Overflow Protein

Alpha	0.05
Error Degrees of Freedom	6
Error Mean Square	5.45

Number of Means	2	3
Critical Range	4.664	4.834

Means with the same letter are not significantly different.

Duncan Grouping	Mean	N	Fraction
A	97.233	3	OO1,SE
B	88.267	3	OU1,SE
C	72.833	3	O1,SE

D.18 Statistical analysis of protein content of the overflow supernatant using defatted chickpea flour at pH 6.6

The SAS System
The GLM Procedure

Class Level Information

Class	Levels	Values
Fraction	3	O1,SU OO1,SU OU1,SU

Number of observations 9

The SAS System
The GLM Procedure

Dependent Variable: Overflow Protein

Source	DF	Sum of Squares	Mean Square	F Value	Pr > F
Model	2	319.0688889	159.5344444	2.49	0.1630
Error	6	384.2000000	64.0333333		
Corrected Total	8	703.2688889			

R-Square	Coeff Var	Root MSE	Overflow Protein Mean
0.453694	10.75709	8.002083	74.38889

Source	DF	Type III SS	Mean Square	F Value	Pr > F
Fraction	2	319.0688889	159.5344444	2.49	0.1630

The SAS System
The GLM Procedure

Duncan's Multiple Range Test for Overflow Protein

Alpha	0.05
Error Degrees of Freedom	6
Error Mean Square	64.03333

Number of Means	2	3
Critical Range	15.99	16.57

Means with the same letter are not significantly different.

Duncan Grouping	Mean	N	Fraction
A	82.367	3	OO1,SU
A			
A	72.733	3	OU1,SU
A			
A	68.067	3	O1,SU

D.19 Statistical analysis of protein content of the overflow sediment using defatted chickpea flour at pH 9.0

The SAS System
The GLM Procedure

Class Level Information

Class	Levels	Values
Fraction	3	O1,SE OO1,SE OU1,SE

Number of observations 9

The SAS System
The GLM Procedure

Dependent Variable: Overflow Protein

Source	DF	Sum of Squares	Mean Square	F Value	Pr > F
Model	2	172.0955556	86.0477778	182.22	<.0001
Error	6	2.8333333	0.4722222		
Corrected Total	8	174.9288889			

R-Square	Coeff Var	Root MSE	Overflow Protein Mean
0.983803	0.737234	0.687184	93.21111

Source	DF	Type III SS	Mean Square	F Value	Pr > F
Fraction	2	172.0955556	86.0477778	182.22	<.0001

The SAS System
The GLM Procedure

Duncan's Multiple Range Test for Overflow Protein

Alpha	0.05
Error Degrees of Freedom	6
Error Mean Square	0.472222

Number of Means	2	3
Critical Range	1.373	1.423

Means with the same letter are not significantly different.

Duncan Grouping	Mean	N	Fraction
A	98.9000	3	OO1,SE
B	92.4667	3	O1,SE
C	88.2667	3	OU1,SE

D.20 Statistical analysis of protein content of the overflow supernatant using defatted chickpea flour at pH 9.0

The SAS System
The GLM Procedure

Class Level Information

Class	Levels	Values
Fraction	3	O1,SU OO1,SU OU1,SU

Number of observations 9

The SAS System
The GLM Procedure

Dependent Variable: Overflow Protein

Source	DF	Sum of Squares	Mean Square	F Value	Pr > F
Model	2	75.2422222	37.6211111	6.78	0.0289
Error	6	33.2866667	5.5477778		
Corrected Total	8	108.5288889			

R-Square	Coeff Var	Root MSE	Overflow Protein Mean
0.693292	3.743968	2.355372	62.91111

Source	DF	Type III SS	Mean Square	F Value	Pr > F
Fraction	2	75.24222222	37.62111111	6.78	0.0289

The SAS System
The GLM Procedure

Duncan's Multiple Range Test for Overflow Protein

Alpha	0.05
Error Degrees of Freedom	6
Error Mean Square	5.547778

Number of Means	2	3
Critical Range	4.706	4.877

Means with the same letter are not significantly different.

Duncan Grouping	Mean	N	Fraction
A	66.100	3	OO1,SU
A			
B A	63.533	3	O1,SU
B			
B	59.100	3	OU1,SU

D.21 Statistical analysis of protein content of the underflow sediment using defatted chickpea flour at pH 6.6

The SAS System
The GLM Procedure

Class Level Information

Class	Levels	Values
Fraction	3	U1,SE UO1,SE UU1,SE

Number of observations 9

The SAS System
The GLM Procedure

Dependent Variable: Underflow Protein

Source	DF	Sum of Squares	Mean Square	F Value	Pr > F
Model	2	3742.642222	1871.321111	592.19	<.0001
Error	6	18.960000	3.160000		
Corrected Total	8	3761.602222			

R-Square	Coeff Var	Root MSE	Underflow Protein Mean
0.994960	6.016830	1.777639	29.54444

Source	DF	Type III SS	Mean Square	F Value	Pr > F
Fraction	2	3742.642222	1871.321111	592.19	<.0001

The SAS System
The GLM Procedure

Duncan's Multiple Range Test for Underflow Protein

Alpha	0.05
Error Degrees of Freedom	6
Error Mean Square	3.16

Number of Means	2	3
Critical Range	3.552	3.681

Means with the same letter are not significantly different.

Duncan Grouping	Mean	N	Fraction
A	58.133	3	UO1,SE
B	18.533	3	U1,SE
C	11.967	3	UU1,SE

D.22 Statistical analysis of protein content of the underflow supernatant using defatted chickpea flour at pH 6.6

The SAS System
The GLM Procedure

Class Level Information

Class	Levels	Values
Fraction	3	U1,SU UO1,SU UU1,SU

Number of observations 9

The SAS System
The GLM Procedure

Dependent Variable: Underflow Protein

Source	DF	Sum of Squares	Mean Square	F Value	Pr > F
Model	2	23.64222222	11.82111111	1.76	0.2499
Error	6	40.24000000	6.70666667		
Corrected Total	8	63.88222222			

R-Square	Coeff Var	Root MSE	Underflow Protein Mean
0.370091	3.839787	2.589723	67.44444

Source	DF	Type III SS	Mean Square	F Value	Pr > F
Fraction	2	23.64222222	11.82111111	1.76	0.2499

The SAS System
The GLM Procedure

Duncan's Multiple Range Test for Underflow Protein

Alpha	0.05
Error Degrees of Freedom	6
Error Mean Square	6.706667

Number of Means	2	3
Critical Range	5.174	5.362

Means with the same letter are not significantly different.

Duncan Grouping	Mean	N	Fraction
A	69.567	3	UO1,SU
A			
A	67.133	3	U1,SU
A			
A	65.633	3	UU1,SU

D.23 Statistical analysis of protein content of the underflow sediment using defatted chickpea flour at pH 9.0

The SAS System
The GLM Procedure

Class Level Information

Class	Levels	Values
Fraction	3	U1,SE UO1,SE UU1,SE

Number of observations 9

The SAS System
The GLM Procedure

Dependent Variable: Underflow Protein

Source	DF	Sum of Squares	Mean Square	F Value	Pr > F
Model	2	11664.44222	5832.22111	1656.88	<.0001
Error	6	21.12000	3.52000		
Corrected Total	8	11685.56222			

R-Square	Coeff Var	Root MSE	Underflow Protein Mean
0.998193	4.779365	1.876166	39.25556

Source	DF	Type III SS	Mean Square	F Value	Pr > F
Fraction	2	11664.44222	5832.22111	1656.88	<.0001

The SAS System
The GLM Procedure

Duncan's Multiple Range Test for Underflow Protein

Alpha	0.05
Error Degrees of Freedom	6
Error Mean Square	3.52

Number of Means	2	3
Critical Range	3.748	3.885

Means with the same letter are not significantly different.

Duncan Grouping	Mean	N	Fraction
A	90.067	3	UO1,SE
B	16.633	3	U1,SE
C	11.067	3	UU1,SE

D.24 Statistical analysis of protein content of the underflow supernatant using defatted chickpea flour at pH 9.0

The SAS System
The GLM Procedure

Class Level Information

Class	Levels	Values
Fraction	3	U1,SU UO1,SU UU1,SU

Number of observations 9

The SAS System
The GLM Procedure

Dependent Variable: Underflow Protein

Source	DF	Sum of Squares	Mean Square	F Value	Pr > F
Model	2	0.69555556	0.34777778	0.07	0.9341
Error	6	30.26000000	5.04333333		
Corrected Total	8	30.95555556			

R-Square	Coeff Var	Root MSE	Underflow Protein Mean
0.022469	3.701086	2.245737	60.67778

Source	DF	Type III SS	Mean Square	F Value	Pr > F
Fraction	2	0.69555556	0.34777778	0.07	0.9341

The SAS System
The GLM Procedure

Duncan's Multiple Range Test for Underflow Protein

Alpha	0.05
Error Degrees of Freedom	6
Error Mean Square	5.043333

Number of Means	2	3
Critical Range	4.487	4.650

Means with the same letter are not significantly different.

Duncan Grouping	Mean	N	Fraction
A	61.067	3	U1,SU
A			
A	60.533	3	UO1,SU
A			
A	60.433	3	UU1,SU

Appendix E

Statistical analysis of starch and protein contents of the overflow and underflow at pH 9.0 using different feed concentrations

E.1 Statistical analysis of the overflow starch content at different feed concentrations

The SAS System
The GLM Procedure

Class Level Information

Class	Levels	Values
Concentration	5	1.5 10.0 15.0 3.0 5.0

Number of observations 15

The SAS System
The GLM Procedure

Dependent Variable: Overflow Starch

Source	DF	Sum of Squares	Mean Square	F Value	Pr > F
Model	4	39.07733333	9.76933333	92.16	<.0001
Error	10	1.06000000	0.10600000		
Corrected Total	14	40.13733333			

R-Square	Coeff Var	Root MSE	Overflow Starch Mean
0.973591	5.977535	0.325576	5.446667

Source	DF	Type III SS	Mean Square	F Value	Pr > F
Concentration	4	39.07733333	9.76933333	92.16	<.0001

The SAS System
The GLM Procedure

Duncan's Multiple Range Test for Overflow Starch

Alpha	0.05
Error Degrees of Freedom	10
Error Mean Square	0.106

Number of Means	2	3	4	5
Critical Range	.5923	.6190	.6346	.6447

Means with the same letter are not significantly different.

Duncan Grouping	Mean	N	Concentration
A	7.6667	3	15.0
B	7.0000	3	10.0
C	4.9000	3	5.0
D	4.1333	3	3.0
E	3.5333	3	1.5

E.2 Statistical analysis of the overflow protein content at different feed concentrations

The SAS System
The GLM Procedure

Class Level Information

Class	Levels	Values
Fraction	5	1.5 10.0 15.0 3.0 5.0

Number of observations 15

The SAS System
The GLM Procedure

Dependent Variable: Overflow Protein

Source	DF	Sum of Squares	Mean Square	F Value	Pr > F
Model	4	259.1800000	64.7950000	78.83	<.0001
Error	10	8.2200000	0.8220000		
Corrected Total	14	267.4000000			

R-Square	Coeff Var	Root MSE	Overflow Protein Mean
0.969260	1.183606	0.906642	76.60000

Source	DF	Type III SS	Mean Square	F Value	Pr > F
Fraction	4	259.1800000	64.7950000	78.83	<.0001

The SAS System
The GLM Procedure

Duncan's Multiple Range Test for Overflow Protein

Alpha	0.05
Error Degrees of Freedom	10
Error Mean Square	0.822

Number of Means	2	3	4	5
Critical Range	1.649	1.724	1.767	1.795

Means with the same letter are not significantly different.

Duncan Grouping	Mean	N	Fraction
A	81.9333	3	1.5
B	80.2333	3	3.0
C	76.1333	3	5.0
D	74.4000	3	10.0
E	70.3000	3	15.0

E.3 Statistical analysis of the underflow starch content at different feed concentrations

The SAS System
The GLM Procedure

Class Level Information

Class	Levels	Values
Fraction	5	1.5 10.0 15.0 3.0 5.0

Number of observations 15

The SAS System
The GLM Procedure

Dependent Variable: Underflow Starch

Source	DF	Sum of Squares	Mean Square	F Value	Pr > F
Model	4	73.95066667	18.48766667	25.28	<.0001
Error	10	7.31333333	0.73133333		
Corrected Total	14	81.26400000			

R-Square	Coeff Var	Root MSE	Underflow Starch Mean
0.910005	1.307215	0.855180	65.42000

Source	DF	Type III SS	Mean Square	F Value	Pr > F
Fraction	4	73.95066667	18.48766667	25.28	<.0001

The SAS System
The GLM Procedure

Duncan's Multiple Range Test for Underflow Starch

Alpha	0.05
Error Degrees of Freedom	10
Error Mean Square	0.731333

Number of Means	2	3	4	5
Critical Range	1.556	1.626	1.667	1.693

Means with the same letter are not significantly different.

Duncan Grouping	Mean	N	Fraction
A	68.2333	3	1.5
B	66.6667	3	5.0
B			
B	66.3000	3	3.0
C	64.0000	3	10.0
D	61.9000	3	15.0

E.4 Statistical analysis of the underflow protein content at different feed concentrations

The SAS System
The GLM Procedure

Class Level Information

Class	Levels	Values
Fraction	5	1.5 10.0 15.0 3.0 5.0

Number of observations 15

The SAS System
The GLM Procedure

Dependent Variable: Underflow Protein

Source	DF	Sum of Squares	Mean Square	F Value	Pr > F
Model	4	32.61066667	8.15266667	45.63	<.0001
Error	10	1.78666667	0.17866667		
Corrected Total	14	34.39733333			

R-Square	Coeff Var	Root MSE	Underflow Protein Mean
0.948058	9.018986	0.422690	4.686667

Source	DF	Type III SS	Mean Square	F Value	Pr > F
Fraction	4	32.61066667	8.15266667	45.63	<.0001

The SAS System
The GLM Procedure

Duncan's Multiple Range Test for Underflow Protein

Alpha	0.05
Error Degrees of Freedom	10
Error Mean Square	0.178667

Number of Means	2	3	4	5
Critical Range	.7690	.8036	.8239	.8370

Means with the same letter are not significantly different.

Duncan Grouping	Mean	N	Fraction
A	7.3333	3	15.0
B	5.2667	3	10.0
C	3.8000	3	5.0
C			
C	3.5667	3	3.0
C			
C	3.4667	3	1.5

DATA APPENDIX

Attached is a CD of the data generated and analyzed in this thesis.